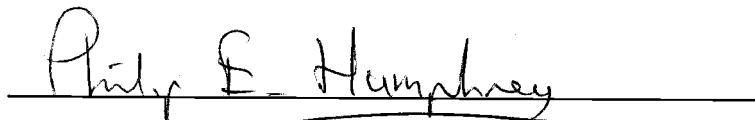


AN ABSTRACT OF THE THESIS OF

Shan Ren for the degree of Doctor of Philosophy in
Forest Products presented on September 27, 1991.

Title: Thermo-Hygro Rheological Behavior of Materials Used
in the Manufacture of Wood-Based Composites

Abstract approved


Dr. Philip E. Humphrey

Thermo-hygro-rheology of wood-adhesive systems plays an important role during the hot pressing process of wood based composites. The principal objective of this research is to quantitatively study the thermo-hygro rheological characteristics of wood-adhesive systems used in such composites. This is with a view to providing material characteristics which may be used in simulation models of industrial hot pressing operations.

For this purpose, a specially designed miniature hot press system mounted on a servo-hydraulic testing machine was used to compress pre-formed fiber networks. The environment for each test was maintained uniform throughout the specimen by pre-treating it inside the system until the desired conditions of temperature and moisture were achieved.

Experiments have been conducted under a range of test conditions of load (1 to 6 MPa), temperature (25 °C to 150 °C) and moisture content (0% to 16%). A five-element rheological model has been developed, and the rheological constants of materials have been determined by incorporating the experimental results in the model.

Each element has been nonlinearly related to prevailing density (rather than stress) of the material. Over almost all of the investigated combinations of temperature and MC, increasing temperature and moisture leads to increased elastic, viscous, delayed elastic and plastic-fractural deformations at given load levels.

The results may aid in the optimization of existing products and the development of new ones.

^c Copyright by Shan Ren
September 27, 1991

All Right Reserved

Thermo-Hygro Rheological Behavior
of Materials Used in the
Manufacture of Wood-Based Composites
by
Shan Ren

A THESIS
submitted to
Oregon State University

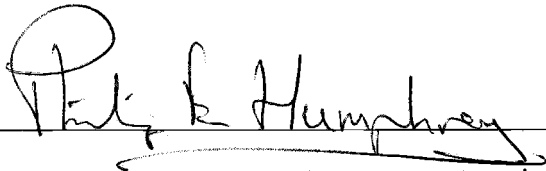
in partial fulfillment of
the requirements for the
degree of

Doctor of Philosophy

Completed September 27, 1991

Commencement June 1992

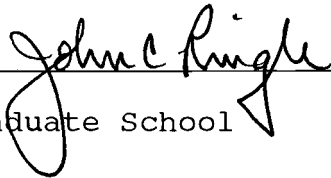
APPROVED:



Professor of Forest Products in Charge of Major



Head of Department of Forest Products



Dean of Graduate School

Data thesis is presented September 27, 1991

Typed by Shan Ren

ACKNOWLEDGEMENTS

This work is dedicated to my teachers, friends and colleagues both in China and USA who have done so many kind things for me.

I would like to express my sincere gratitude and appreciation to my advisor, Dr. Philip E. Humphrey, for his guidance, attention and help.

A special thanks must go to Dr. E. Wolff, Dr. D. Thomas, Dr. J. Karchesy, Dr. R. Leichti and Dr. E. Tice for their encouragement and help as my committee members.

I also want to thank Dr. Holbo for his kindly help during equipment improvement.

Finally, I want to thank my parents and my wife for all their continuous support, encouragement, care and understanding during my graduate career.

TABLE OF CONTENTS

CHAPTER 1. INTRODUCTION	1
CHAPTER 2. LITERATURE REVIEW	6
2.1. Introduction	6
2.2. Rheological behavior of wood composite materials	9
2.2.1. Application of rheological principles.	9
2.2.2. Rheological behavior of wood composites.	14
2.2.2.1. Rheological behavior of wood materials	16
2.2.2.2. Rheological behavior of adhesives.	16
2.3. Effects of wood composite's structure on rheological behavior	18
2.3.1. Effects of wood furnish material structures	21
2.3.2. Effects of the adhesive matrix structure	24
2.3.3. Effects of interfacial structure	26
2.4. Effects of temperature and moisture	27
2.4.1. Temperature effects	32
2.4.2. Moisture effects	35
2.4.3. Effects of temperature and moisture on the rheological and bonding behavior of adhesives	38
2.5. Effects of adhesive and adhesion on rheological behavior	41
CHAPTER 3. RESEARCH STRATEGY	45
3.1. Introduction	45
3.2. Structure of test materials	45
3.3. Rheological behavior at the SMAS level	47

3.4. The link between system density and rheological characteristics	53
3.5. Temperature and moisture effects	54
3.6. Research process	54
CHAPTER 4. MATERIALS AND METHODS	56
4.1. Materials	56
4.1.1. Specimen preparation	58
4.2. Experimental design	59
4.2.1 The experimental approach	60
4.2.2. Compression and deformation	62
4.2.2.1. Compression	62
4.2.2.2. Deformation	65
4.2.3. Investigating the combined effects of temperature and moisture	67
4.3. Equipment design	72
4.3.1. Affecting loading and measuring deformation	74
4.3.1.1. Compression measurement and control . .	75
4.3.1.2. Deformation measurement and control . .	76
4.3.2. Temperature measurement and control	78
4.3.2.1. Test system temperature measurement and control	79
4.3.2.2. Specimens temperature measurement and control	80
4.3.3. Specimen moisture measurement and control . .	82
4.3.3.1. vapor measurement	82
4.3.3.2. Moisture condition control	84
4.3.4. Computer control and data acquisition system	86

4.3.5. MTS machine control	88
4.4. Experimental test sequence	89
CHAPTER 5. DATA ANALYSIS	91
5.1. Determination of rheological properties	91
5.1.1. Overall strategy for finding elements properties	92
5.1.2. Process for evaluating E1	94
5.1.3. Process for evaluating PMF	97
5.1.4. Process for evaluating K1	100
5.1.5. Process for evaluating E2	102
5.1.6. Process for evaluating K2	103
5.2. Determination of thermo-hygro-effects	107
CHAPTER 6. RESULTS AND DISCUSSION I	113
--Preliminary evaluation of the model--	
6.1. Evaluation of the physical principles of the model	113
6.2. Rheological parameters	116
6.3. General evaluation of the model	118
6.3.1. Prediction of instantaneous behavior	120
6.3.2. Prediction of time dependent behavior	121
6.3.3. The workable range of the model	123
6.3.4. Prediction of environmental effects	123
6.3.5. Predicting initial thickness	125
CHAPTER 7. RESULTS AND DISCUSSION II.	128
--Thermo-hygro rheological behavior--	
7.1. Causes of the rheological behavior of wood furnish materials under compression	128

7.1.1.	Predicted behavior of EE1 for a given cycle	130
7.1.2.	predicted behavior of EPMF for a given loading cycle	131
7.1.3.	Predicted behavior of EV1 for a given loading cycle	133
7.1.4.	Predicted behavior of EE2 and EV2 for a given loading cycle	134
7.1.5.	Predicted behavior of all five elements combined	137
7.2.	Structural effects	141
7.3.	Temperature effects	143
7.4.	Moisture effects	148
7.5.	Energy consumption of rheological behavior	153
CHAPTER 8. CONCLUSIONS AND POSSSIBLE FUTURE RESEARCH . .		156
8.1.	Conclusions of current research	156
8.2.	Possible future research	157
BIBLIOGRAPHY		159
APPENDICES		
APPENDIX I.	Computer programs for operating test system and quantifying rheological properties of materials	167
APPENDIX II.	Five elements properties	189
APPENDIX III.	Regression results	206

LIST OF FIGURES

Figure	Page
2.1. Rheological elements; a) elastic element, b) viscous element, c) plastic element	10
2.2. Burger's four-element model	14
2.3. A typical curve of adhesion development for powder PF to wood system. (from Humphrey and Ren, 1989)	18
2.4. Schematic illustration of particle mat structure (from Suchsland, 1967).	20
2.5. Nine links of an adhesive bond (according to Marra, 1981)	25
2.6. Predicted temperature distribution (from Humphrey, 1989).	33
2.7. Progresssive changes in predicted vertical moisture distribution during hot pressing (from Humphrey, 1989)	37
2.8. Development of wood-adhesive adhesion under different forming temperatures and moisture conditions (from Humphrey and Ren, 1989).	40
2.9. Four stages identified for the analysis of bond strength development (from Ren, 1988) . . .	42
3.1. A typical rheological behavior of a wood composite material under compression.	49
3.2. A five-element rheological model.	49
4.1. The basic principle of the test method.	61
4.2. A typical pressure vs time curve ($P = 4 \text{ MPa}$) . .	63
4.3. Typical deformation vs time curve for the loading curve shown as Fig. 4.2. ($MC = 4 \%$, $T = 120^\circ \text{C}$, $P = 4 \text{ MPa}$)	66
4.4. A typical curves of stress and deformation vs time in the first section (I) of the load control curve.	67

Figure	Page
4.5. A typical temperature vs time curve during pre-treat and test processes. (MC = 10%, target $T = 100^{\circ}\text{C}$, density = 250 kg/M ³).	68
4.6. A typical curve of vapor pressure vs time. ($T = 100^{\circ}\text{C}$, MC = 4%, $P_v = .038\text{ MPa}$)	72
4.7. A miniature thermal pressing system.	74
4.8. The compression control and measurement scheme.	75
4.9. LVDT assembly photograph (LVDT verically assembled besides the press	77
4.10. Test system temperature measurement and control	79
4.11. The temperature measurement system for the specimens.	81
4.12. Vapor pressure measurement arrangement.	83
4.13. The temperature and moisture control system.	86
4.14. Computer control and data collection system	87
4.15. A complete test system	88
5.1. A section (part I) of a typical test curve for deriving rheological constants.	93
5.2. E1 vs density for a typical test condition ($T = 100^{\circ}\text{C}$, MC = 4%).	96
5.3. Initial stage of compression for quantifying PMF	97
5.4. PMF vs density data and an exponentially fit curve for a typical test condition ($T = 100^{\circ}\text{C}$, MC = 4%).	99
5.5. K1 vs density data and an exponentially fit curve for a typical test condition ($T = 100^{\circ}\text{C}$, MC = 4%).	101

Figure	Page
5.6. E2 vs density data and an exponentially fit curve for a typical test condition (T = 100 °C, MC = 4%).	103
5.7. K2 vs density data and an exponentially fit curve for a typical test condition (T = 100 °C, MC = 4%).	105
5.8. One example of the five constants vs density (T = 150 °C, MC = 16%).	106
5.9. The effects of the structure (density) and temperature on EE1	107
5.10. The effects of the structure (density) and moisture on EE1	108
6.1. Predicted thickness versus time curve for a given load curve.	114
6.2. Typical predicted temperature effects on rheological deformation (MC = 4 %, T = 25, 120 °C).	115
6.3. Typical predicted moisture effects on deformation (T = 100 °C, MC = 0, 10 %).	116
6.4. Typical variation of the five elements with density (T = 100 °C, MC = 4%).	117
6.5. Typical variation of E1 under different temperature and moisture conditions	118
6.6. Comparisons between experimental and predicted deformation for a specially designed loading cycle	119
6.7. Comparisons of predicted and experimental instantaneous compression behavior (effect of EE1) for loading curve as Fig. 6.6. shown.	120
6.8. Comparisons between instantaneous relaxation deformation of EE1 and compression deformation of EPMF + EE1 for loading curve as Fig. 6.6. shown.	121
6.9. Predicted and tested time-dependent behaviors for the loading given in Fig.6.6.	122

6.10	Predicted temperature effects on rheological behavior for loading curve shown in Fig. 6.6. (MC = 16 %, T = 25, 100, 120, 150 °C).	124
6.11.	Examples of predicted moisture effects on rheological behavior for the loading curve shown in Fig. 6.6 (T = 100 °C, MC = 0, 4, 10, 16 %).	125
6.12	Prediction of initial thickness from known required final thickness and pressing conditions (P = 6 MPa, T = 100 °C, MC = 0 %).	126
7.1	Curves representing typical rheological behavior of a fiber network under compression (T = 100 °C, MC = 10 %).	129
7.2.	Predicted behavior of EE1 (derived from loading cycle of Fig.7.1, T = 100 °C, MC = 10 %).	131
7.3.	Predicted behavior of EPMF (derived from loading cycle of Fig.7.1, T = 100 °C, MC = 10 %).	132
7.4.	Predicted behavior of EV1 (derived from loading cycle of Fig.7.1, T = 100 °C, MC = 10 %)	134
7.5.	Predicted behavior of EE2 (derived from loading cycle of Fig.7.1, T = 100 °C, MC = 10 %).	135
7.6.	Predicted behavior of EE2/EV2 (derived from loading cycle of Fig.7.1, T = 100 °C, MC = 10 %)	137
7.7.	A reconstructed rheological curve from the behaviors of the five elements (combination of Fig.7.1, 7.2, 7.3, 7.4, 7.5, 7.6).	138
7.8.	Five-element deformation after initial instantaneous deformation (combination of EE1, EPMF, EV1, EE2 and EE2/EV2).	139
7.9.	An example E1 curve varies with specimen's thickness changes during the test.	141

Figure	Page
7.10. EPMF element properties at three different conditions of temperature and moisture content .	143
7.11. Temperature effects on fibers network deformation (MC = 4 %)	144
7.12. The effects of temperature on E1 (at MC = 10) %	145
7.13. The effects of temperature on PMF (at MC = 10 %)	145
7.14. The effects of temperature on K1 (at MC = 10 %)	146
7.15. The effects of temperature on E2 (at MC = 10 %)	146
7.16. The effects of temperature on K2 (at MC = 10 %)	147
7.17. Moisture effects on overall deformation (T = 150 °C, P = 4 MPa)	149
7.18. The effects of moisture conditions on E1 (at T = 150 °C)	149
7.19. The effects of moisture conditions on PMF (at T = 150 °C)	150
7.20. The effects of moisture conditions on K1 (at T = 150 °C)	150
7.21. The effects of moisture conditions on E2 (at T = 150 °C)	151
7.22. The effects of moisture conditions on K2 (at T = 150 °C)	151
7.23. Energy (force * distance) consumption during typical of rheological deformation of the material.	154

LIST OF TABLES

Table	Page
4.1. The range of compressing pressures used in the experiments	65
5.1. How the five elements are effected by density, temperature and moisture content	109
6.1. Appoximate working rangs of the model	123

**THERMO-HYGRO RHEOLOGICAL BEHAVIOR
OF MATERIALS USED IN THE
MANUFACTURE OF WOOD-BASED COMPOSITES**

CHAPTER 1. INTRODUCTION

Thermo-hygro-rheology of wood-adhesive systems used in structural composites plays an important role in determining optimum process schedules for hot pressing. It also affects structures and associated properties of the final products. However, hot pressing is a complicated process. The wood-adhesive system (wood: fibers, flakes or particles; adhesives, and interface) simultaneously and continuously sustains physical and chemical changes. Most of these vary throughout the composite during hot pressing. Rheological behavior (which includes elastic, delayed elastic, viscous, plastic and micro-fractural types of mechanism) varies depending upon the structure and properties of the material and the localized thermodynamic conditions that occur within the product as hot pressing progresses. Temperature and moisture interactively affect these processes.

Both recoverable and permanent types of deformation occur at various stages of the pressing process. The deformations are effected by many physical factors, and the rheological behavior in turn affects the entire physical system (including mechanisms such as heat and moisture transfer, and adhesion).

A fundamental understanding and the ability to make quantitative predictions of the rheological behavior of wood-adhesive systems during hot pressing are increasingly demanded for the development and improvement of high quality products. This is necessary in order to completely understand, effectively design and precisely control both the wood-adhesive system and the hot pressing process.

A study of the rheological behavior of wood-adhesive furnish materials under highly controlled conditions of load, temperature and moisture were conducted to characterize the rheological phenomena of wood composite furnish material. The principal objective of this research was to establish a quantitative understanding of the elastic, plastic, visco and micro-fracture types of behavior of the systems under the ranges of conditions that occur during hot pressing. Such understanding (material models) may be incorporated within simulation models which account for the interaction of rheology, thermodynamics (heat and moisture transfer with phase change) and adhesion in the hot pressing process. The models will ultimately be used as tools for product development and process optimization.

The following constituent objectives were established for the project:

1. To apply the concepts of rheology to study the characteristics of wood composite furnish materials under

diverse thermo-hygro (temperature and adsorbed moisture) condition.

2. To establish a model representing the thermo-hygro-rheological characteristics of the wood furnish materials under compression.

3. To develop new experimental techniques for determining rheological properties (the main focus of the work) and experimentally verifying the thermo-hygro-rheological model.

4. To provide rheological constants of wood composite materials in order to permit simulation of industrial pressing operations (incorporation of rheological behavior in a global three dimensional simulation model).

5. To provide a better understanding of the nature of the thermo-hygro-rheological behavior of wood-adhesive systems during hot pressing.

To realize the objectives of this research, new techniques were developed to offer a direct and automated means for investigating physical phenomena that occur during compression of furnish materials. For this purpose, specimens were tested under a range of accurately controlled steady-state conditions of temperature and moisture content. A specially designed test system capable of applying dynamic force in a highly controlled way were developed. This consisted of a miniature hot press system which was mounted

on a computer controlled servo-hydraulic testing machine. Environments for each test were maintained constant and uniform throughout the specimen by pre-treating it inside the system until the desired conditions of temperature and moisture were achieved. Desired experimental test conditions were maintained constant during the subsequent test cycle by controlling the temperature and water vapor pressure of the atmosphere inside the sealed pressing system.

Experiments were conducted under a range of test conditions (in particular load, temperature and equilibrium moisture content). Information about strain and stress versus time were derived from each selected combination of compression pressure, temperature and moisture content.

Development of the above experimental techniques was the principal objective of the research. However, a non-linear five-element rheological model has also been developed as a preliminary attempt to describe the rheological characteristics of wood-adhesive systems. The rheological constants of materials were therefore determined from the experimental results. The rheological behavior and the effects of temperature and moisture content may then be characterized.

The first part of this thesis reviews rheological concepts and applications, and the main physical aspects of wood composites manufacturing are outlined. Then, the research strategy is fully described. Fundamental issues in

structure analysis, rheological behavior and computational implications during hot pressing are briefly discussed. Efforts to understand and numerically reproduce hygro-thermo-rheological behavior are contemplated. Following the literature and background discussion, the methods for quantifying the rheological constants of composite materials from experimental data are developed. Next the experimental methods, test equipment and materials are described. The fourth part of the thesis concerns data analysis and computation. It is here that rheological constants are actually quantified. Then, the application of the five-element rheological model is considered.

The results of the research may aid in our understanding of the underlying mechanisms that affect rheological behavior of wood furnish materials at each stage during hot pressing. Innovations in experimental techniques and numerical methods of simulation are enabling us to develop effective models and experimental techniques which may prove to be useful tools. This research may motivate further study of the rheological mechanisms that occur during hot pressing.

CHAPTER 2. LITERATURE REVIEW

2.1. Introduction

As one of the important engineering materials, wood composites are receiving increasing attention. The continuous improvement of quality and performance of wood-based composites and the efficient utilization of the wood and other natural fiber materials from the renewable natural resources continuously stimulate the development of wood-based composite materials. This interest has, however, only recently occurred as attempts to study the materials fundamentally. Before that, trial and error methods were used.

Traditional products such as wood composites face many serious demands on its quality and performance. The improvement and development of new wood composite materials require more fundamental understanding and higher engineering performance standards.

Thermo-hygro-rheology is an important aspect for effectively designing and precisely controlling both the structure and manufacturing (hot pressing) processes. However, hot pressing is a complicated process. It involves simultaneous physical and chemical changes within the wood-adhesive systems. Most mechanisms occur differentially throughout the composite during hot pressing and they

directly or indirectly effect the rheological behavior. The main physical processes may be classified into the following main areas (Humphrey, 1982; Humphrey and Bolton, 1985, 1989a):

- thermo-hygro-rheological behavior of the wood-adhesive system (time-dependent densification and stress relaxation).
- adhesive polymerization and adhesion.
- heat and moisture transfer (with phase change) within the wood-adhesive system.

These processes, as well as the structure of the materials, are complex. The intricacy is not only from the component materials but also from their interactions. The natural variability of the structure and properties of wood materials also complicate these interactions. The densification resulting from compression greatly affects the structure and properties of the wood-adhesive system which, in turn, effects the progress of the other mechanisms (such as vapor convection and associated heat transfer).

A number of research workers have studied the physical and chemical phenomena of wood composites related to hot pressing (including for example, Strickler, 1959; Suchsland, 1967; Humphrey and Bolton, 1979; Humphrey, 1982; Smith, 1982; Humphrey and Bolton, 1985; Zavala, 1985; Geimer et al., 1985; Kamke and Casey, 1988b; Ren, 1988; Humphrey and Bolton, 1989a, 1989b; Bolton and Humphrey, 1989a; Humphrey

and Ren, 1989; Hata, 1990a; Wolcott et al., 1989). Most have used empirical methods, which provide good experimental data to support general descriptions of the process. Few, however, attempted to address the problem numerically and thus provide the necessary fundamental understanding (Humphrey, 1982; Kayihan and Benjamin, 1983; Humphrey and Bolton, 1989a, 1989b; Wolcott et al., 1990). A limited number of researchers have worked theoretically, and some hypotheses have been developed (Chow, 1969; Collett, 1972). However, most of them did not include the rheological behavior of materials during hot pressing. None of these have apparently been supported or verified experimentally.

Experimental techniques, numerical methods and computing technologies have enabled viable models and techniques to be developed for studying the wood-adhesive system. Humphrey (1982) pointed out that computer simulation of physical phenomena during hot pressing process (incorporating heat and moisture transfer, adhesion and rheological behavior) may enable us to quantitatively predict the complete physical processes during hot pressing. However, before this may be achieved, each of the three areas (rheological behavior, heat and moisture transfer and adhesion aspects) must be quantified individually.

The rheological behavior of wood-adhesive systems during hot pressing, and the effects that temperature and moisture conditions have on these processes are the main

concern of this literature review and the research to follow. Interactions between thermo-hygro-rheological behavior and the other main physical processes will be only briefly discussed here.

2.2. Rheological behavior of wood composite materials

Wood-adhesive systems are rheological materials: the materials display elastic, viscous and plastic effects. Since wood composites products generally exhibit visco-elastic behavior in service, they are well known as visco-elastic materials, although they also display plastic and micro-fractural behaviors during manufacture.

The principles of rheology and its application to wood-adhesive systems will be discussed in the following sections.

2.2.1. Application of rheological principles

Rheology is a science developed from classical mechanics to study the time-dependent behavior of materials under load. According to the principle of rheology, the behavior of the materials may be represented by the superposition of the behaviors of elastic, plastic and viscous mechanisms (Eirich, 1958; Wang, 1984; Lodge et al., 1985; Bodig and Jayne, 1986; Findley, 1976). These basic

elements can be applied to represent the relationship between stress and strain of the materials (Fig. 2.1).

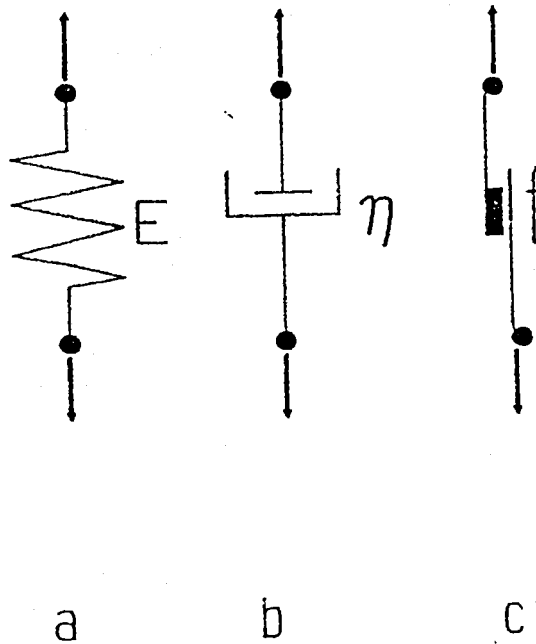


Figure 2.1. Rheological elements; a) elastic element, b) viscous element, c) plastic element.

Elastic elements:

Elastic elements are represented by springs (Fig.2.1.a). An immediate elastic strain response is obtained upon loading. The response is time independent and the energy absorbed by the materials upon deformation is fully recoverable when the applied force is removed and the system returns to its original dimensions (Zhao, 1982). The

chief characteristic of elastic strain therefore is complete reversibility.

Using common notation for the generalized Hooke's law for an isotropic materials subject to an uniaxial loading:

$$\epsilon = \frac{\sigma}{E} \quad (2.1)$$

where, E: coefficient of elasticity.
 σ : stress.
 ϵ : strain.

Hooke's law represents material relationships where time dependency is excluded, whereas all processes occurring in response to an externally applied force are somewhat time dependent. Materials that obey Hooke's law (usually only at low strain levels) are said to be linearly elastic. However, it is entirely possible that a material may behave in a nonlinear elastic fashion (which may be represented by more than one linear spring combined together or by a single nonlinear spring).

Viscous elements:

Viscous elements are represented by dash-pots (Fig. 2.1.b). Materials that obey Newton's law are said to be ideally viscous (Newtonian). Viscous behavior is a time dependent response to external forces (Zhao, 1982).

Applying common notation of Newton's law:

$$\epsilon = \frac{\sigma t}{K} \quad (2.2)$$

where, K: coefficient of viscosity.
t: time.

The energy absorbed by the system is entirely dissipated by non-mechanical (internal) processes and there is no inherent tendency of the material to assume its original dimensions. A relationship between strain and time exists for any particular stress history.

Plastic elements:

Another ideally approximated by many materials in their response to external forces is that of the St. Venant material which is purely plastic (Lu, 1983). Plastic elements are represented by friction blocks (Figure 2.1.c.) where no strain occurs until the applied load exceeds the yield stress of the material. When an externally applied load reaches the yield stress, then high strain will immediately occur.

$$\sigma = f \quad (2.3)$$

where, f: friction stress.

This deformation will remain when load is removed. Plastic strain is defined as time independent although some

time dependent strain is often observed to accompany plastic strain.

Models for the rheological characteristics of a material may, therefore, be established by applying a number of the above basic elements in different arrangements.

A general model for visco-elastic materials:

Several models have been applied to composite materials. Burger's model, the most valid and applicable viscoelastic model, will be discussed here, since it has been used extensively.

Burger's model includes four elements to represent three different types of deformation: elastic, viscous and delayed elastic. Figure 2.2. shows the four-element model.

If the model is analyzed under constant uniaxial loading conditions, it may be simply described by the creep equation (Wang, 1984; Bodig and Jayne, 1986):

$$\epsilon = \sigma * \left(\frac{1}{E1} + \frac{t}{K1} + \frac{1}{E2} \left(1 - e^{-\frac{E2*t}{K2}} \right) \right) \quad (2.4)$$

where, E1: property of elastic element 1.
 E2: property of elastic element 2.
 K1: property of viscous element 1.
 K2: property of viscous element 2.
 t: time.

Burger's model has been used to express a diverse range of types of visco-elastic material behavior (Findley, 1976). Its has also been applied to wood composites (for example, Bodig and Jayne, 1986; Smulski and Ifiu, 1987; Smulski, 1989; Tang and Simpson, 1990).

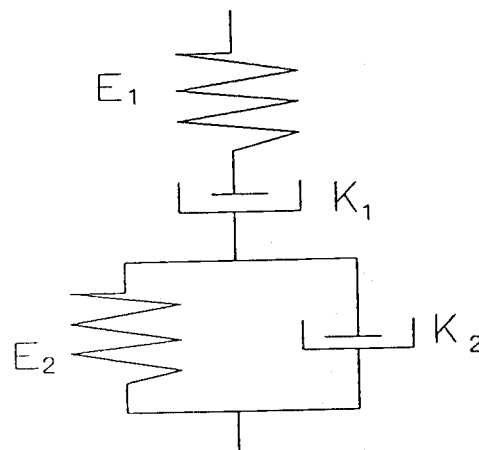


Figure 2.2. Burger's four-element model.

2.2.2. Rheological behavior of wood composites

Several studies involving the mechanical behavior of wood composite materials during manufacturing have been reported (Strickler, 1959; Suchsland, 1967; Bolton and Humphrey, 1989c; Smulski, 1989; Wolcott et al., 1990; Hata,

1990a). However, visco-elastic behavior has been given relatively little in-depth attention.

Since Kunesh (1961) first pointed out that hot pressed wood materials behave inelastically, several visco-elastic theories have been applied to wood composite manufacturing (Laufenburg, 1983; Kelley et al., 1987; Wolcott et al., 1990). However, most rheological models were developed for studying homogeneous solid materials under small deformation ranges or for studying materials in the liquid state. Their direct application to wood composites during hot pressing is limited by the fact that the relatively large deformation causes dramatic change in the structure and properties of wood-adhesive system.

Clearly, the rheological behavior of wood composites during hot pressing depends on the structure and behavior of the component materials (wood, adhesive and interface) and their interaction. External load and internal stress distribution and relocation; densification and partial fracture of the wood elements (while they are compressed, bent and twisted); intensive heat and moisture transfer; migration and penetration of adhesive as well as the development of adhesion; all these physical changes influence the rheological behavior of the system.

The rheological behavior of the materials therefore should be investigated not only as a system, but also in terms of the properties and behavior of the components.

2.2.2.1. Rheological behavior of wood materials

Cell wall compression theory has recently been studied by Kasal (1989). Wolcott and Kamke (1990) applied the theories of cellular materials and the visco-elasticity theory of amorphous polymers of Ferry (1980) in their study of compression of wood materials. These projects endeavored to directly apply and transform theories for other materials to wood composites. The structure of the wood composite and its effects on plastic deformation were not declared clearly. As stated earlier, however, it also involved (in addition to pure plastic deformation) micro-fracture and spatial rearrangement of wood elements. Since the above mechanical models oversimplified the causes of relative large deformation during hot pressing, their further refinement is limited.

2.2.2.2. Rheological behavior of adhesives

Rheological theory of adhesives must properly account for cohesion and adhesion (Marra, 1981; Ryutoku et al., 1990). A Torsional Braid Analysis (TBA) technique was developed by Steiner and Warren (1981, 1987) to study the rheology of adhesives as they cure. This was the first research which clearly attempted to study the rheological

properties of adhesives beyond the gelation stage which can be used in wood composites; even although these authors only considered changes in modulus of rigidity. However, the experimental conditions were obviously different from those that apply within composites during hot pressing. It did not include the effects of wood furnish materials and the variation of moisture content. Both of the above may significantly effect adhesion at the micro-structure level (Humphrey and Ren, 1989; Ren, 1988).

Humphrey and Ren (1989) appear to be first to directly study the isothermal adhesion kinetics of adhesive to wood bonds. Figure 2.3 shows an adhesion development curve for a powder phenolic to wood system. At the early stages of bond formation the adhesion strength appeared to depend on the instantaneous viscosity of the adhesive. As polymerization progressed, the adhesion appeared to increase.

The case of cohesion of adhesive of identical chemistry and molecular structure provides a basis for examining the rheological aspects of adhesive behavior (such as degree of polymerized and adsorption interdiffusion processes). The only important restraints that limit cohesion-type bonding concern the rheological character of the adhesive (Kaelble, 1971; Ren and Humphrey, 1990).

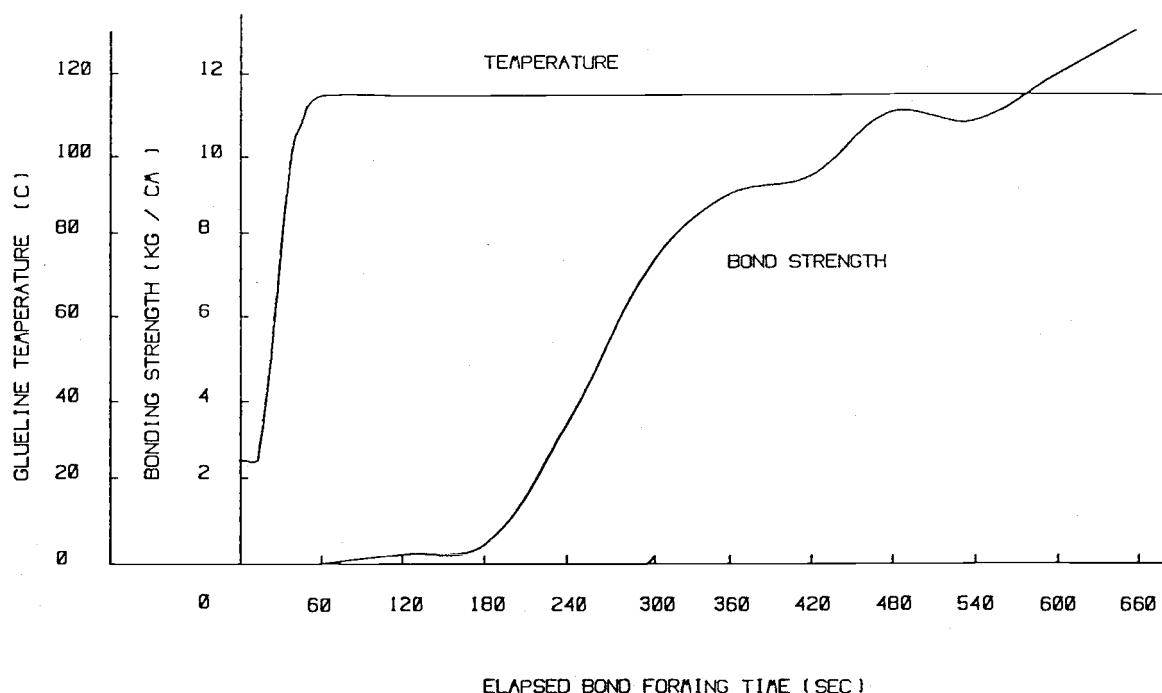


Figure 2.3. A typical curve of adhesion development for powder PF to wood system (from Humphrey and Ren, 1988).

Clearly, the area of wood-adhesive interactions and the flow processes associated with bond development and the ability to resist stress is highly complex. This is beyond the scope of the present work but should, in this authors' opinion, be the subject of much further study.

2.3. Effects of wood composite's structure on rheological behavior

This section concerns the structures of wood-adhesive systems and their effects on behavior during hot pressing. Changes in structure (for instance, fiber orientation,

element structures or variation) of wood composites that occur during hot pressing have attracted little attention; most wood composites have been designed by trial-and-error methods without much prior knowledge of how their structure affects their behavior during processing. Once certain raw material structures had been found to yield products with moderately useful properties, they have been used with little further thought towards correction or improvement. This situation has changed somewhat recently with the application of scientific techniques. However, the progressive change in structure that occurs in composite materials during hot pressing is still not very refined.

Most reported methods for studying and analyzing the system during hot pressing processes were based on some idealized and simplified structure of the materials; where wood elements were allocated linear mechanical properties, uniform physical properties and stable geometric structures. These were placed in a non-continuous polymerized adhesive matrix, and adhesion between the wood and adhesive had been assumed to provide a joint which perfectly transferred stress (Strickler, 1959; Suchsland, 1967; Delollis, 1968; Humphrey, 1982; Zavala, 1985; Ren, 1988; Wolcott et al., 1990). For instance, many researchers preferred to simplify the structure to the wood and adhesive and assumed uniformly distributed porosity (Suchsland, 1967; Harless et al., 1987; Kelley et al., 1987; Wolcott et al., 1990).

The concept of simplified structure neglected that large deformations occurs along with a range of physical and chemical mechanisms. Although some ideal structural model may simplify the research work and create the opportunity to directly apply the theories from other areas, it obviously restricts further analysis.

A description of particleboard in terms of a statistical model of its structural variation was reported (Suchsland, 1967) (Fig.2.4).

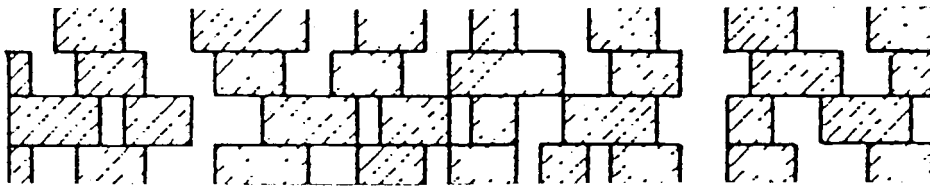


Figure. 2.4. Schematic illustration of particle mat structure (from Suchsland, 1967).

The real structure (macro and micro) of wood-based composites are quite different from those over-simplified models (Mataki et al., 1972; Mark, 1972). Non-uniform spatial distribution of component materials is a general

characteristic of wood composite structures (Humphrey, 1982). For instance, wood composites are formed from wood furnish materials (particles, veneers, and fibers) which are only partially adhesive coated.

Sources of randomized structural variability include: fracture, distortion and overlap of fibers or layers, adhesive extraction or over-penetration, non-satisfied phase contact, etc. (Collett, 1970; Humphrey, 1982; Geimer et al., 1985; Bolton and Humphrey, 1988). Progressive changes in structure may result from differential consolidation through a composite's thickness. Such density profiles are due to progressive migration of heat and moisture as the press closes.

2.3.1. Effects of wood furnish material structures

Two main sources of random variability may be identified in the composites; these are associated first with the variability of the wood material, and secondly with the geometry and orientation of the wood elements in the consolidated composites. If wood-based composites are to be considered engineering materials, then understanding of their micro-structure will be necessary during both design and manufacturing.

The effects of wood structure and properties on composite structure and properties have been investigated by

too many workers to be cited individually; a selection includes (Kollman et al., 1975; Liang, 1981; Rosen, 1979; Strickler 1959; Siau, 1984; Skarr, 1972; Humphrey, 1982; Stewart, 1979; Stanish, 1986; Wengent and Mitchell, 1979; Marian, 1966; Chow, 1969; Clay and Kramer, 1988; Marra, 1981). The following research areas may be identified:

- wood structure and physical properties
- wood chemical properties
- wood surface energy and wettability
- wood properties affecting heat and mass transfer in the vicinity of the bond (permeability, hygroscopicity, conductivity, void volume etc.).
- orientation of wood elements in the composite.
- moisture content and temperature of wood.

Unfortunately, there appears to be very few reports concerning how wood composite structures change during the hot pressing process and how these effect the composite formation process and properties (Suchsland, 1967; Humphrey, 1982). Some of the above factors will be briefly considered in turn.

It is clear that wood structure and the orientation of components within both solid wood and composites has an effect on the performance of wood-adhesive systems. Upon compression of composite mats, densification will occur. Many anatomical characteristics of the interacting surfaces will then affect the nature of the compression and adhesion

process that may follow. These are likely to vary in response to general characteristics associated with species (cell wall structure) and such factors as the anatomical differences between earlywood and latewood (Clay and Kramer, 1988). For example, latewood generally has superior mechanical properties, but it is contended that the higher density (cell wall thickness) of this material results in more variation in swelling and shrinkage. This may lead to high stresses on the micro-structures both during hot pressing and in service.

The surface characteristics of wood furnish material directly influence the internal stress distribution. It also effects adhesive distribution and subsequent strength of adhesives bonds (Chow, 1969; Collett, 1972; Kelley, 1983; Wellons, 1980; Young, 1982). Earlywood exhibits good accessibility to adhesive mainly due to the larger voids of the fiber lumen. This generates a larger active surface area for adhesion but larger deformation (strain) is necessary to achieve a given density and interfacial contact.

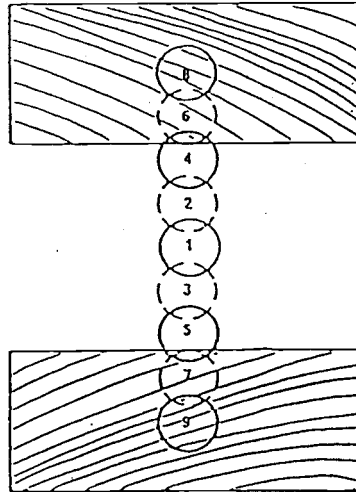
In order to improve and design wood composite structures, quantitative description of structure and associated properties is more valuable than a statistical descriptive model. Some researchers have tried to link the mechanical behavior of composites to the characteristics of cellulose and lignin (Mark, 1972; Wolcott et al., 1990). The application of these theories during hot pressing has not

been completed, although such approaches may well have considerable merit.

2.3.2. Effects of the adhesive matrix structure

Marra (1981) likened the adhesive bond to a chain with nine links. Each of the nine links can be associated with specific types of behavior that affect both bonding and final product performance (see Figure 2.5.).

In Marra's model, links 8 and 9 represent the physical, chemical, and anatomical properties of wood; links 6 and 7 represent the nature of the subsurface of the zone, while links 4 and 5 represent the interfacial area where adhesion forces of wood and adhesive are supposed to engage one another. Links 2 and 3 are the adhesive layer that could be most strongly influenced by the chemical and physical properties of the wood. The center link reflects adhesive cohesion. Mechanical properties may, then, result from the behavior of any link in this hypothetical chain. This structural model demonstrates the wood-adhesive adhesion structure. However, it was not experimentally verified and does not provide any real data about how the structure progressively develops.



- Link 1: The adhesive film.
 Links 2 and 3: Intra-adhesive boundary layer, strongly influenced by the adherent.
 Links 4 and 5: Adhesive-adherent interface, site of adhesion forces.
 links 6 and 7: Adherent subsurface, partially fractured in preparing the surface.
 links 8 and 9: Adherent proper.

Figure 2.5. Nine links of an adhesive bond (according to Marra, 1981)

The molecular structure of most adhesives continuously changes with time and temperature from a linear, or partially cross-linked (pre-polymerized) form to a fully cured three-dimensional structure. The adhesive's properties therefore vary during hot pressing. Such variations lead to the generation of three-dimensional networks throughout the composite (Kelley, 1983; Nelson, 1974; Gent and Hamed, 1981; Kyokong et al. 1986; Rice, 1981). However, the adhesive structure is not a continuous (inter-connected) matrix

within wood composites since the quantity of adhesive is not normally sufficient to cover the total surface area of the wood furnish material. Furthermore, conventional formation techniques are not precisely controlled, and the interfacial structure of the wood composite is non-uniform (Humphrey, 1982; Ren and Humphrey, 1990).

2.3.3. Effects of interfacial structure

The interface is not only a geometrical boundary between the wood material and adhesive, but also between adjacent materials' elements. The interface is influenced by physical-chemical processes taking place during the interaction of wood and adhesive at the stage of composite formation (such as inter-diffusion of adhesive and other fluids, selective sorption, and catalytic effects). Furthermore, the effects of heat and moisture on the material influences stress levels at the interfaces; the later is due on part to dimensional changes of the cell wall that occur with moisture changes. (Castle and Watts, 1989; Ren and Humphrey, 1990).

The interfacial properties may effect hygro-thermo-mechanical compatibility of the components. The physical-chemical effects define phase contact completeness, and the nature, number and strength of physical and chemical bonds which are generated.

Reduction and elimination of the interfacial imperfections can be directly associated with the processes of internal stress relaxation (Kelley et al., 1987). Such effects may be of critical importance in the adhesion mechanisms in wood based composites and paper.

Techniques to fully analyze the structure of wood-adhesive interfaces are, unfortunately, still beyond our knowledge.

2.4. Effects of temperature and moisture

Heat and moisture affect the mechanical properties of the system, and this results in variations of structure during manufacturing, and in variations in service performance. Simultaneous heat and moisture transfer results in transient gradients of temperature, within-void vapor pressure, cell-wall moisture content, adhesive polymerization, and wood furnish material softness during hot pressing.

Springer (1988) suggested three steps for studying the hygro-thermo effects of materials. First, the distribution of temperature and moisture content inside the material are calculated. This work in the wood composite area has been tackled by Humphrey and his co-workers (Humphrey, 1982; Humphrey and Bolton, 1989a; Siau, 1984; Bowen, 1970; Hata, 1990). Second, from the known temperature and moisture

conditions, the hygro-thermal deformation and stress are calculated. Third, changes in properties and performance due to temperature and moisture are determined. Little research in the later two steps has been conducted on wood composites manufacturing.

A number of theories have been developed for a better understanding the mechanism of heat and moisture transfer both in solid wood and in wood-based composites. According to the reported research, temperature and moisture vary with time in a predicted manner (Humphrey, 1982). Heat is conducted into the system from platens that attain temperatures in the range of 70 to 230 °C. Both conductive and convective heat transfer occurs inside the system. Initially, moisture in the system (bound in the cell walls and associated with the adhesives) near the heated platens vaporizes, the partial pressure of water vapor increases in the outer portions of the porous system, and the vapor convects vertically to the center and horizontally to the edges of the composite. Examples of such investigations are quite numerous and included those reported by Humphrey (1982), Humphrey and Bolton (1989a), Skaar (1972, 1981), Siau (1979, 1980), Rosen (1979), Bowen (1970), Kamke and Casey (1988a).

However, the thermo-hygro effects on rheological behavior of the wood-adhesive system have not been quantitatively and directly studied until recently.

In the consideration of composite materials during hot pressing, several parameters should be considered (Humphrey, 1982, Humphrey and Bolton 1985, 1989a, Bolton and Humphrey, 1989c; Shout and Summerscales, 1981; Springer, 1988; Wolcott et al., 1990) as following:

- a. temperature inside the material as functions of position and time.
- b. moisture concentration inside the material as functions of position and time.
- c. total amount of moisture inside the materials as functions of time.
- d. moisture and temperature effects on stress-strain distribution inside the material as functions of position and time.
- e. rheological behavior of the material as a function of time.

Variations of each of the above variables that occur within the composite should be studied because they reflect the thermo-hygro conditions under which the composite structure is formed.

Since the theories governing the thermo-hygro effects on composite materials has not been completely developed, Tsai (1988) assumed that micromechanical theories remain valid for the range of hygrothermal conditions that occur in composites, that laminated plate theory and failure criteria remain valid and only that the stiffness and strength

properties are effected. These assumptions may be used to simplify the modeling of temperature and moisture effects on engineering composite application. Since the mechanics which developed from general condition can be used for certain range of hygrothermal change, many theories from other research may also be applied to the thermo-hygro effects of composites. Micromechanics is used here because it can reduce the number of variables. However, Tsai's suggestion was developed for mainly with in-service behavior of composites in mind, rather than for the manufacturing process.

The provision of numerical models which account fundamentally for the contributory mechanism during hot pressing is very important. Several researchers have attempted to simulate the system using numerical methods of integration. Carruthers (1959) attempted to model temperature change or rate of heat penetration in particleboard. Bowen (1970) applied a two dimensional model to describe heat transfer in particleboard pressing, but he did not directly calculate convective heat transfer; this limited his model. Kayihan and Johnson (1983) developed a model which considered both heat and moisture flow theoretically. However, it was a one dimensional model and was short of rigorous physical analysis. Some relatively empirical research involving steam injection has also been reported recently (Hata, 1990).

Those works may be represented by one successful and realistic three-dimensional model which was established by Humphrey (1982) for heat and moisture transfer during hot pressing.

In this model, the physical dimensions of the composite while in the press are divided into small increments of length. Simulation progresses by considering interactions between these defined regions for small time increments. If the time increments are sufficiently small, steady-state conditions of temperature and moisture as well as vapor pressure may be approximated, and simple equations may be used to calculate flow of energy and vapor during each increment. Updating the status of all regions at the end of each time increment enables simulation to proceed. The updating procedure involves the calculation of new equilibrium conditions of temperature, adsorbed moisture content, vapor pressure and relative humidity for each region.

This model describes the heat and moisture transfer which takes place when a mattress of wood particles or fibers is hot pressed. It produces three dimensional distributions of temperature, absorbed moisture content, and within void vapor pressure and relative humidity. The physics underlying the above mentioned researches on heat and moisture transfer will be briefly outlined in the following sections.

2.4.1. Temperature effects

Heat may be transferred in wood composite materials in three ways: conduction, convection and radiation (Humphrey, 1982; Humphrey and Bolton, 1989a, 1989b; Kamke and Casey, 1988a; Kollman et al., 1975). Heat conduction and convection are thought to play a major role in the hot pressing of wood composites; radiation is not thought to be significant.

During hot pressing, heat is transferred from the press platens to the center of the board until the temperature at the center of the board approaches that of the platens. On the other hand, when the temperature increases, differences between the board and outside temperature increase and some (usually relatively little) heat is transferred from the edge of the board to the atmosphere by Newtonian cooling. Far greater amounts of heat and water are lost through the edges due to the escape of water vapor. The unsteady-state heat transfer is therefore in three dimensions and is a function of time and the material's structure. A number of equations have been developed in this area. Most of them have limited applicability and are not conceptually difficult to derive (Welty et al., 1976; Zhang, 1983).

The rate of conductive heat transfer clearly depends on the magnitude of the temperature gradient and the thermal conductivity coefficient of the materials (Humphrey, 1982; Shao, 1989; Hata, 1990). Primary among the material

properties which effect conductivity are density, moisture content and the structure of the material (which effects the conductive pathways).

The combination of thermodynamic processes operative within wood-adhesive system during pressing are similar in their fundamental nature to those in solid wood during drying, but their variation is more complex since the structure continuously changes during pressing. The steepness of gradients and the resultant hostility of the environment within panels make rigorous understanding of the processes all the more important.

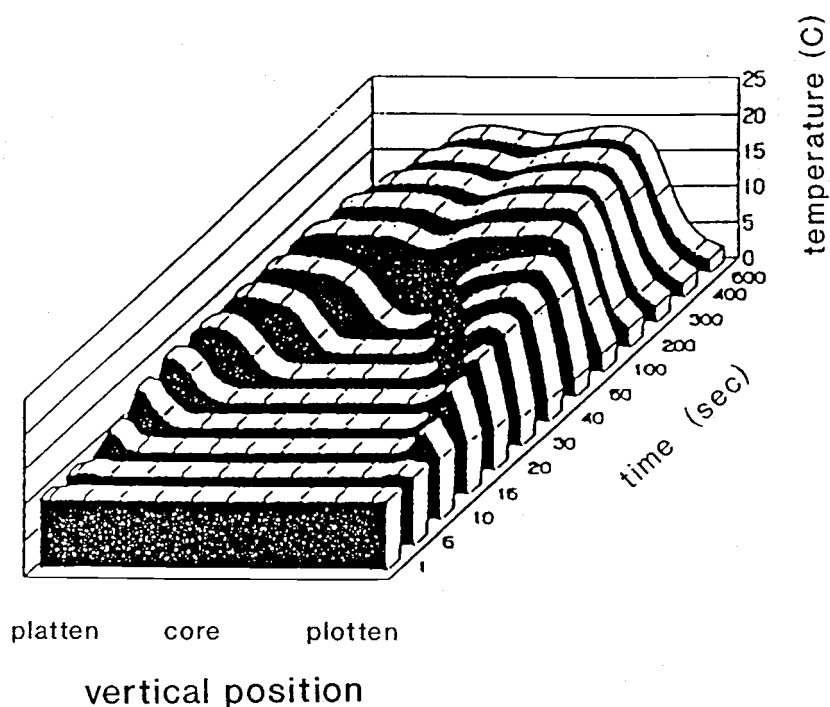


Figure 2.6. Predicted temperature distribution (from Humphrey, 1989).

Figure 2.6. shows a typical computer simulated temperature distribution within an industrial panel in three dimensions. With time increases, the vertical position temperature distribution continuously varies until equal to the platen temperature.

Heat may influence the mechanical behavior due to the glass transition temperature (T_g) of the component materials, effects of moisture condition, and adhesive polymerization. Wood composites contain polymeric component materials. The effect of heat on the mechanical behavior, therefore, may be described by the equilibrium principle of temperature and time. This approach was originally developed for chemical engineering and the polymer industry. Mathematical applications of this principle, such as the Williams-Landel-Ferry (WLF) equation, which is popular in the polymer composites areas may possibly be applied here (Ferry, 1980; Seferis and Nicolais, 1983; Wolcott et al., 1990, Nelson et al., 1974). Wolcott and Kamke (1990) appear to be first to apply the WLF equation in the wood composite area by trying to quantify the effects of temperature on the viscoelastic behavior of the materials.

Since the rate of temperature rise will determine the adhesive polymerization rate and softness of the structure, both the heat and the associated adhesion influence the rheological behavior of the system. The adhesive effects will be discussed later.

2.4.2. Moisture effects

During the early stages of research, a number of workers noted that overall furnish moisture content effects physical properties of composites (Smith, 1982; Suchsland, 1967; Bolton and Humphrey, 1989b; Liang, 1981; Jr. Nelson, 1986; Simpson, 1980; Siau, 1980; Skarr, 1981). Strickler (1959) pointed out that the distribution of moisture affects layer density, modulus of rupture and elasticity, internal bond strength, and dimensional stability of particleboard.

The internal stresses and associated local densification are clearly associated with movement of water within the materials during pressing (Suchsland, 1967; Zavalar, 1986). Some investigations (Humphrey and Ren, 1989, Ren, 1988) have suggested that tensile strength of wood composites is maximized when they are formed at steady-state of moisture contents between 8 to 10%.

It should also be remembered that localized moisture values vary greatly within such panels during pressing, so initial moisture values do not provide any fundamental information upon which the processes may be characterized (Humphrey, 1982).

In general terms, free water evaporates from liquid surfaces as energy is applied. As the moisture content of a system of wetted wood materials decreases below fiber

saturation point the attraction between the wood and the adsorbed water molecules increases (Siau, 1980; Skarr, 1972; Moore, 1983; Pimentel and Spratly, 1969), and so does the energy needed to remove them. In the pressing of most wood composites, phase change and subsequent convection of water vapor contributes more than conduction to the rapid transfer of heat energy into the board center. This has been asserted by a number of workers (Strikler, 1959; Siau, 1979) and confirmed by Humphrey (1982, 1989).

The rate at which moisture moves through the composite is clearly a function of energy input, the energy associated with the change of phase of adsorbed water into water vapor, and subsequent diffusion and re-adsorption of the vapor (Skarr, 1972; Humphrey, 1982). This diffusion of water vapor leads to the re-distribution of adsorbed water within the system and the development of gradients of moisture content in the three dimensions of the composite. Moisture will be lost from the edges of the composite where only the partial pressure of the water vapor in the surrounding atmosphere. Escape of vapor from the surfaces of the composite in the press will be prevented by the presence of the platens.

Moisture movement from one location to another therefore relies upon localized gradients of temperature and moisture content, together with the hygroscopicity and permeability of the materials.

A typical simulated moisture distribution within an industrial panel in three dimensions is shown as Figure.2.7. With the time increases, the vertical position moisture content also varies.

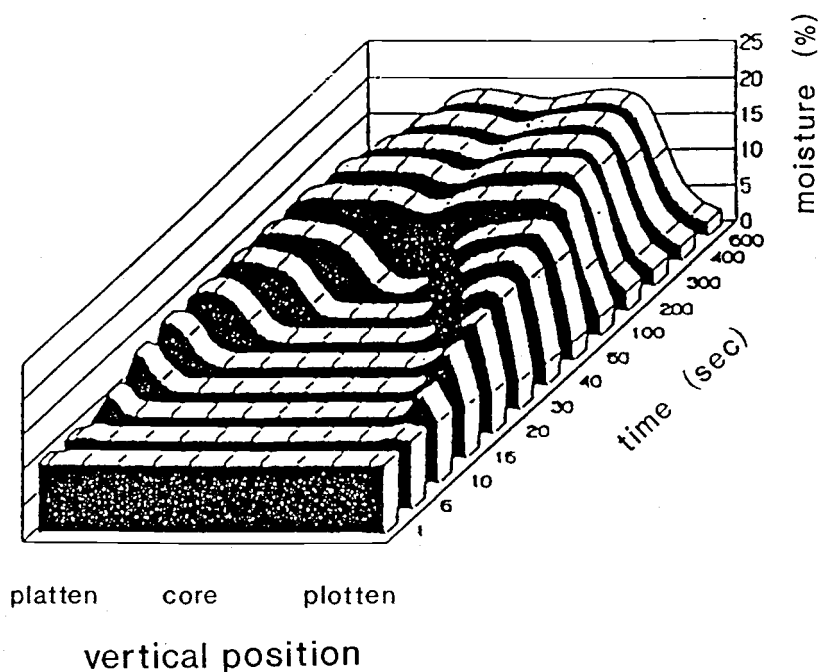


Figure.2.7. Progressive changes in predicted vertical moisture distribution during hot pressing (from Humphrey, 1989).

The effects of moisture on mechanical behavior during the hot pressing is an important factor. Unfortunately, no report about the moisture effects on the rheological behavior of wood-adhesive systems during hot pressing can be found.

2.4.3. Effects of temperature and moisture on the rheological and bonding behavior of adhesives

A brief and preliminary review of the effects of localized temperature and moisture conditions on the behavior of adhesive is discussed in this section - although it is not the main focus of the present work.

As would be expected for a thermosetting adhesive, the influence of temperature on the development of bond strength is significant, especially in the initial stages of the bonding formation. The viscosity of many adhesives is clearly effected by their temperature. The higher the temperature the lower the viscosity. This is providing that polymerization does not overcome this effect. Such changes in the rheological properties of adhesives while within composites during hot pressing are still not well understood (Anderson et al., 1977; Humphrey and Bolton, 1979, 1985; Steiner and Warren, 1981; Brady and Kamke, 1987; Steiner and Warren, 1987; Humphrey and Ren, 1989; Ren and Humphrey, 1990). When all other factors (such as moisture content) are held constant, bond strength development is a function of temperature and forming time (Kaelble et al., 1971; Anderson et al., 1977; Ren, 1988).

$$S = f(T, t) \quad (2.5)$$

Where: S = accumulated strength (Pa)
 T = forming temperature (°C)
 t = forming time (sec)

Indeed, for many adhesive systems investigated, it has been found that bond strength follows the Arrhenious relationship (when the log of isothermal strength development rate is proportional to absolute temperature (Humphrey and Ren, 1989)).

With care, the principle of superposition (and numerical methods) may be used to predict the development of bond strength under different temperature conditions. This concept also can be used when attempting to model the unsteady-state temperature and moisture conditions that occur during pressing (as described in sections above).

The combined influences of both moisture content and temperature on the development of adhesion is also significant (Ren, 1988). Recent studies reported that the moisture content of 10% produced higher bonding rates in wood-adhesive adhesion than those at 4% and 16% in an actual controlled steady-state condition of moisture (Humphrey and Ren, 1989). Wellons (1982) pointed out that the moisture in wood determines glueline moisture content and thus effects both the depth of adhesive penetration and the curing time of aqueous adhesives. Figure 2.8. shows the development of adhesion under different moisture conditions (4, 10, and 16%) and temperatures of 115 °C and 110 °C. In this work, both temperatures and moisture content clearly affected the early stages of adhesion. This suggests there is a range of

moisture values which are optimum for the rapid initiation of adhesion.

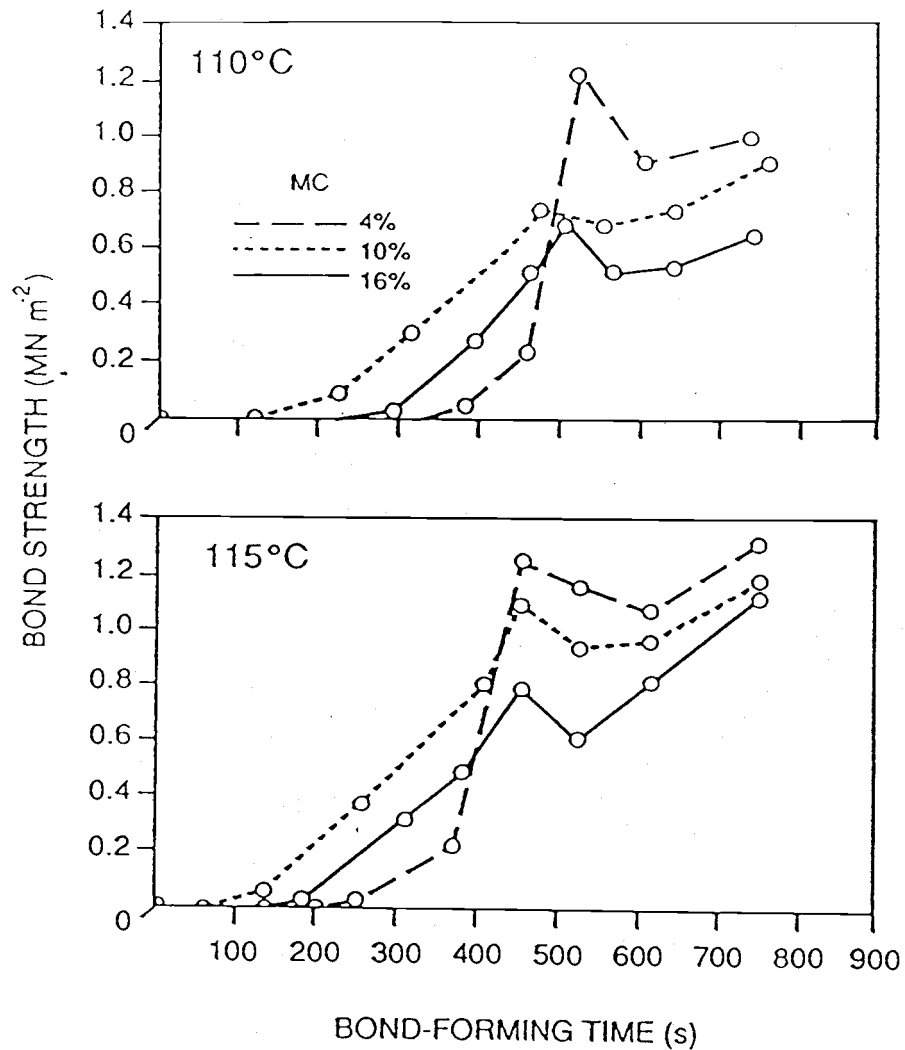


Figure 2.8. Development of wood-adhesive adhesion under different forming temperatures and moisture conditions (from Humphrey and Ren, 1989).

The effects of adhesive and adhesion on rheological behavior during pressing will be reviewed in the following section.

2.5. Effects of adhesive and adhesion on rheological behavior

Some rheological characteristics of adhesives and their interaction with the conditions that occur during hot pressing have been observed (Steiner and Warren, 1981; Ren and Humphrey, 1990). However, because the contribution of the rheological behavior of the adhesive to the behavior of wood-adhesive system is complex, the behavior of adhesive during hot pressing has not been understood clearly.

The rheological characteristics of adhesive continuously change during hot pressing while the adhesive polymerizes from linear molecules to a three dimensional network. The behavior of adhesive and its effects on rheological behavior of wood-adhesive system play varying roles at different stages during the hot pressing process. By dividing adhesion development that occur during hot pressing into four stages, A, B, C and D as in Figure 2.9, the rheological behavior of the adhesive and its effects on the behavior of wood-adhesive system may be analyzed based on the different stages.

Stage "A" may correspond to the adhesive melting, squeezing and compressing, migrating and penetrating within the system. Wood-adhesive adhesion is negligible and only the result of viscous restraint. Since at this stage, true

adhesion does not take place, cohesive forces hold adjacent molecules of adhesive together.

Stage "B" may be the result of condensation reactions to form larger molecules and small networks. The viscosity of the adhesive is likely to increase rapidly but it still may be regarded as a fluid. The adhesive is soft and can become somewhat thermoplastic-like on heating. Its effects on the system therefore, is relatively small and may be omitted because of its low resistance to external load.

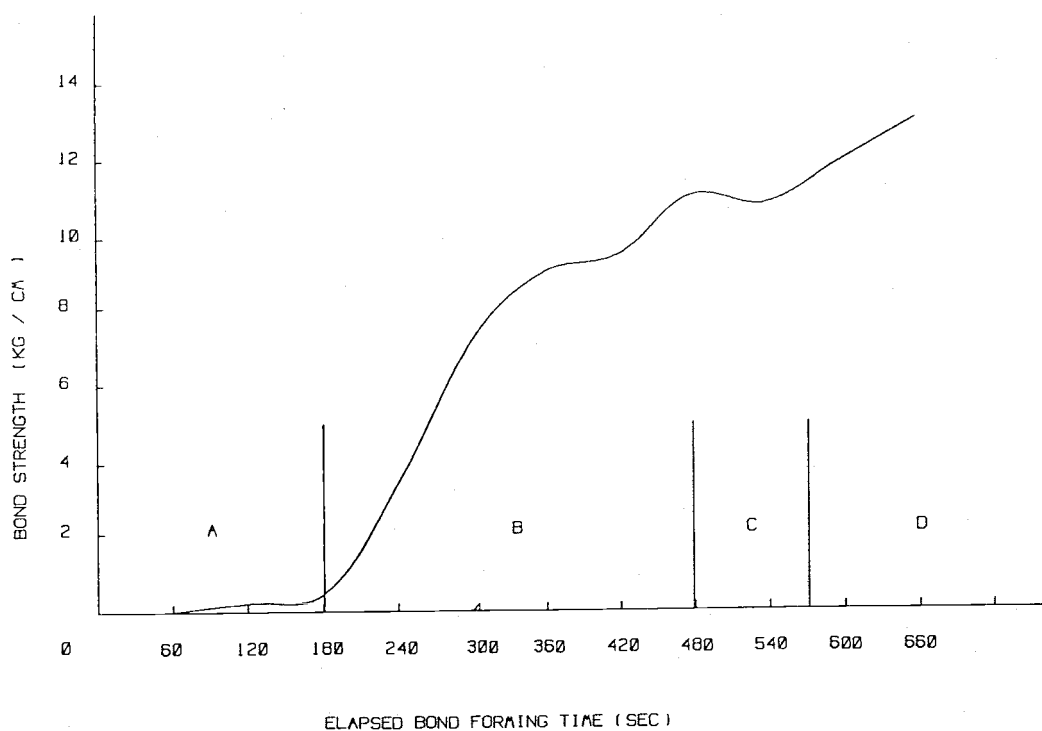


Figure 2.9. Four stages identified for the analysis of bond strength development (Ren, 1988).

The stage "C" corresponds to a slow development or reduction in adhesion. The cause of this discontinuity is not known. It may be that the adhesive begins to form a three-dimensional network where the initial or temporary molecular bonds are broken and rearranged. The viscosity of the adhesive may change relatively little during this stage.

Stage "D" of adhesion is well developed. The adhesive has reached a high level of chain-extension cross-linking reactions of the thermosetting adhesives results in a fully cured system. The deformation of the systems (both creep and relaxation), may be restricted by the fully cured non-continuous adhesive matrix. Since the adhesive matrix is non-uniformly distributed through the composite, localized micro-fracture may occur due to localized internal stress concentrations. The residual water vapor pressure inside the composite also may cause or increase this micro-fracture of wood-adhesive system upon press opening.

The whiskers of polymer (phenolic) drawn from the surfaces of adhesive-wood bond during the tension test at elevated temperature were observed (Ren and Humphrey, 1990). This suggests that the adhesive is deformable under such elevated temperatures and does display some thermo-plastic characteristics. There were short adhesive whiskers distributed non-continuously over the surface. Changes in viscosity of the adhesive would, most likely, affect the relative importance of adhesion deformation in the polymer.

According to the above discussions, the rheological behavior of wood composites during hot pressing clearly depends on the structure and behavior of the component elements (wood, adhesive and interface), environmental conditions, and their interaction.

CHAPTER 3. RESEARCH STRATEGY

3.1. Introduction

The present research concentrates on an unified structure to study the rheological characteristics of the materials more than that of specific industrial products. In this way, the results may be generally useful for both scientific investigation and broad industrial application.

The study is focused on the combined rheological characteristics of wood, adhesive and interface during hot pressing. In future studies, the functions of the component materials within wood composites during this process and their relationship with other physical processes during pressing may be studied.

It is therefore an objective of the present work to develop the techniques and rheological models to numerically evaluate the rheological characteristics of furnish material behavior under the diverse conditions that occur during the hot pressing. Physical descriptions may be established based on the theoretical analysis and experimental results.

3.2. Structure of test materials

Since most deformation occurs within the wood fraction of the composite materials (not within the adhesive and

interfaces), the wood components dominate the rheological behavior of the whole system during hot pressing.

Rheological behavior of the other components within the system are thought to be relatively insignificant compared with the behavior of wood furnish materials -- especially during the initial stages of hot pressing. At this stage, the contribution of the adhesive rheological behavior and polymerization is likely to be small.

Therefore, the rheological behavior of wood-adhesive system during hot pressing may be then approximately described by the behavior of wood furnish materials in a certain circumstances. The present research, consequently, is focused on the mechanism of wood furnish materials behavior during compression. The effects of the adhesive and interface on the rheological behavior of wood-adhesive system during hot pressing have been assumed to be relatively minor factors in initial stage of hot pressing process.

This research is conducted on samples which fall into the semi-macro structural (SMAS) level (dimensions lie between the micro-structure and industrial products). A study at the SMAS level may establish some connections between studies which based on micro-structure and macro-structure so that the research results may be useful for both industrial application and scientific analysis.

3.3. Rheological behavior at the SMAS level

When an external force is applied to a network of fibers or flakes, stress is transferred within the system through contact points of varying effective interfacial area. Stress is not therefore transferred through the network uniformly or continuously. Stresses which are transferred through this effective interfacial area may be called the effective stresses. The concept of the effective stress and effective interfacial area reflects the structure, property and mechanical response of wood composites based on their micro-structure. This concept may also be used to represent the material's "memory" of its history of behavior sustained during manufacture.

Under each applied force condition, the localized micro-structure of wood-based composites leads to a diversity of internal stresses. The variation of the effective interfacial area causes the variation of the effective stress:

$$\sigma_i = \frac{F}{S_i} \quad (3.1)$$

where: F: applied force, (N)
 S: effective interfacial area, (M²)
 σ : effective stress, (Pa).
 i: position within the board.

Consequently, if the localized strength of materials is less than the effective stress, high levels of localized deformation occur. Localized effective interfacial area is

partially or completely reconstructed. Especially at the initial stages of hot pressing, the effective interfacial area is relatively small and the localized concentrated effective stress may be enormously larger than the externally applied load. Plastic deformation may be partly caused by localized micro-structure fracture but large part due to material relocation.

With the densification, the effective interfacial area is rapidly increased and the effective stress is continuously redistributed. The effective stress may subsequently level off until it approaches the value of external stress. In other words, the effect of external load is shared by more and more of the components within the composite as the density increases. Localized micro-fracture and the quantity of micro-structural relocation are reduced. The component materials begin to act together as an united (composite) material which consists of the behavior of wood, adhesive and interface. The effects of this sequence on the rheological characteristics of wood-adhesive system are outlined in sections to follow.

Figure 3.1. represents the typical rheological behavior of a wood composite material under compression.

Rheological behavior may therefore, be classified into four different sources of strain (plastic and micro-fracture, elastic, viscous, and delayed elastic). A five-

element rheological model has been established to describe these types of behavior (Figure 3.2).

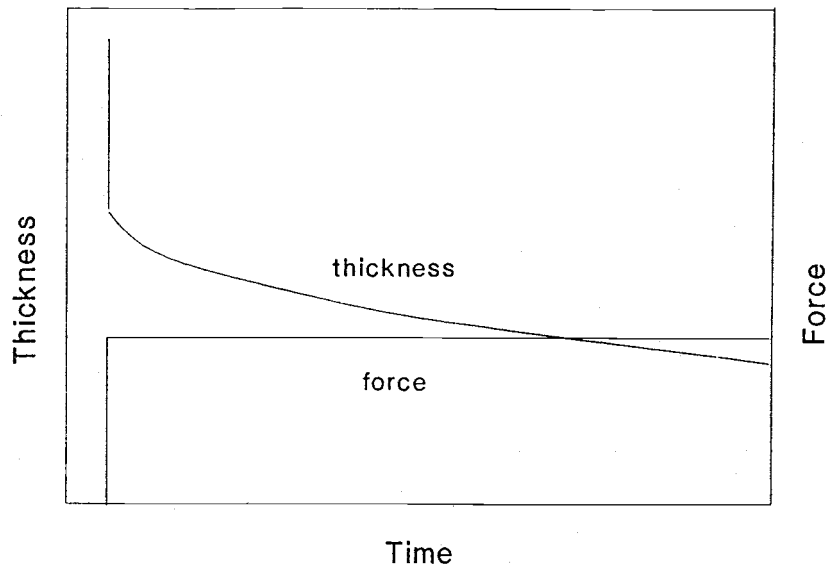


Figure 3.1. Typical rheological behavior of a wood composite material under compression.

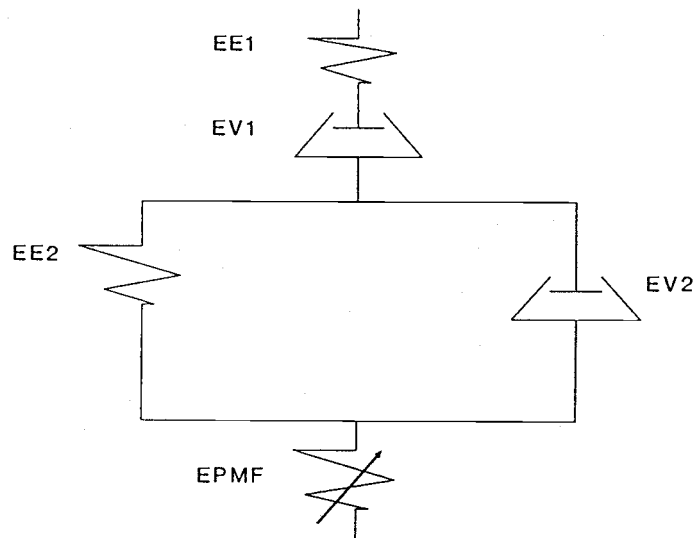


Figure 3.2. A five-element rheological model.

The role of each element is considered in turn. As pointed out in chapter 2, upon compression, the materials are instantaneously deformed due to elastic, plastic and micro-fracture behavior. The recoverable instantaneous deformation may be represented by an elastic (spring) element (EE1 in Fig. 3.2). The applied load is proportional (though nonlinearly) to the deformation, the response is time independent, and the energy absorbed by the material upon deformation is fully recovered when the external force is removed.

The non-recoverable instantaneous deformation is caused by the Plastic and Micro-Fracture (PMF) effects which can be modeled by an Element of Plastic and Micro-structure Fracture (EPMF). No strain occurs until the effective stresses exceed the yield strength of the localized micro-structures. At that time, the micro-structure yields and some micro-fracture takes place, and a portion of the micro-structure is relocated. Since the yield strength depends upon the micro-structure of the material, it changes continuously while the structure changes. Such structural changes are non-recoverable. PMF behavior appears to play an important role in wood composites manufacture; especially in the initial stages of consolidation. It is here proposed to develop a new element to represent this behavior which includes the plastic relocation and partial fracture of the micro-structure.

After instantaneous modes of deformation, the material continues to deform, even under constant load. This deformation is attributable to non-recovable viscous behavior and delayed elastic behavior. The later is recoverable after sustained unloading.

Non-recovable viscous behavior can be modeled by a viscous element (EV1) which is represented by a dash-pot. The energy absorbed by the system is entirely dissipated and there is no inherent tendency to assume original dimensions. Delayed elastic deformation may be presented by elastic (EE2) and viscous elements (EV2) arranged in parallel.

Since each element represents part of the rheological behavior, the deformation of the material is a superposition of the five elements' behaviors. It is not conceptually difficult to mathematically describe the combined effects of these elements. This model may be represented by the following structural equation:

$$RB = EE1 + EPMF + EV1 + EE2/EV2 \quad (3.2)$$

where, RB : represents the rheological behavior.
 + : serial connection.
 / : parallel connection.

A mathematical description of the five-element model could be represented by the following rheological equations:

$$\sigma + \left(\frac{\frac{K_1}{E_1 PMF}}{E_1 + PMF} + \frac{K_1 + K_2}{E_2} \right) \frac{d\sigma}{dt} + \left(\frac{\frac{K_1 K_2}{E_1 PMF}}{\frac{E_1 + PMF}{E_2}} \right) \frac{d^2\sigma}{dt^2} = K_1 \frac{d\epsilon}{dt} + \frac{K_1 K_2}{E_2} \frac{d^2\epsilon}{dt^2} \quad (3.3)$$

where, E1 : represents constant of EE1. Pa.
 K1 : represents constant of EV1. Pa * sec..
 PMF: represents constant of EPMF. Pa.
 E2 : represents constant of EE2. Pa.
 K2 : represents constant of EV2. Pa * sec..
 σ : stress. Pa.
 ϵ : strain. mm/mm.
 t : time. sec.

At least some of the elements for present system behave in a nonlinear fashion. Since the materials sustain very large deformation (strain) during hot pressing, the variation of the structure significantly effects the behavior. It appears from preliminary analysis that reasonably reliable predictions of the materials' behavior may be made if the nonlinear nature of the system is linked to a structural property -- namely that of density. This assumption will be discussed in the next section and will be developed further in chapter 5.

Consequently, the definition of each element should be considered here as functions of structural properties, such as density. Any variation of the stress or density may vary the rheological characteristics of each element.

3.4. The link between system density and rheological characteristics

Density was applied here to establish the links between the rheological behavior and structure. The use of density is convenient since density changes continuously as pressing proceeds and may be easily inferred. Localized density variation, which represents how the micro-structure varies under localized effective stress and the combined effects of temperature and moisture condition, shows the nature of rheological behavior of wood composite during hot pressing. It is fully acknowledged that more refined analyses could be developed which account for micro-structural changes which may not directly be associated with density changes. Such analyses are, however, likely to be very complex and have yet to be developed.

The study of the rheological behavior in terms of density is therefore an acceptable rigorous approach. It also may offer easily measured and controlled parameters which will be convenient for potential industrial development work. The present approach really was, however, likely to provide particular useful models in the short term.

3.5. Temperature and moisture effects

Although, heat and moisture transfer have been studied before, relationships between temperature and moisture content and rheological behavior during hot pressing have not been quantitatively established. The effects of these variables on rheological behavior are an important part of this research.

Rheological behavior of wood composite furnish materials first was studied under steady-state conditions of temperature and moisture. Then, the effects of unsteady-state conditions of temperature and moisture, which occur during hot pressing, may be dealt with numerically in future work based on the results of the analysis from the steady-state conditions.

In the present research, experiments were performed on specially formed fibers disks while under a average of iso-thermo-hygro-conditions. Iso-thermo-hygro conditions were obtained by the specially designed experimental technique and equipments.

3.6. Research process

According to the previous analysis, this research work was conducted to understand the rheological behavior of wood furnish materials under the conditions that occur during the

hot pressing process. This research included: 1) applying rheological concepts to the hot pressing process, 2) establishing a rheological model of the materials, and 3) developing experimental techniques and equipment to provide experimental results. Rheological behavior as functions of structure (density), temperature and moisture condition have been investigated and predicted. Efforts to understand and numerically reproduce the thermo-hygro-rheological behavior of the tested materials have been contemplated.

The experiments were conducted under a range of test conditions of compression pressure, temperature and moisture content while all other conditions were held constant (the thermodynamic environments are maintained constant and uniform throughout each test). Under these conditions, varying stresses were applied and resultant deformation was recorded. The non linear characteristics of five model elements were determined from the experimental results. This procedure was repeated for a range of steady-state temperature and moisture conditions to enable a non-linear thermo-hygro-rheological model to be developed and experimentally verified.

CHAPTER 4. MATERIALS AND METHODS

4.1. Materials

Wood fibers were selected as the primary test material in the investigation since they can be used to study the properties of wood materials without (or at least with reduced) influence of the natural variability of solid wood. Furthermore, it is considered that the greatest potential for new product development depends on the use of individual fibers (rather than flakes, particles or veneers). Since wood fibers can be formed in different methods and in different dimensions, the natural defects of wood fiber may be uniformly distributed throughout the test specimens and the influence of defects may be minimized. Therefore, the results of wood fiber study are more effective and accurate than that of other type of wood materials to show us the real nature of materials and as possible references for further research work.

Wood fibers for this research were obtained from the Evanite Hardboard Mill (Corvallis, Oregon). The raw material for the fiber process came from several sources including plywood mill residues (predominately, 90 - 95%), and wood chips of whole trees (5 - 10%). Wood fiber used in the present study consisted of about 95% Douglas-fir (Pseudotsuga menziesii) and 5% Hemlock (Tsuga heterophylla).

Wood fibers were defiberated with a thermo-mechanical defiberator (TMP method) at the Evanite mill. Therefore, the properties of fiber were less influenced than that of other manufacturing methods, for example, the effects of chemical methods. The fibers, which were collected near to the port of the defiberator, did not include adhesive or wax. They were stored at about 75% MC in a cold room (8 to 10 °C) to avoid possible bio-degradation, prior to use.

In addition to fibers, flakes of poplar wood (Populus spp.) were selected as the second test material. The result of this research obviously may be related with flakeboard manufacture. Poplar wood flakes were selected since it was also used in a cooperative project with Michigan Technological University (investigating unconventional pressing cycles at high moisture content and low temperature).

Since this thesis is mainly concerned with physical principles and experimental techniques, the discussion about the behavior of flakes will not be included; they are only included to demonstrate the capability of the experimental techniques.

A wide range of materials may be investigated in the future with the developed techniques. For instance, wood veneer may be selected as test material to investigate the behavior of plywood and laminated veneer lumber (LVL). Furthermore, the rheological properties of combinations of

natural and synthetic fibers could be investigated. These may well be important constituents of composites of the future.

4.1.1. Specimen preparation

Preparation of wood fiber specimens

A metered quantity of fiber was blended with an excess (95%) of water in a laboratory blender until the fibers were well separated. The blending time was short (30 sec) so that the fiber structure and properties were not mechanically disturbed.

The fiber slurry was then transferred to a hand sheet forming system. The water was vacuumed from the fiber slurry through a fine screen, and a relatively uniform fiber network was formed.

The wet fiber disks were conditioned in a range of environments to achieve target equilibrium moisture contents.

With this system, the dimensions of wood fiber disks may be varied in response to the maximum required consolidation pressure available. In the present work, the disks were 90 mm in diameter, 25 mm in thickness and weighed 14 grams in the oven-dry condition. The specimens could be

compressed at a pressure of 8 MPa on the available servo-hydraulic machine (capacity of 50 KN).

Circular specimens were adopted here because they do not contain any square corners which may perturb uniform boundary conditions.

Preparation of wood flake specimens

Flakes' average dimensions were 50 mm length, 10 mm width and 0.5 - 0.8 mm thickness. These were formed into disks carefully by hand to reduce possible variation. The flake disks were similarly pre-treated in conditioning rooms to reach the required equilibrium moisture content values. The flake disks were 90 mm in diameter, 20 mm in thickness and weight of 14 grams in the oven-dry condition.

New specimens were used for each test to produce comparable results.

4.2. Experimental design

The experimental methods described here were designed to provide an experimental and quantitative understanding of rheological behavior and how both the temperature and moisture condition affect the behavior. Therefore, applied load, deformation, density variation, temperature and moisture contents were the main parameters considered in

this experimental design. Experimental design will be deliberated as following:

1. How to design experimental processes and select experimental parameters.
2. How to precisely perform the compression test, efficiently study the deformation process and the effects of temperature and moisture content.

4.2.1 The experimental approach

During the experiments, the environment was maintained constant and uniform throughout each test by pre-treating the specimen inside the test system until the desired conditions of temperature and moisture were attained throughout. Desired test conditions then, were maintained constant during each test by controlling the atmosphere inside the sealed testing system at the appropriate temperature and water vapor pressure.

Each specimen was tested under accurately controlled compressing pressures and steady-state condition of temperature and moisture. The stress and strain were measured and recorded for analysis. Following the experimental test, the specimens' dimensions and weight were recorded to double check whether the moisture content of specimen were accurately controlled during each test.

Experiments have been conducted under ranges of mean compression pressures (P). The rheological constants of the specimens may therefore be determined from the experimental results. The basic principle of the test is shown as Figure 4.1.

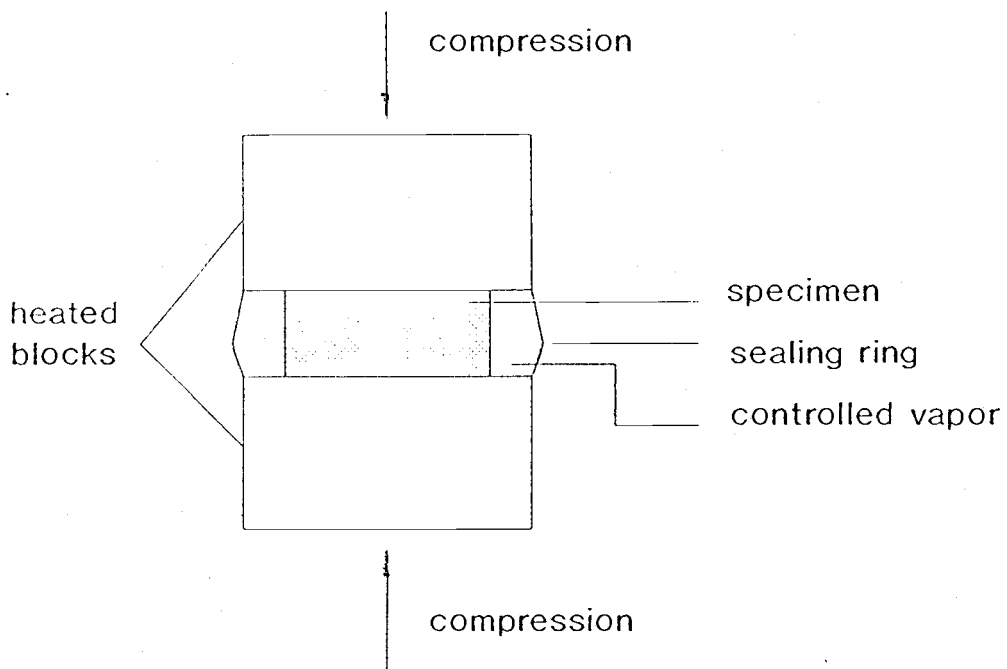


Figure 4.1. The basic principle of the test method.

Firstly, the temperature was held constant and the loads and deformations were measured for a range of moisture contents. Then, the moisture content of specimens was held constant and the loads and deformations were measured at a

range of temperatures. The combined effects of temperatures and moisture conditions were investigated in this way.

4.2.2. Compression and deformation

4.2.2.1. Compression

Compression pressures were pre-selected in the light of two main factors. First, since the results of our research may be used to improve existing products and also to design new composite materials, maximum pressures (the highest values used) should be comparable to peak loads applied in industry. More importantly, pressures should be selected based on scientific research requirements for understanding the fundamental mechanisms of wood composite materials.

The compressing pressures (platen pressures) conventionally used for wood composites vary both within and among each pressing cycle. Peak pressures typically range from 1 to 8 MPa. Pressures (P) were selected in the present work ranged between 1 and 6 MPa. Such a range enables material constants (such as elasticity, viscosity and plasticity), to be evaluated effectively.

A typical compressing pressure versus time curve applied to the specimens in this research is shown in Figure 4.2. From this curve, we can observe the compressing

pressure curve was designed with 22 steps for obtaining a diverse range of information about the material.

This curve may be sub-divided into three sections. Section I is the most important part and enables most rheological properties of the material to be obtained. Section II was included to enable the changes in rheological characteristics of the material to be quantified over an extended period. Section III was included to enable the relaxation of materials to be analyzed after maximum stresses have passed. The "spring-back" phenomena during hot pressing may relate to this section of the test cycle.

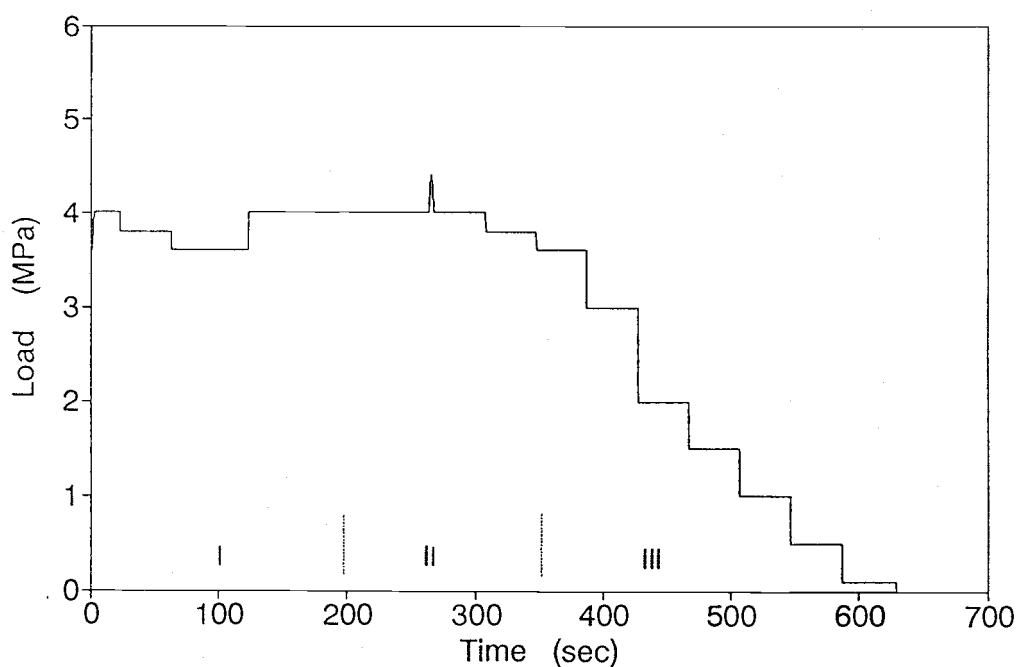


Figure 4.2. A typical pressure vs time curve
($P = 4$ MPa).

In the present research, the main emphasis was placed on the application of rheological concepts to the material, the establishment and verification of models, and the development of experimental techniques to support them. Indeed, the latter is the primary focus of the present work; model development is only of a preliminary nature to demonstrate the approach. Therefore, only the first section of the experimental test results will be applied in the analysis in this thesis.

Since the compressing pressures have to be varied within very small ranges during each test (to meet the requirements of the analytical techniques), pressure reductions during each test were limited to 5% of the average pressure (P). The maximum compressing pressure was 10% larger than the average pressure (P) to produce some extra required elastic-plastic deformation. The elastic-plastic properties of the material may then be derived from the resultant deformations. Since the density of the material clearly varied during each test, several average compression pressures (1, 2, 4, 6 Mpa) were used to establish a relationship between the rheological behavior and the structure (in terms of density). The range of pressing cycles employed are shown as Table 4.1.

Actual compressing pressures applied to the specimens inevitably deviated somewhat from the above control (or target) values. This was due to the limited sensitivity of

test machine controlling system. However, this kind of variation was very small (within $\pm 0.1\%$ of the target values).

Table 4.1. The range of compressing pressures used in the experiments.

Section	Step No.	Duration (sec.)	Compression Pressure (Mpa)			
I	1	0.4	0.0	0.0	0.0	0.0
	--	2	0.9	1.8	3.6	5.4
	3	2.0	1.0	2.0	4.0	6.0
	4	20	1.0	2.0	4.0	6.0
	5	40	0.95	1.9	3.8	5.7
	6	60	0.90	1.8	3.6	5.4
	--	7	140	1.0	2.0	4.0
	8	2.0	1.1	2.2	4.4	6.6
	9	0.2	1.1	2.2	4.4	6.6
	10	2.0	1.0	2.0	0.0	6.0
II	11	40	1.0	2.0	4.0	6.0
	12	40	0.95	1.9	3.8	5.7
	13	40	0.90	1.8	3.6	5.4
	14	40	1.0	2.0	4.0	6.0
	--	15	40	1.0	2.0	4.0
III	16	40	0.5	1.5	1.5	1.5
	17	40	0.5	1.0	1.0	1.0
	18	40	0.5	0.5	0.5	0.5
	19	2.0	0.1	0.1	0.1	0.1
	20	40	0.1	0.1	0.1	0.1
	--	21	1.4	-0.8	-0.8	-0.8
	22	0.4	0.0	0.0	0.0	0.0

4.2.2.2. Deformation

The deformation of specimens during each compression test cycle was measured and recorded (deformation could also be controlled with the system, but such position control was not used in the main part of this investigation). A typical

curve of deformation versus time derived from the compression curve of Figure 4.1. is shown in Figure 4.3.

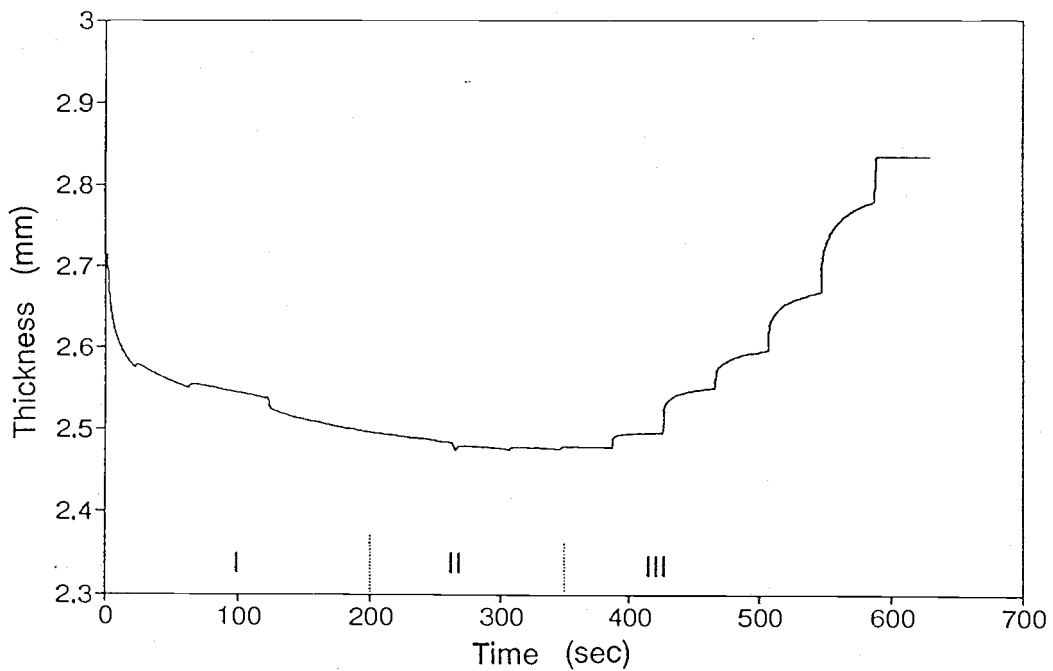


Figure 4.3. Typical deformation vs time curve for the loading curve shown as Fig. 4.2.
(MC = 4%, T = 120 °C, P = 4 MPa)

Figure 4.4. shows more detail of load and resultant deformation sustained during the first section of the test curve (period I). The details of how the five constants for the material may be derived from this curve will be discussed in chapter 5.

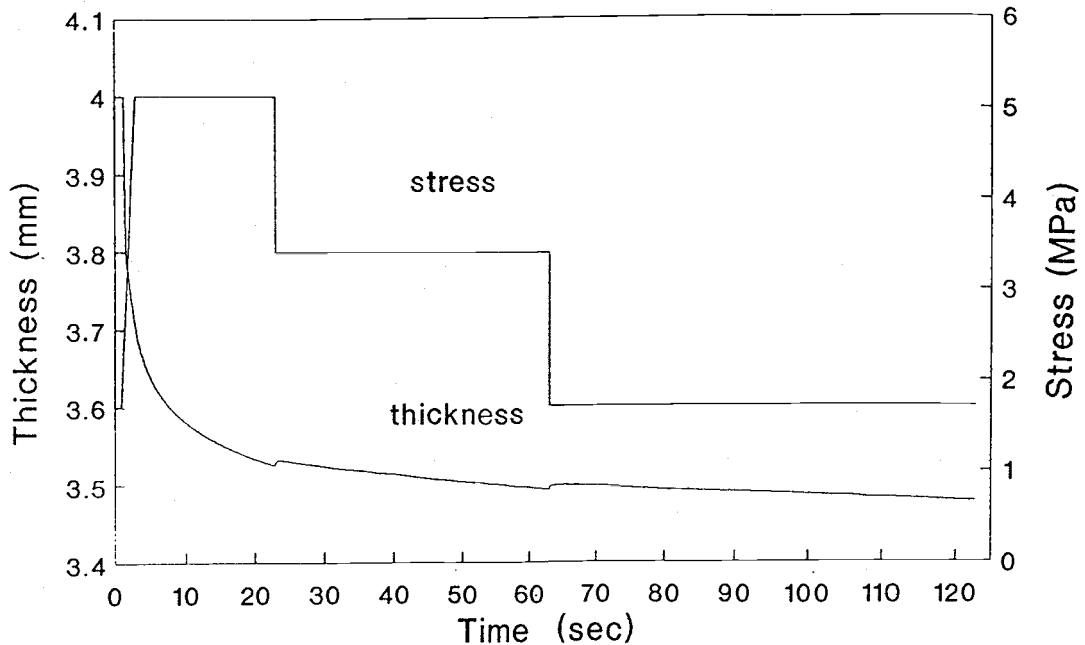


Figure 4.4. A typical curves of stress and deformation vs time in the first section (I) of the load control curve.

4.2.3. Investigating the combined effects of temperature and moisture

Effects of temperature

The temperature of wood composite materials varies from room temperature to about 200 °C during industrial hot pressing. Considering the thermo-degrading susceptibility of

wood materials, a temperature range of 25 to 150 °C was selected for the present research. Temperatures of 25, 100, 120 and 150 °C were employed in the investigation. A broader range and more intermediate values may be explored in future research.

To achieve a constant and uniform temperature condition prior to each test, pre-treating processes within the test system itself were necessary. Figure 4.5. shows a typical temperature curve during a complete pre-treating and compressing cycle.

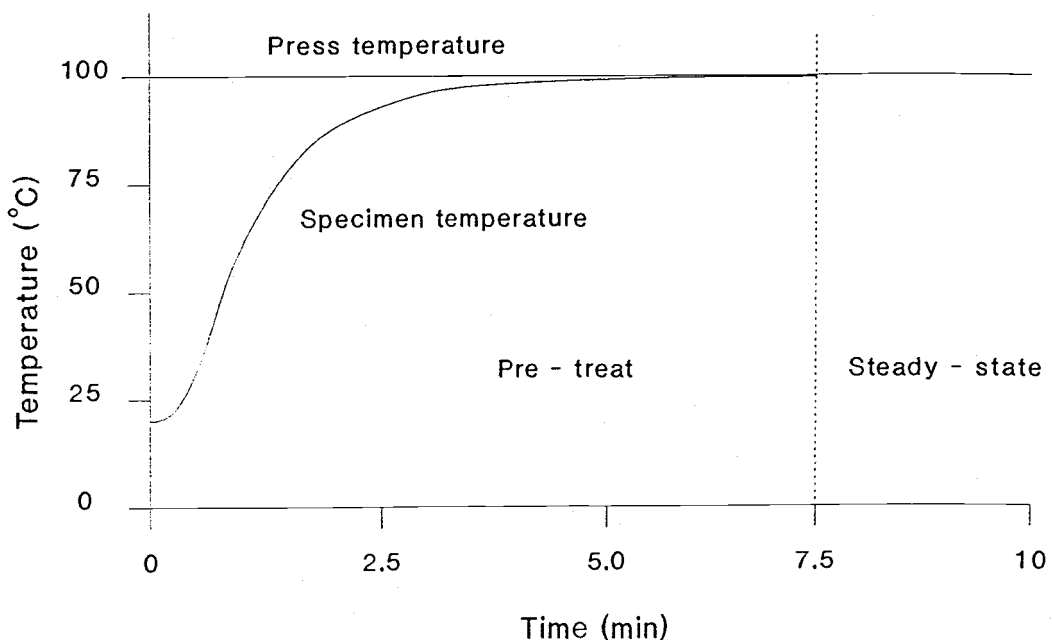


Figure 4.5. A typical temperature vs time curve during pre-treat and test processes (MC = 10%, target T = 100 °C, density = 250 kg/M³).

From Fig. 4.5, we can see that the temperature of the specimen was raised from room temperature to the desired value. The temperature was then maintained constant during the compression test. The time needed to achieve a desired temperature varies with test temperatures, moisture content, density and fiber mass (specimen thickness for a given density).

Effects of moisture

The most difficult parameter to control and measure during each test was moisture content. In the present research, the temperature and pressure of water vapor were selected as the two variables to control the moisture contents of the hygroscopic specimens. We know that the equilibrium moisture content (EMC) of natural fibers is a function of the relative humidity (RH) and temperature of the environment, and the RH is also a function of vapor pressure and temperature. Therefore, if we can control temperature and vapor pressure, then we can effectively control the EMC.

An important consideration in measuring the partial pressure of water vapor in an atmosphere surrounding and penetrating the specimens was how to distinguish it from air pressure. Air was trapped inside the testing system and its pressure varied when the treatment vessel volume was varied

and when the temperature changed. In order to overcome this problem, the system was evacuated (air removed) prior to testing. In this way, subsequently measured pressures were entirely due to the vapor; the air pressure effects were thereby all but eliminated.

A vacuum pumping system was applied to produce sufficient evacuation at the beginning of each pre-treatment process. There was little residual air, and its effects on controlled pressures were calculated and compensated. In this way, we may assume that measured and compensated internal pressures were due to water vapor derived from moisture in the specimens or that added prior to system closure. Providing sufficient supplemental liquid water was added prior to the system being sealed, then the water that was inevitably lost during evacuation may not dry out the sample. After sealing and heating, sufficient water remained to enable the necessary vapor pressure accumulation to affect the necessary EMC when equilibrium was eventually reached.

Several assumptions are necessary in this approach.

a. Simpson's equation (1973) has been used here to relate EMC, relative humidity and temperature for wood fibers. The inaccuracy of this equation was assumed small enough to be accepted. In future studies, it may be necessary to characterize the hygroscopicity of particular fiber type.

From Simpson's equation:

$$MC = \left(\frac{K1 * K2 * h}{1 + K1 * K2 * h} + \frac{K2 * h}{1 - K2 * h} \right) * \frac{1800}{W} \quad (4.1)$$

where: $K1 = 3.73 + 0.003642T - 0.0001547T^2$
 $K2 = 0.647 + 0.001053T - 0.000001714T^2$
 $W = 216.9 + 0.01961T - 0.00572T^2$
 $h = P_{\text{vapor}} / P_{\text{saturate}}$
 $MC = \text{moisture content.}$
 $T = \text{temperature}$

b. The final weight of tested (compressed) specimens can be used to indicate the final MC of the specimens after testing. This provided a means of evaluating the quality of control achieved during each test.

A range of moisture contents between 0 and 16% was selected (0, 4, 10, 16%). Figure 4.6. shows a typical vapor pressure curve measured during a pre-treating and compressing sequence.

In order to realize the experimental design, a new test system has been specially designed. This apparatus effectively consists of a miniature circular hot press with the provision for accurate load and temperature control. In addition, an attached environmental control system has been designed and used in this research. Peripheral sealing of the platens enables the atmospheres of controlled RH and temperature to be maintained around the specimen. A digital computer control system has been developed which enhances the servo-hydraulic test machine (MTS) performance thus enabling both compressive pressure and thickness of

specimens to be controlled dynamically. A digital data acquisition system was also used to collect the test data. More details about equipment design is presented in the next section.

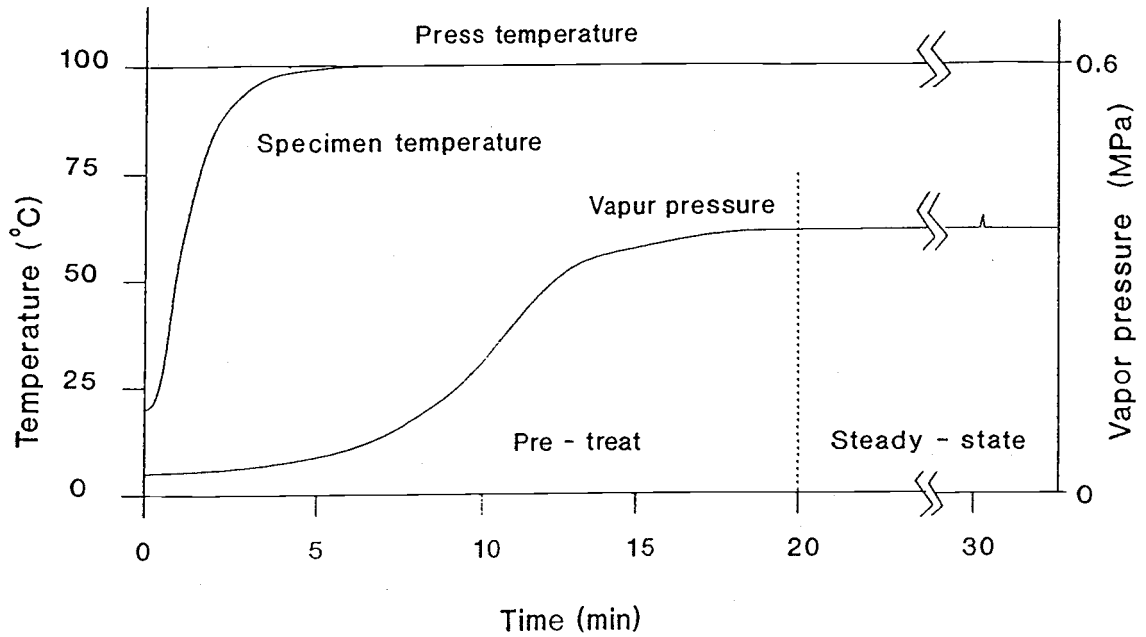


Figure 4.6. A typical curve of vapor pressure vs time.
 ($T = 100\text{ }^{\circ}\text{C}$, $MC = 4\%$, $P_v = .038\text{ MPa}$)

4.3. Equipment design

According to the previous discussion, the test equipment should perform the following functions:

1. Compress specimens with precise controllability and accurate measurement of load and deformation.
2. Maintain isothermal conditions in three dimensions throughout the specimens during each test.
3. Maintain iso-hygro conditions in three dimensions throughout the specimens during each test.
4. Provide capability of computer controlling the testing and data acquisition processes.
5. Experimental capability to conduct future research under unsteady-state conditions.

It was impossible to adapt any existing equipment to conduct this work. Therefore, new experimental arrangement was developed. This system and its development was the primary objective of the present research project. Figure 4.7. shows the miniature device which was developed for this research.

For the experimental miniature hot pressing system to have good heat transfer properties, the heat energy storage capacity (thermal mass) must be large enough to avoid large temperature variations during heat transfer from the platens to the test specimens. Insulation was designed to control internal distribution of temperature.

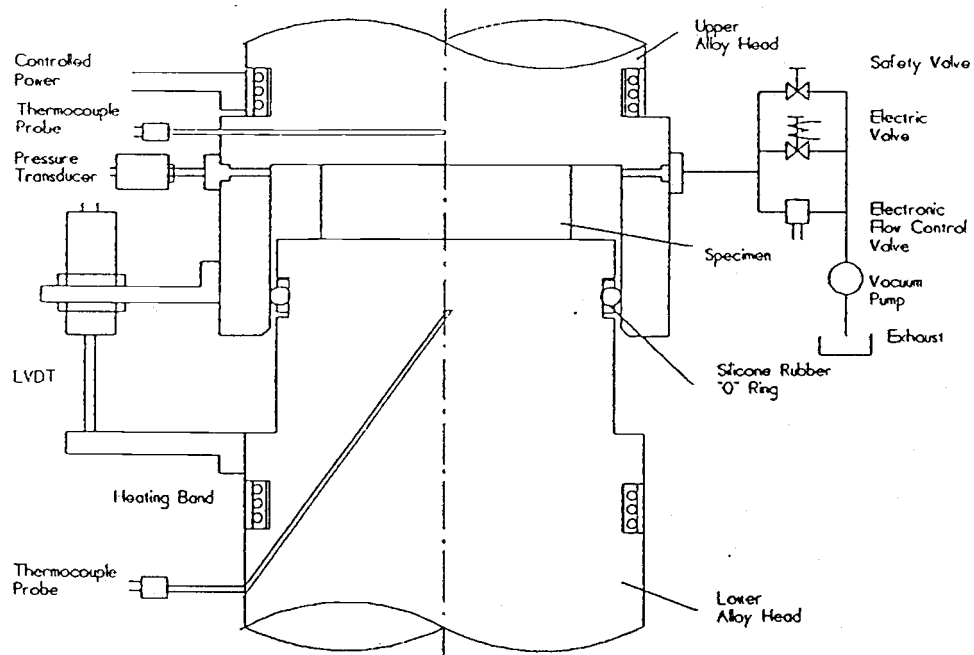


Figure. 4.7. A miniature thermal pressing system.

4.3.1. Affecting loading and measuring deformation

Two parts of the miniature hot press were assembled on the machine. One was attached to the top frame and the other was on the piston of the machine. The piston was able to be driven up or down by hydraulic power from a fast response power unit and control valve. A load cell of 50-KN capacity and LVDT of 150 mm range were applied to obtain a large test range. An extra LVDT of 50 mm range was directly assembled beside (60 mm away from) the hot press for precise measurement. Linking the LVDT directly on the pressing heads

improved the accuracy of measurements by avoiding vibration and the effects of thermally induced distortion of the MTS frame.

4.3.1.1. Compression measurement and control

In the load control situation (Fig. 4.8), desired compression pressure for each test was first generated by a computer program (see appendix I: a program for generating control loading pressure data). An operating program (see appendix I: a program for test operation) then converted the digital data to analog form by means of a digital to analog converter; this signal was transmitted to the MTS microprocessor.

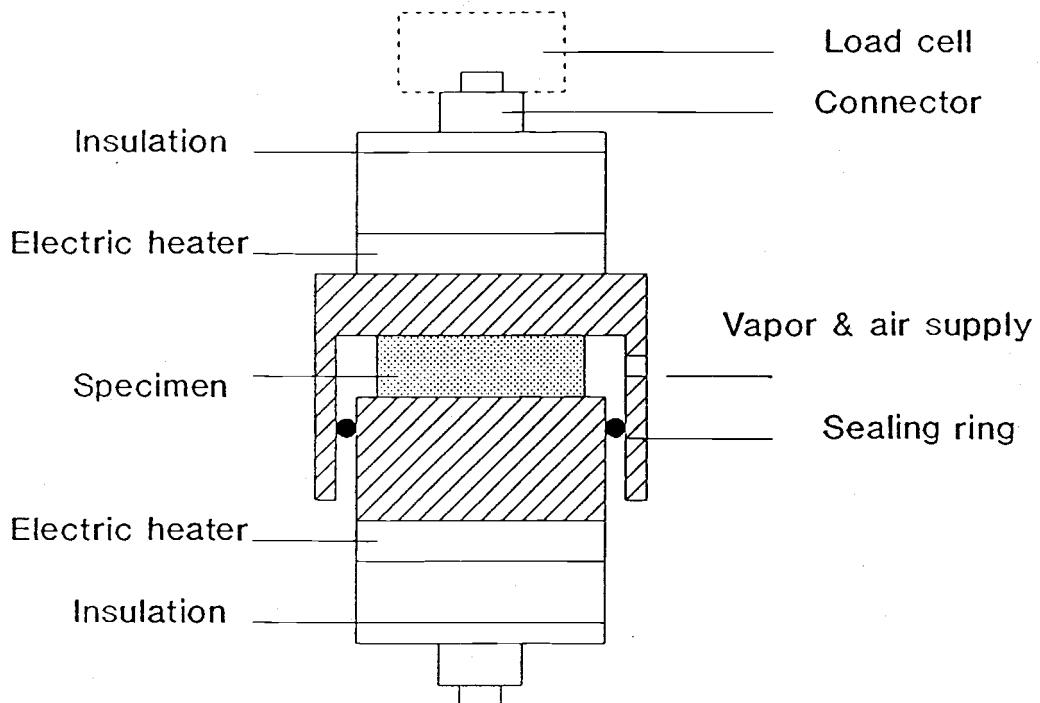


Figure. 4.8. The compression control and measurement scheme.

In the control loop, the desired control data (target value) was repeatedly compared with the measured value from load cell, and control system decided whether the load should be increased or not. If the actual load sensed by the load cell was less than the control value, the hydraulic system drove the piston up. The press was closed and pressure increased until the actual pressure approached the target value. The MTS machine then maintained the system constant (final position) until the next control cycle began. The signal analysis and control cycle were repeated every 0.2 seconds.

4.3.1.2. Deformation measurement and control

During compression, the relative movement between the top and bottom parts of the press was measured by the LVDT and collected by the computer with the data acquisition system so that the relationship of the compressing pressure and the deformation of materials can be established. A rigid material with high temperature resistance was used to connect the 50 mm LVDT to the miniature hot press. This minimized temperature influences.

The control system was also designed to be operated under position control so that deformation of materials could be controlled and resultant variations in stresses be measured. However, throughout the present research, load

control was used to establish the stress-strain relationships.

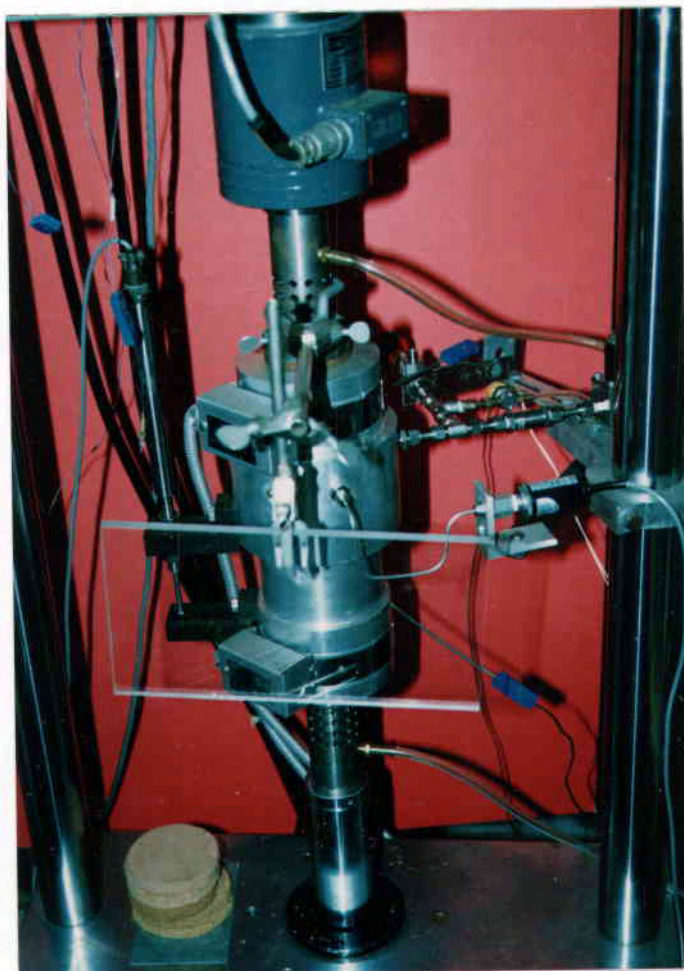


Figure 4.9. LVDT assembly photograph (LVDT vertically assembled besides the press).

Since the two main variables, load and deformation, were measured by the load cell and LVDT, and recorded by the computer, which revealed a noisy signal related to some equipment system components, no-matter how careful we were, there were still some experimental errors. Much of the noise

was dealt with by passing the signal through a filter prior to digitization. But some random errors remained.

However, the nonlinear regression of the large quantity of experimental data at high correlation coefficient may minimized these errors' influences (see chapter 5).

4.3.2. Temperature measurement and control

The desired temperature conditions encompassed a large range for the different tests though they were constant during each test. Two temperature variables (test system temperature and specimen temperature) should be considered here. Each of them will be addressed individually. The following functions are necessary for this part of the equipment design:

1. the tests must be conducted at temperatures varying between 20 to 150 °C.
2. the target temperature must be controlled within quite fine limits (± 0.5 °C).
3. heat transfer rates within the equipment and into the specimens should be maximized.
4. the sources of heat energy should be large enough and well enough controlled to minimize variation of temperature.

4.3.2.1. Test system temperature measurement and control

Thermocouples were used to measure sample and equipment temperatures. Two electrical band-heaters, two EUROTHERM analog temperature controllers (model 917) and two thermocouple probes (which were mounted inside the pressing heads) were used to measure and control the two parts of test system separately. Figure 4.10. represents the arrangement of band-heater and thermocouple probe on lower part of test system.

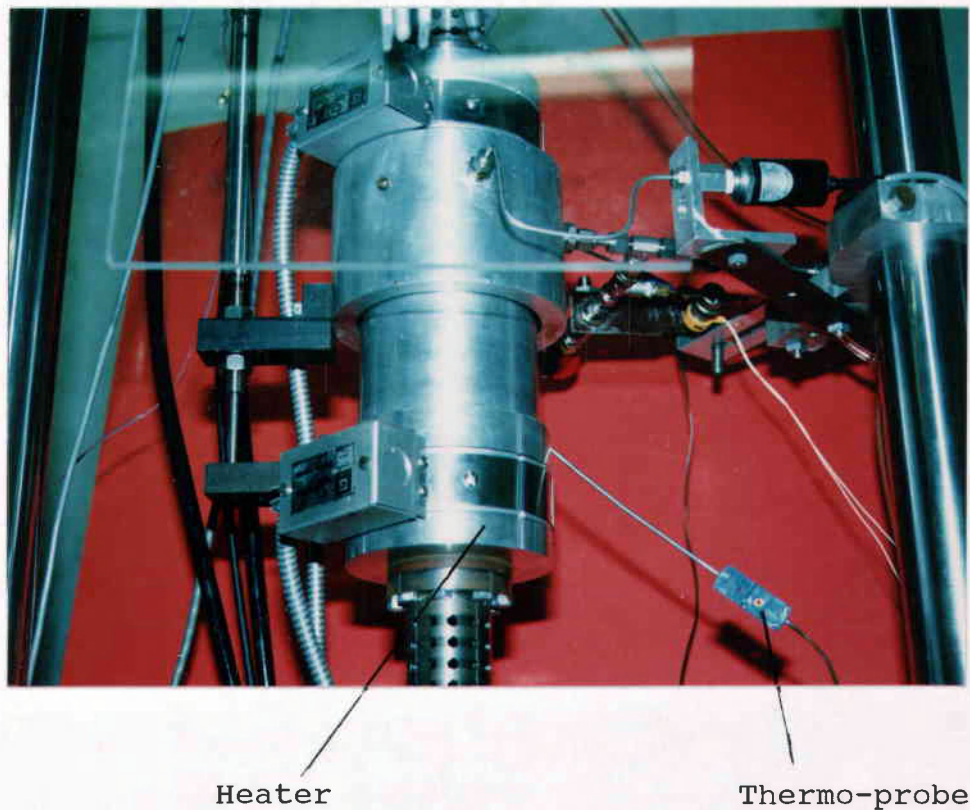


Figure. 4.10. Test system temperature measurement and control (photo).

Temperature of test system was measured by thermocouple probes inside the heated platens and controlled by the temperature controllers. In addition to measurement and control of the internal temperature of each pressing head, their interfacial temperatures between specimen and the metal were also measured during each test. This measurements were designed for control the internal temperature during each test.

High heat conductivity and capacity alloy was used to make the test system can transfer heat energy quickly, and avoid any temperature variation due to heat transfer from plates to the test specimens and to outside atmosphere.

The special designed press shell was for three dimensional temperature controlling purpose. (later we will discuss it also worked for moisture controlling purpose.)

In this way, the test system could be sealed and maintain at constant temperature condition.

4.3.2.2. Specimen temperature measurement and control

The test with steady-state condition of temperature demands the temperature uniform distributed within the sample in three dimensions. Therefore, a miniature press was designed with a relatively large annular region surrounding the pressing surfaces so that heat transfer was uniform and edge effects were minimized. The alloy shell was special

designed to cover the edge of sample to make the heat transfer uniformly in three dimensions. A silicon rubber "O" sealing ring was utilized here to seal the test system while still allowing sliding motion (see Fig. 4.11).

Specimen temperatures were measured during the pre-heat period in order to judge when uniformity have been reached and whether it was constant during the test.

Internal temperature were measured with two thermocouples (Type "T"). One was placed at the geometric center of each specimen and another was positioned near the sample / platen interface. When the center temperature was equal to the surface temperature, then, it was assumed that temperature was uniformly distributed throughout the specimens and steady-state temperature had been reached.

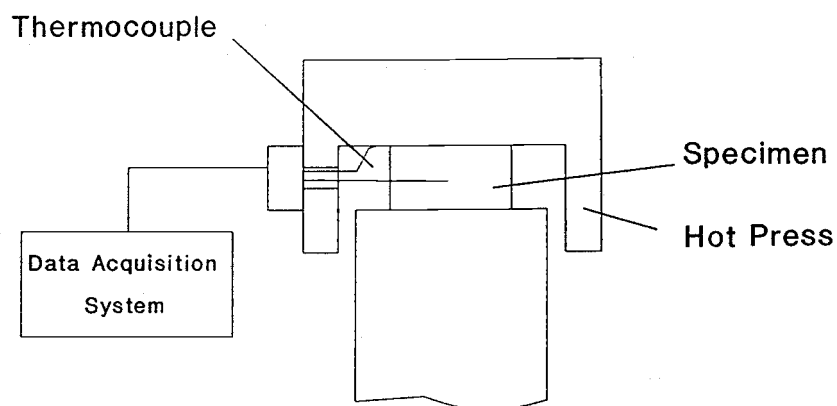


Figure 4.11. The temperature measurement system for the specimens.

At each combined temperature and moisture conditions, two or three pre-tests were conducted to measure the temperatures of the specimens and system, and to judge how much time (average time) was needed for stability to be reached. During "real" test, only the sample / platen interfacial temperature was measured. Temperature of center of specimen was not included in "real" tests since measurement may have interfered with the thermal and mechanical behavior of the materials.

4.3.3. Specimen moisture measurement and control

Moisture condition of specimen may be measured directly, but achieving and maintaining a target value within the system is more difficult to accomplish. In many circumstance, the parameters which may be converted to calculate the moisture content were measured and controlled instead of directly control and measurement of MC.

Therefore, as pointed out earlier, the temperature and vapor pressure were the two variables used in this project to indirectly measure and control the MC of the specimens.

4.3.3.1. vapor measurement

An absolute pressure transducer was employed to measure gas pressure inside test system. Silicone oil was applied

within the connecting tube which connected the pressure transducer to test system. This was to avoid possible water effects on the transducer. The vapor pressures were collected by computer data acquisition system for further analysis. Since the test was operated under a steady-state moisture condition, constant values of vapor pressure were desired during each test.

Figure 4.12. shows how to measure and collect the vapor pressure data. Since one important consideration was how to measure it and how to separate it from residual air pressure which was tracked inside system when hot press was closed, a new method has been applied here to measure vapor pressure under vacuum circumstances.

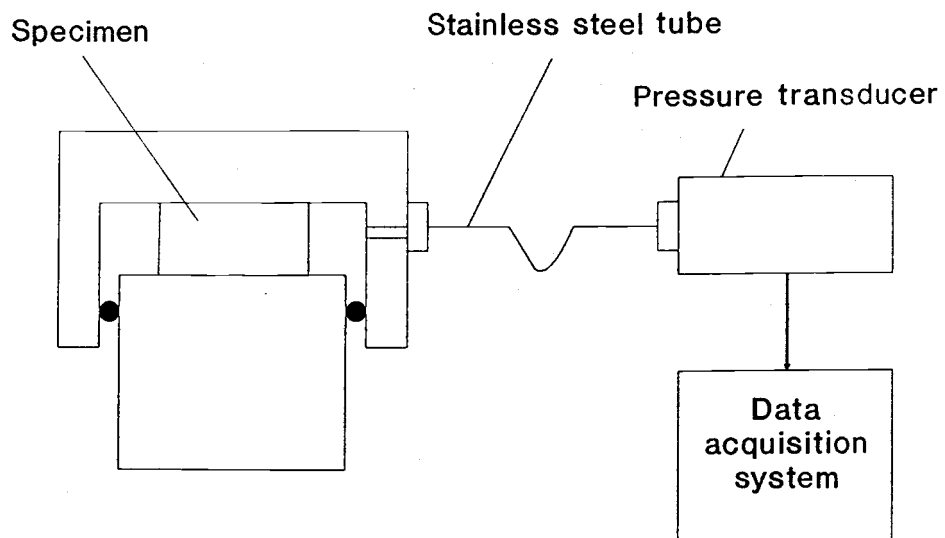


Figure 4.12. Vapor pressure measurement arrangement.

4.3.3.2. Moisture condition control

The vapor pressure measurement and control system consisted of the following main components:

1. a vacuum pump to remove most of the air from the system prior each test.
2. an electrical valve which opens or closes the test system to produce vacuum condition at beginning of each test.
3. an proportionally opening electronic servo-valve allowing excess vapor to be let out off the system to maintain the pressure at the designed values.
4. a pressure measurement and proportional feedback control circuit to enable preselected vapor pressure values to be maintained.
5. a manual adjustable safety valve for avoiding possible pressure overshooting damage or explosion.
6. a high temperature resistant silicon rubber "O" ring to seal the test system while allowing physical movement.

The vapor pressure corresponding to desired RH at prevailing temperature was pre-set on the specially constructed vapor control unit. Having carefully positioned on the lower platen, the system was sealed (by moving up the lower part of press), the electrical valve was opened, and

the internal air was evacuated. The electrical valve was then closed.

As heat was transferred into the material, the vapor pressure gradually increased. When this reached the value necessary to achieve the target RH, then the control valve opened. Excess water was ejected until isothermal condition were reached. While heat was being transferred to the center of the specimens, some moisture inevitably migrated. Time was allowed for moisture gradients to uniform prior to testing. At this time, it was assumed that the required EMC and temperature prevailed throughout the specimens.

Once the system arrived isothermal and isohygro conditions, the target vapor pressure was maintained constant value. This clearly necessitated automatic venting of vapor as the volume of the vessel decreased. When vapor pressure exceeded the pre-selected value, the control unit would proportionally open the electronic servo-valve and let the extra vapor be evacuated out by the vacuum pump until the internal pressure equaled to the preselected value. The vacuum pump was necessary because the target partial pressure of water vapor often was below atmospheric pressure (at low MC values and / or low temperatures).

Figure 4.13. shows the process of how to measure and control vapor pressure within system.

Since a complete vacuum was impossible to achieve, there was always some residual air inside the test system

after it was closed. The pressure from the residual air also changed with temperature change (thermal expansion and contraction). However, these effects were relative small compared to the vapor pressures. In any case, they were subtracted (compensated for).

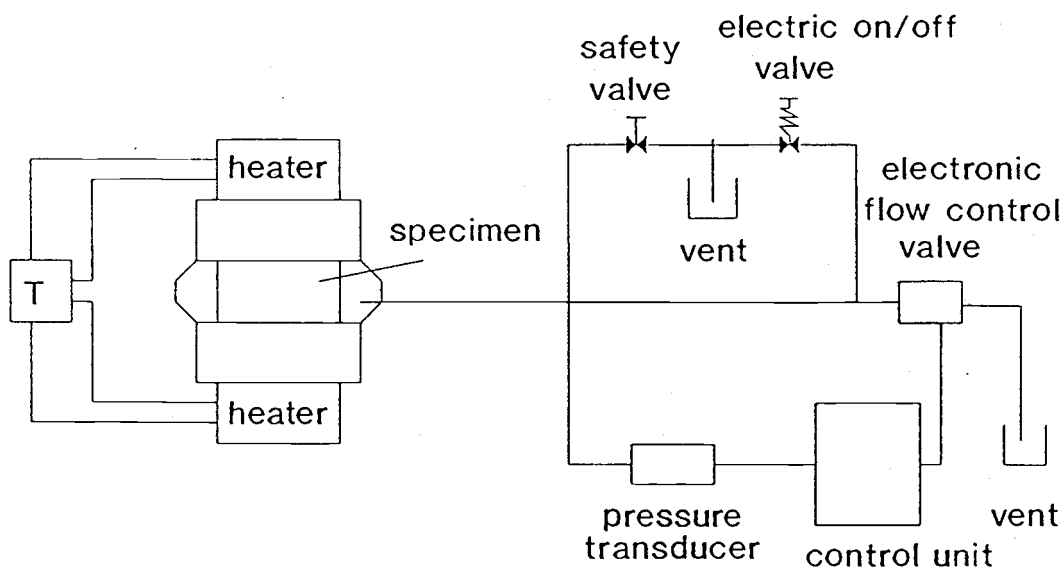


Figure 4.13. The temperature and moisture control system.

4.3.4. Computer control and data acquisition system

The physical properties of the specimens changed during each compressing test and this reacquired use of responsive control approach. A computer control and data acquisition system has been developed. This included the following functions:

1. Controlling the piston movement with load or position as control variables.
2. Measuring and recording the conditions of load, material deformation before and during each test cycle.
3. Collecting temperature, vapor pressure data.

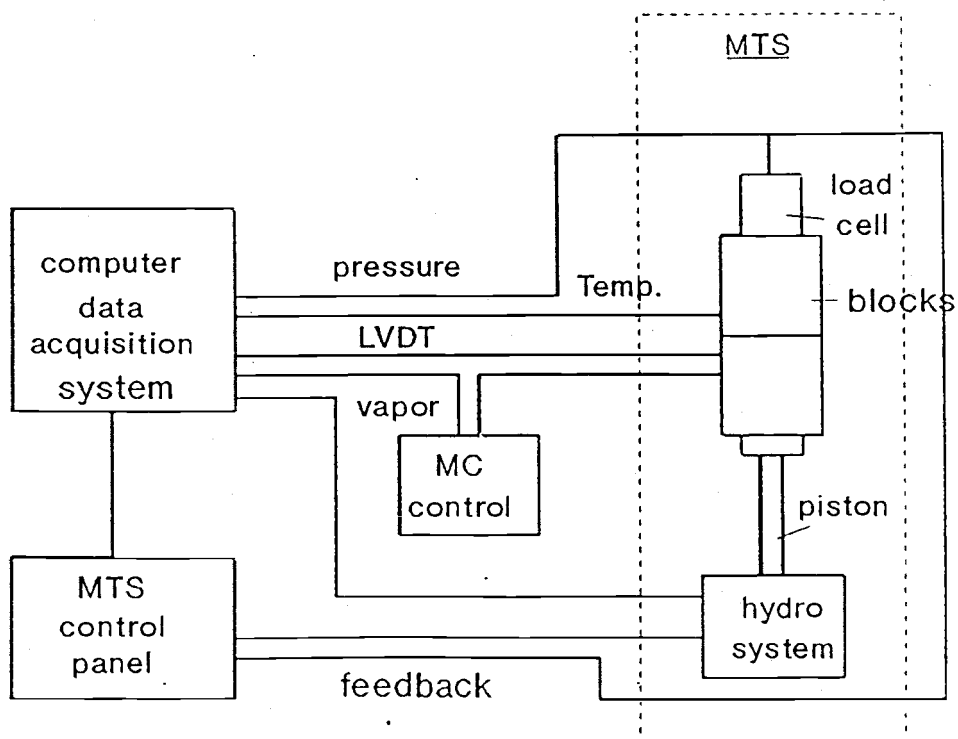


Figure. 4.14. Computer control and data collection system.

The compression pressure and specimens deformation which were measured by the load cell and LVDT, and the temperatures and vapor pressure which were measured from the thermocouple and pressure transducer were collected through

a data acquisition system, which transferred the analog data to digital data, and recorded by the computer.

4.3.5. MTS machine control

Since the original function generator of the MTS machine was not able to produce the necessary complex serial control curves, a computer control system was designed to replace the original function generator of MTS and to enhance the performance of the machine.

After the computer control system was incorporated, the complicated press behavior could be programmed via a PC.

Figure 4.15. shows the complete test system.

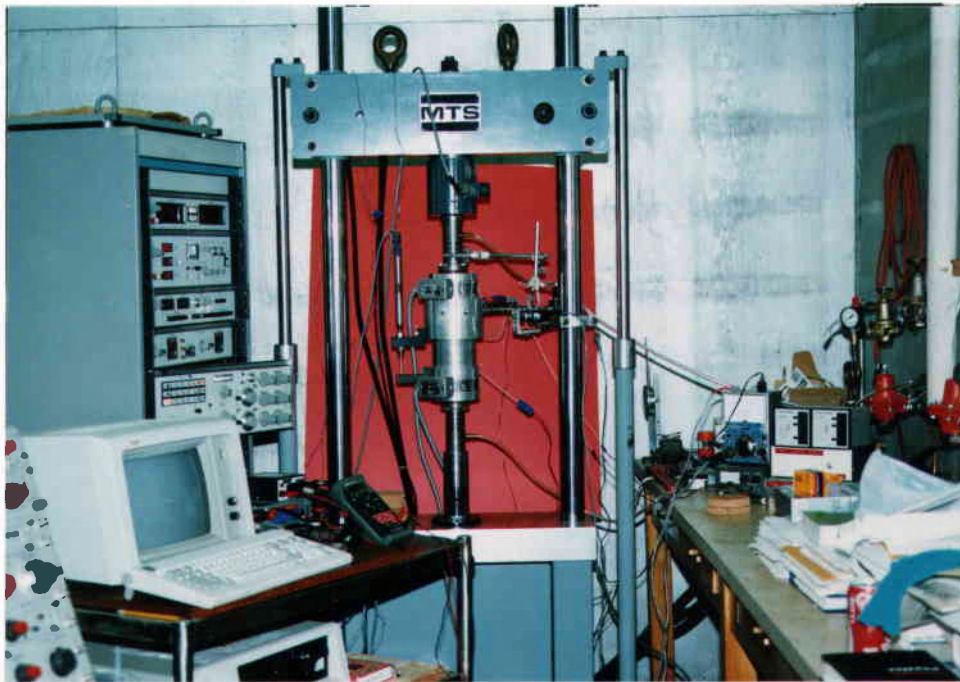


Figure 4.15. A complete test system (photo).

4.4. Experimental test sequence

Circular specimens 90 mm diameter and 25 mm thick were put in several conditioning rooms to achieve the required wood moisture contents. Following pre-treatment, the specimen was immediately placed in the test system, and the temperature and vapor control systems were adjusted to the required values. The miniature press was first closed to a pre-determined position where the two parts of the press just touched the bottom and top surface of the specimen. This position was maintained for the duration of the pre-treatment period. In this way, the specimen usually quickly reached the required steady-state temperature. At the same time, water vapor was generated. The vapor pressure and temperature were increased around the specimens.

The flexible silicon rubber "O" seal ring kept the system insulated for controlling the environment at each test. When the target pre-selected hot pressing condition was approached, the electronic valve was activated by the vapor controlling system which functioned depending on the signal from vapor pressure transducer which measures the system vapor condition. During each test, the deformations of the materials were measured in response to the load control cycle.

Repetition of this procedure for different pressing conditions enabled the rheological characteristics of the

specimens during steady-state temperature and moisture conditions to be evaluated. New specimens were prepared for each test. Results were specific to the material, temperature, moisture content and mean platen pressure used for each test.

CHAPTER 5. DATA ANALYSIS

5.1. Determination of rheological properties

The following should be regarded as a preliminary attempt to derive rheological models for the materials. In order to determine the rheological properties, recall the definition of the proposed rheological model (equation 3.3):

$$\sigma + \left(\frac{K_1}{\frac{E_1 PMF}{E_1 + PMF} + \frac{K_1 + K_2}{E_2}} \right) \frac{d\sigma}{dt} + \left(\frac{K_1 K_2}{\frac{E_1 PMF}{E_1 + PMF} E_2} \right) \frac{d^2\sigma}{dt^2} = K_1 \frac{d\epsilon}{dt} + \frac{K_1 K_2}{E_2} \frac{d^2\epsilon}{dt^2}$$

For wood composite materials under conditions of compression:

$$\epsilon = \frac{\sigma}{E_1} + \frac{\sigma}{PMF} + \frac{\sigma t}{K_1} + \frac{\sigma}{E_2} \left(1 - e^{\left(\frac{-E_2 t}{K_2} \right)} \right) \quad (5.1)$$

- where, E1 : elastic element (EE1) property (Pa)
 response to instantaneous elastic behavior.
 K1 : viscous element (EV1) property (Pa * sec)
 response to irreversible viscous behavior.
 PMF: plastic-fracture element (EPMF) property
 (Pa) response to fracture and plastic
 behavior during compression.
 E2 : elastic element (EE2) property (Pa)
 response to delayed elastic behavior.
 K2 : viscous element (EV2) property (Pa * sec)
 response to delayed elastic behavior.
 t : time (sec)
 σ : stress (Pa)
 ε : strain (mm/mm)

Determination of these properties requires an analysis of the rheological behavior and related mathematical description, which has been discussed earlier. A physical-mathematical method has been developed here for doing this work.

The following assumptions have been made:

1. Specimen structures and properties are continuously and uniformly distributed throughout.
2. Rheological properties may change as the micro-structure changes and this is directly related to the prevailing density of the materials (an important assumption discussed earlier).
3. The dimensions of the specimens only change in the direction of thickness. The variation of diameter (poisson's effect) is relatively small (due to the porous nature of the network) and will be neglected.

5.1.1. Overall strategy for finding elements' properties

Figure 5.1 shows a section of a typical test curve. The properties of each of the five elements have been inferred by judicious interpretation of deformations resulting from specific parts of the loading cycle.

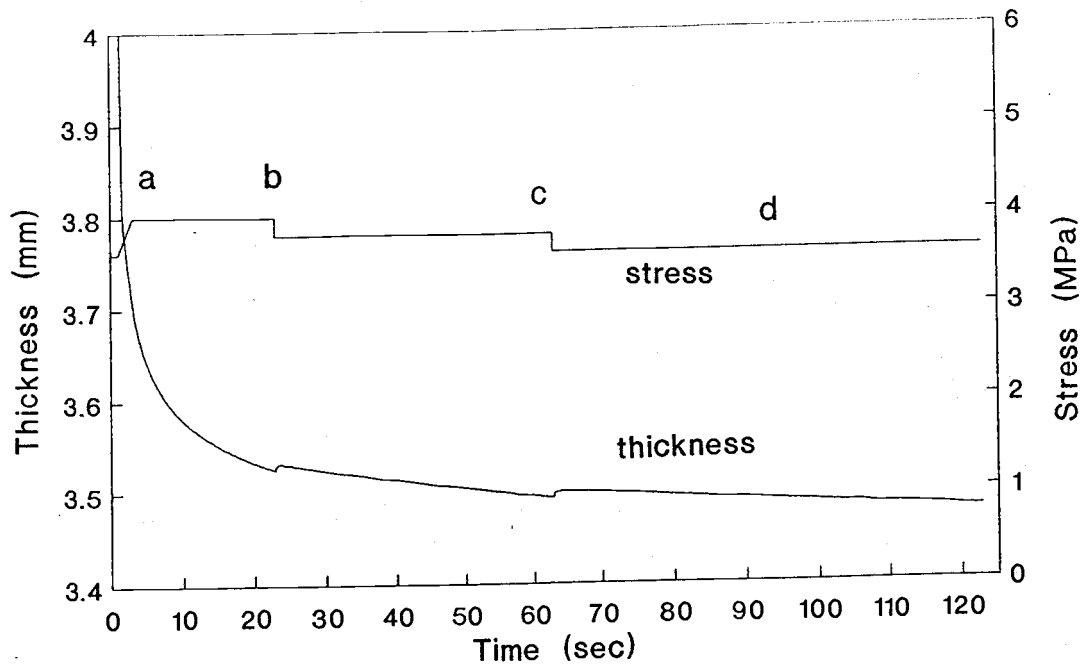


Figure 5.1. A section (part I) of a typical test curve for deriving rheological constants.

a. The values of E_1 and K_1 can be directly calculated from the relationship of stress and strain of each test result. The relationship between these constants and density (element property = $f(\rho)$, where, ρ = density), then, can be established by mathematical or statistical methods from a group of test results.

b. Applying the equation of E_1 to separate PMF (plastic and fracture characteristics) from each test result, and then, evaluating the PMF component as a function of density.

c. Applying the equations of E1, PMF and K1 to get the E2 values in each test result, and evaluating E2 as a function of density from the group of test results (for different P values).

d. Applying the equations of E1, PMF, K1 and E2 to obtain the K2 values in each test result, and evaluating K2 as a function of density from the group test results.

In this way, the relationships between the element's properties and the material's density may be established. More details of how to get those constants and how to find the equations will be discussed in the following sections.

5.1.2. Process for evaluating E1

During the first part of each test, compressive pressure is reduced twice (see Figure 5.1. points b and c), though the pressure is only reduced by a very small amount (the difference is 5 % of the average load during section I of the loading cycle). During these rapid unloading stages, the specimens undergo two instantaneous relaxation (expansion) responses, which, to first approximatise, only involve instantaneous elastic deformation of EE1. Values are specific to the average density that prevailed during the unloading period (which was almost instantaneous) and it follows that:

at point b:

$$\begin{aligned}\Delta\sigma_b &= \sigma_{b1} - \sigma_{b2} \\ \epsilon_b &= (\text{thickness}_{b1} - \text{thickness}_{b2}) / \text{thickness}_{b1}\end{aligned}$$

$$El_b = \frac{\Delta\sigma_b}{\epsilon_b} \quad (5.2)$$

at point c: (same as above)

$$El_c = \frac{\Delta\sigma_c}{\epsilon_c} \quad (5.3)$$

A number of elastic properties are obtained from a group of tests conducted under a range of mean compressing pressures (1, 2, 4, 6 MPa), specific densities (related to thickness) and steady-state conditions of temperature and moisture (points on Fig.5.2). Each test condition was repeated two to three times.

A regression equation based on the data which is presented in Figure 5.2. then, is generated; this curve is superimposed on the data in figure 5.2.

$$El = e^{A+B\rho} \quad (5.4)$$

where, A and B: constants
 ρ : density

The regression equation represents the variation of El with density while the material is at a specified thermo-hygro state, and this establishes the constitutive relationship between El and density.

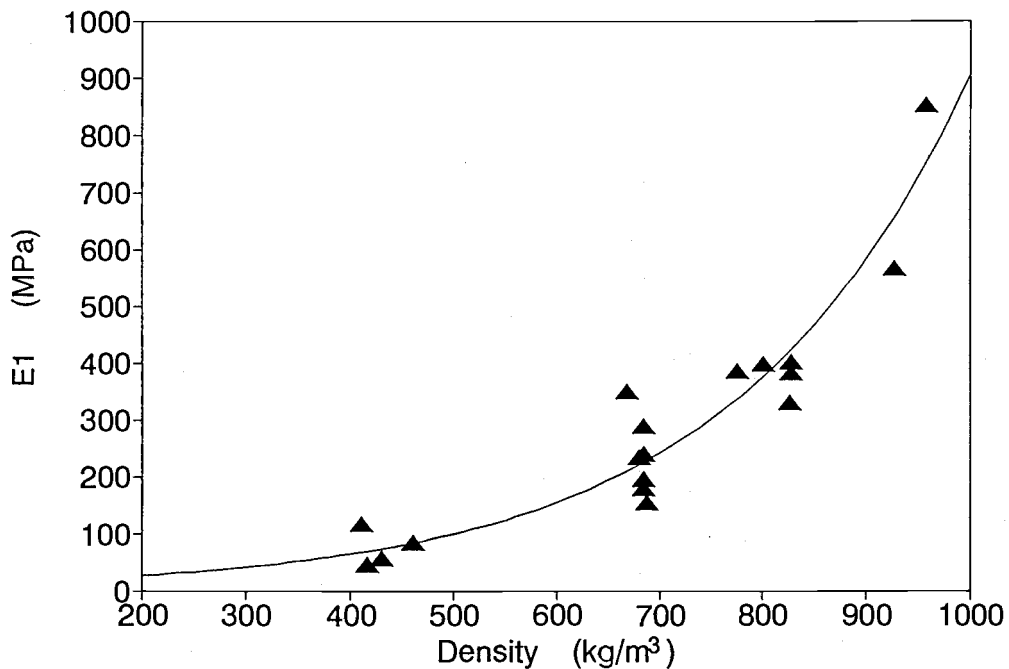


Figure 5.2. E1 vs density for a typical test condition ($T = 100^{\circ}\text{C}$, $\text{MC} = 4\%$).

It is necessary to be aware that the above established work assumes plastic, delayed elastic and viscous types of behavior do not take place during the short time periods while the load decreases and resultant thickness increases occur at points of b and c. Though some of the elemental effects must in fact occur, they are likely to be small enough to be neglected (at least in the first analysis). Hence the deformations at points b and c are assumed to be caused only by the effects of EE1.

It will also be assumed that interactions among the five elements do not occur or significantly effect the

accuracy of the present work. However, such interactions may prove to be necessary in future refinement of the models.

5.1.3. Process for evaluating PMF

During the initial stage of the compressive pressure increase, rapid stress increases (Figure 5.3) produce localized structural failures and micro-structural relocation, as well as elastic deformation. It is assumed that the instantaneous elastic deformation, fiber fractures and relocation happen as a direct consequence of compression (the applicaiton of pressure) at each step of stress increase.

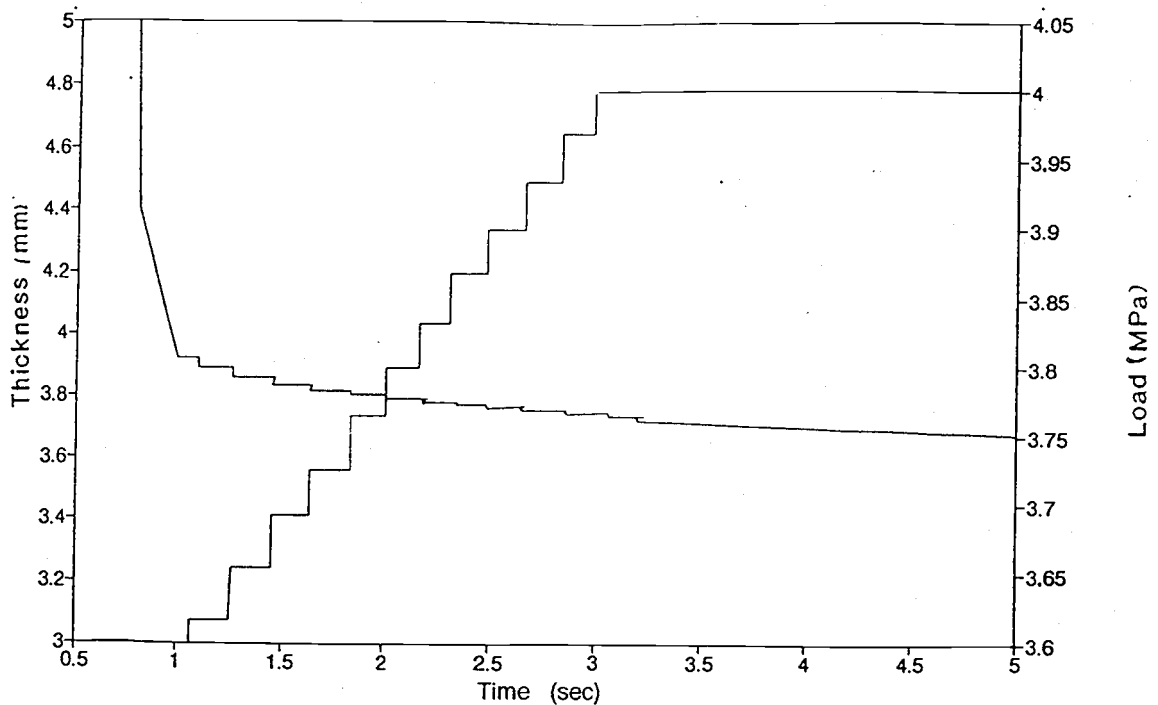


Figure 5.3. Initial stage of compression for quantifying PMF.

Since the effects of EV1, EE2/EV2 are assumed to be small enough to be neglected at each stepwise stress increase, the strain due to both EE1 and EPMF behaviors at each density condition (thickness) is given by:

$$\epsilon_{instant.} = \epsilon_{elastic} + \epsilon_{PMF} \quad (5.5)$$

Differences in responses during instantaneous load increases and decreases may be used to distinguish between elastic and fractural mechanisms. A method is developed here to separate the EPMF and EE1 properties at this initial stage of compression. We subtract the strain of EE1 from the total instantaneous strain so that the strain of EPMF may be calculated as a consequence of a rapid load change. Therefore, when loads increase almost instantaneously, strain of EE1 can be calculated:

$$E1 = e^{A+Bp}$$

$$\epsilon_{EE1} = \frac{\Delta \sigma}{E1} \quad (5.6)$$

PMF can then be quantified:

$$PMF = \frac{\Delta \sigma}{(\epsilon_{instant} - \epsilon_{PMF})} \quad (5.7)$$

Different PMF values also are derived from groups of test results based on density, the same as when calculating E1. Figure 5.4. presents values for the property of plastic-micro-fractural element with the density and a regression curve ($PMF = e^{A+B\rho}$) resulting from those data.

A relationship between the instantaneous plastic behavior and the material density then is established.

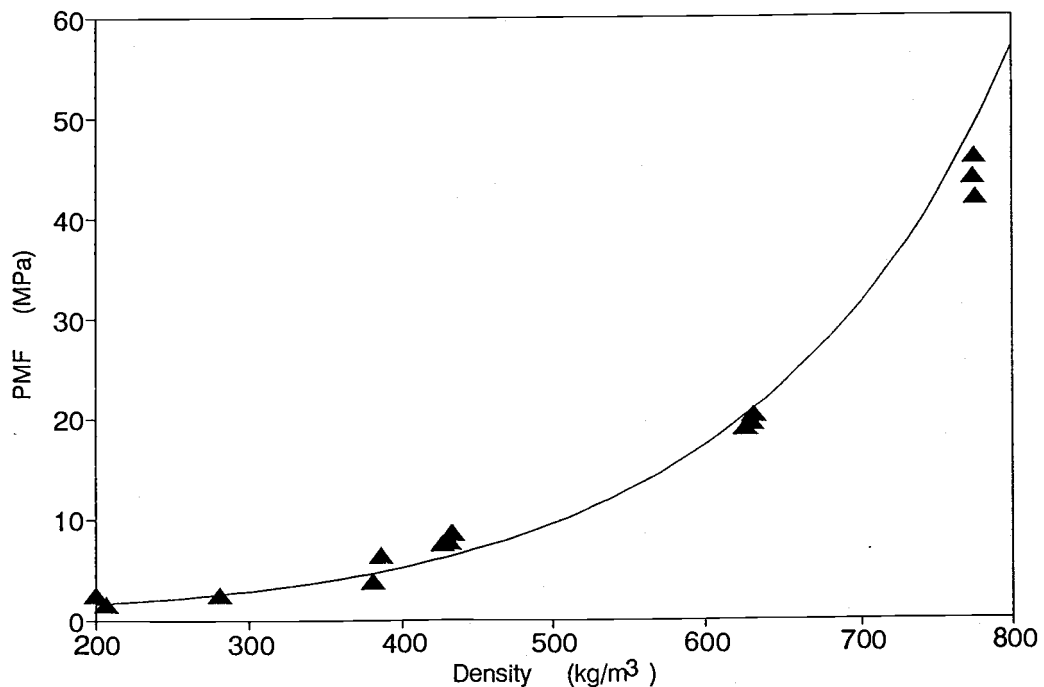


Figure 5.4. PMF vs density data and an exponentially fit curve for a typical test condition ($T = 100\text{ }^{\circ}\text{C}$, $MC = 4\%$).

5.1.4. Process for evaluating K1

Let us first consider EV1's behavior. It is observed that during a period of sustained stress, the deformation continuously varied (Figure 5.1. stage d).

$$\epsilon_{EE2/EV2} = \frac{\sigma}{E2} e^{-\frac{E2t}{K2}} \quad (5.8)$$

if $t \rightarrow \infty$, then, $\epsilon_{EE2/EV2} \rightarrow 0$

If time is long enough, the deformation of EE2/EV2 is apparently so small with increasing time that its effect may be neglected. The deformation of EE2/EV2 is approximately zero and it follows that:

$$\epsilon = \frac{\sigma}{E_1} + \frac{\sigma}{PMF} + \frac{\sigma t}{K_1} + \frac{\sigma}{E_2} \quad (5.9)$$

A method has therefore been developed to divide the behavior of EV1 from that of the other elements. The slope of the thickness versus time curve (Fig. 5.1. d) is represented by the following equation:

$$\frac{\epsilon}{\Delta t} = \frac{\sigma}{K1} \quad (5.10)$$

where, $\epsilon = (\text{thickness}_1 - \text{thickness}_2) / \text{thickness}_1$
 $\Delta t = \text{time}_1 - \text{time}_2$

The property of EV1 is therefore given by:

$$K_1 = \frac{\sigma \Delta t}{\varepsilon} \quad (5.11)$$

Different K_1 values based on different densities can be derived from groups of test results by applying a range of compressing pressures while the specimen is under constant and similar environmental condition. Figure 5.5 shows the K_1 versus density relationship, and a regression curve for those data ($K_1 = e^{A+B\rho}$).

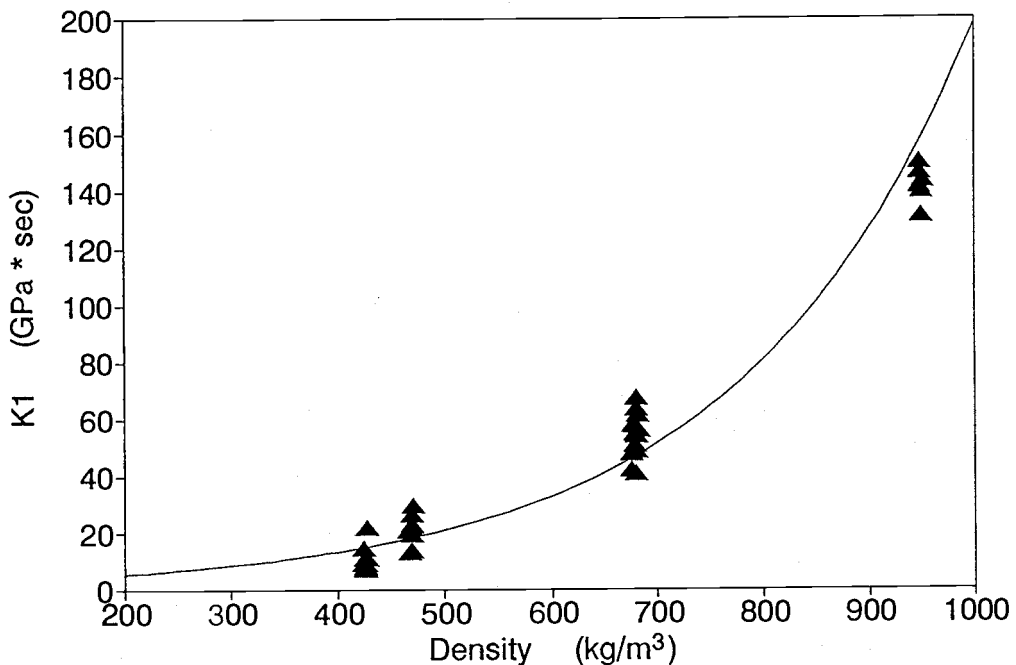


Figure 5.5. K_1 vs density data and an exponentially fitted curve for a typical test condition ($T = 100^\circ\text{C}$, $\text{MC} = 4\%$).

5.1.5. Process for evaluating E2

As we discussed in the previous section, at that part of the curve (Fig. 5.1. d) from which the K1 value is derived, the effect of EV2 is so small that its contribution to the total behavior appears to become insignificant. Therefore, if we could carefully calculate the other elemental deformations accumulated at this stage, the delayed elastic deformation will be approximately equal to the deformation of element EE2 (since the $\epsilon_{EE2/EV2} = 0$). The strain can be described by the following equation:

$$\epsilon_{total} = \epsilon_{EE1} + \epsilon_{PMF} + \epsilon_{EV1} + \epsilon_{EE2} \quad (5.12)$$

We subtract the strains of EV1, EE1 and EPMF from the total strain to obtain the strain of EE2, and then calculate a value of E2.

In this procedure, the cumulative contribution of EV1 under changing density values (and EV1 values) must be taken into account.

$$E2 = \frac{\sigma}{\epsilon_{EE2}} \quad (5.13)$$

Again, the effect of density on E2 may be explored by conducting tests under a range of mean loading values (P). Figure 5.5 shows such a set of E2 values and a regression curve ($E2 = e^{A+Bp}$) based on those data.

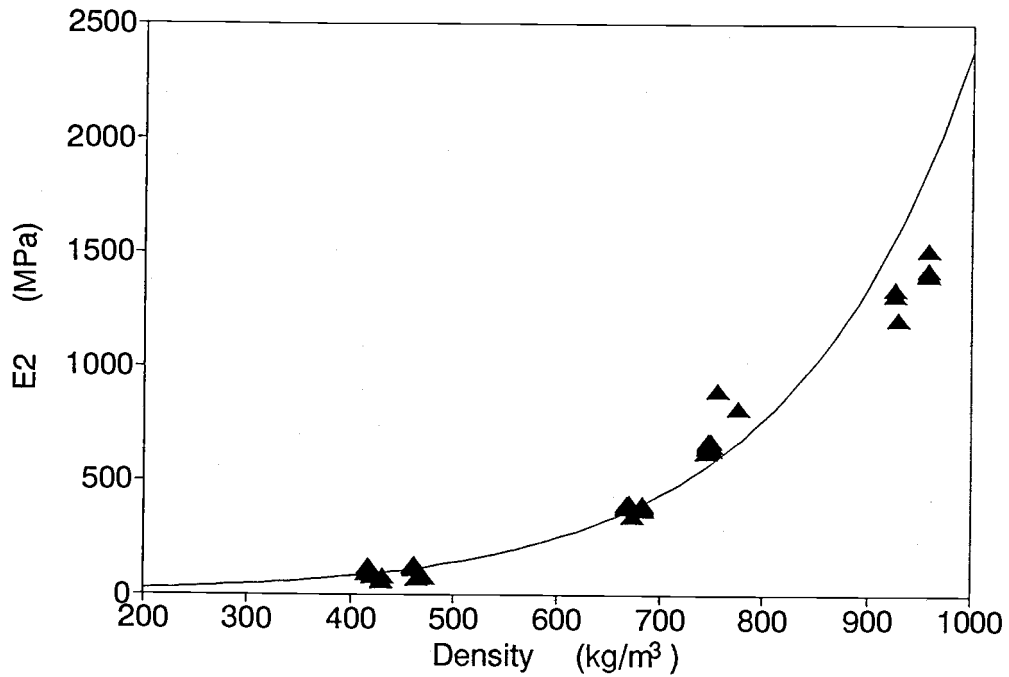


Figure 5.6. E2 vs density data and an exponentially fitted curve for a typical test condition ($T = 100^{\circ}\text{C}$, $\text{MC} = 4\%$).

5.1.6. Process for evaluating K2

Since the other four elemental properties (E1, PMF, K1 and E2) have been quantified, the deformation of EV2 may be approximated as the result of the deformations of other elements subtracted from the total deformation. Therefore, the strain of EV2 can be quantified by the following equation:

$$\epsilon_{EE2/EV2} = \epsilon_{total} - \epsilon_{EE1} - \epsilon_{PMF} - \epsilon_{EV1} - \epsilon_{EE2} \quad (5.14)$$

Since deformation of EE1, EPMF, EV1 and EE2 can be calculated, the strain of EE2/EV2 is given by:

$$\epsilon_{EE2/EV2} = \frac{\sigma}{E2} \left(e^{\frac{-E2t}{K2}} \right) \quad (5.15)$$

The value of K2 can be quantified from the following equations:

$$\begin{aligned} \ln \epsilon_{EE2/EV2} &= \ln \left(\frac{\sigma}{E2} \right) - \frac{E2t}{2.3K2} \\ K2 &= \frac{E2t}{2.3 \left[\ln \left(\frac{\sigma}{E2} \right) - \ln \epsilon_{EE2/EV2} \right]} \end{aligned} \quad (5.16)$$

By applying the same procedure as those for the other elemental properties, a group of experimental data can be used to establish the relationship between the K2 and density. Figure 5.6 represents the values of K2 and a regression curve ($K2 = e^{A+B\rho}$) based on these values.

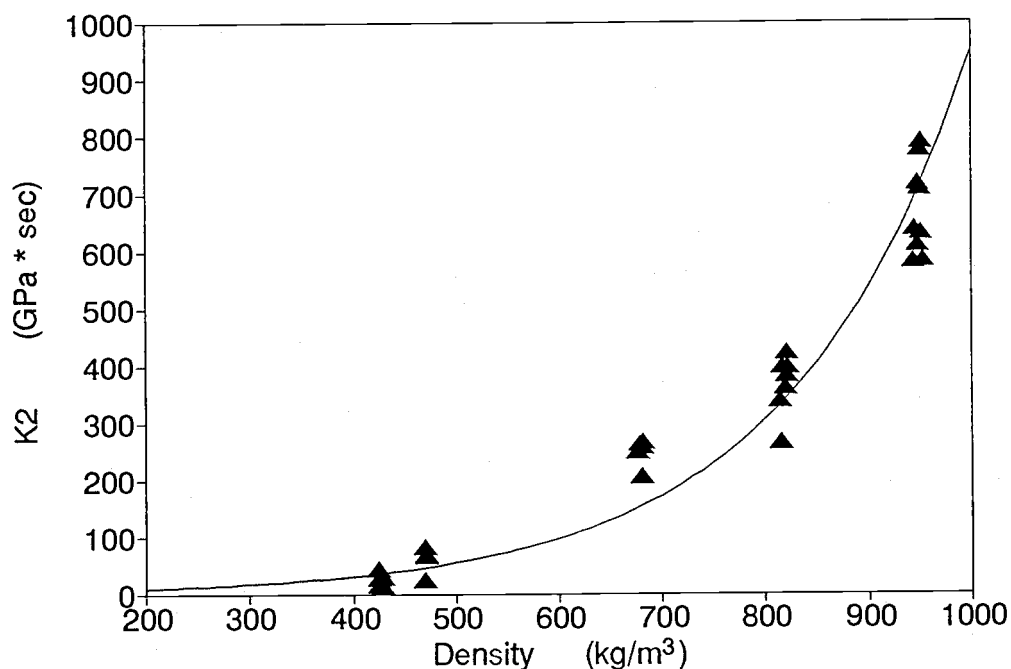


Figure 5.7. K2 vs density data and an exponentially fitted curve for a typical test condition ($T = 100^{\circ}\text{C}$, $\text{MC} = 4\%$).

Figure 5.8. shows how all five elements vary with density under a typical isothermo-hygro condition. The complete information of the whole range of temperature and moisture conditions investigated, and the nonlinear regression results are presented in Appendix II.

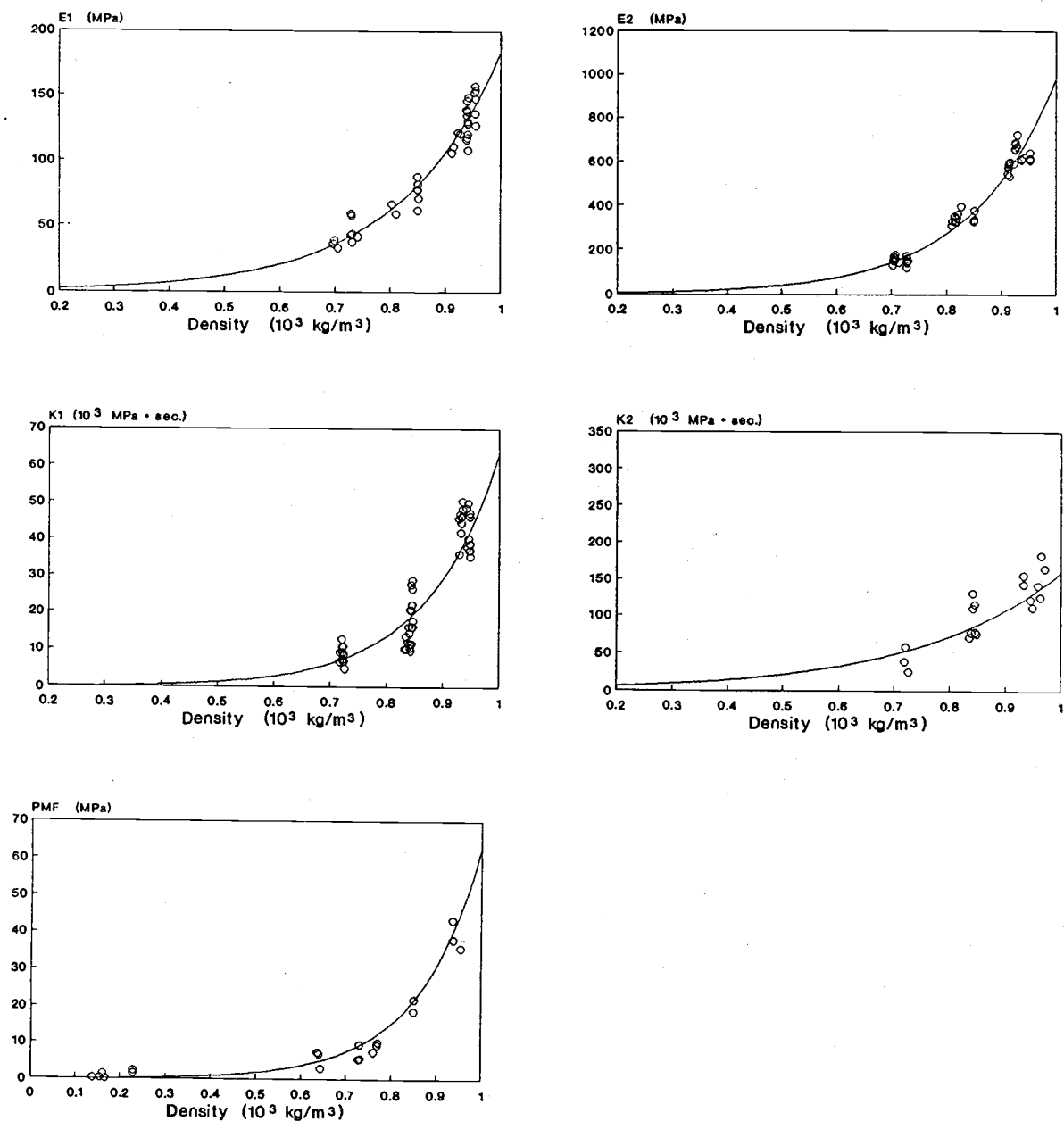


Figure 5.8. One example of the five constants vs density ($T = 150^\circ\text{C}$, $\text{MC} = 16\%$). (see Appendix II for the whole set).

5.2. Determination of thermo-hygro-effects

Having derived an approach to obtain relationships between the density and the rheological properties of materials under specific thermo-hygro conditions, the effects of temperature and moisture conditions on the rheological properties then, can be quantified by repeating this procedure. Figure 5.9 and Figure 5.10 demonstrate how the properties of five elements are effected by temperature and moisture content (complete information is given in Appendix II). Further discussion about thermo-hygro-effects is given in chapter 7.

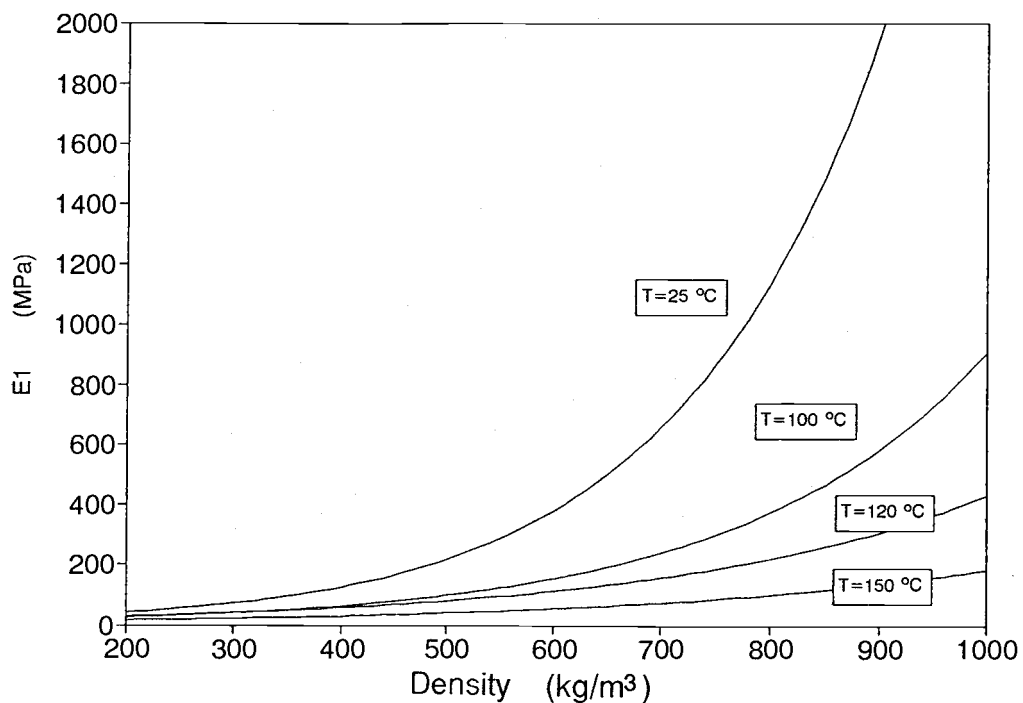


Figure 5.9. The effects of structure (density) and temperature on EE1.

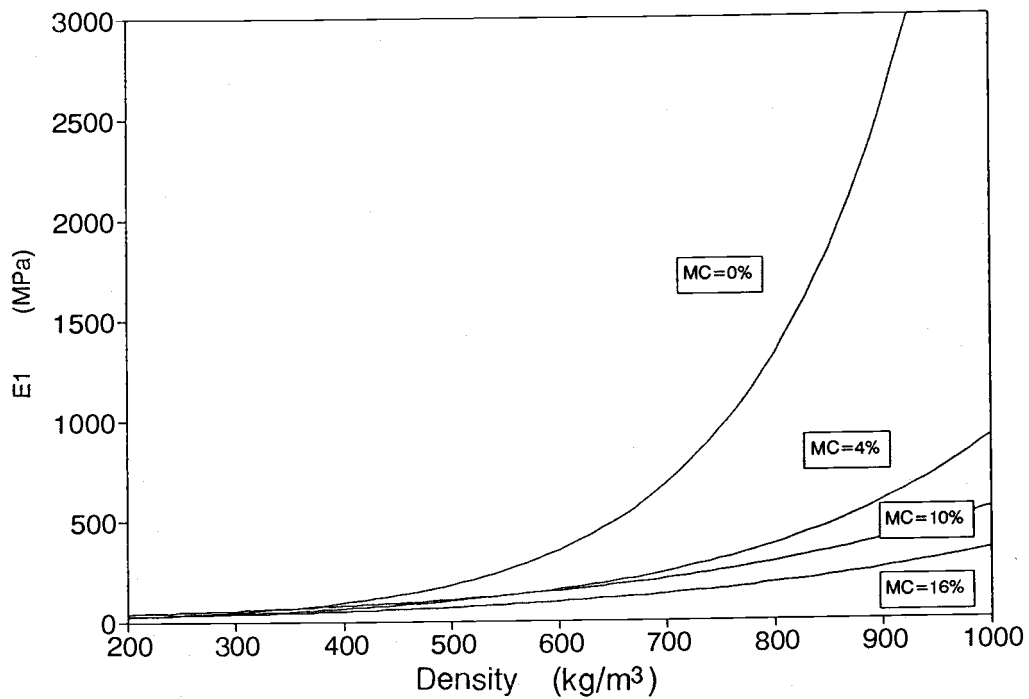


Figure 5.10. The effects of density and moisture on E_1 .

Table 5.1 summarizes the results of regression analysis of the element's behavior with density, temperature and moisture conditions. Complete regression analysis results are given in Appendix III.

Table 5.1. How the five elements are effected by density, temperature and moisture content.

EE1 = EXP (A + B *ρ)

Temp. °C	MC %	R	A	B
<hr/>				
5	0	0.964	2.72063	0.006364
100	0	0.946	2.65174	0.005479
120	0	0.912	2.59871	0.00553
150	0	0.914	2.33204	0.005544
25	4	0.904	1.88442	0.00662
100	4	0.950	2.39771	0.004411
120	4	0.864	3.05273	0.003255
150	4	0.866	2.63164	0.00321
25	10	0.932	1.79215	0.006473
100	10	0.808	2.73551	0.003331
120	10	0.783	1.68379	0.004109
150	10	0.841	-2.0938	0.008054
25	16	0.940	2.47814	0.003677
100	16	0.919	2.22265	0.002998
120	16	0.754	2.25415	0.002787
150	16	0.956	-0.21987	0.005431

EPMF = EXP (A + B * ρ)				
Temp. °C	MC %	R	a	b
25	0	0.888	-0.50492	0.008332
100	0	0.887	-0.85454	0.008572
120	0	0.913	-0.99294	0.007296
150	0	0.901	-1.26273	0.007391
25	4	0.888	-1.37924	0.009034
100	4	0.925	-0.7362	0.005974
120	4	0.894	-1.15077	0.006281
150	4	0.903	-0.39131	0.004438
25	10	0.882	-0.71583	0.00683
100	10	0.948	-0.94233	0.005706
120	10	0.947	-0.6012	0.005182
150	10	0.981	-4.58683	0.011842
25	16	0.963	-0.20318	0.004803
100	16	0.924	-0.72868	0.005008
120	16	0.829	-0.86604	0.004606
150	16	0.814	-2.94695	0.007086
EV1 = EXP (A + B * ρ)				
Temp. °C	MC %	R	A	B
25	0	0.976	7.03929	0.008572
100	0	0.918	7.05826	0.006731
120	0	0.938	6.72563	0.006975
150	0	0.899	6.58855	0.006413
25	4	0.986	7.2095	0.006741
100	4	0.917	7.69316	0.004504
120	4	0.943	6.8686	0.005591
150	4	0.945	5.44764	0.006515
25	10	0.957	6.99715	0.006353
100	10	0.929	6.97595	0.004208
120	10	0.862	4.95519	0.006469
150	10	0.874	2.09287	0.00956
25	16	0.967	7.3551	0.004358
100	16	0.972	5.4637	0.005804
120	16	0.962	2.94444	0.008896
150	16	0.920	3.31537	0.007739

EE2 = EXP (A + B * ρ)				
Temp. °C	MC %	R	A	B
25	0	0.989	2.09391	0.008599
100	0	0.974	2.0031	0.007899
120	0	0.968	1.76593	0.00736
150	0	0.958	1.29433	0.007898
25	4	0.969	1.50248	0.008205
100	4	0.975	2.10239	0.005674
120	4	0.955	2.76024	0.005139
150	4	0.952	1.96528	0.00523
25	10	0.972	1.94875	0.007296
100	10	0.985	2.27419	0.004879
120	10	0.985	3.19372	0.003712
150	10	0.933	-0.88903	0.011727
25	16	0.952	2.56073	0.00484
100	16	0.985	1.47303	0.005417
120	16	0.941	2.60589	0.003975
150	16	0.981	0.45006	0.006443

(Table 5.1. continued)

EV2 = EXP (A + B * ρ)

Temp. °C	MC %	R	A	B
<hr/>				
25	0	0.940	7.71583	0.010469
100	0	0.949	7.14709	0.009689
120	0	0.920	8.13388	0.006967
150	0	0.979	4.82398	0.011632
25	4	0.972	6.67971	0.010772
100	4	0.951	8.06327	0.005701
120	4	0.928	6.86583	0.006274
150	4	0.900	6.61729	0.006925
25	10	0.962	5.89206	0.012053
100	10	0.943	6.81938	0.006213
120	10	0.916	6.26179	0.006568
150	10	0.876	5.74813	0.005891
25	16	0.963	7.48219	0.006749
100	16	0.907	5.97159	0.00699
120	16	0.897	6.52881	0.005758
150	16	0.867	7.99562	0.003984

CHAPTER 6. RESULTS AND DISCUSSION I

--Preliminary evaluation of the model--

Following establishment of the rheological model and quantification of the rheological parameters of the tested materials (from experimental results), it is necessary to find if the model logically and usefully represents the material's behavior. Only a preliminary evaluation is presented in this chapter since the main focus of the research was development of the experimental techniques.

6.1. Evaluation of the physical principles of the model

The relations between stress and strain:

Figure 6.1. shows an example of load-deformation relation predicted by the model. With a given loading cycle, the deformation continuously varies.

Since the structure and associated properties of wood composite materials during compression varies continuously, the deformations are not only time dependent but also structure dependent.

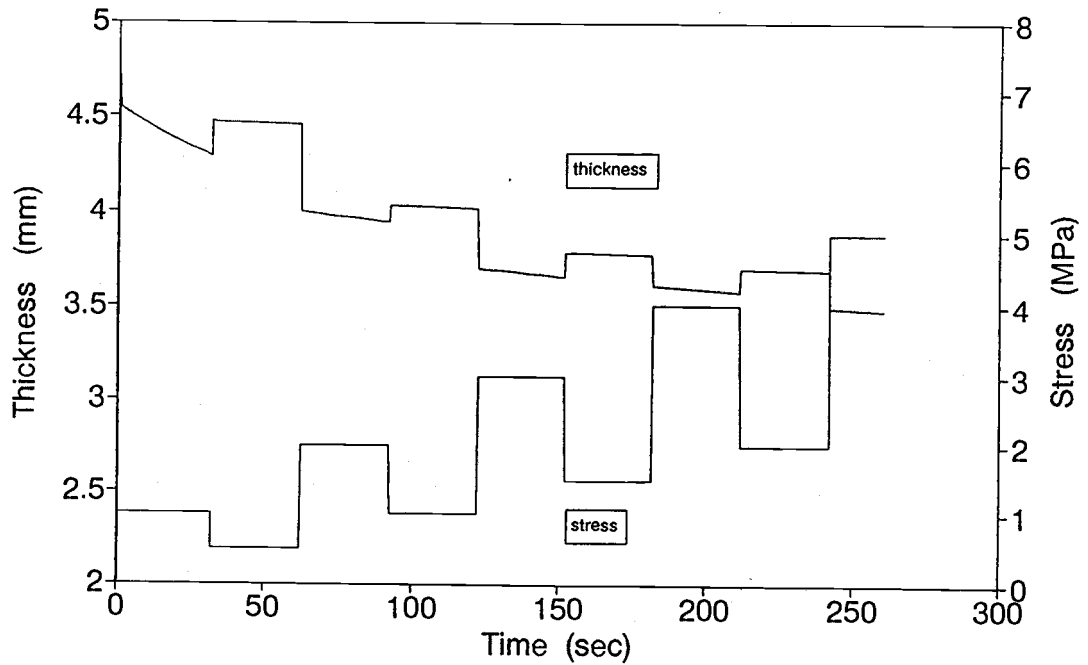


Figure 6.1. Predicted thickness versus time curve for a given load curve.

Temperature effects:

It is well known that the wood materials are easily softened and deformed under high temperatures. Figure 6.2. shows deformation curves predicted by the model under different isothermal conditions when the moisture content was held constant. As expected, the higher deformations were predicted under the higher temperature conditions (Fig. 6.2. curve of 120 °C).

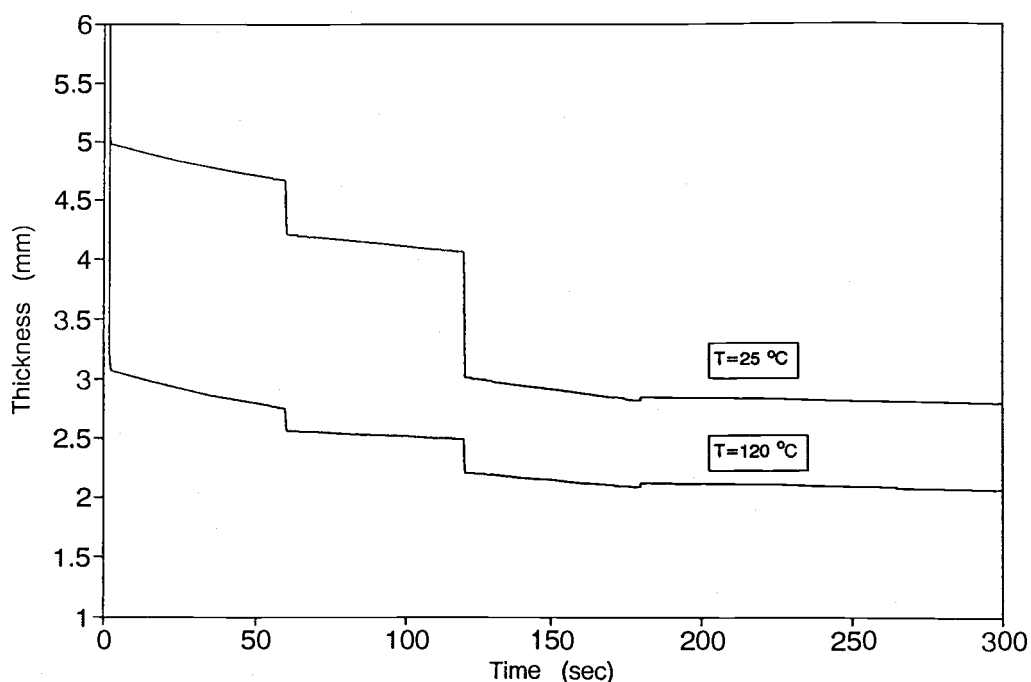


Figure 6.2. Typical predicted temperature effects on rheological deformation (MC = 4 %).

Moisture effects:

Moisture effects on the mechanical behavior are a little more complex than those for temperature. However, under high moisture conditions, the thermal effects are quite obvious. The higher moisture contents make the materials more easily relocated and deformed — as would be expected from well known effects of cell wall moisture on properties. From the predicted curves in Figure 6.3, the effects of the moisture were observed when the temperature was held constant.

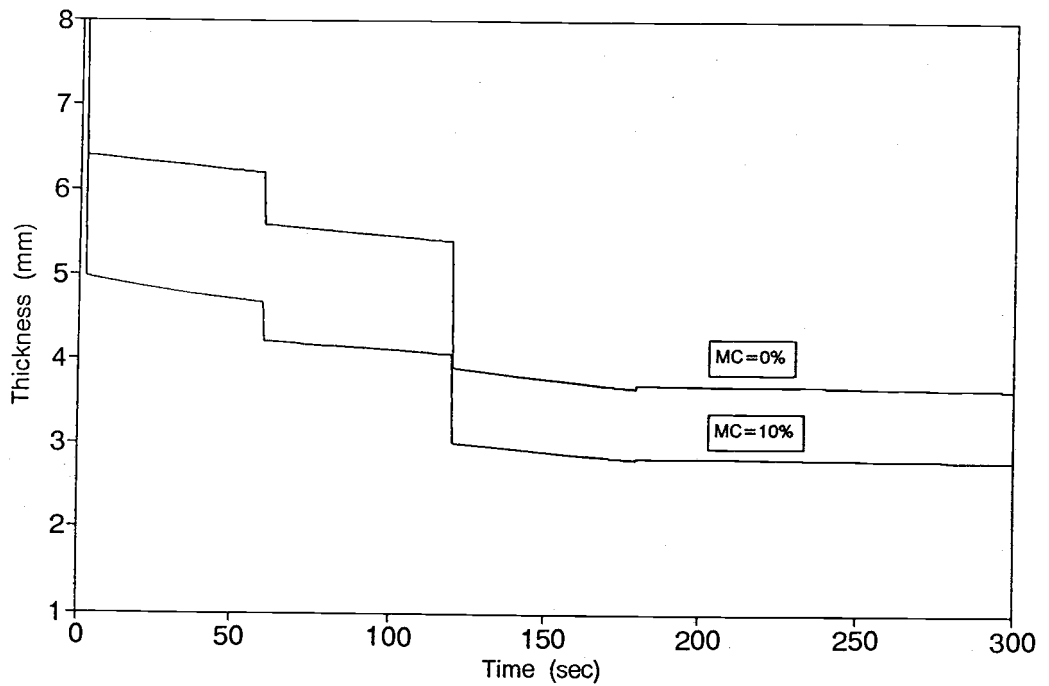


Figure 6.3. Typical predicted moisture effects on deformation ($T = 100\text{ }^{\circ}\text{C}$).

6.2. Rheological parameters

Figure 6.4. suggests that some of the derived rheological properties are logically dependent on density. Furthermore, for example, Figure 6.5 shows that the $E1$ values increase with density, but temperature reduction coupled with moisture increase causes the $E1$ curve to shift downward.

According to the values of these parameters and the rheological model discussed in chapter 3 and 5, elements of $EE1$ and $EPMF$ are more sensitive than the other elements

during the initial stages of the compression cycle. With time increases, the sensitivity of EE2 increases while that of EV2 decreases. EV1's influence is relatively small over the times of concern here. Since this is a preliminary evaluation, a complete range of tests have not been conducted here.

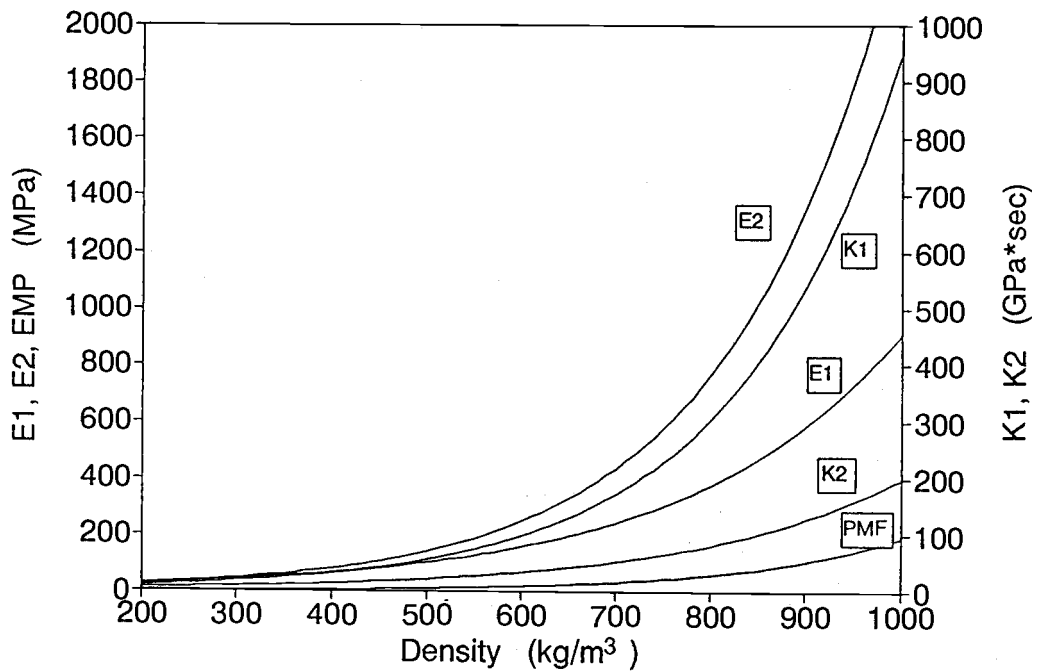


Figure 6.4. Typical variation of the five elements with density ($T = 100\text{ }^{\circ}\text{C}$, $\text{MC} = 4\%$).

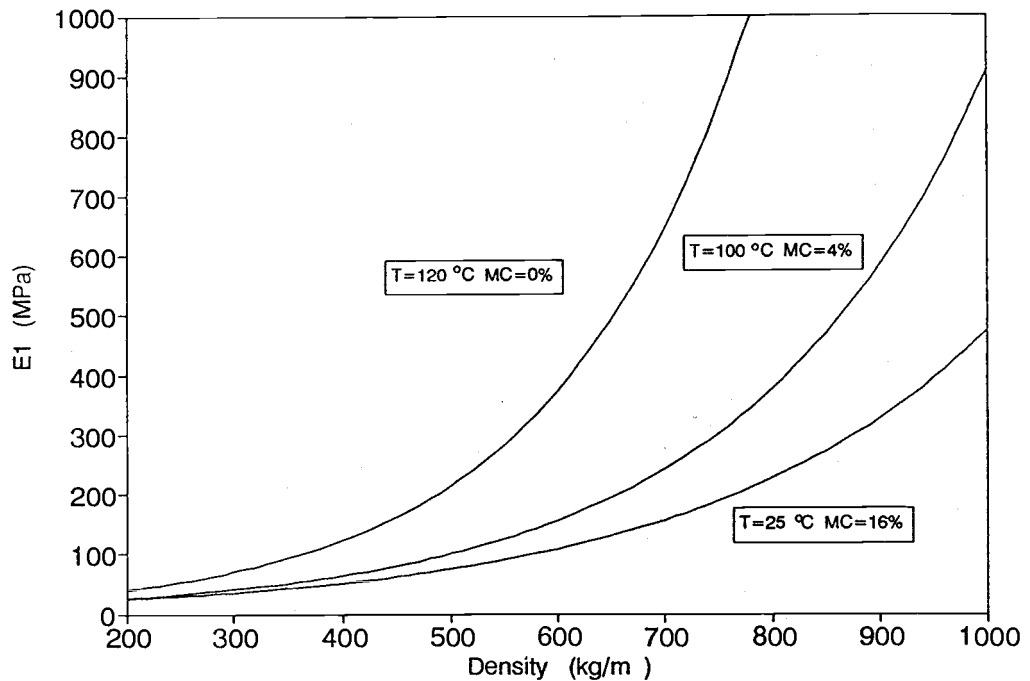


Figure 6.5. Typical variation of E1 under different temperature and moisture conditions.

6.3. General evaluation of the model

Absolute evaluation of accuracy of the elements is difficult in the absence of supporting literature. Comparisons will therefore be made between predicted and experimentally measured behavior for a range of dynamic loading cycles.

Figure 6.6. shows specially designed experimentally executed loading and corresponding deformation curves, together with the deformation curve predicted by the model.

The difference between the two curves reflects the quality of the model. Discrepancies are generally relatively small and will be discussed in a little more detail in following sections.

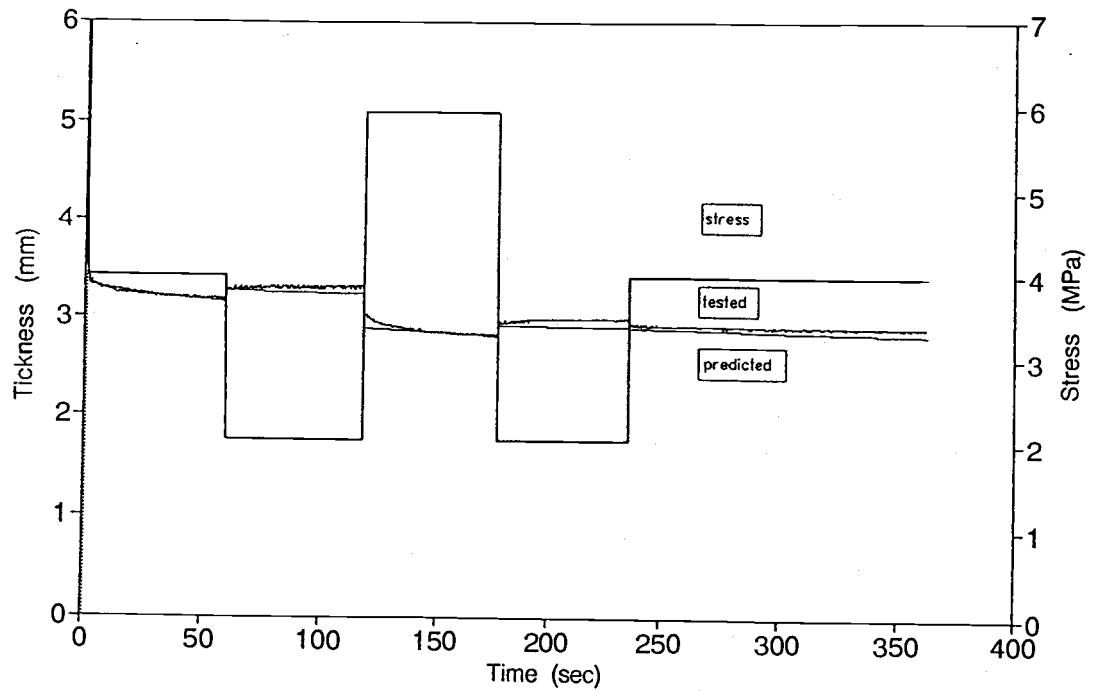


Figure 6.6. Comparisons between experimental and predicted deformation for a specially designed loading cycle.

6.3.1. Prediction of instantaneous behavior

From Figure 6.7. we can see that there are some differences between the predicted and experimental results. The discrepancy is within 7%.

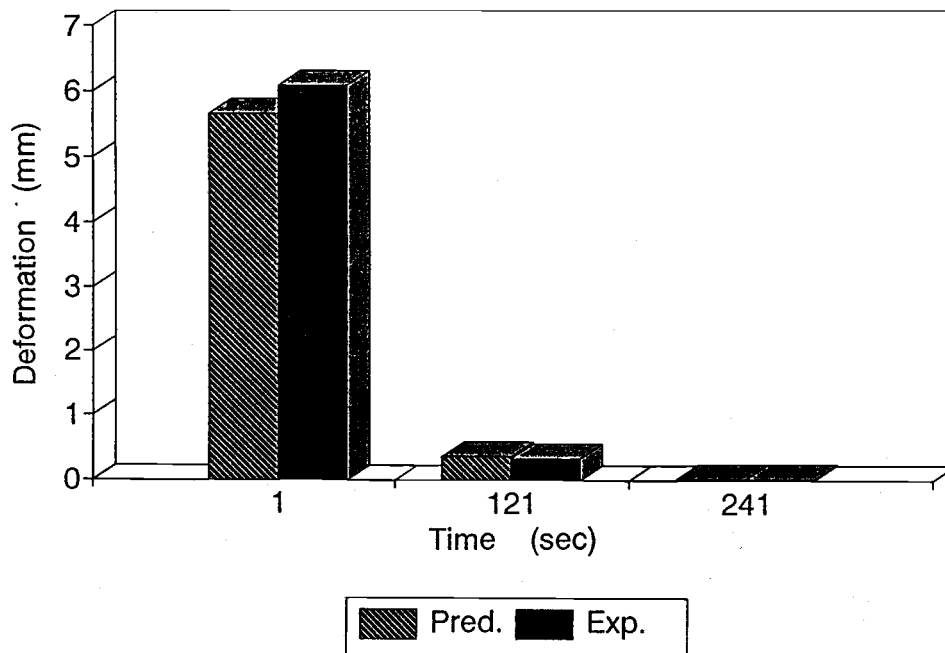


Figure 6.7. Comparisons of predicted and experimental instantaneous compression behavior (effect of EE1) for loading curve as Fig. 6.6 shown.

Figure 6.8 shows the difference between the results of instantaneous compression (at 121 sec) and relaxation (at 181 sec) under similar differential stresses. The deformation of compression (including effects of EPMF and EE1) obviously differs from that of relaxation (with only

effect of EE1). Therefore, the effects of EE1 can not represent the completed instantaneous deformation of compression conditions during wood composite manufacture. The EPMF is necessary to be developed to study this kind of behavior.

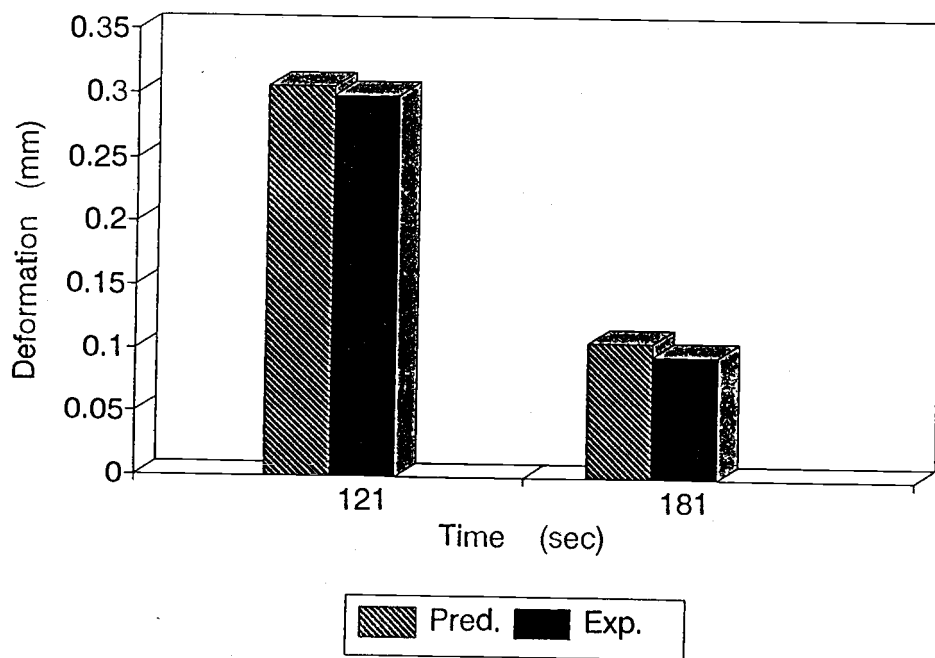


Figure 6.8. Comparisons between instantaneous relaxation deformation of EE1 and compression deformation of EPMF + EE1 for loading curve as Fig. 6.6. shown.

6.3.2. Prediction of time dependent behavior

Time dependent behavior mainly consists of the delayed elastic deformation and the viscous deformation which are

represented by EE2, EV2, and EV1. However, with the changes of structure (density), the rheological properties also vary.

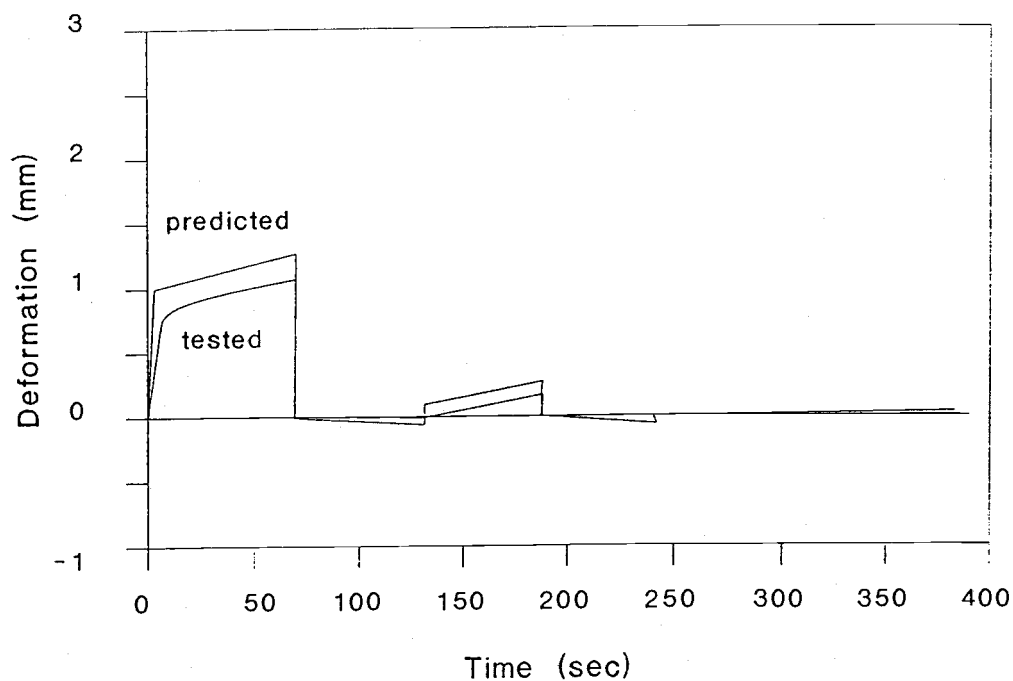


Figure 6.9. Predicted and tested time-dependent behaviors for the loading given in Fig. 6.6.

From Figure 6.9 we can see that the time dependent behavior was quite well predicted, especially at the later stages of deformation. The discrepancy in the early stages was less than 8%, and at the late stages was less than 5%.

6.3.3. The workable range of the model

The useful range of the loading pressure, density, temperature and moisture conditions is shown in Table 6.1.

Table 6.1. Approximate working ranges of the present model.

Compression pressure:	0 -- 7 MPa
Density:	250 -- 1200 kg / m ³
Temperature:	25 -- 180 °C
Moisture content:	0 -- 16 %

6.3.4. Prediction of environmental effects

Temperature effects:

Figure 6.10 shows a typical example of predicted curves of rheological deformation that take place under a range of temperature conditions. Since the thermo-effects on properties of each element can be quantified and predicted, the thermo-effects on the rheological behavior of the whole material also can be predicted.

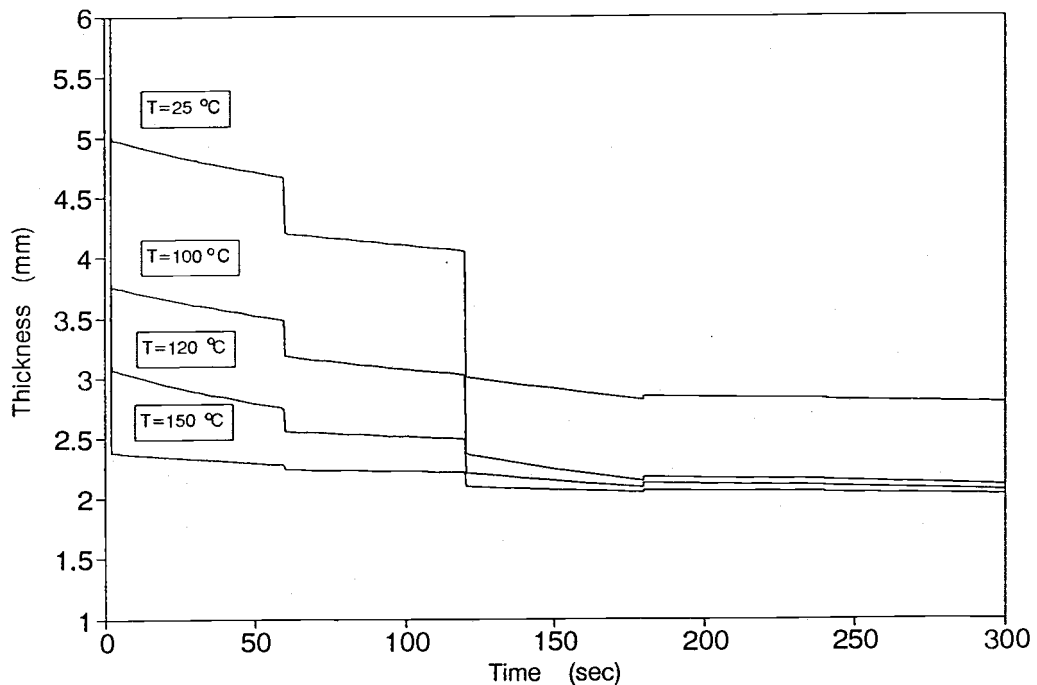


Figure 6.10. Predicted temperature effects on rheological behavior for loading curve shown in Fig. 6.6.
(MC = 16%, T = 25, 100, 120, 150°C).

Moisture effects:

Since the hygro effects on properties of each element can be quantified and predicted, the hygro effects on the rheological behavior also can be quantified and predicted. Figure 6.11. shows examples of predicted curves for deformation taking place under a range of moisture conditions.

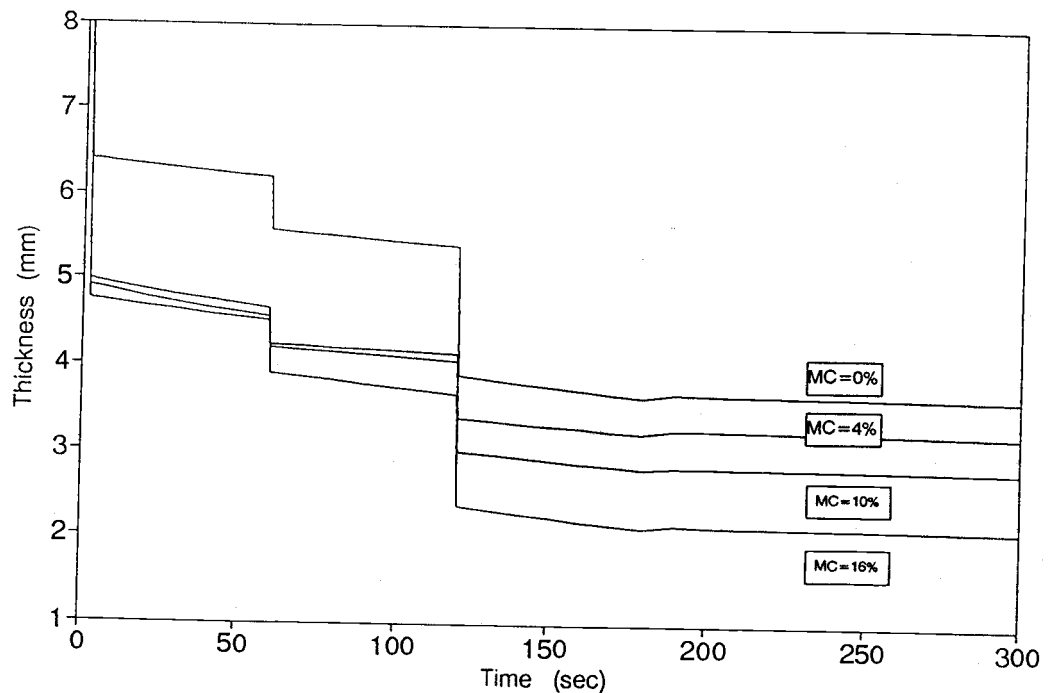


Figure 6.11. Examples of predicted moisture effects on rheological behavior for the loading curve shown in Fig. 6.6 ($T = 100\text{ }^{\circ}\text{C}$, $MC = 0, 4, 10, 16\%$).

6.3.5. Predicting initial thickness

The model may be applied in many ways to study the materials behavior. For instance, if a specific density is needed after compression, we can apply the model inversely from the desired density (final thickness) to predict initial thickness based on different compression cycles and environmental conditions. Then we may design a loading cycle and select initial thickness of specimen to produce required

thickness. Figure 6.12. shows an example of how to predict the initial thickness under a designed condition of loading, temperature and moisture (steady-state condition in this example) from known final thickness. Applying inversely calculation based on the model and test conditions, the initial thickness can be predicted (deformation start at right).

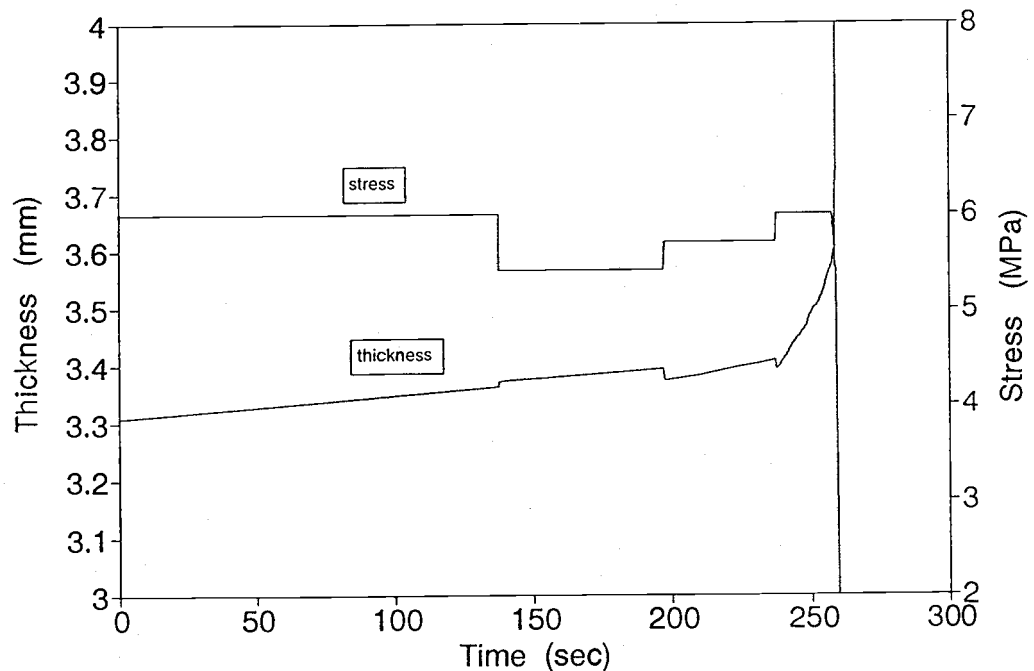


Figure. 6.12. Prediction of initial thickness from known required final thickness and pressing conditions ($P = 6$ MPa, $T = 100$ °C, $MC = 0$ %).

Due to the limited ranges of load, temperature and moisture investigated, the capability of this model has been verified only over a relatively narrow range.

The applicability of the model to other composite materials is not clear. However, having established the experimental and numerical approaches, it should be feasible to apply similar techniques to a diverse range of raw material combinations.

The present research has focused on experimental techniques. However, some brief discussion about thermo-hygro effects on the behavior will also be presented in the next chapter.

Some specific examples of material behavior that does not fall within the assumptions of the general rheological theories will also be considered.

CHAPTER 7. RESULTS AND DISCUSSION II

--Thermo-hygro rheological behavior--

Thermo-hygro-rheological behavior of wood furnish materials (as functions of density, time, temperature and moisture condition) during compression will be deliberated in this chapter.

The underlying mechanisms which may influence rheological characteristics are addressed in section 7.1, then sections 7.2, 7.3 and 7.4 present the effects of the structure, temperature and moisture respectively. The energy consumption of the rheological deformation are addressed in section 7.5.

7.1. Causes of the rheological behavior of wood furnish materials under compression

Clearly, the wood furnish materials are deformed and partially damaged (micro-structurally) under the influence of varying compressive pressures. The materials sustain intricate elastic, delayed elastic, viscous, plastic-micro-fracture changes, and these progress in an unsteady-state fashion as pressing proceeds (Fig. 7.1). Therefore, the behavior is the superposition of the five different elemental behaviors.

Theoretically, the rheological behavior of the materials should be a superposition of the five elements' behavior and their interactions (although the later have not been included in the present models). After the rheological parameters of the tested materials have been obtained, the contribution of each element may then be predicted for a given loading cycle.

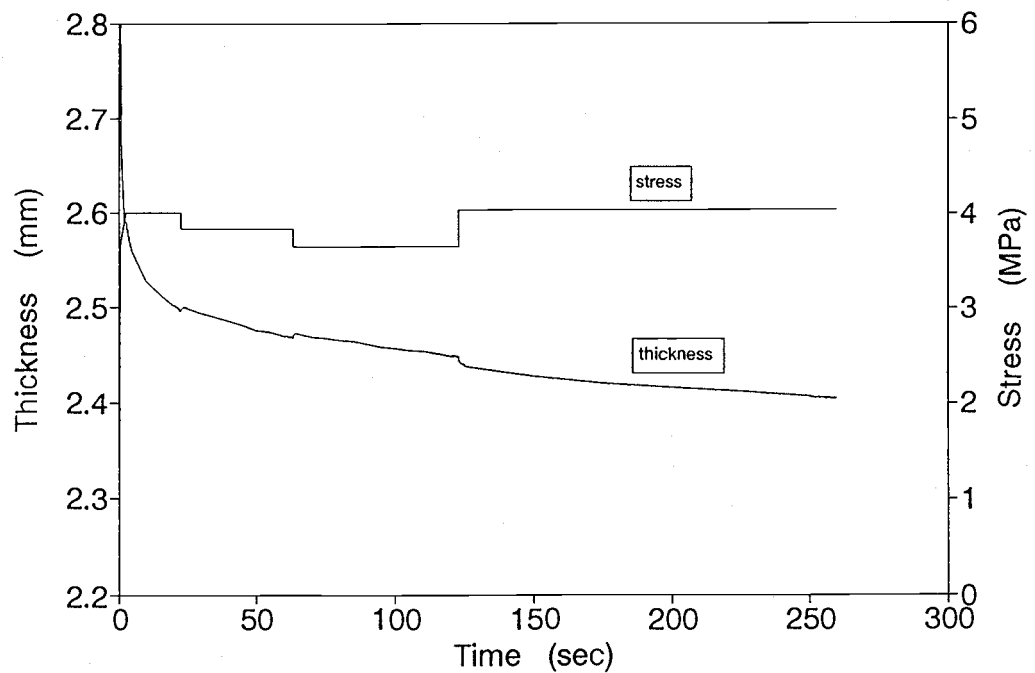


Figure 7.1. Curves representing typical rheological behavior of a fiber network under compression ($T = 100^{\circ}\text{C}$, $\text{MC} = 10\%$).

7.1.1. Predicted behavior of EE1 for a given loading cycle

Since E1 is affected by density, the actual deformation of EE1 is caused not only by varied stress but also by changes in structure.

The behavior of EE1 varies nonlinearly with density, but the deformation of EE1 may be cumulatively predicted:

$$\epsilon_{EE1} = \frac{\sigma}{E1} = \frac{(th - the1)}{th}$$

$$the1 = th \left(1 - \frac{\sigma}{E1}\right) \quad (7.1)$$

where, th: given thickness.
the1: EE1 effected thickness.

Deformation of EE1 = th - the1.

Applying this equation (7.1) to the experimental data will enable the deformation of this element during a specified test to be predicted. In this procedure, element values (which continuously change with density) are obtained from the measured thickness versus time data. Stress values are those actually used in the corresponding compression tests. This approach has been used for all the following elements. Figure 7.2. shows the predicted behavior of EE1 under the given loading sequence.

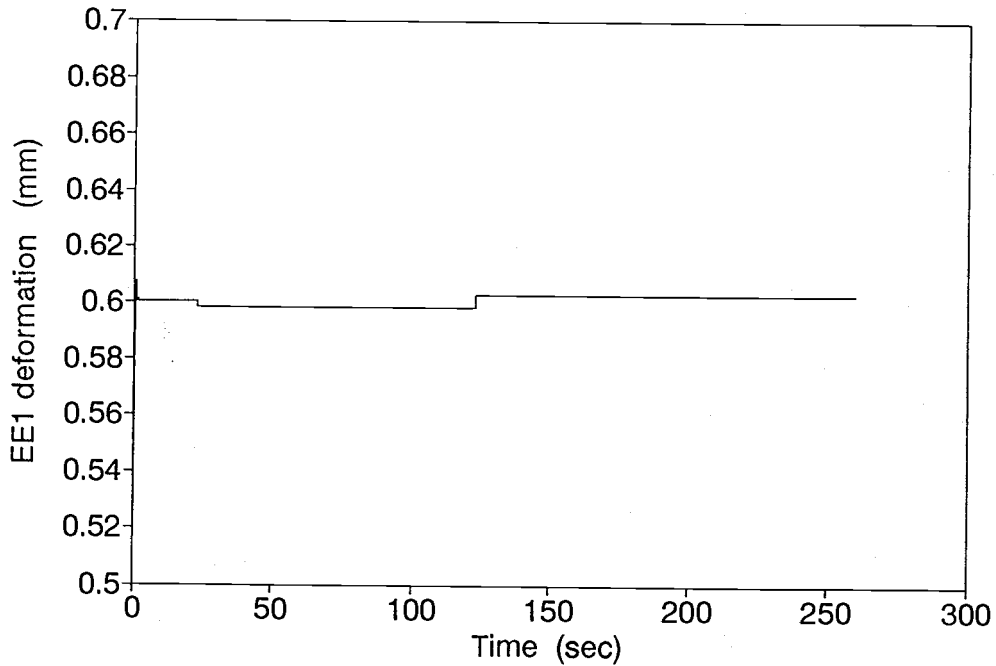


Figure 7.2. Predicted behavior of EE1 (derived from loading cycle of Fig. 7.1, $T = 100^{\circ}\text{C}$, $\text{MC} = 10\%$).

7.1.2. predicted behavior of EPMF for a given loading cycle

Deformation sustained by EPMF consists of the deformations from given stress and from consequential changes in density. Since the behavior of EPMF varies in a nonlinear fashion with density, a calculation of the deformation of EPMF during any given testing cycle may be predicted (Fig. 7.3).

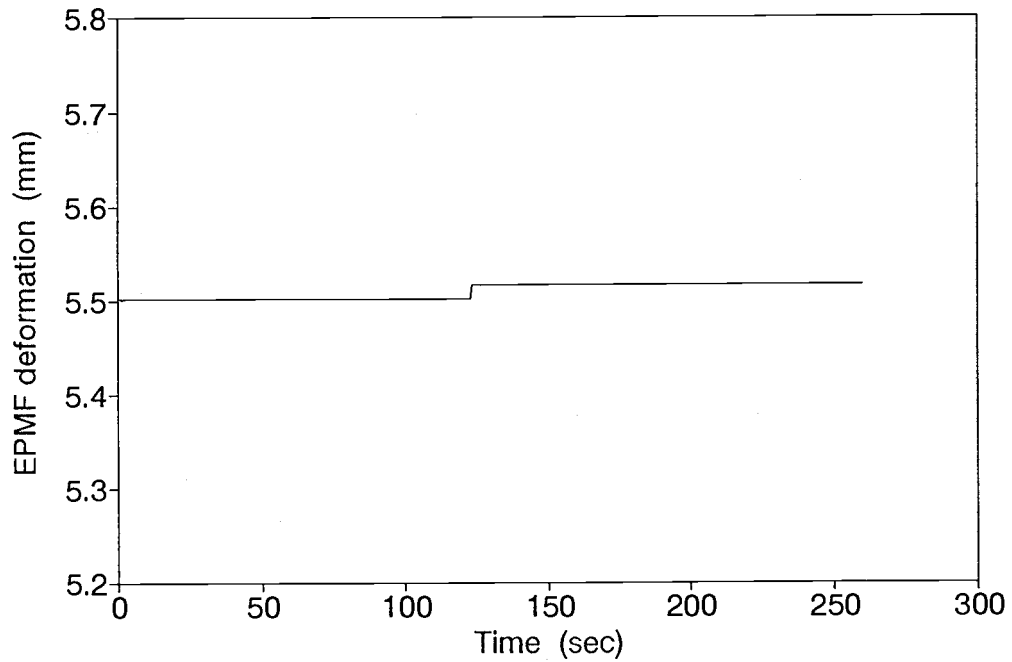


Figure 7.3. Predicted behavior of EPMF (derived from loading cycle of Fig. 7.1, $T = 100^{\circ}\text{C}$, $\text{MC} = 10\%$).

$$\epsilon_{PMF} = \frac{\sigma}{PMF} = \frac{(th - th_{pmf})}{th}$$

$$th_{pmf} = th \left(1 - \frac{\sigma}{PMF} \right) \quad (7.2)$$

where, th : given thickness.
 th_{pmf} : EPMF effected thickness.

Deformation of EPMF = $th - th_{pmf}$.

7.1.3. Predicted behavior of EV1 for a given loading cycle

Following initial instantaneous deformation, the material continuously deformed under constant compression. This deformation mainly consists of delayed elastic deformation from both EE2 and EV2, and the viscous deformation of EV1. However, the values of E1 and PMF also vary with the continuously changing density. This means that the deformation of these two elements are also effected. The deformation of this stage can be shown as the equation shown at the start of chapter 5.

Since the behavior of EV1 is nonlinear and based on density, a calculation of the deformation of EV1 at each test may be conducted as follows.

$$\epsilon_{EV1} = \frac{\sigma t}{K1} = \frac{(th - thv1)}{th}$$

$$thv1 = th \left(1 - \frac{\sigma t}{K1}\right) \quad (7.3)$$

where, th: given thickness.
thv1: EV1 affected thickness.
t: time.

Deformation of EV1 = th - thv1.

Applying equation (7.3) to the experimental data supplies the actual deformation from this element and how it varies during the given testing cycle (Fig. 7.4). Since K1

is a function of density, any variation of load, which may cause the variation of deformation, may affect the behavior of EV1. Therefore, deformation of EV1 does not vary continuously with the load.

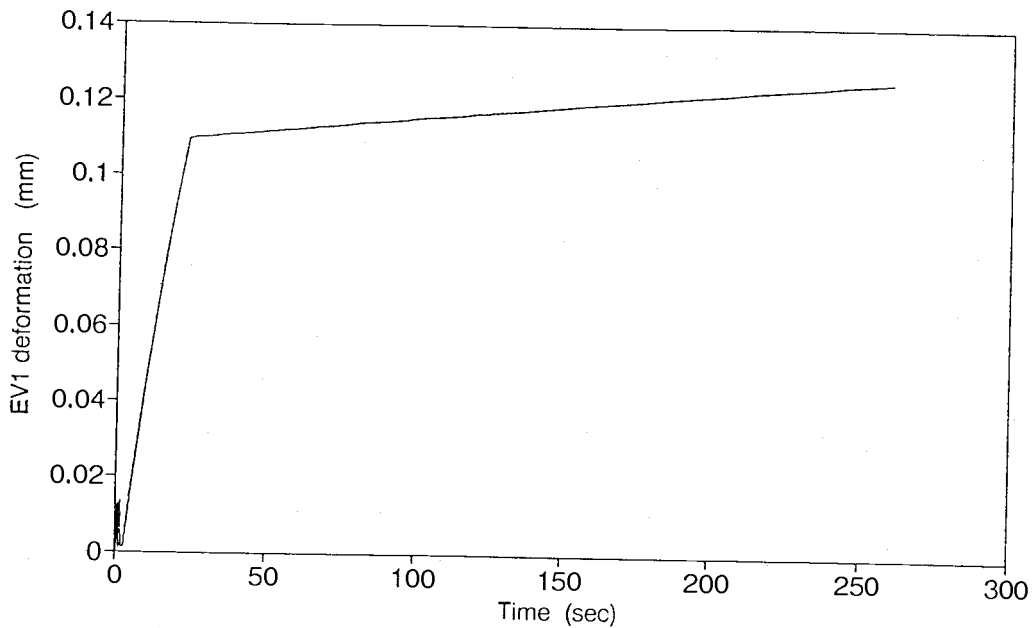


Figure 7.4. Predicted behavior of EV1 (derived from loading cycle of Fig. 7.1, $T = 100\text{ }^{\circ}\text{C}$, $MC = 10\%$).

7.1.4. Predicted behavior of EE2 and EV2 for a given loading cycle

The behavior of EE2 and EV2 (delayed elastic) is represented by the following equation:

$$\epsilon_{(\text{delayed elastic})} = \frac{\sigma}{E2} - \frac{\sigma}{E2} e^{\frac{-E2 t}{K2}} \quad (7.4)$$

Behavior of EE2:

The deformation of EE2 also is stress and density induced. It is the total deformation subtracted by the deformations of other elements.

It follows that:

$$\epsilon_{EE2} = \frac{\sigma}{E2} = \frac{(th - the2)}{th}$$

$$the2 = th \left(1 - \frac{\sigma}{E2}\right) \quad (7.5)$$

where, th: given thickness.
the2: EE2 effected thickness.

Deformation of EE2 = th - the2.

Again, deformation from this element may be predicted (Fig.7.5.).

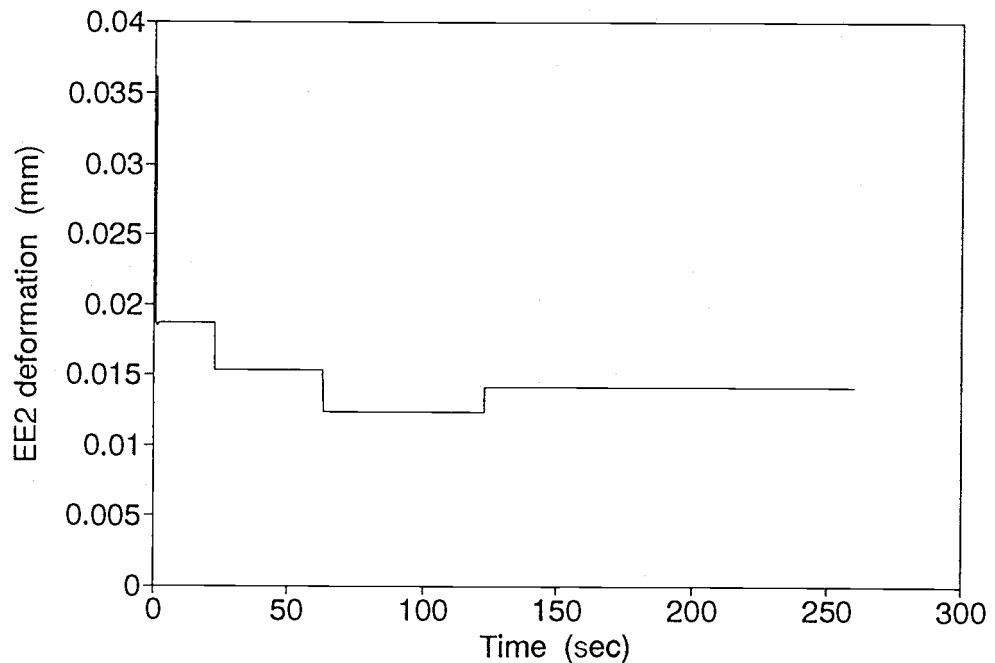


Figure 7.5. Predicted behavior of EE2 (derived from loading cycle of Fig. 7.1, T = 100 °C, MC = 10 %).

Behavior of EV2:

The actual deformation of EE2 associates to the properties of EV2. The values of EE2/EV2 (see equation 7.6) is given by the strains of EE1, EPMF, EV1 and EE2 subtracted from the total strain.

$$\epsilon_{EE2/EV2} = \epsilon_{total} - \epsilon_{EE1} - \epsilon_{PMF} - \epsilon_{EV1} - \epsilon_{EE2}$$

$$\epsilon_{EE2/EV2} = \frac{\sigma}{E2} e^{\left(\frac{-E2t}{K2}\right)} \quad (7.6)$$

$$the2v2 = th \left(1 - \frac{\sigma}{E2} e^{\left(\frac{-E2t}{K2}\right)}\right) \quad (7.7)$$

where: th: given thickness.
the2v2: EE2 and EV2 affected thickness.
t: time.

Deformation of EE2/EV2 = th - the2v2.

The strain of EV2 may be reconstructed individually or in the form of EE2/EV2 (equation 7.6) for each test.

As for the other elements, applying this equation (7.7) to the experimental data enables the actual deformation from this element and how it varies to be predicted (Fig. 7.6).

It should be remembered that EE2 and EV2 both change continuously with changing density. The impact of this is most obvious when loads change instantaneously. Then, density and corresponding element values change greatly and this results in apparent instantaneous delayed elastic deformation. This is clearly contrary to expected behavior

associated with the acknowledged effect of density on elemental properties. The superposition of the behavior of these two elements will show the delayed elastic behavior (Fig. 7.8).

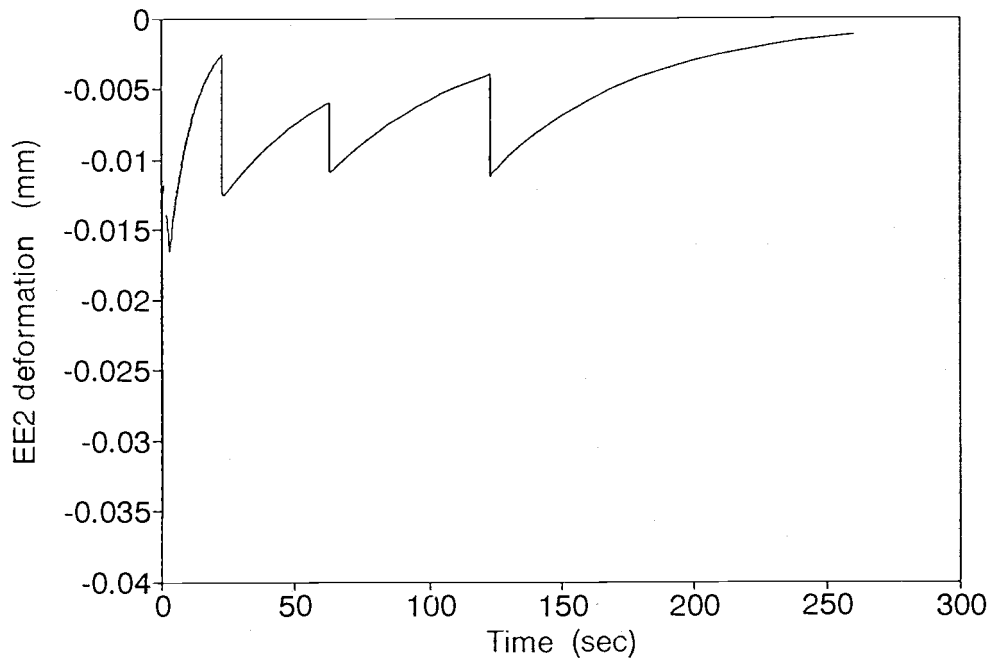


Figure 7.6. Predicted behavior of EE2/EV2 (derived from loading cycle of Fig. 7.1, $T = 100^{\circ}\text{C}$, $\text{MC} = 10\%$).

7.1.5. Predicted behavior of all five elements combined

Figure 7.7 shows a curve reconstructed from the behavior of the five elements as discussed above. Figure 7.8 shows the deformations of five elements at each stage of compression after instantaneous deformation. It may help us to understand the rheological behavior of each element.

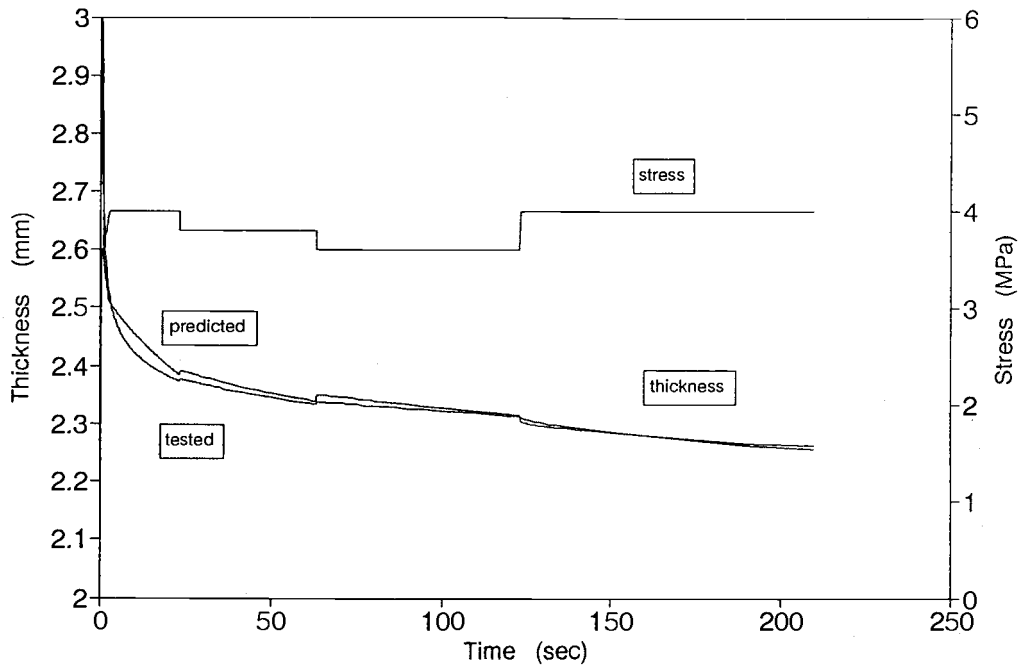


Figure 7.7. A reconstructed rheological curve from the behaviors of the five elements (combination of Fig.7.1, 7.2, 7.3, 7.4, 7.5, 7.6).

The deformation in the initial stage of compression mainly is from the effects of EPMF and EE1 which reflects the relocation and fracture of the fibers (EPMF, Fig.7.3), and elastic effects (EE1, Fig. 7.2). With time increases, the deformation continuously increases even during periods of constant compression. One part of this increase is from the delayed elastic effect; the effect of EE2/EV2 rapidly increases from negative values to zero (EE2/EV2, Fig. 7.6 and 7.8) so that the deformation of the EE2 is delayed (EE2, Fig. 7.5 and 7.8). However, this delay also depends on the variation of density. Another part of the time-dependent deformation is due to viscous deformation (EV1 in Fig. 7.4

deformation is due to viscous deformation (EV1 in Fig. 7.4 and 7.8). Deformations of these three elements continuously varied with time (Fig. 7.1. and 7.8).

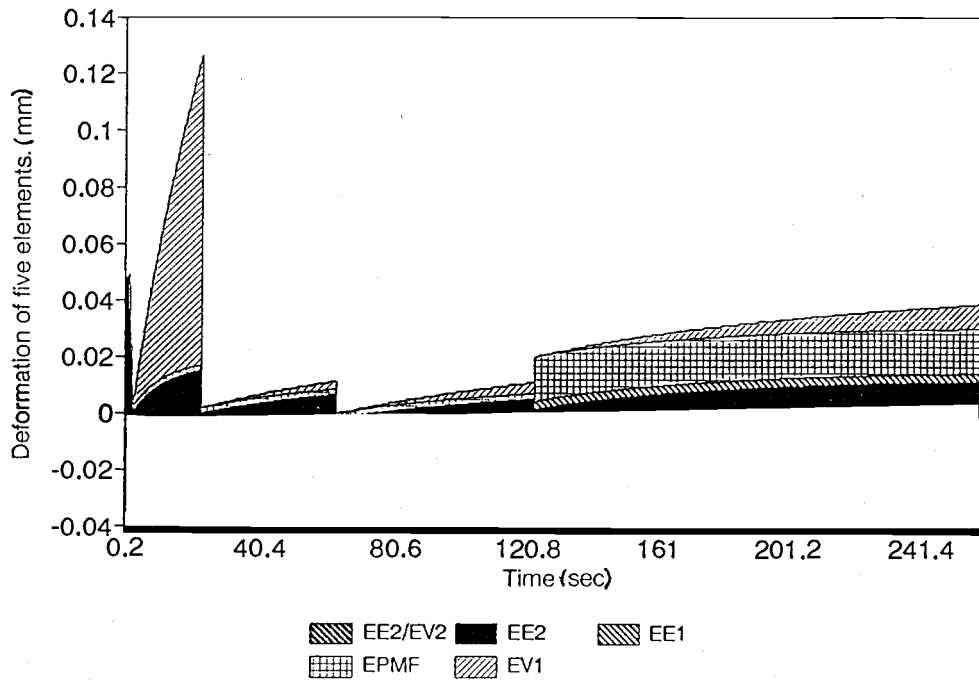


Figure. 7.8. Five-element deformation after initial instantaneous deformation (combination of Fig. 7.2, Fig. 7.3, Fig. 7.4, Fig. 7.5, Fig. 7.6).

With density increases, the effects of EPMF and EE1 also vary. This suggests that with increasing density, fracture and relocation of the micro-structure also takes place. High density could possibly lead to more uniform internal stress distributions.

After a certain time period, the delayed elastic deformation is fully developed and subsequent deformation rates are approximately linear (when values of EE2/EV2

strain mainly is from EV1 (the viscous properties of the fiber network, and the effects of EE1, PMF, and EE2/EV2 on the materials varied insignificantly).

If the behavior of the five elements could be controlled in a desired way, the hot pressing process and the quality of final products may be improved. For instance, in order to avoid any destruction of wood-adhesive adhesion, the adhesive should not be fully polymerized until the deformation (behavior) of EE1 and EPMF are fully developed.

Since the property of EE1 increases with density, under similar stress conditions, the higher E1 value leads to lower strains and that results in reduced spring back (thickness increase). Therefore, EE1 may be manipulated to avoid internal failure during hot press opening. The localized internal bond strength should be larger than the internal stress upon press opening to avert EE1 product failure.

The dimensional stability of wood composite materials at later stage of hot pressing (even after pressing) mainly depends on the behavior of EV1, EE2 and EV2 from Fig. 7.8. The larger the values of these elements, the less time-dependent deformation (relaxation process) will occur. Therefore, the better dimensional stability.

This research therefore, is important for its potential application in product manufacture (hot pressing).

7.2. Structural effects

A study of the rheological behavior in terms of structural properties is important, especially for engineering composite materials. The structure and associated properties change continuously as pressing proceeds (see Fig. 7.9) and it directly effects the manufacturing process and the properties of the final product.

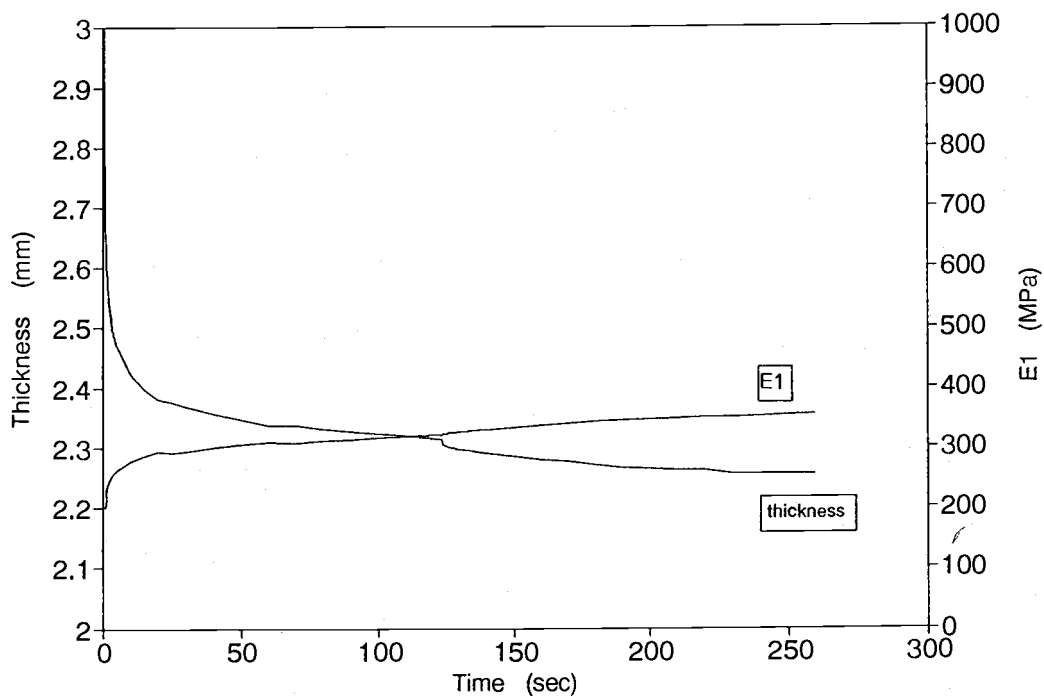


Figure 7.9. An example E1 curve varies with specimen thickness change during the test.

Generally, the rheological behavior of materials is described as a function of stress, strain or rate of strain. However, in the consideration of wood-based composites hot pressing, the structure (for instance, the micro-structure distribution, fiber orientation, density profile, raw materials properties, and the wood-adhesive system) which directly influences total mechanical properties becomes an extremely important factor.

The rheological behavior of materials during compression depends on the effects of structure (as we have already discussed at chapter 3), as well as on time. When the materials are densified, they form a lot of open or closed voids, varying in shape and size. Voids within the system are formed due to extraction or volatilization products of chemical reactions of adhesive solvents, moisture adsorbed by the adhesive and wood material, the porous nature of wood, and "defects" due to unsuccessful formation processes. The effective surface areas within materials vary and these are linked to internal stress distributions. At lower densities, the voids are large and the effective surface area is low. The effective stress (which only acts on the non-porous part of the system) therefore is concentrated on the effective surface area and it may approach that at high density condition. At high density conditions, the voids are reduced and the mean effective surface (contact) is increased, and the effective

stress therefore, may be relatively low. Consequently, with the densification process, material properties continuously change, and the contribution of each element behavior also varied (Fig. 7.10).

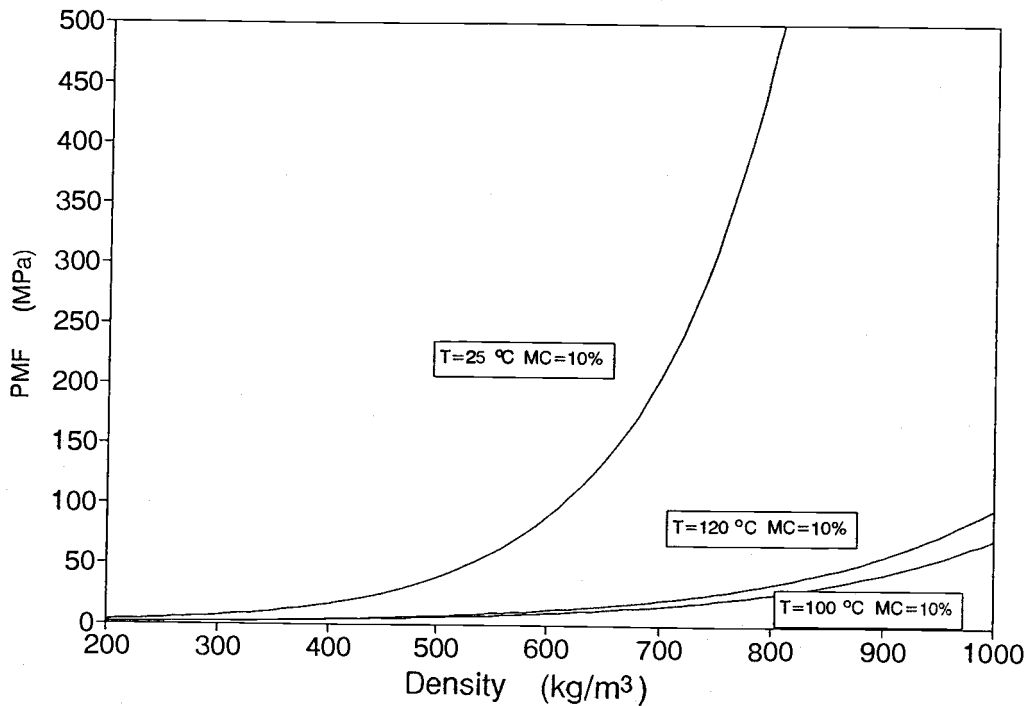


Figure 7.10. EPMF element properties at three different conditions of temperature and moisture content.

7.3. Temperature effects

The effects of temperature on the rheological behavior appear to be significant, especially in the initial stages of compression. The higher the temperature, the larger the initial deformation. This is demonstrated in Figure 7.11,

which shows thermo-rheological behavior during steady-state compression for a range of temperatures (in this case, all at 10% moisture content and similar compression conditions).

To determine the magnitudes of the thermal effects, it is necessary to determine the thermal effects on each element properties and their behavior. Thermo-effects on the composites are directly related with the thermo-effects on each element's property. Figures 7.12 to 7.16 show the thermo-effects on element properties. More information about the thermo-effects on rheological properties of materials may be found in Appendix II.

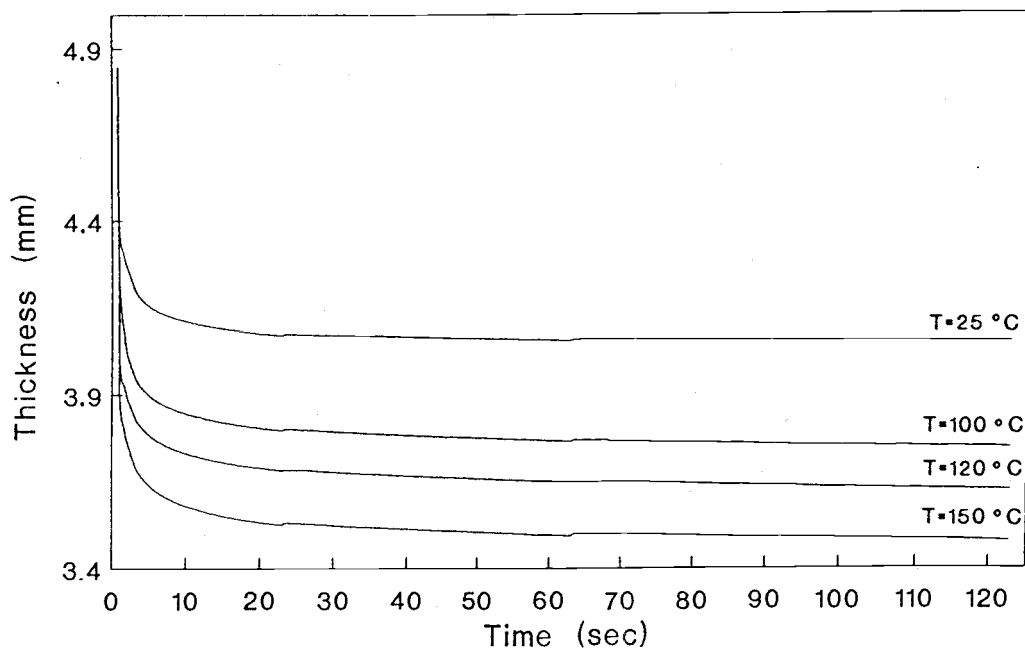


Figure.7.11. Temperature effects on fiber network deformation (MC = 4 %).

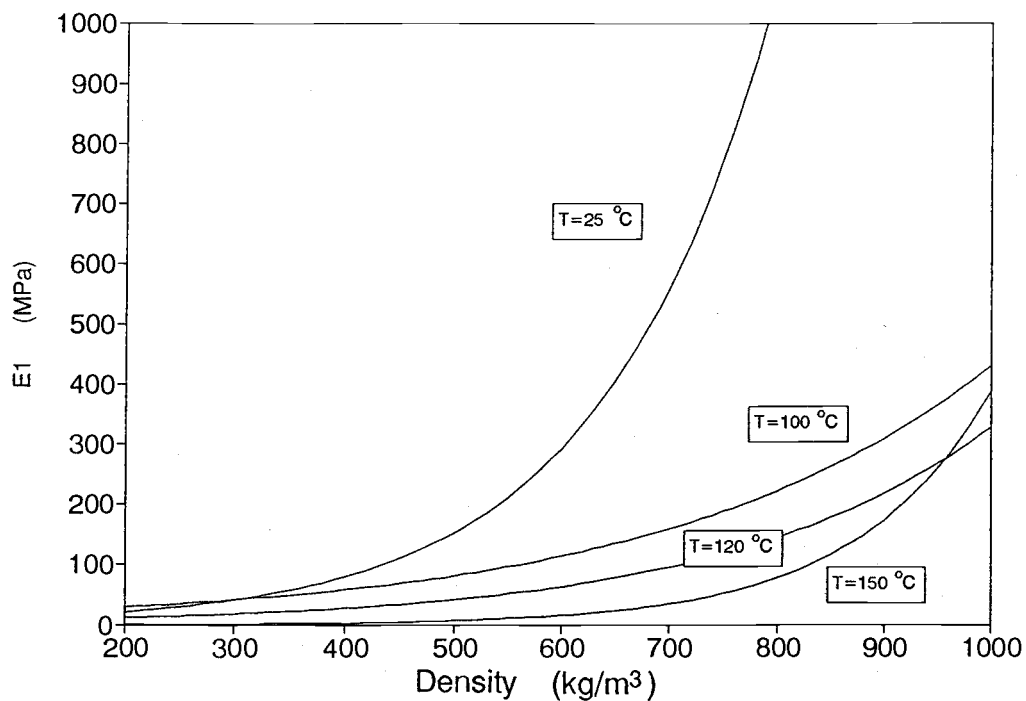


Figure 7.12. The effects of temperature on E_1
(at MC = 10) %

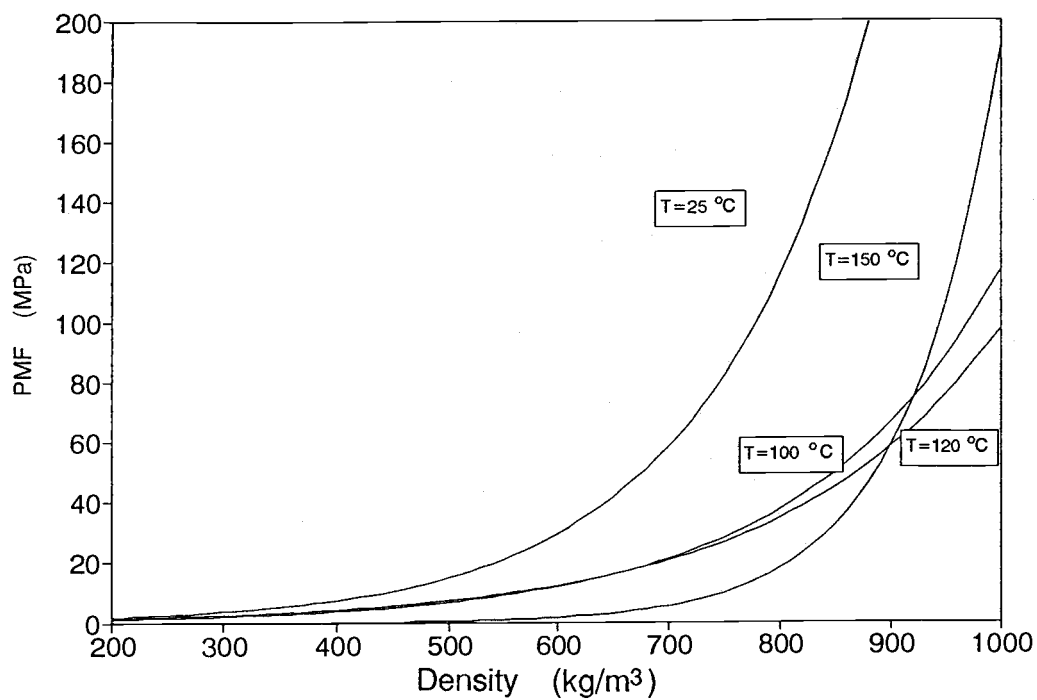


Figure 7.13. The effects of temperature on PMF
(at MC = 10 %).

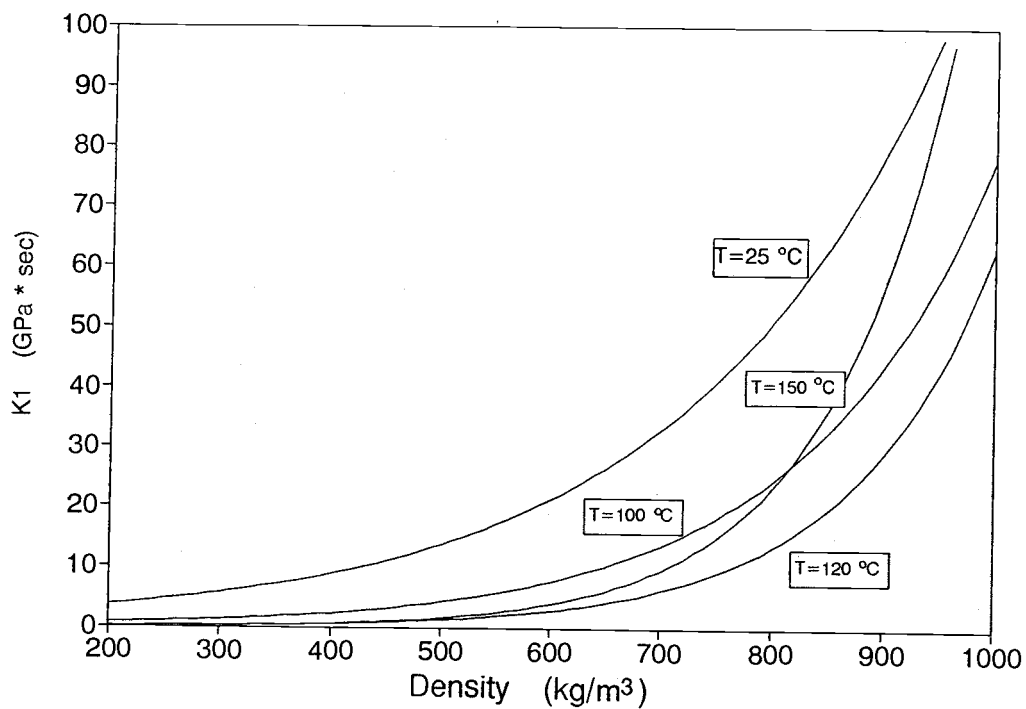


Figure 7.14. The effects of temperature on $K1$ (at MC = 10 %).

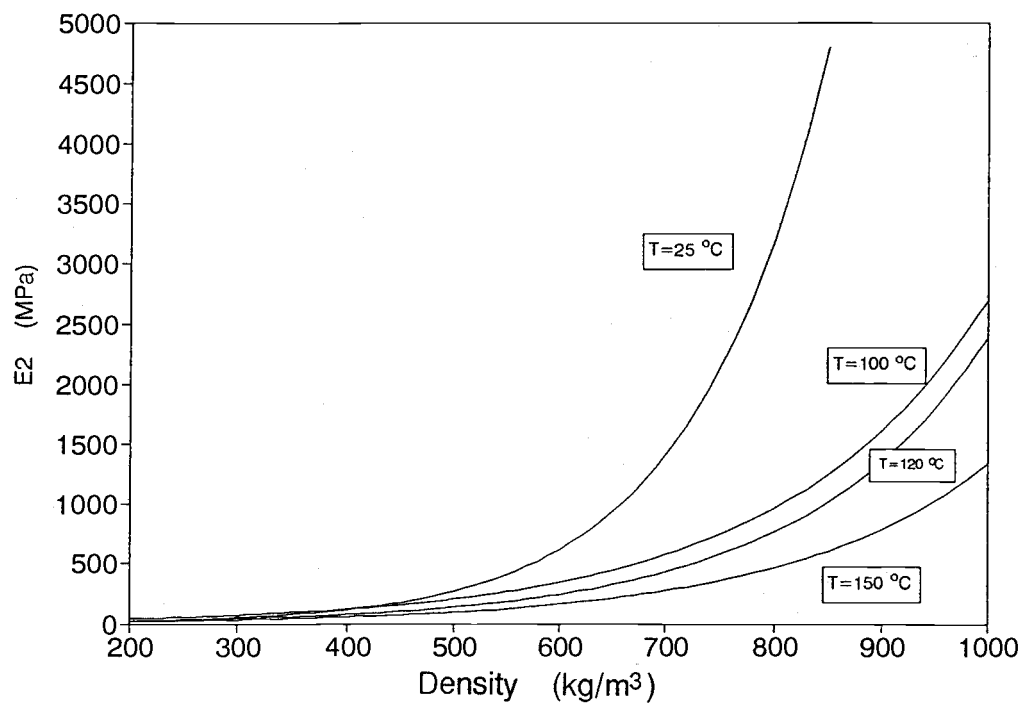


Figure 7.15. The effects of temperature on $E2$ (at MC = 10 %).

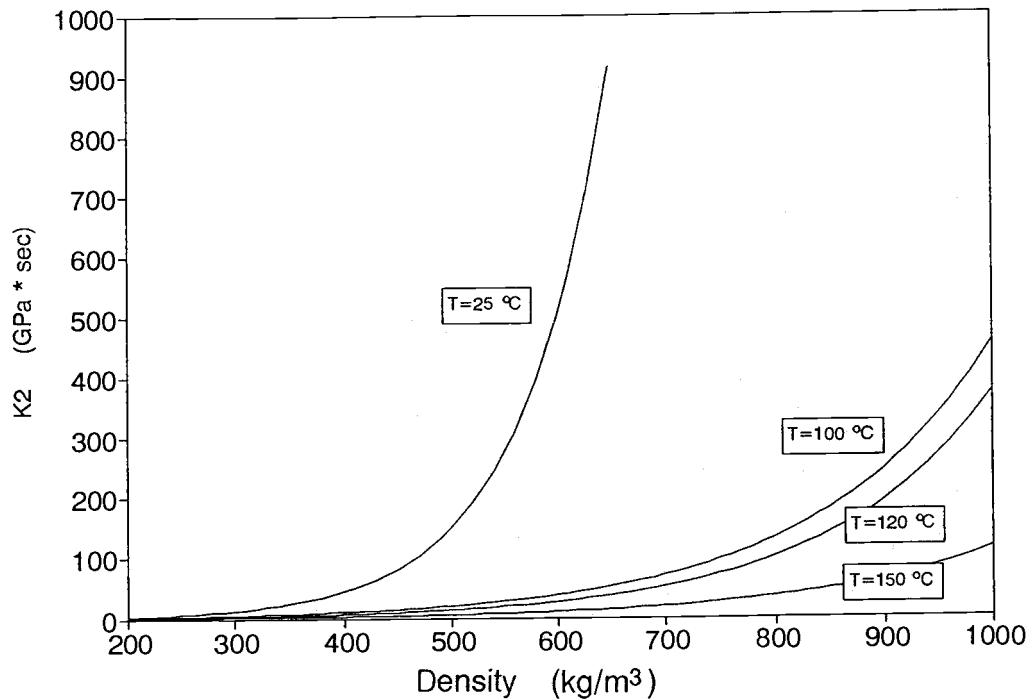


Figure 7.16. The effects of temperature on K_2 (at MC = 10 %).

Under different temperature conditions, the rheological properties of materials vary with density in different fashions. Within most test ranges, higher temperatures cause lower element property values, that means the more thermo-effects on deformation of the materials.

Clearly, this information suggests that the thermal effects of rheological properties of materials can be quantified.

It is interesting to see some significant difference of thermo-effects on the materials at 150 °C. The elements' properties first vary predictably (as at other lower temperatures) with density until about 700 kg/m³. The deformation of the material then, increase significantly so that the values of element properties at 150 °C disproportional higher than at under lower temperatures (such as 100 and 120 °C). This information may help us to produce dimensional stabilized products. The relationship between this phenomena and hygro-effects on the rheological behavior will be discussed in the next section.

7.4. Moisture effects

The effect of moisture on the rheological behavior of fiber network is also significant. Figure 7.17 shows the hygro-rheological behavior during consolidation at a range of moisture conditions (0, 4, 10, 16%), a constant temperature (150 °C) and similar mean compression conditions (4 MPa). As expected, we can see that increasing moisture content results in greater rheological deformation (Fig. 7.17).

Figure 7.18 to 7.22 show the hygro-effects on the element properties.

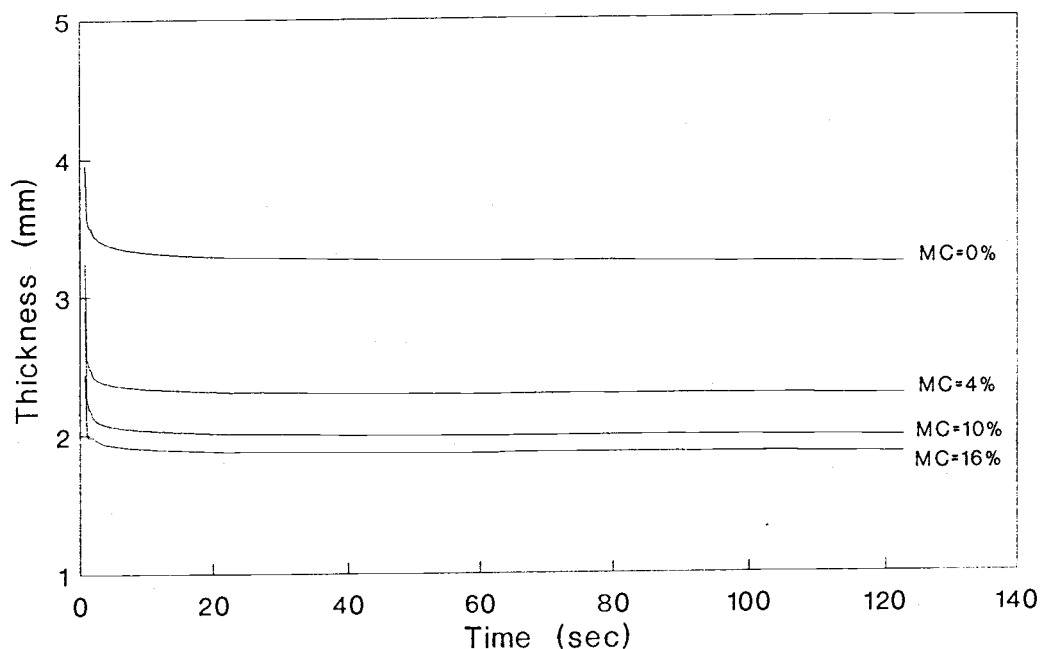


Figure 7.17. Moisture effects on overall deformation
($T = 150^{\circ}\text{C}$, $P = 4\text{ MPa}$)

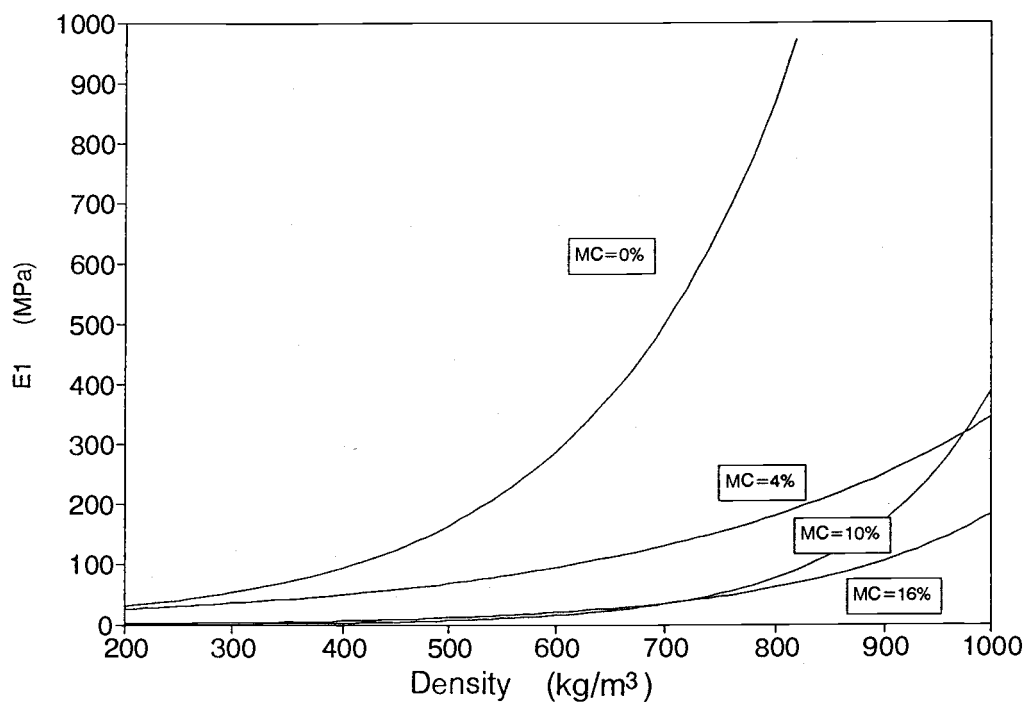


Figure 7.18. The effects of moisture conditions
on E_1 (at $T = 150^{\circ}\text{C}$).

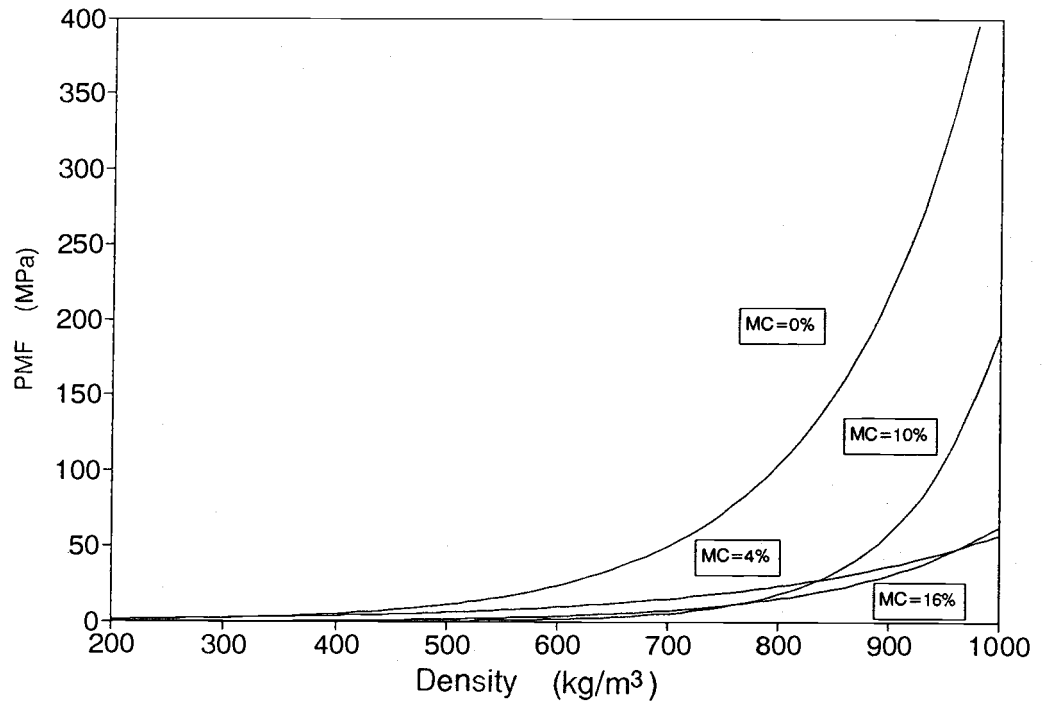


Figure 7.19. The effects of moisture conditions on PMF (at $T = 150^{\circ}\text{C}$).

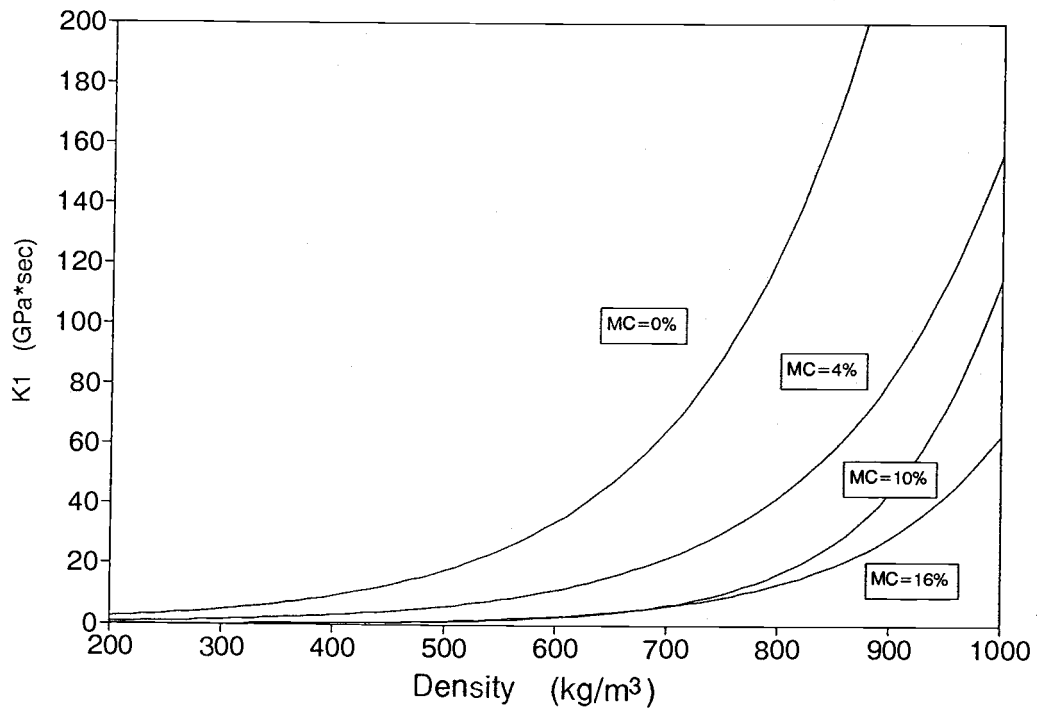


Figure 7.20. The effects of moisture conditions on $K1$ (at $T = 150^{\circ}\text{C}$).

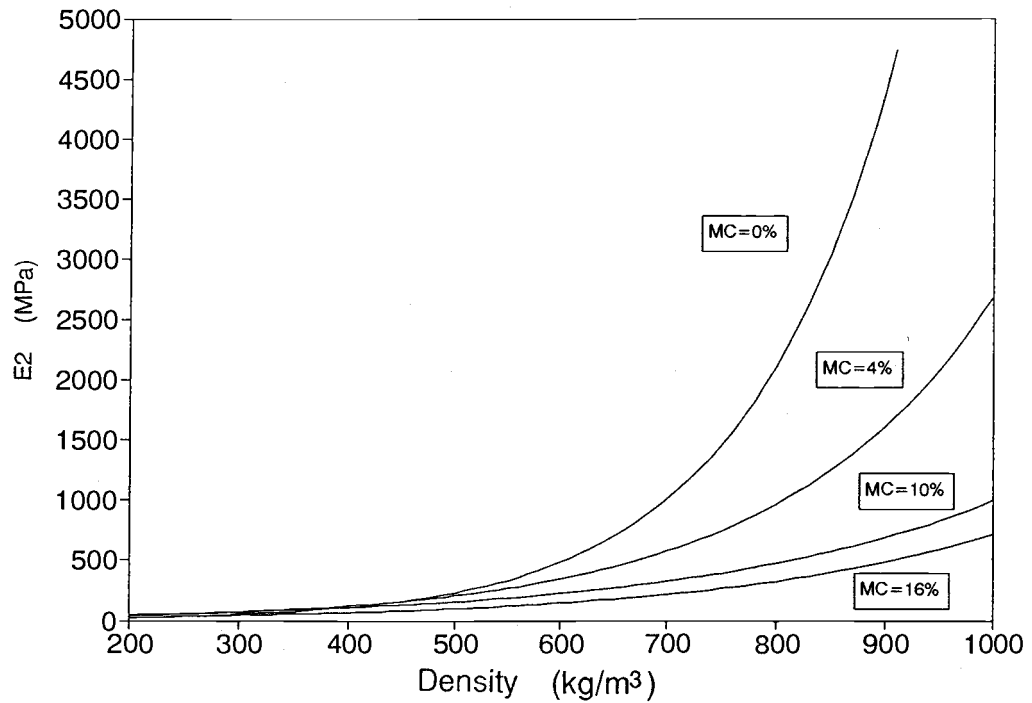


Figure 7.21. The effects of moisture conditions on E_2 (at $T = 150^\circ\text{C}$).

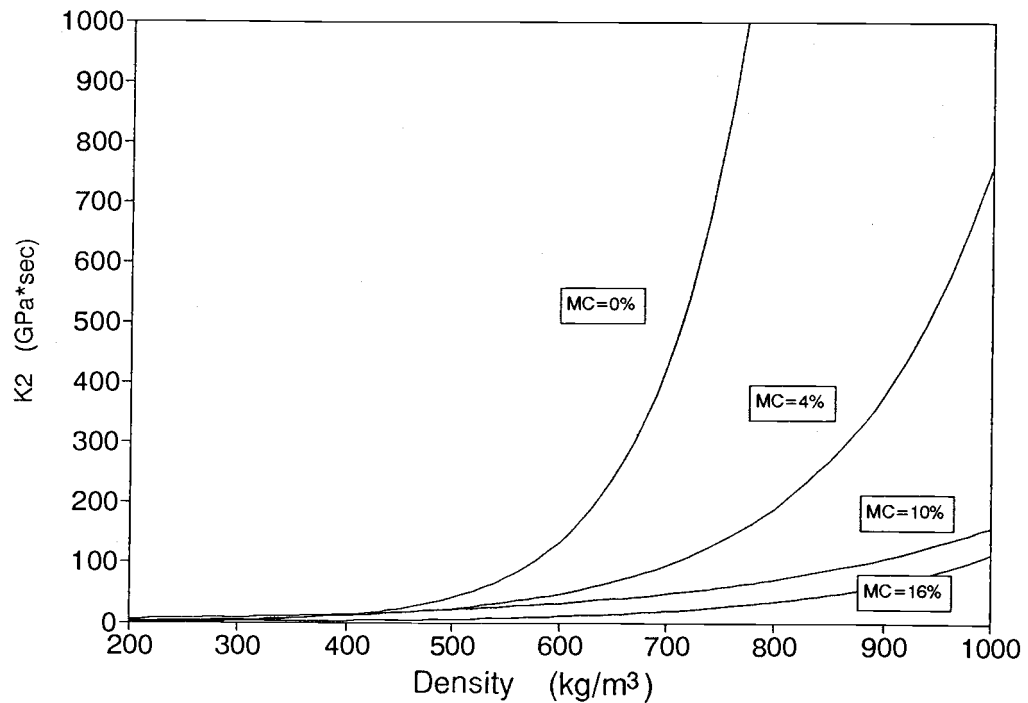


Figure 7.22. The effects of moisture conditions on K_2 (at $T = 150^\circ\text{C}$).

properties of materials. This information may help us to produce high quality and dimensional stable products and may stimulate further research in this direction.

7.5. Energy consumption of rheological behavior.

It is interesting to see that the energy associated with deformation may be calculated as compression progresses. This may be done for the whole material and also for each element separately. Such an approach may provide useful insights into the relative importance of each of the mechanisms involved and may also provide a means for reducing energy consumption (mechanical) in manufacture.

Figure 7.23 indicates that the energy (force * deformation) consumed during compression results mainly from EE1 and EPMF at the initial stages of compression. After initial instantaneous deformation, the EV1 element is the major energy consumer during the subsequent stage of compression, and EV1 also continuously consumes a certain amount of energy during later stages of the process. However, EE2/EV2 together are definitely an important factor which should be considered to reduce energy consumption in hot pressing and the time dependent characteristics of the materials. On the other hand, since the energy which is stored by EE2/EV2 together can not be immediately released when the hot press is opened, the stability of the final

products may be effected by this factor. It seems reasonable to reduce the energy of EE2/EV2 as a small value as possible. Since after initial stage, the Force varies relative small, the quantity of deformation of each element may be used to indicate the energy consumption.

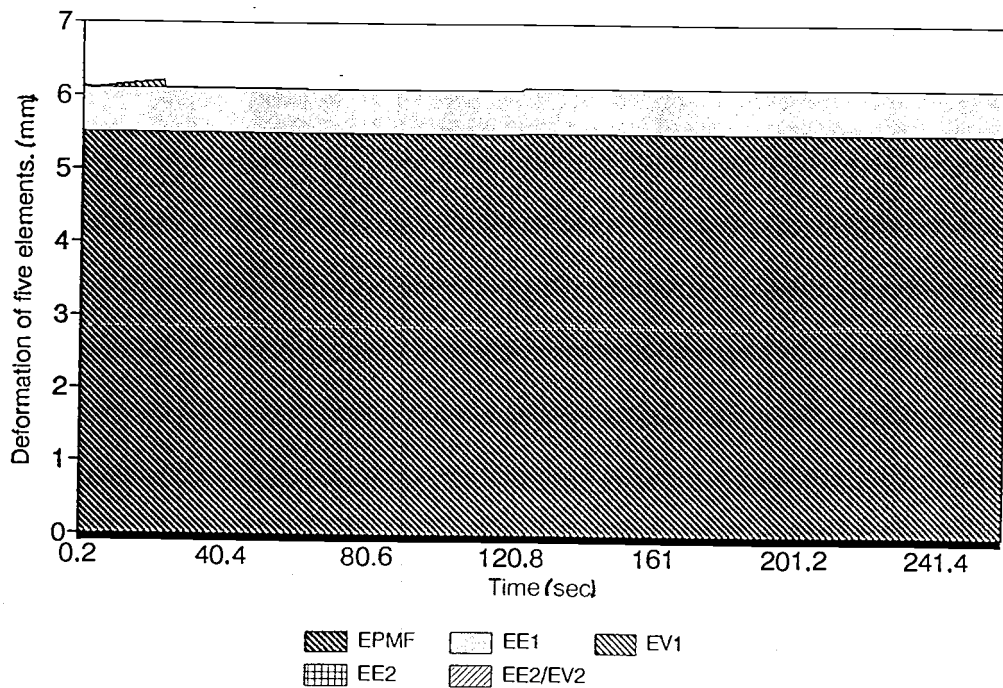


Figure 7.23. Energy (force * distance) consumption during typical of rheological deformation of the material.

From the above, it appears that a viable method to reduce energy during hot pressing is to achieve the final density distribution early in the pressing cycle, and then try to prevent the deformation of EE2, EV1 and EV2. Since after initial compression, the density has already achieved

relatively high values, the deformation of other elements can be manipulated by relative small external changes in stress. However, large increases making stage may increase the number and magnitude of deformation may cause the micro-fractures and this which may effect final products properties. Furthermore, to achieve final thickness too fast may induce some extra variation of density profile (which is developed with time) and that also effects the final products' performance.

This discussion presents preliminary results of this research. There are still many questions remaining. However, this research may stimulate further development of the rheological mechanics during hot pressing, both from theoretical and experimental standpoints.

CHAPTER 8. CONCLUSIONS AND POSSIBLE FUTURE RESEARCH

8.1. Conclusions of current research

The following are the principal conclusions of the current work:

1. Techniques and equipment have been developed to investigate the rheological phenomena that occur during the compression of wood fiber networks.

2. A five-element rheological model has been established offering a means for investigating and ultimately predicting the rheological behavior that occurs during industrial hot pressing.

3. Experimentally quantifying rheological properties of wood composite furnish materials has been developed.

4. Thermo-hygro effects on the rheological behavior of wood composite materials have been investigated at moisture contents from 0 to 16%, temperatures from 25 to 150 °C and stress ranging between 0 and 6 MPa.

5. Elastic-viscous-plastic-micro-fracture deformation has been defined and quantified.

8. Elemental behaviors have been quantitatively studied individually.

The research described here was designed to provide an experimental and quantitative understanding of the

rheological behavior and the combined effects of temperature and moisture content. Ultimately it is expected that such techniques will give us more flexibility to select suitable component materials, and to design hot pressing processes to achieve required structures and properties of final products. If we can control the behavior of each of the component materials (to make them deform in a predictable fashion), we may efficiently produce high quality products from wood materials.

8.2. Possible future research

1. If more investigation could be done over a larger range of conditions, the rheological behavior of wood and wood composite materials, and their effects on other physical aspects may then be quantitatively understood.

2. The results of this study will ultimately be combined with those from parallel studies of: 1) heat and moisture transfer and 2) adhesion kinetics, so that the interaction of physical mechanisms operative during hot pressing may be understood quantitatively.

3. The application and improvement of the techniques we developed for this research may lead to further research to improve industrial products and manufacturing processes.

4. Micro-structural analysis may enable the rheological characteristics of materials to be linked to the materials' structure.

5. The behavior of adhesives and interfaces during hot pressing also should be investigated so that the complete wood-adhesive system can be better understood.

BIBLIOGRAPHY

- Anderson, G.P., S.J. Bennett, and K.L. DeVries. 1977. Analysis and testing of adhesive bonds:155-182, 185-229. Academic Press, Inc., New York.
- Bentun, A., and S. Mindess, 1990. Fiber reinforced cement composites:378-434. Elsevire Science Publishers. LTD., UK.
- Bodig, J., and B. Jayne. 1986. Mechanics of wood and wood composites. Van Nostrand Reinhold Company Inc., New York, N.Y.
- Bolton, A.J., and P.E. Humphrey. 1977. Measurement of the tensile strength development of urea formaldehyde resin-wood bonds during pressing at elevated temperatures. J. Inst. Wood Sci. 7(5):11-14.
- Bolton, A.J., and P.E. Humphrey. 1988. The hot pressing of dry-formed wood-based composites. Part I. A review of the literature, Identifying the primary physical processes and the nature of their interaction. Holzforschung 42(6):403-406.
- Bolton, A.J., P.E. Humphrey and P.K. Kavvouras. 1989a. The hot pressing of dry-formed wood-based composites. Part III. Predicted vapor pressure and temperature variation with time, compared with experimental data from laboratory boards. Holzforschung. 43(4):265-274.
- Bolton, A.J., P.E. Humphrey and P.K. Kavvouras. 1989b. The hot pressing of dry-formed wood-based composites. Part IV. Predicted variation of mattresss moisture content with time. Holzforschung. 43(5):345-349.
- Bolton, A.J., P.E. Humphrey and P.K. Kavvouras. 1989c. The hot pressing of dry-formed wood-based composites. Part VI. The importance of stresses in the pressed mattress and their relevance to the minimisation of pressing time, and the variability of board properties. Holzforschung. 43(6):406-410.
- Bowen, M.E. 1970. Heat transfer in particleboard during pressing. Ph.D. Thesis, Colorado State University. Fort Collins, CO.
- Brady, D.E., and F.A. Kamke. 1988. Effects of hot-pressing parameters on resin penetration. For. Prod. J. 38(6):63-68.

- Carlsson, L.A., and R.B. Pipes. 1987. Experimental characterization of advanced composite materials. Printice-Hall, Englewood Cliffs, N.J.
- Carruthers, J.F.S. 1959. Heat penetration in the pressing of plywood. Forest Prod. Res. Bull. No.44. H.M.S.O., London.
- Castle, J.E. and J.F. Watts. 1989. Surface analytical techniques for studying interfacial phenomena in composite materials. In Interfacial phenomena in composite materials '89. Ed. by Jones, F.R. Butterworth & Co. Ltd. UK.
- Chow, S.Z. 1969. A kinetics study of the polymerization of PF resin in the presence of cellulose materials. Wood Sci. 1(4):215-221.
- Collett, B.M. 1972. A review of surface and interfacial adhesion in wood science and related fields. Wood Sci. Tech. 1(6):1-42.
- Collett, B.M. 1970. Scanning electron microscopy: A review and report of research in wood science. Wood and Fiber 2(2):113-133.
- Delollis, N.J. 1968. Theory of adhesion: mechanism of bond failure and mechanism of bond improvement. Part 1: Evaluation and present status of the theories of adhesion. Adhesive Age. 11(12):21-25.
- Dinwoodie, J.M. 1983. Properties and performance of wood adhesives:1-57, Wood adhesives: Chemistry and technology. Marcel Dekker, Inc., NY.
- Eirich, F.R. 1958. Rheology: theory and applications. Volume II. Academic press Inc., New York.
- Ferry, J.D. 1980. Viscoelastic properties of polymers. John Wiley and Sons, New York, NY.
- Findley, W.N. 1976. Creep and relaxation of non-linear visco-elastic materials. North-Holland publishing Company. New York, NY.
- Geimer, R.L., R.J. Mahoney, S.P. Loehnerts, and R.W. Meyer. 1985. Influence of processing-induced damage on strength of flakes and flakeboards. For. Prod. Lab. Res. No.463. For. Prod. Lab., Madison, WI.

- Gent, A.N., and G.R. Hamed. 1981. In Adhesive bonding of wood and other structural materials. 54-64. EMMSE Projectt, Materials research Lab. Pennsylvania State Univ. University Park, PA.
- Harless, T.E.G., F.G. Wagner, P.H. Short, R.D. Seale, P.H. Mitchell and D.S. Ladd. 1987. A model to predict the density profile of particleboard. Wood and Fiber Sci. 19(1):81-92.
- Hata, T., 1990. Production of particleboard with steam-injection. Part 1. Wood and Fiber Sci. 24(2):65-78.
- Humphrey, P.E., and A.J. Bolton. 1979. Urea formaldehyde resin bond strength development with reference to wood particleboard manufacture. Holzforschung 33(4):129-133.
- Humphrey, P.E. 1982, Fundamental aspects of wood particleboard manufacture. Ph.D. thesis, Univ. of Wales, U.K.
- Humphrey, P.E., and A.J. Bolton. 1985. Development of bond strength as resin cures and resultant effects on wood-based composites during hot pressing. Wood Adhesives in 85 - Status and needs. Madison, WI.
- Humphrey, P.E., and A.J. Bolton. 1989a. The hot pressing of dry-formed wood-based composites. Part II. A simulation model for heat and moisture transfer, and typical results. Holzforschung 43(3):199-206.
- Humphrey, P.E., and A.J. Bolton. 1989b. The hot pressing of dry-formed wood-based composites. Part V. The effect of board size: comparability of laboratory and industrial pressing. Holzforschung 43(3):401-405.
- Humphrey, P.E., and S. Ren. 1989. Bonding kinetics of thermosetting-adhesive systems used in wood-based composites: The combined effect of temperature and moisture content. J. Adhesion Sci. Technol. 3(5):397-413.
- Humphrey, P.E., 1989. Moisture related problems in wood processing and products: theory and practice. Execustive summaries, FPRS annual meeting, Reno, Nevada, 1989.
- Kaelble, D.H. 1971. Physical Chemistry of Adhesive:117-180,349-375,388-423,450-486. Wiley-Interscience, NY.

- Kamke, F.A., and L.J. Casey. 1988a. gas pressure and temperature in the mat during flakeboard manufacture. For. Prod. J. 38(3):41-43.
- Kamke, F.A., and L.J. Casey. 1988b. Fundamentals of flakeboard manufacture: internal-mat conditions. For. Prod. J. 38(6):38-44.
- Kasal, B. 1989. Behavior of wood under transverse compression. M.S. thesis, Virginia Polytechnic Institute and State University, Blacksburg, VA.
- Kayihan, F., and J.A. Johnson. 1983. Heat and moisture movement on wood composite materials during the pressing operation - a simplified model. Numerical methods in heat transfer. 2:511-531.
- Kelley, S.S., T.G. Rials, and W.G. Glasser. 1987. Relaxation behavior of the amorphous components of wood. J. Mater. Sci. 22:617-624.
- Kelley, S.S., and R.A. Young. 1983. Bond formation by wood surface reactions: Part III--Parameters affecting the bond strength of solid wood panels. For. Prod. J. 33(2):21-27.
- Kollman, F.F.P., E.W. Kuenzi, and A.J. Stamm. 1975. Principles of wood science and technology II. Wood materials: 387-423. Springer-Verlag.
- Kunesh, R.H. 1961. The inelastic behavior of wood: a new concept for improved panel forming processes. For. Prod. J. 11(9):395-406.
- Kunesh, R.H. 1968. Strength and elastic properties of wood in transverse compression. For. Prod. J. 18(1):65-72.
- Kyokong, B. et al., 1986. Fracture behavior of adhesive joints in poplar. Wood and Fiber Sci. 18(4):499-525.
- Laufenburg, T.L. 1983. Characterizing the nonlinear behavior of flakeboards. Wood and Fiber Sci. 15(1):47-58.
- Lehmann, W.F. 1965. Simplified test of internal bond in particleboard. For. Prod. J. 15(5):223-224.
- Liang, S.Z. 1981. Wood drying: 31-46. Forestry Publisher Co., Beijing. In Chinese.

- Lodge, A.S., M. Renardy and J.A. Nohel. 1985. Viscoelasticity and rheology. Academic press, Inc. New York.
- Lorence K, 1981. Rapid method to determine internal bond and density variation of particleboard. For. Prod. J. 31(12):51-53.
- Lu, R.S. 1983. Plastic mechanics. Industry Publisher Co., Beijing. In Chinese.
- Marian, J.E. 1966. Surface properties as physics-chemical phenomena. Holzforschung, 16(5):134-148.
- Mark, R.E., 1972. Mechanical behavior of the molecular component of fiber. In Theory and design of wood and fiber composite materials. Ed. by Jayne, B.A. Syracuse University Press, NY.
- Marra, A.A. 1981. In Adhesive bonding of wood and other structural materials:371-374,378-385. EMMSE Project, Materials research Lab. Pennsylvania State Univ. University Park, PA.
- Mataki, Y., 1972. Internal structure of fiberboard and its relation to mechanical properties. In Theory and design of wood and fiber composite materials. Ed. by Jayne, B.A., Syracuse University Press, NY.
- Moore, W.J. 1983. Basic Physical Chemistry. Prentice-Hall. Inc. Englewood Cliffs, NJ.
- Nelson, R.M. 1986. Diffusion of bound water in wood. Wood Sci.Tech. Vol 20:125-135.
- Nielsen, L.E. 1974. Mechanical properties of polymers and composite. Marcel Dekker, Inc. New York.
- Petersen, R.G. 1985. Design and analysis of experiments:112-145,166-202. Academic Press, NY.
- Pimentel, G.C., Spratly, R.D. 1969. Understanding chemical thermodynamics. HoldenDay, Inc., San Francisco.
- Ren, S. 1988. Bonding kinetics of thermosetting adhesive systems used in composites. M.S. thesis. Oregon State University, Corvallis, Oregon.
- Ren, S. and P.E. Humphrey, 1990. Wood-adhesive failure surfaces and their relationship with the development of bond strength. Technical Forum of FPRS annual meeting, Salt Lake City, June. 1990.

- Rice, J.T. 1981. In Adhesive bonding of wood and other structural materials, et al. Marcel Dekker Inc. NY.
- River, B.H. 1981. A Method for Measuring Adhesive Shear Properties. Adhesives Age. Dec.:30-33.
- Rosen, H.N. 1979. Psychromeric relationships and equilibrium moisture content of wood at temperature above 100 °C. Proceedings wood moisture content relationships:76-83. Blacksburg, Virginia.
- Ruedy, T.C., and J.A. Johnson. 1979. Glueline fracture of wood adhesive compact-tension specimens at various grain orientation configurations:201-218. The first international conference on wood fracture. Forintek Canada Corp. Vancouver, BC.
- Ryutoku, Y. et al. 1990. Adhesion and bonding in composites. 1-4, 283-335. Marcel Dekker Inc. NY.
- Schnivina, A.P. 1972. Elastic behavior of wood fiber. In Theory and design of wood and fiber composite materials. Ed. by Jayne, B.A. Syracuse University Press, NY.
- Seferis, J.C., and L. Nicolais. 1983. The role of the polymeric materials in the processing and structural properties of composite materials: 127-146, 481-502. Plenum Press, NY.
- Shao, M. 1990. Thermal conductivity of wood fiber net work. MS. Thesis, Oregon State University, Corvallis, Oregon.
- Shen, K.C., Crlarroll, M.N. 1969. A new method for evaluation of internal strength of particleboard. For. Prod. J. 19(8):17-22.
- Shout, D, and J.Summerscales. 1981. Elastic and thermal properties of composites. In Fiber composite hybid materials. Ed. by Hancox, N.L. Macmillon Publishing Co. Inc.
- Siau, J.F. 1984. Transport processes in wood. Springer-Verlag:11-32.
- Siau, J.F. 1980. Nonisothermal moisture movement in wood. Wood Sci.13(1):11-13.

- Siau, J.F. 1979. The effect of temperature and moisture content on physical changes in wood. Proceedings wood moisture content relationships:76-83. Blacksburg, Virginia.
- Simpson, W.T. 1973. Predicting equilibrium moisture content of wood by mathematical models. Wood and Fiber 5(1):41-49.
- Skarr, C. 1972. Water in wood :27-71, 127-170. Syracuse University Press, NY.
- Smith, D. 1982. Waferboard press closing strategies. For. Prod. J. 32(3):40-45.
- Smulski, S.J, and Geza Ifiu. 1987. Flexural behavior of glass fiber reinforced hardboard. Wood and Fiber Sci. 19(3):313-327
- Smulski, S.J. 1989. Creep function for wood composite materials. Wood and Fiber Sci. 21(1):45-54.
- Springer, G.S. 1988. In Composites design, 4th edition. Composite design. Ed. by Tsai. S.W. :16-1 to 16-18. Think Composites, Dayton, Ohio.
- Stanish, M.A. 1986. The roles of bound water chemical potential and gas phase diffusion in moisture transport through wood. Wood Sci. Tech.(19):53-70.
- Stewart, H.A.1979. Some surfacing defects and problems related to wood moisture content. Proceedings wood moisture content relationships:70-75. Blacksburg, Virginia.
- Steiner, P.R., and S.R. Warren. 1981. Rheology of wood adhesive cure by torsional braid analysis. Holzforschung 35(6):273-278.
- Steiner, P.R., and S.R. Warren. 1987. Behavior of Urea-formaldehyde wood adhesives during early stages of cure. For.Prod.J. 37(1):20-22.
- Strickler, M.D. 1959. The effect of press cycles and moisture content on properties of Douglas Fir flakeboard. For. Prod. J. 9(7):203-207.
- Suchsland, O. 1967. Behavior of a particleboard mat during the press cycle. For. Prod. J. 17(2):51-57
- Tsai, S.W. 1988. Composites design. Think composites. Dayton, Ohio.

- Tang, Y.F., and W.T. Simpson. 1990. Perpendicular to grain rheological behavior of loblolly pine in press drying. *Wood and Fiber*. 22(3):326-342.
- Wang, Q.H. 1984. Textbook of rheology of materials. Civil Engineering Press Inc., Beijing. In Chinese.
- Wellons, J.D. 1980. Wettability and gluability of Douglas fir veneer. *For. Prod. J.* 30(7):53-55.
- Welty, J.R., C.E. Wicks, and R.E. Wilson. 1976. Fundamentals of momentum, heat, and mass transfer. John Wiley and several edition sonos New York.
- Wengent, E.M., and P.H. Mitchell. 1979. Psychrometer relationships and equilibrium moisture content of wood at temperatures below 100 °C. Symposium of wood moisture content, temperature, and humidity relationships:4-11. Blacksburg, Virginia.
- White, M.S. 1977. Influence of resin penetration on the fracture toughness of wood-adhesive bonds. *Wood Sci.* 10(1): 6-14.
- Wolcott, M.P., B. Kasal, F.A. Kamke and D.A. Dillard. 1989. Testing small wood specimens in transverse compression. *Wood and Fiber Sci.* 21(3):320-329.
- Wolcott, M.P., F.A. Kamke and D.A. Dillard. 1990. Fundamentals of flakeboard manufacture: viscoelastic behavior of the wood component. *Wood and Fiber Sci.* 22(4):345-361.
- Young, R.A. 1982. Bond formation by wood surface reactions: Part 1. *Wood Sci.* 14 (3):110-119.
- Zavala, D.Z. 1985. Analysis of processes operative within plywood during hot pressing. Ph.D. thesis. Oregon State University, Corvallis, OR.
- Zhang, B.G. 1980. Heating Engineering: 52-58. Light Industry Publisher Co. Beijing. In Chinese.
- Zhao, H. 1982. Elastic Mechanics. Mechanical Eng. Publisher Co., Tianjing. In Chinese.
- Zisman, G. 1963. Influence of constitution on adhesion. *Ind. and Eng. Chem.* 55(10):19-38.

APPENDICES

APPENDIX I

Computer programs for operating test system
and quantifying rheological properties of materials.

There are five computer programs in this appendix:

- | | |
|---|-----|
| 1. Program for operating test system | 168 |
| 2. Program for calculating the EE1 and EV1
properties from test results. | 179 |
| 3. Program for calculating the EPMF property. | 183 |
| 4. Program for calculating the EE2 property. | 185 |
| 5. Program for calculating the EV2 property. | 187 |

```

DECLARE SUB genctda (alldat!, load!)

10
'   WOOD COMPOSITES HOT PRESSING SIMULATION TEST PROGRAM
'   1989-7-26 BY SHAN REN FOR Ph.D THESIS.
CLS
LOCATE 10, 10, 1, 1
PRINT "WELCOME TO THE COMPOSITES MANUFACTURING SIMULATION TEST SYSTEM"
LOCATE 15, 28
PRINT "PART III TEST"
100 IF INKEY$ = "" THEN GOTO 100

PRINT "   The functions of this program are:"
PRINT "   1. Composites manufacturing multi-simulation test:"
PRINT "       a. dynamic and static test on materials stress and strain,"
PRINT "       b. steady state condition test,"
PRINT "       c. unsteady state condition test,"
PRINT "       d. hygrothermo-effects,"
PRINT "       e. heat and moisture transfer measure and control,"
PRINT "       f. vapor condition,"
PRINT "   2. Experimental equipments control:"
PRINT "       a. minature insulated pressing system,"
PRINT "       b. data collection and conversion system, "
PRINT "   3. Enhancing and Controlling MTS test function:"
PRINT "       a. using IBM pc and Data Translation DT2805-DT707T board"
PRINT "           replace MST function generator"
PRINT "       b. control and collect test parameters at same time"
PRINT "   4. Notes: "
PRINT "       a. temperature preseted and controlled by the equipment of eurotherm"
PRINT "       b. vapor pressure measured and controlled by extra control part,"
PRINT "       c. initial vaccume condition is produced by a vaccume system,"
PRINT "       d. deformation is measured by a extra high quality LVDT."
PRINT

300 IF INKEY$ = "" THEN GOTO 300

400 'define constants.
DEFINT A-Z
BASE.ADDRESS = &H2EC
COMMAND.REGISTER = BASE.ADDRESS + 1
STATUS.REGISTER = BASE.ADDRESS + 1
DATA.REGISTER = BASE.ADDRESS
COMMAND.WAIT = &H4
WRITE.WAIT = &H2
READ.WAIT = &H5

500
CCLEAR = &H1
CERROR = &H2
CCLOCK = &H3
CSAD = &HD
CADIN = &HC
CRAD = &HE' + 128
CDAOUT = &H8 + 128
CSTOP = &HF
CRESET = &H1

TOP.RANGE# = 10
BOTTOM.RANGE# = -10

BASE.FACTOR# = 4096
BASE.CHANNELS = 8
GAIN(0) = 1
GAIN(1) = 10
GAIN(2) = 100
GAIN(3) = 500

```



```

600  'stop and clear the board
      OUT COMMAND.REGISTER, CSTOP
      TEMP = INP(DATA.REGISTER)
      WAIT STATUS.REGISTER, COMMAND.WAIT
      OUT COMMAND.REGISTER, CCLEAR

1000 ' set parameters

PRINT "TEST NUMBER (ONE ... ..) = ?";
INPUT NTST$

PRINT "NUMBER OF THERMOCOUPLES = ?";
INPUT NTHM

PRINT "NUMBER OF PRESSURE TRANSDUCERS = ?";
INPUT NPT

PRINT "NUMBER OF DISPLACEMENT TRANSDUCERS = ?";
INPUT NLVDT

1300 'selecte the dac channels.
PRINT "ENTER DESIRED DAC CHANNEL "; '(1 FOR PROGRAME CHECK AND 0 FOR OPERATION)";
PRINT "0 IS TO OPERATE MTS, 1 IS TO CHANGE LVDT RANGE."

1500
S = 1
PRINT "A/D START CHANNEL ( 1 TO 7 )"; S
ADSCHAN = S - 1
IF ADSCHAN < 0 THEN GOTO 1500
IF ADSCHAN > (BASE.CHANNELS - 1) THEN GOTO 1500

1600
ADECHAN = 7
PRINT "A/D END CHANNEL ( 1 TO 7 )"; ADECHAN
IF ADECHAN < 0 THEN GOTO 1600
IF ADECHAN > (BASE.CHANNELS - 1) THEN GOTO 1600

1700
NCHAN = ADECHAN - ADSCHAN + 1
NCHAN# = NCHAN
IF NCHAN < 1 THEN NCHAN = NCHAN + BASE.CHANNELS

2000 ' select procedures of operation
PRINT "SELECT PROCEDURES: "
PRINT "          1. GENERATE CONTROL DATA FILE "
PRINT "          2. SET REFERENCE DATA, "
PRINT "          3. TEST,"
PRINT "          4. EXIT"
INPUT sp$

SELECT CASE sp$
  CASE "1"
    PRINT "GENERATE CONTROL DATA FILE ..."
    genctda 32700, 32700
    GOTO 2000
  CASE "2"
    PRINT "GENERATE THE REFERENCE DATA ..."
    GOTO 2100
  CASE "3"
    PRINT " TEST !!!"
    GOTO 2200
  CASE "4"
    GOTO 10000
  CASE ELSE
    GOTO 2000
END SELECT

2100 'referenc data proceduce
      OPEN "a:datrf" + NTST$ FOR INPUT AS #1

```

```

GOTO 2500

2200 'open data file for output and input data
    OPEN "C:\mts\DATCT" + NTST$ FOR INPUT AS #1

2500 'input control data from the data file
    INPUT #1, alldat
    PRINT "ALLDAT ="; alldat

PRINT "TEST TIME (SECONDS) = ?"; alldat / 5

2600
ncon# = alldat
nconvers# = ncon#
IF nconvers# > 32700 THEN nconvers# = 32700
PRINT "NUMBER OF CONVERSIONS = ?"; nconvers#

2800 'dimension array to hold high and low byte of a/d data.
DIM ADL(NCHAN), ADH(NCHAN)
DIM AD#(nconvers# * 10)
DIM ctvolt(nconvers#)
DIM load#(nconvers#)

FOR j = 1 TO alldat
    INPUT #1, z, load#(j)
NEXT j
CLOSE #1

3000
PRINT "                                START TEST   ???"
```

3100 IF INKEY\$ = "" THEN GOTO 3100
CLS
LOCATE 10, 18, 1, 1
PRINT "TEST STARTED !!! PLEASE WAIT !!!";

```

3200 'check error
    WAIT STATUS.REGISTER, COMMAND.WAIT
    STATUS = INP(STATUS.REGISTER)
    IF (STATUS AND &H80) THEN GOTO 9500

    OUT COMMAND.REGISTER, CSTOP
    TEMP = INP(DATA.REGISTER)
    WAIT STATUS.REGISTER, COMMAND.WAIT
    OUT COMMAND.REGISTER, CCLEAR

3500 'start loop
BEEP
X! = TIMER
FOR I = 1 TO alldat

3600 'input control data from data file
    WAIT STATUS.REGISTER, COMMAND.WAIT
    STATUS = INP(STATUS.REGISTER)
    IF (STATUS AND &H80) THEN GOTO 9500

    OUT COMMAND.REGISTER, CSTOP
    TEMP = INP(DATA.REGISTER)
    WAIT STATUS.REGISTER, COMMAND.WAIT
    OUT COMMAND.REGISTER, CCLEAR

    DAVOLTS# = load#(I)

    RANGE# = TOP.RANGE# - BOTTOM.RANGE#
    DATA.VALUE# = (DAVOLTS# - BOTTOM.RANGE#) * 4096 / RANGE#
    DATA.VALUE# = CINT(DATA.VALUE#)
    IF DATA.VALUE# > 4095 THEN DATA.VALUE# = 4095

```

```

'record control data
ctvolt(1) = DATA.VALUE#

WAIT STATUS.REGISTER, COMMAND.WAIT
OUT COMMAND.REGISTER, CDAOUT

WAIT STATUS.REGISTER, WRITE.WAIT, WRITE.WAIT
OUT DATA.REGISTER, 0 ' DACSELECT

'divide dac data into high and low bytes and write both bytes
'to the data in register, waiting for a clear data in full flag
'before each write.

DAHIGH = INT(DATA.VALUE# / 256)
DALOW = DATA.VALUE# - DAHIGH * 256
WAIT STATUS.REGISTER, WRITE.WAIT, WRITE.WAIT
OUT DATA.REGISTER, DALOW
WAIT STATUS.REGISTER, WRITE.WAIT, WRITE.WAIT
OUT DATA.REGISTER, DAHIGH

'check error

WAIT STATUS.REGISTER, COMMAND.WAIT
STATUS = INP(STATUS.REGISTER)
IF (STATUS AND &H80) THEN GOTO 9500

4000 'SET A/D PARAMETERS FOR TEMPERATURE MEASURE (gain of 3).
      'SET A/D PARAMETERS FOR PRESSURE AND POSITION MEASURE (gain of 0).

FOR q = 1 TO 10

IF q > 4 THEN GOTO 4020
ADCHANNEL = q - 1
ADGAIN = 3
LT = 0
GOTO 4060

4020
IF q <> 5 THEN GOTO 4030
ADCHANNEL = 4
ADGAIN = 0
LT = LT#
GOTO 4060

4030
IF q > 8 THEN GOTO 4050
ADCHANNEL = q - 1
ADGAIN = 0
LT = 0

4050
IF q <> 9 THEN GOTO 4055
ADCHANNEL = 4
ADGAIN = 1
LT = 0

4055
IF q <> 10 THEN GOTO 4060
ADCHANNEL = 4
ADGAIN = 2
LT = 0

4060
'set a/d parameters command to set up the a/d converter.
'wait until the board ready flag is set then write the
'set a/d parameters command byte to the command register.

WAIT STATUS.REGISTER, COMMAND.WAIT
OUT COMMAND.REGISTER, CADIN

```

'wait until the board data in full flag is clear, then
'write the a/d gain byte to the data in register.

```
WAIT STATUS.REGISTER, WRITE.WAIT, WRITE.WAIT
OUT DATA.REGISTER, ADGAIN
```

'wait until board data in full flag is clear,
'write the a/d start channel byte to the data in register.

```
WAIT STATUS.REGISTER, WRITE.WAIT, WRITE.WAIT
OUT DATA.REGISTER, ADCHANNEL
```

'read the A/D, high AND low BYTES, into arrays, waiting for a set
'data out ready (of ready) flag before each read.

4400

```
WAIT STATUS.REGISTER, READ.WAIT
ADL = INP(DATA.REGISTER)
WAIT STATUS.REGISTER, READ.WAIT
ADH = INP(DATA.REGISTER)
```

b = a + q

AD#(b) = ADH * 256 + ADL + LT

```
WAIT STATUS.REGISTER, COMMAND.WAIT
STATUS = INP(STATUS.REGISTER)
IF (STATUS AND &H80) THEN GOTO 9500
```

NEXT q

a = b

```
WAIT STATUS.REGISTER, COMMAND.WAIT
STATUS = INP(STATUS.REGISTER)
IF (STATUS AND &H80) THEN GOTO 9500
```

' set up a control loop to feedback signal to LVDT cycle
' for entering a small measurement range.

4500

```
IF I > 5 THEN GOTO 4900
LVDT0# = -.01
GOTO 4910
```

4900

```
IF I < 9 THEN GOTO 4905
LT# = (AD#(55) - AD#(85))
```

4905

```
' -.15 FOR P2, -.10 FOR P6, -.12 FOR P4
LVDT0# = ((AD#(55) * (10 / 4096)) * 2 - 10) - .12
```

4910

DAVOLTS# = LVDT0#

```
RANGE# = TOP.RANGE# - BOTTOM.RANGE#
DATA.VALUE# = (DAVOLTS# - BOTTOM.RANGE#) * 4096 / RANGE#
DATA.VALUE# = CINT(DATA.VALUE#)
IF DATA.VALUE# > 4095 THEN DATA.VALUE# = 4095
```

```
WAIT STATUS.REGISTER, COMMAND.WAIT
OUT COMMAND.REGISTER, CDAOUT
```

```
WAIT STATUS.REGISTER, WRITE.WAIT, WRITE.WAIT
OUT DATA.REGISTER, 1' DACSELECT
```

'divide dac data into high and low bytes and write both bytes
'to the data in register, waiting for a clear data in full flag
'before each write.

```
DAHIGH = INT(DATA.VALUE# / 256)
DALOW = DATA.VALUE# - DAHIGH * 256
WAIT STATUS.REGISTER, WRITE.WAIT, WRITE.WAIT
```

```

      OUT DATA.REGISTER, DALOW
      WAIT STATUS.REGISTER, WRITE.WAIT, WRITE.WAIT
      OUT DATA.REGISTER, DAHIGH

      'check error
      WAIT STATUS.REGISTER, COMMAND.WAIT
      STATUS = INP(STATUS.REGISTER)
      IF (STATUS AND &H80) THEN GOTO 9500

NEXT I

5000
Y! = TIMER
z! = Y! - X!
u! = z! / alldat
CLOSE #2

REDIM load#(0)
REDIM ADL(0), ADH(0)

BEEP
5100
      ' to set da channel 1 to output 0.
      DAOUT# = -.01

      RANGE# = TOP.RANGE# - BOTTOM.RANGE#
      DATA.VALUE# = (DAOUT# - BOTTOM.RANGE#) * 4096 / RANGE#
      DATA.VALUE# = CINT(DATA.VALUE#)
      IF DATA.VALUE# > 4095 THEN DATA.VALUE# = 4095

5200
      WAIT STATUS.REGISTER, COMMAND.WAIT
      OUT COMMAND.REGISTER, CDAOUT

      WAIT STATUS.REGISTER, WRITE.WAIT, WRITE.WAIT
      OUT DATA.REGISTER, 1 ' DACSELECT

      'divide dac data into high and low bytes and write both bytes
      'to the data in register, waiting for a clear data in full flag
      'before each write.

      DAHIGH = INT(DATA.VALUE# / 256)
      DALOW = DATA.VALUE# - DAHIGH * 256
      WAIT STATUS.REGISTER, WRITE.WAIT, WRITE.WAIT
      OUT DATA.REGISTER, DALOW
      WAIT STATUS.REGISTER, WRITE.WAIT, WRITE.WAIT
      OUT DATA.REGISTER, DAHIGH

      'check error
      WAIT STATUS.REGISTER, COMMAND.WAIT
      STATUS = INP(STATUS.REGISTER)
      IF (STATUS AND &H80) THEN GOTO 9500

      OUT COMMAND.REGISTER, CSTOP
      TEMP = INP(DATA.REGISTER)
      WAIT STATUS.REGISTER, COMMAND.WAIT
      OUT COMMAND.REGISTER, CCLEAR

5300
CLS

LOCATE 5, 10, 1, 1
PRINT "          T E S T   C O M P L E T E   !"
LOCATE 15, 10
PRINT "DATA CONVERSION IS IN PROGRESS !   PLEASE WAIT !!!"
LOCATE 22, 10
PRINT "          T I M E   F O R   P R E P A R I N G   N E X T   T E S T   !!!"
LOCATE 25
PRINT

```

```

5600 'calculate and print all converted a/d voltages,
      'formatting the spacing to indicate first and last channel readings.

5900      WAIT STATUS.REGISTER, COMMAND.WAIT
          STATUS = INP(STATUS.REGISTER)
          IF (STATUS AND &H80) THEN GOTO 9500

6000      OPEN "C:\data\DIGDAT" + NTST$ FOR OUTPUT AS #4
          IF sp$ = "2" THEN
              OPEN "A:datarf" + NTST$ FOR OUTPUT AS #3
          ELSE OPEN "C:\MTS\DATA" + NTST$ FOR OUTPUT AS #3
          END IF

6050      'set values for system of thermocouples, pressure and LVDT

          'SENPT = sensitivity of pressure transducers (PSI/VOLT)
          'SENLT = sensitivity of position transducers (in/volt)

6100      SENPTVP# = ((150 / 14.2) / 10.2) / 10 'vapor pressure (MPa/V)
          SENPTLP# = ((5000 / (3.1415 * 9.2 * 9.2 / 4)) / 10.2) / 10 ' (MPa/M2)/V
          SENLT1# = 25.4 / 10 'LVDT position (mm/V)
          SENLT2# = 25.4 / 2 'piston position (mm/V)

6150 'ZEROVP! = zero output of vapor pressure trans in volts
      'ZEROLP! = zero output of lead pressure trans in volts
      'ZEROLT! = zero output of lved in volts

6200      'start loop to consider data for each cycle
          ZEROVP# = 0
          ZEROLP# = 0
          LVREF1# = 9.36 '2.239 'lvrf1!
          LVREF2# = 4 '13.29 '12.29 'lvrf2!

6300      OUT COMMAND.REGISTER, CSTOP
          TEMP = INP(DATA.REGISTER)
          WAIT STATUS.REGISTER, COMMAND.WAIT
          OUT COMMAND.REGISTER, CCLEAR

      FOR eloop = 1 TO nconvers#

6500      'select thermocouple channels

          ADGAIN = 3
          FACTOR# = (10 / BASE.FACTOR#) / GAIN(ADGAIN)

          FOR CHANT = 1 TO 4
              'calculate the a/d reading in volts.
              b = (eloop - 1) * 10 + CHANT
              UNI.VOLTS# = AD#(b) * FACTOR#
              BI.VOLTS# = UNI.VOLTS# * 2 - (10 / GAIN(ADGAIN))
              TRAW# = BI.VOLTS#
              IF CHANT <> 1 THEN GOTO 6700
6600      'obtain reference cold junction voltage
              CJV# = TRAW#
              CJT# = CJV# * 1000! / .5
              CJREF# = 38.66698 * CJT# + 4.373944E-02 * (CJT# ^ 2!) - 2.497418E-05 * (CJT# ^ 3!)

6700      'obtain voltage for current channel
              VNT# = TRAW#

6750      'apply cold junction corrected voltage (IN MICROVOLTS)
              VF# = (VNT# * 1000000!) + CJREF#

6800      'apply cubic conversion factors to get temperature
              TEMP# = 2.507424E-02 * VF# - 4.492068E-07 * (VF# ^ 2!) + 7.994254E-12 * (VF# ^ 3!)

```

```

6900 'save results in data file and print on screen
      IF CHANT = 2 THEN
        PRINT #3, USING "####.##,"; TEMP#;
      END IF

6950
NEXT CHANT

7200
ADGAIN = 0
FACTOR# = (10 / BASE.FACTOR#) / GAIN(ADGAIN)

      'calculate the a/d reading in volts.
FOR CHANP = 5 TO 8 'press and vapor data
      'obtain voltage for current channel

c = (eloop - 1) * 10 + CHANP

      UNI.VOLTS# = AD#(c) * FACTOR#
      BI.VOLTS# = UNI.VOLTS# * 2 - (10 / GAIN(ADGAIN))
      VNP# = BI.VOLTS#

7300      'calculate pressure
      IF (CHANP = 5) THEN
        THICK1# = (LVREF1# + VNP#) * SENLT1#
        THICK1# = THICK1# - PIST#
        PRINT #3, USING "##.#####,"; THICK1#;
        'strain! = 18 - THICK1#
        strain! = 12 - THICK1#
        PRINT #4, USING "##.#####,"; strain!;
        'PRINT #4, AD#(c);
        IF eloop = 10 THEN THRF# = THICK1#
      ELSEIF (CHANP = 6) THEN
        PRESVP# = (VNP# - ZEROVP#) * SENPTVP#
        PRINT #3, USING "####.#####,"; PRESVP#;
        PRINT #4, AD#(c);
      ELSEIF (CHANP = 7) THEN
        THICK2# = (LVREF2# + VNP#) * SENLT2#
        PRINT #3, USING "##.#####,"; THICK2#;
        'PRINT #4, AD#(c);
        IF eloop = 6 THEN MTS# = THICK2#
        IF eloop = 9 THEN MS# = MTS# - THICK2#
        PIST# = MS#
      ELSEIF (CHANP = 8) THEN
        PRESLP# = -(VNP# - ZEROVP#) * SENPTLP#
        PRINT #3, USING "##.#####,"; PRESLP#;
        'PRINT #4, AD#(c);
      END IF

7370
NEXT CHANP

7380
ADGAIN = 1
FACTOR# = (10 / BASE.FACTOR#) / GAIN(ADGAIN)
      'calculate the a/d reading in volts.
c = (eloop - 1) * 10 + 9
      UNI.VOLTS# = AD#(c) * FACTOR#
      BI.VOLTS# = UNI.VOLTS# * 2 - (10 / GAIN(ADGAIN))
      LT1# = BI.VOLTS#
      THICK# = (LT1#) * SENLT1#
      IF eloop = 10 THEN T1# = THICK#
      TH1# = T1#
      THICK9# = THRF# - (TH1# - THICK#)
      PRINT #3, USING "##.#####,"; THICK9#;
      'PRINT #4, AD#(c);

7390
ADGAIN = 2
FACTOR# = (10 / BASE.FACTOR#) / GAIN(ADGAIN)

```

```

      'calculate the a/d reading in volts.
c = (eloop - 1) * 10 + 10
  UNI.VOLTS# = AD#(c) * FACTOR#
  BI.VOLTS# = UNI.VOLTS# * 2 - (10 / GAIN(ADGAIN))
  LT1# = BI.VOLTS#
    THICK# = (LT1#) * SENLT1#
    IF eloop = 10 THEN T2# = THICK#
    TH2# = T2#
    THICK0# = THRF# - (TH2# - THICK#)
    PRINT #3, USING "###.#####,"; THICK0#;
    'strain! = 18 - THICK0#
    strain! = 12 - THICK0#
    PRINT #4, USING "###.#####,"; strain!;
    'PRINT #4, AD#(c);

7400  'record control data
st! = (5000 / (3.1415 * 9.2 * 9.2 / 4)) / 10.2
R! = st! / 10
  ctv# = ctvolt(eloop) * RANGE# / 4096
  ctp# = -(ctv# + BOTTOM.RANGE#) * R!
  IF eloop = ctvolt THEN ctp# = 0
  PRINT #3, USING "###.#####,"; ctp#;

7500  'record each loop test time
      'calculate each loop time
      TIME! = eloop * .2

      PRINT #3, USING "####.##,"; TIME!
      PRINT #4, USING "####.##,"; TIME!
      'PRINT #4, TIME!

7800
NEXT eloop
CLOSE #3
CLOSE #4

7900 'print out time of total and each loop
PRINT u!, w! - V!
8200
IF sp$ = "2" THEN 2000
9500  'program error explain
      'stop the dt2805 board and empty the data out register
      'wait until the dt2805 board ready flag is set,
      'then write the read error register command byte
      'to the command register
      OUT COMMAND.REGISTER, CSTOP
      TEMP = INP(DATA.REGISTER)
      WAIT STATUS.REGISTER, COMMAND.WAIT
      OUT COMMAND.REGISTER, CERROR

      'wait until the dt2805 board data out ready flag is set,
      'then read the dataout register to get the error register low byte
      WAIT STATUS.REGISTER, READ.WAIT
      ERR1 = INP(DATA.REGISTER)

      'wait until the dt2805 board data out ready flage is set,
      'then read the data out register to get the error register high byte.
      WAIT STATUS.REGISTER, READ.WAIT
      ERR2 = INP(DATA.REGISTER)

      'check the error flag.
      IF ERR1 > 0 THEN
        PRINT "PROGRME ERR ARE:"
        PRINT "ERR1 ="; ERR1
      ELSEIF ERR2 > 0 THEN
        PRINT "PROGRME ERR ARE:"
        PRINT "ERR2 ="; ERR2
      END IF

```



```

10000
END

SUB genctda (alldat!, load!) STATIC

' this is the part 3 of a composites manufacturing simulation test system
' this program is for creating a data file
' and the file will be used to control mts machine
,
CLS
LOCATE 5, 10
PRINT " WELCOME TO COMPOSITES MANUFACTURING SIMULATION TEST SYSTEM"
LOCATE 10, 10
PRINT "                                PART III "
LOCATE 15
PRINT
PRINT "                                *****"
PRINT "                                *                                * "
PRINT "                                *      MTS CONTROL DATA GENERATING PROGRAM !      *"
PRINT "                                *                                *"
PRINT "                                *****                                "
10050 IF INKEY$ = "" THEN GOTO 10050
CLS
LOCATE 2
PRINT
'DIM load!(alldat)
'DIM pload!(alldat)

10100 'creat a data file
PRINT "DATA FILE SELECT:"
PRINT
PRINT "      1. MTS TEST REFERENC DATA,"
PRINT "      2. MTS TEST CONTROL DATA"
PRINT "      3. EXIT"
INPUT sf$
10150
PRINT " DATA FILE NUMBER =      ? "
INPUT ndaf$

SELECT CASE sf$
CASE "1"
PRINT " Reference data file generation !"
GOTO 10200
CASE "2"
PRINT "Test control data file generation !"
GOTO 10300
CASE "3"
PRINT "EXIT SUB !"
GOTO 10900
CASE ELSE
GOTO 10100
END SELECT

10200
OPEN "a:rfct" + ndaf$ FOR OUTPUT AS #1
GOTO 10400
10300
OPEN "C:\MTS\datct" + ndaf$ FOR OUTPUT AS #1

10400
PRINT " how many test stages =      ?"
INPUT stage

PRINT " totle test time =      (sec.) ? "
INPUT tt

alldat = tt * 5
PRINT #1, alldat
PRINT alldat

```

```

PRINT " diameter of test disks = (mm)"
INPUT disk!
a! = (3.1415 * 9.2 * 9.2 / 4)
st! = (5000 / a!) / 10.2 'maximum stress m(N/M2)
PRINT "maximum stress = "; st!
R! = st! / 10
10500
FOR I = 1 TO stage
  PRINT "the "; I; "stage of "; stage; " pressing time = ? "
  INPUT timstg!
  PRINT "start press pressure = (m(N/M2)) "
  INPUT ps!
  pstart! = ps! / R!
  PRINT "end press pressure = (m(N/M2)) "
  INPUT pe!
  pend! = pe! / R!
10600
  'taveg!(i) = (tend(i) - tstart(i)) / timstg
  pdiff! = (pend! - pstart!)
  peach! = pdiff! / (timstg! * 5)

  IF I = 1 THEN tm = 1
  FOR j = tm TO (timstg! * 5 + tm - 1)

    IF pend! <> pstart! THEN
      pvalue! = pstart!
    ELSE
      pvalue! = pend!
    END IF

    each! = peach! * (j - tm + 1)
    pload! = pvalue! + each!
    load! = pload!

    PRINT #1, j, load!
    PRINT J, load!
  NEXT j
  tm = j
  IF ((j - 1) / 5) >= tt THEN 10650

NEXT I

10650
CLOSE #1

10700 ' check time and data numbers

PRINT " total time = ?"; j - 1
d = 5 * tt
PRINT " total data = ?"; d

IF ((j - 1) / 5) <> tt THEN
  PRINT " setted wroung time !!!"
ELSEIF d <> alldat THEN
  PRINT "setted wroung data !!!";
END IF

10900

END SUB

```

```

PROGRAM CST.FOR
c*****
c this program calculates the rheological constants
c of wood-adhesive system during hot pressing from
c experimental results, and to creat a E1, E1P, K1 data file
c for futher analysis.
c 7-26-1990 by Shan Ren, improved on 2-2-1991
c*****
      REAL*8 (A-H,O-Z)
      REAL*8 th(630*5),Strs(630*5)
      CHARACTER*3 U
      CHARACTER*2 N$
      CHARACTER*4 W,V
      CHARACTER*5 X,Z
      CHARACTER*6 Y
      WRITE(*,*) 'NUMBER OF TEST = '
      READ(*,*) N$
      WRITE(*,*) 'CONDITION OF TEST'
      READ(*,*) NCS
      U='DEF'
      V='CTE1'
      W='E1P'
      X=U // N$
      Y=V // N$
      Z=W // N$
      OPEN(UNIT=7,FILE='C:\SHAN\X')
      OPEN(UNIT=8,FILE='C:\SHAN\Y')
      OPEN(UNIT=9,FILE='C:\SHAN\Z')
c
      input data
      N=630*5
      DO 100 I=1,N
        READ(7,*)TIME,TH(I),STRS(I)
100    CONTINUE
      CLOSE(UNIT=7)
      WRITE(8,*)'Te No=','N$', 'INTI H 0.2=',TH(1), '1='TH(5)
      WRITE(8,*)'TIME,LOAD,DENSITY,THICK,E1,STRAIN,STRESS '
c      calculate of elastic element 1: ";
c      calculate the elastisity of elastic element 1 at vary c      condition.
c      Strain = Stress / E
      DO 200 I=23,63,40
        T=I*5
        AVT1=(TH(T)+TH(T-1)+TH(T-2))/3
        AVT2=(TH(T+1)+TH(T+2)+TH(T+3))/3
        STN1=(AVT1-AVT2)/AVT1
        STS1=STRS(T)-STRS(T+1)
        IF(STN1.EQ.0) THEN GOTO 150
        E1=ABS(STS1/STN1)
        DENS=(140000 /((3.14156*9.2*9.2/4)*AVT1))
150    CONTINUE
        WRITE(8,'F4.1') T/5
        WRITE(8,'F6.4') STRS(T)
        WRITE(8,'F9.5') DENS
        WRITE(8,'F9.6') AVT1
        WRITE(8,'F13.6') E1
        WRITE(8,'F8.5,1X,F8.5') STN1,STS1
200    CONTINUE
c      for i > 265
      DO 300 T=1325,1335
        STN1=(TH(T)-TH(T+1))/TH(T)
        STS1=STRS(T)-STRS(T+1)
        IF(STN1.EQ.0) THEN GOTO 250
        IF(T.GT.1325) THEN STS1=-STS1
        E1=(STS1/STN1)
        DENS=(140000)/((3.14156*9.2*9.2/4)*TH(T))
250    CONTINUE
        WRITE(8,'F4.1') t/5
        WRITE(8,'F6.4') Strs(t)
        WRITE(8,'F9.5') dens
        WRITE(8,'F9.6') th(t)
        WRITE(8,'F13.6') E1
        WRITE(8,'F8.5,1X,F8.5') Stn1,Sts1
300    CONTINUE

```

```

c   for elastical element 1: E1 at 307.2 sec.
DO 400 T=1536,2936,200
    AVT1=(TH(T)+TH(T-1)+TH(T-2))/3
    AVT2=(TH(T+1)+TH(T+2)+TH(T+3))/3
    STN1=(AVT1-AVT2)/AVT1
    STS1=STRS(T)-STRS(T+1)
    IF(STN1.EQ.0) THEN GOTO 350
    E1=(STS1/STN1)
    DENS=(140000)/((3.14156*9.2*9.2/4)*AVT1)
350  CONTINUE
    WRITE(8,'F4.1') t/5
    WRITE(8,'F6.4') Strs(t)
    WRITE(8,'F9.5') dens
    WRITE(8,'F9.6') avt1
    WRITE(8,'F13.6') E1
    WRITE(8,'F8.5,1X,F8.5') Stn1,Sts1
400  CONTINUE
c   for elastical element 1: E1 at 589.2 sec.
    STN1=(TH(2945)-TH(2946))/TH(2945)
    STS1=STRS(2945)-STRS(2946)
    IF(STN1.EQ.0) THEN GOTO 500
    E1=ABS(STS1/STN1)
    DENS=(140000)/((3.14156*9.2*9.2/4)*TH(2945))
500  CONTINUE
    WRITE(8,'F4.1') 589.2/5
    WRITE(8,'F6.4') Strs(2945)
    WRITE(8,'F9.5') dens
    WRITE(8,'F9.6') th(2945)
    WRITE(8,'F13.6') E1
    WRITE(8,'F8.5,1X,F8.5') Stn1,Sts1
c   Calculate the E1P:
c   E1P = Stress / Strain
c   Strain=Stress/P+Stress/E1=Stress*((E1+P)/P*E1)
c   P = 1/(1/E1P - 1/E1)
    WRITE(9,*)'TIME,STRESS,DENSITY,THICK,E1P,STRAIN,STS1'
DO 600 T=1,6
    STN1=(TH(T)-TH(T+1))/TH(T)
    STS1=STRS(T)-STRS(T+1)
    IF(STN1.EQ.0) THEN GOTO 550
    E1P=(STS1/STN1)
    DENS=(140000)/((3.14156*9.2*9.2/4)*TH(T))
550  CONTINUE
    WRITE(9,'F4.1') T/5
    WRITE(9,'F6.4') STRS(T)
    WRITE(9,'F9.5') DENS
    WRITE(9,'F9.6') TH(T)
    WRITE(9,'F13.6') E1P
    WRITE(9,'F8.5,1X,F8.5') STN1,STS1
600  CONTINUE
DO 700 T=10,15
    STN1=(TH(T)-TH(T+1))/TH(T)
    STS1=STRS(T)-STRS(T+1)
    IF(STN1.EQ.0) THEN GOTO 650
    E1P=(STS1/STN1)
    DENS=(140000)/((3.14156*9.2*9.2/4)*TH(T))
650  CCONTINUE
    WRITE(9,'F4.1') T/5
    WRITE(9,'F6.4') STRS(T)
    WRITE(9,'F9.5') DENS
    WRITE(9,'F9.6') TH(T)
    WRITE(9,'F13.6') E1P
    WRITE(9,'F8.5,1X,F8.5') STN1,STS1
700  CONTINUE
c   for elastical element 1 and plastic element: E1P at
c   123 sec.
    STN1=(TH(615)-TH(616))/TH(615)
    STS1=STRS(615)-STRS(616)
    IF(STN1.EQ.0) THEN GOTO 800
    E1P=STS1/STN1
    DENS123=(140000)/((3.14156*9.2*9.2/4)*TH(615))
800  CONTINUE
    WRITE(9,'F4.1') 123

```

```

WRITE(9,'F6.4') STRS(615)
WRITE(9,'F9.5') DENS
WRITE(9,'F9.6') TH(615)
WRITE(9,'F13.6') E1P
WRITE(9,'F8.5,1X,F8.5') STN1,STS1
c  when i < 265
DO 900 T=1315,1325
    STN1=(TH(T)-TH(T+1))/TH(T)
    STS1=STRS(T)-STRS(T+1)
    IF(STN1.EQ.0) THEN GOTO 850
    E1P=(STS1/STN1)
    DENS=(140000)/((3.14156*9.2*9.2/4)*TH(T))
850  CONTINUE
    WRITE(9,'F4.1') T/5
    WRITE(9,'F6.4') STRS(T)
    WRITE(9,'F9.5') DENS
    WRITE(9,'F9.6') TH(T)
    WRITE(9,'F13.6') E1P
    WRITE(9,'F8.5,1X,F8.5') STN1,STS1
900  CONTINUE
c  calculate the visco element 1: k1
c  ek1 = Strs*t / K1 ; K1 = Strs*t/ek1
c  CALCULATE OF ELASTIC ELEMENTS 2 = ";
c  stn = stnk1 + stne2
c  stnk1 = Sts*t/K1 = (he1-h2)/he1
c  the2 = (tht!/(1-stnk1))
WRITE(8,*)'TIME, STRESS, DENSITY, THICK, K1, E '
DO 1000 I=200,260,5
    T=I*5
    TH=ABS(TH(T-1)+TH(T)+TH(T+1))/3
    THA=ABS(TH(T+24)+TH(T+25)+TH(T+26))/3
    DENS=(140000)/((3.14156*9.2*9.2/4)*TH)
    STNK1=ABS(TH-THA)/TH
    THK1=ABS(TH/(1-STNK1))
    IF((TH-THA).EQ.0) THEN GOTO 950
    K1=(STRS(T)*5)/STNK1
    THKAP=ABS((TH-THA)/5)
    KAP=STRS(T)/K1
950  CONTINUE
    WRITE(8,'F 4.1') I
    WRITE(8,'F6.4') STRS(T)
    WRITE(8,'F9.5') DENS
    WRITE(8,'F9.6') TH
    WRITE(8,'F13.6') K1
    DTHE2=THK1-THA
    THE2=TH-DTHE2
    STNE2=(DTHE2)/TH
    IF(STNE2.EQ.0) THEN GOTO 980
    E2=ABS(STRS(T)/STNE2)
980  CONTINUE
    WRITE(8,'F12.6') E2
1000 CONTINUE

DO 1100 I=150,260,10
    T=I*5
    TH=ABS(TH(T-1)+TH(T)+TH(T+1))/3
    THA=ABS(TH(T+49)+TH(T+50)+TH(T+51))/3
    DENS=(140000)/((3.14156*9.2*9.2/4)*TH)
    STNK1=ABS(TH-THA)/TH
    THK1=ABS(TH/(1-STNK1))
    IF((TH-THA).EQ.0) THEN GOTO 1050
    K1=(STRS(T)*10)/STNK1
    THKAP=ABS((TH-THA)/10)
    KAP=STRS(T)/K1
1050 CONTINUE
    WRITE(8,'F 4.1') i
    WRITE(8,'F6.4') Strs(t)
    WRITE(8,'F9.5') dens
    WRITE(8,'F9.6') th
    WRITE(8,'F13.6') K1
    DTHE2=THK1-THA
    THE2=TH-DTHE2

```

```
      STNE2=(DTHE2)/TH
      IF(STNE2.EQ.0) THEN GOTO 1080
      E2=ABS(STRS(T)/STNE2)
1080   WRITE(8,'F12.6') E2
1100  CONTINUE
      CLOSE(UNIT=8)
      CLOSE(UNIT=9)
      STOP
      END
```

```

PROGRAM CSTE2.FOR
c*****
c this program is to calculate the rheological constants
c of wood-adhesive system during hot pressing from
c experimental results, and to creat an E2 data file
c for futher analysis.
c 7-26-1990 by Shan Ren, improved on 2-2-1991
c*****
      REAL*8 (A-H,O-Z)
      REAL*8 TH(300*5), STRS(300*5)
      CHARACTER*3 NC$, U,V
      CHARACTER*2 N$
      CHATATER*4 W
      CHARACTER*5 X
      CHARACTER*6 Y,Z
      WRITE(*,*) 'NUMBER OF TEST = '
      READ(*,*) N$
      WRITE(*,*) 'CONDITION OF TEST'
      READ(*,*) NC$
      U='ALC'
      V='DEF'
      W='CSET'
      X=U // NC$
      Y=V // N$
      Z=W // N$
      OPEN(UNIT=7,FILE='C:\SHAN\X')
      OPEN(UNIT=8,FILE='C:\SHAN\Y')
      OPEN(UNIT=9,FILE='C:\SHAN\Z')
c    input parameters
      READ(7,*) AE1, BE1, AP, BP, AK1, BK1
      CLOSE(UNIT=7)
c    input data
      N=300*5
      DO 100 I=1,N
        READ(8,*) TIME, TH(I), STRS(I)
100    CONTINUE
      CLOSE(UNIT=8)

c    CALCULATE OF ELASTIC ELEMENT 2: ";
c    at t >> t0, ee2 = eetotal-ee1-ek1-ep, ee2k2 = 0
c    strn = stnk1 + stne2
      WRITE(9,*) 'TEST NUMBER =', 'N$'
      WRITE(9,*) 'TIME, DENSITY, LOAD, THICK, THICKC, E2'
      DO 200 I=50,300,5
        T=I*5
        TH=(TH(T-1)+TH(T)+TH(T+1))/3
        THB=(TH(T-24)+TH(T-25)+TH(T-26))/3
        DENS=(140000)/((3.14156*9.2*9.2/4)*
c        Calculate the each element constant:
c
c
c
        E1=EXP(AE1+BE1*DENS)
        P=EXP(AP+BP*DENS)
        K1=EXP(AK1+BK1*DENS)
c
c    calculate the ee1:
        EE1=(STRS(T)-STRS(T - 25))/E1
        THE1=(TH*(1-EE1))
        DTHE1=(TH-THE1)
c    calculate the ep:
c    check maximin value of stress:
        IF (SM.LE.STRS(T)) THEN SM=STRS(T)
        ST=SM
        IF(SM.GT.STRS(T)) THEN ST=SM
        ST1=ST-STRS(T-25)
        EP=ST1/P
        THP=(TH*(1-EP))
        DTHP=(TH-THP)
        IF (STM.GE.STRS(T)) THEN DTHP=0
        STM=ST

```

```
c      calculate the ek1:
      EK1=STRS(T)*25/K1
      THK1=ABS(TH*(1 - EK1))
      DTHK1=ABS(THK1 - TH)
c      calculate the EE2:
      ETOTAL=ABS(TH-THB)/TH
      EE2=ABS(ETOTAL-EE1-EP-EK1)
      THE2=ABS(TH*(1-EE2))
      DTHE2=ABS(THE2-TH)
      IF(EE2.EQ.0) THEN GOTO 150
      E2=(STRS(T)/EE2)
c      CALCULATE THE DEFORMATION:
      DTH=(DTHE1+DTHP+DTHE2+DTHK1)
      THA=TH-DTH
150    CONTINUE
      WRITE(9,'F4.1') T
      WRITE(9,'F6.4') STRS(T)
      WRITE(9,'F8.4') DENS
      WRITE(9,'F8.6,1X,F8.6') TH,THA
      WRITE(9,'F12.6') E2
200    CONTINUE
      STOP
      END
```



```

PROGRAM CSTK2.FOR
c*****
c this program calculates the rheological constants of
c wood-adhesive system during hot pressing from
c experimental results and to create a K2 data file
c for further analysis.
c 7-26-1990 by Shan Ren, improved on 2-2-1991
c*****
      REAL*8 (A-H,O-Z)
      REAL*8 TH(300*5),STRS(300*5)
      CHARACTER*2 N$
      CHARACTER*3 NC$
      CHARACTER*4 W
      CHARACTER*5 X
      CHARACTER*6 Y,Z
      WRITE(*,*)'NUMBER OF TEST = '
      READ(*,*) N$
      WRITE(*,*)'CONDITION OF TEST = '
      READ(*,*) NC$
      U='ALC'
      V='DEF'
      W='CSTK'
      X=U//NC$
      Y=V//N$
      Z=W//N$
      OPEN(UNIT=7,FILE='C:\SHAN\X')
      OPEN(UNIT=8,FILE='C:\SHAN\Y')
      OPEN(UNIT=9,FILE='C:\SHAN\Z')
c    input parameters
      READ(7,*)AE1,BE1,AP,BP,AK1,BK1,AE2,BE2
      CLOSE(UNIT=7)
c    input data
      N=300*5
      DO 100 FOR I=1,N
        READ(8,*)TIME,TH(I),STRS(I)
100    CONTINUE
      CLOSE(UNIT=8)
c    CALCULATE THE VISCO ELEMENT 2: K2
      ee2k2 = etotal-ee1-ee2-ek1-ep
      ee2k2' =S/K1 + S / K2 * (e(-E2*t/K2))
c    K2 = E2*t*log(e)/(log(strs/E2)-log( *** ))
      WRITE(9,*)'TEST NUMBER =', 'N$'
      WRITE(9,*)'TIME, LOAD, DENSITY, THICK, THKC, K2'
      DO 200 I=50,300,5
        T=I*5
        TH=(TH(T-1)+TH(T)+TH(T+1))/3
        THB=(TH(T-24)+TH(T-25)+TH(T-26))/3
        DENS=(140000)/((3.14156*9.2*9.2/4)*TH)
c      Calculate the each element constant:
c
c
      E1=EXP(AE1+BE1*DENS)
      P=EXP(AP+BP*DENS)
      K1=EXP(AK1+BK1*DENS)
      E2=EXP(AE2+BE2*DENS)
c
c    calculate the ee1:
      EE1=(STRS(T)-STRS(T-25))/E1

      THE1=(TH*(1-EE1))
      DTHE1=(TH-THE1)
c    calculate the ep:
c    check maximin value of stress:
      IF(SM.LE.STRS(T)) THEN SM=STRS(T)
      ST=SM
      IF(SM.GT.STRS(T)) THEN ST=SM
      ST1=ST-STRS(T - 25)
      EP=ST1/P

      THP=(TH*(1-EP))
      DTHP=(TH-THP)
      IF(STM.GT.STRS(T)) THEN DTHP=0

```

```

STM=ST
c   calculate the ek1:
    EK1=STRS(T)*25/K1
    THK1=ABS(TH*(1-EK1))
    DTHK1=ABS(THK1-TH)
c   calculate the ee2:
    EE2=(STRS(T)/E2)
    THE2=ABS(TH*(1-EE2))
    DTHE2=ABS(THE2-TH)
c   calculate the EV2:
    ETOTAL=ABS(TH-THB)/TH
    E2K2=ABS(ETOTAL-EE1-EE2-EK1-EP)
    THE2K2=ABS(TH*(1+E2K2))
    DTHE2K2=ABS(THE2-TH)
    L=LOG(E2*E2K2/STRS(T))
    IF (L.EQ.0) THEN GOTO 150
    K2=(E2*25)/(L)
c   calculate the deformation:
150  CONTINUE
     DTH=(DTHE1+DTHP+DTHE2+DTHK1-DTHE2K2)
     THA=TH-DTH
     WRITE(9,'4.1') T
     WRITE(9,'F6.2') STRS(T)
     WRITE(9,'F8.4') DENS
     WRITE(9,'F8.6,1X,F8.6') TH,THA
     WRITE(9,'F12.6') K2
200  CONTINUE
     CLOSE(UNIT=8)
     STOP
     END

```

```

c*****
c this program calculates the rheological constants
c of wood-adhesive system during hot pressing from
c experimental results and to creat E1P and P data file
c for futher analysis.
c 7-26-1990 by Shan Ren, improved on 2-2-1991
c*****
      READ*8 (A-H,O-Z)
      REAL*8 TH(270*5),STRS(270*5),A(27*5)
      CHARACTER*2 N$
      CHARACTER*3 NT$
      CHARACTER*4 W
      CHARACTER*5 X
      CHARACTER*6 Y,Z
      WRITE(*,*)'NUMBER OF TEST ='
      READ(*,*)N$
      WRITE(*,*)'CONDITION OF TEST = '
      READ(*,*)NT$
      U='ACL'
      V='DEF'
      W='CSTP'
      X=U//NT$
      Y=V//N$
      Z=W//N$
      OPEN(UNIT=7,FILE='C:\SHAN\X')
      OPEN(UNIT=8,FILE='C:\SHAN\Y')
      OPEN(UNIT=9,FILE='C:\SHAN\Z')
c      input parameters of E1 from equation
      READ(7,*)AE1,BE1
      CLOSE(UNIT=7)
c      input data
      N=270*5
      DO 100 I=1,N
        READ(8,*)TIME, TH(I),STRS(I)
100    CONTINUE
      CLOSE(UNIT=8)
c      Calculate the E1P:
c      E1P = Stress / Strain
c      Strain = Stress/P + Stress/E1 = Stress ((E1+P)/P*E1)
c      P = 1/(1/E1P - 1/E1)
      WRITE(9,*)'Te No=','N$', 'int h 1=' (1), th(5)
      WRITE(9,*)'time,load,density,thick,P,E1c,Strain,Sts1'
      DO 200 T = 1 TO 6
        dens=(140000)/((3.14156*9.2*9.2/4)*th(t))
        Stn1=(th(t)-th(t+1))/th(t)
        Sts1=Strs(t)-Strs(t+1)
        IF(Stn1.EQ.0) THEN GOTO 150
        E1P=(Sts1/Stn1)
        E1c=EXP(ae1+be1*dens)
        IF(E1P.EQ.0) THEN GOTO 150
        P=1/(1/E1P-1/E1c)
150      WRITE(9,'F4.1') t/5
        WRITE(9,'F6.4') Strs(t)
        WRITE(9,'F8.4') dens
        WRITE(9,'F8.6') th(t);
        WRITE(9,'F12.6,1X,F12.6') P,E1c
        WRITE(9,'F8.5,1X,F8.5') Stn1,Sts1
200    CONTINUE
      DO 300 T=10,15
        DENS=(140000)/((3.14156*9.2*9.2/4)*TH(T))
        STN1=(TH(T)-TH(T+1))/TH(T)
        STS1=STRS(T)-STRS(T+1)
        IF(STN1.EQ.0) THEN GOTO 250
        E1P=(STS1/STN1)
        E1C=EXP(AE1+BE1*DENS)
        IF(E1P.EQ.0) THEN GOTO 250
        P=1/(1/E1P-1/E1C)
250    CONTINUE
        WRITE(9,'F4.1') T/5
        WRITE(9,'F6.4') STRS(T)
        WRITE(9,'F8.4') DENS

```

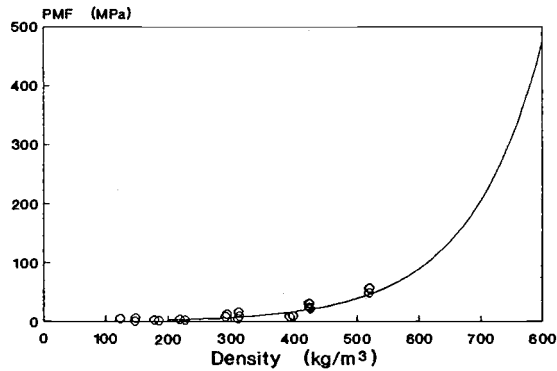
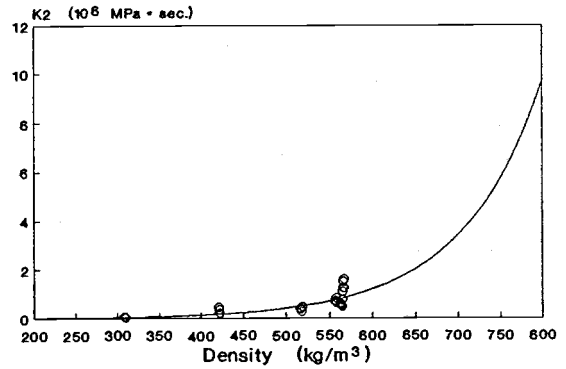
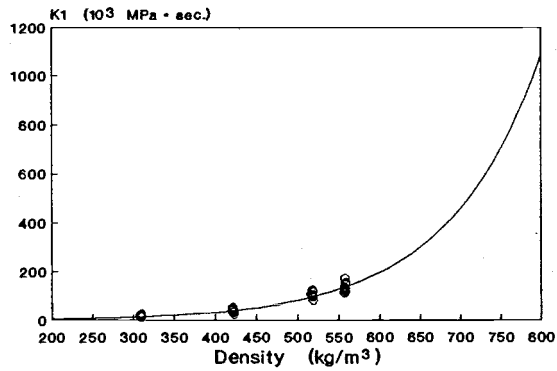
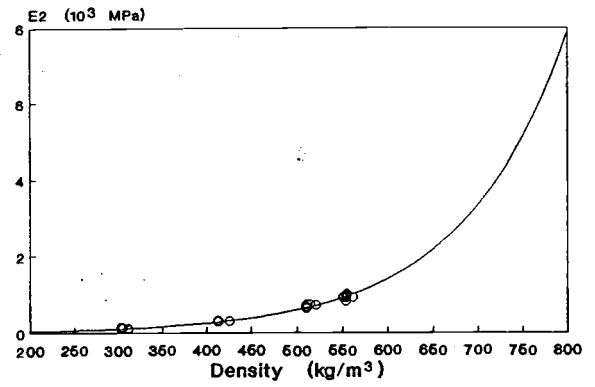
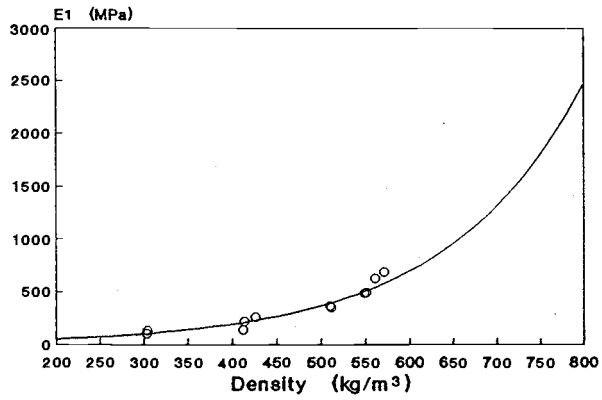
```

        WRITE(9,'F8.6') TH(T)
        WRITE(9,'F12.6,1X,F12.6') P,E1C
        WRITE(9,'F8.5,1X,F8.5') STN1,STS1
300  CONTINUE
c    for elastical element 1 and plastic element: E1P at c c    123 sec.
    DENS=(140000)/((3.14156*9.2*9.2/4)*TH(615))
    STN1=(TH(615)-TH(616))/TH(615)
    STS1=STRS(615)-STRS(616)
    IF(STN1.EQ.0) THEN GOTO 400
    E1P=(STS1/STN1)
    E1C=EXP(AE1+BE1*DENS)
    IF(E1P.EQ.0) THEN GOTO 400
    P=1/(1/E1P-1/E1C)
400  WRITE(9,'F4.1') 123
    WRITE(9,'F6.4') STRS(615)
    WRITE(9,'F8.4') DENS
    WRITE(9,'F8.6') TH(615)
    WRITE(9,'F12.6,1X,F12.6') P,E1C
    WRITE(9,'F8.5,1X,F8.5') STN1,STS1
c    when i < 265
    DO 500 T=1315,1325
        DENS=(140000)/((3.14156*9.2*9.2/4)*TH(T))
        STN1=(TH(T)-TH(T+1))/TH(T)
        STS1=STRS(T)-STRS(T+1)
        IF(STN1.EQ.0) THEN GOTO 450
        E1P=(STS1/STN1)
        E1C=EXP(AE1+BE1*DENS)
        IF(E1P.EQ.0) THEN GOTO 450
        P=1/(1/E1P-1/E1C)
450  WRITE(9,'F4.1') T/5
    WRITE(9,'F6.4') STRS(T)
    WRITE(9,'F8.4') DENS
    WRITE(9,'F8.6') TH(T)
    WRITE(9,'F12.6,1X,F12.6') P,E1C
    WRITE(9,'F8.5,1X,F8.5') STN1,STS1
500  CONTINUE
c    calculate the plasiticity
    WRITE(9,*) 'EXTRA CALCULATION'
    STSP=STRS(1325)-STRS(1315)
    STNP=(TH(1315)-TH(1336))/TH(1315)
    P=STSP/STNP
    DENS=(140000)/((3.14156*9.2*9.2/4)*TH(1315))
    WRITE(9,'F4.1') 1315/5
    WRITE(9,'F6.4') STRS(1315)
    WRITE(9,'F8.6') DENS
    WRITE(9,'F8.6') TH(1315)
    WRITE(9,'F12.6,1X,F12.6') P,E1C
    WRITE(9,'F8.5,1X,F8.5') STN1,STS1
    CLOSE(UNIT=9)
    STOP
    END

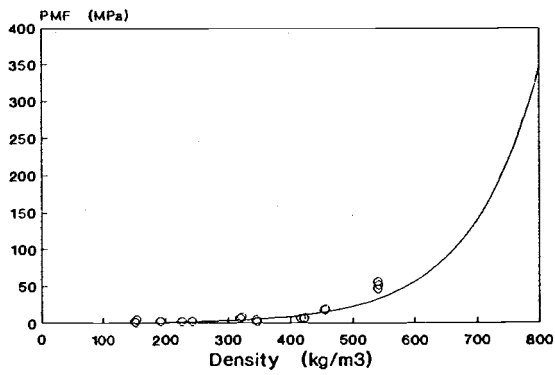
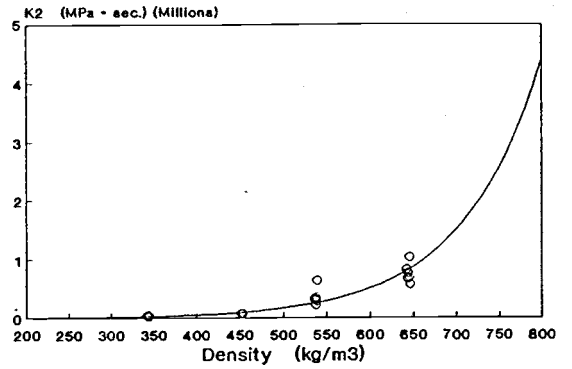
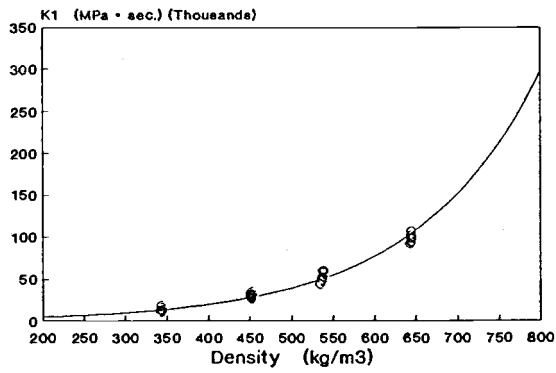
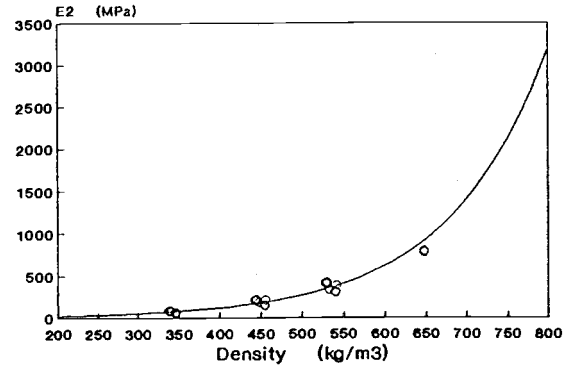
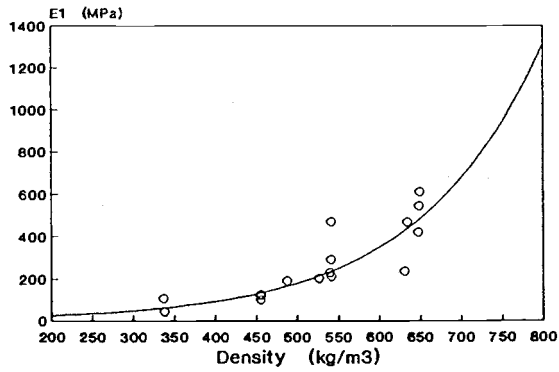
```

APPENDIX II

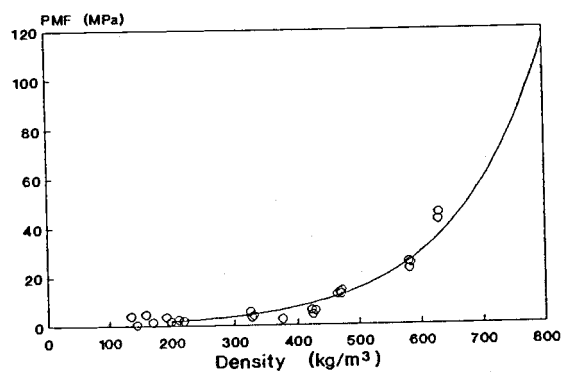
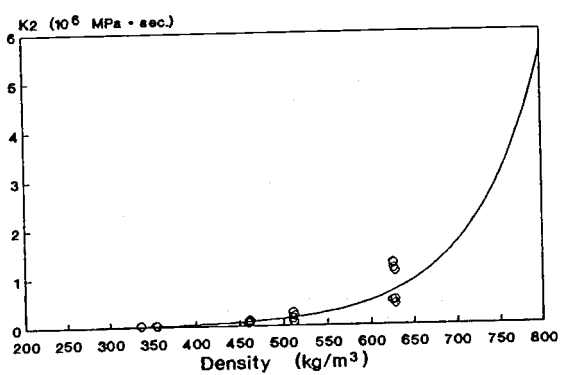
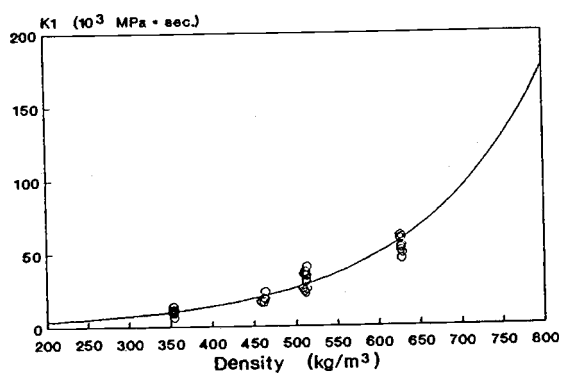
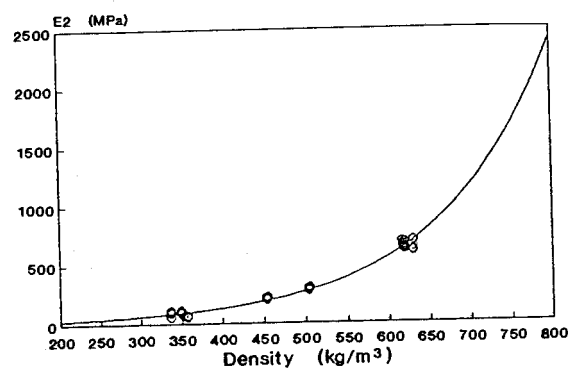
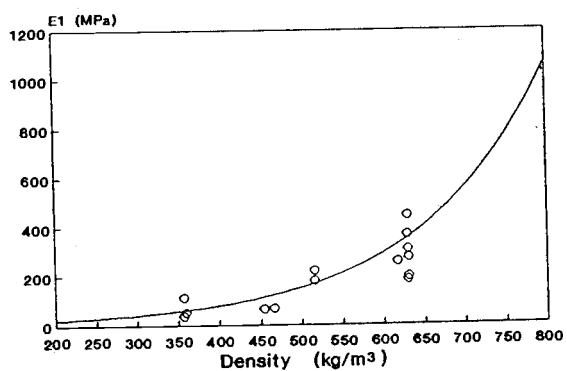
Five elements properties



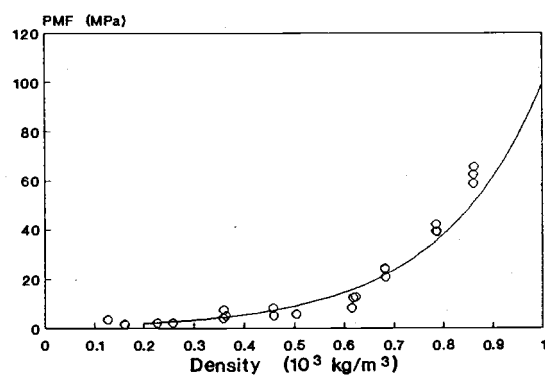
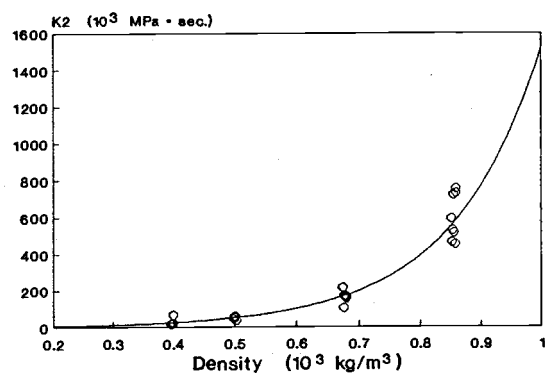
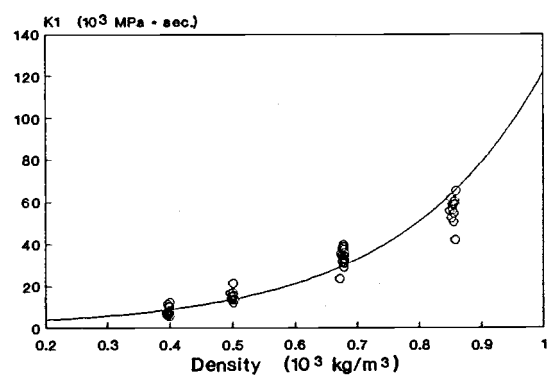
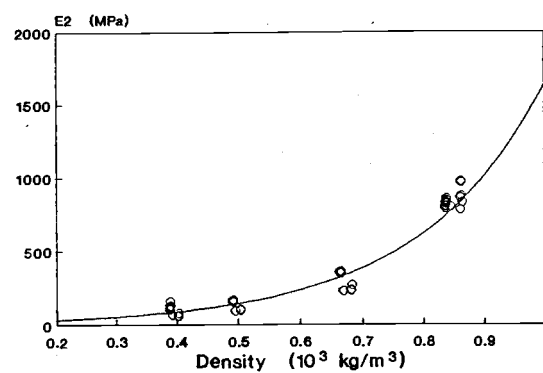
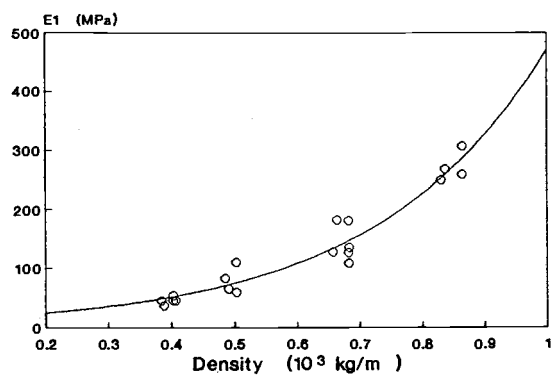
Element properties on $T = 25\text{ }^{\circ}\text{C}$, $MC = 0\%$.



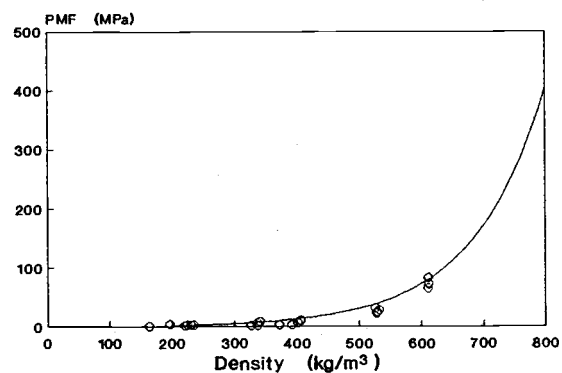
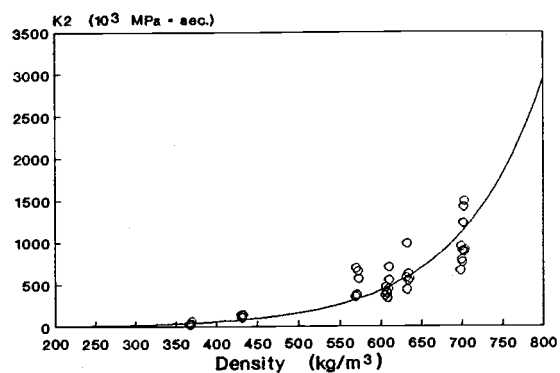
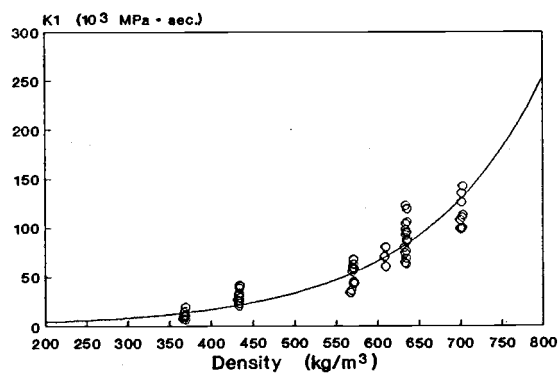
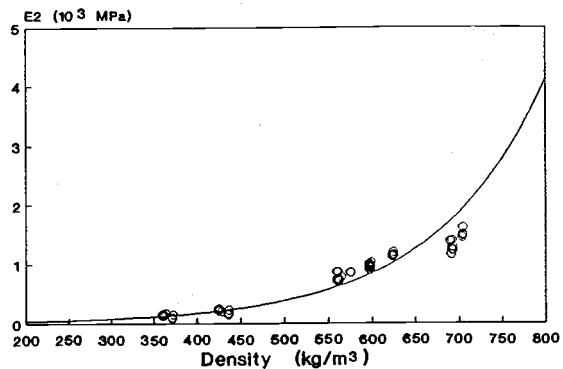
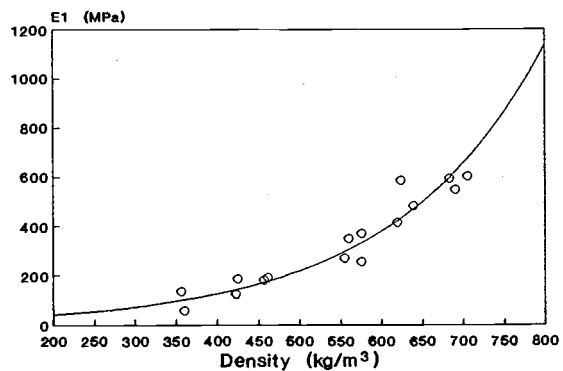
Element properties on $T = 25\text{ }^{\circ}\text{C}$, $\text{MC} = 4\%$.



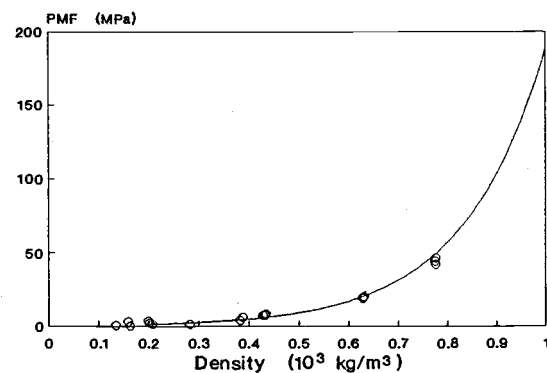
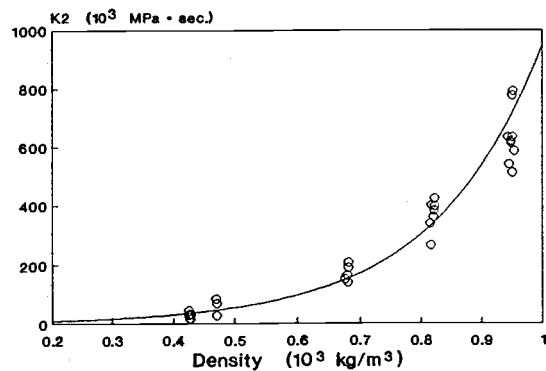
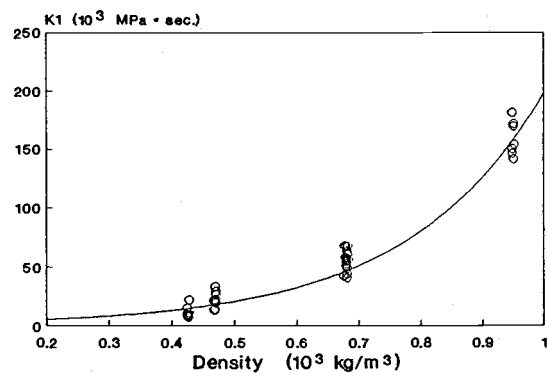
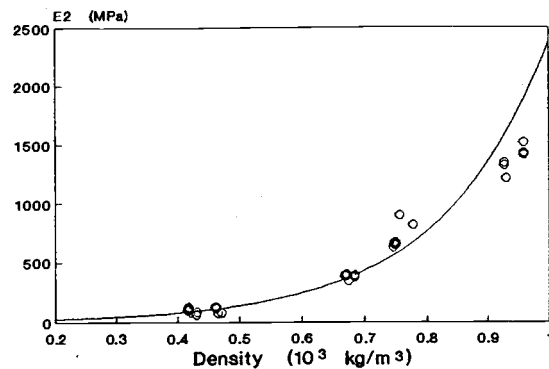
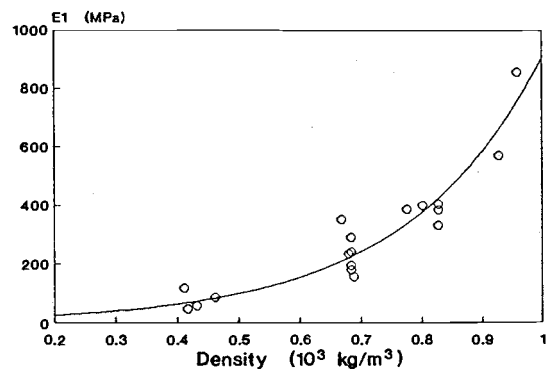
Element properties on $T = 25\text{ }^{\circ}\text{C}$, $MC = 10\%$.



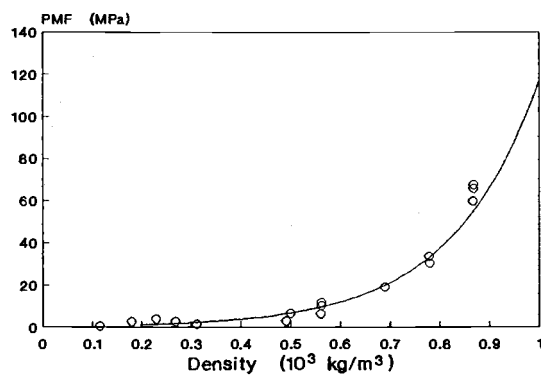
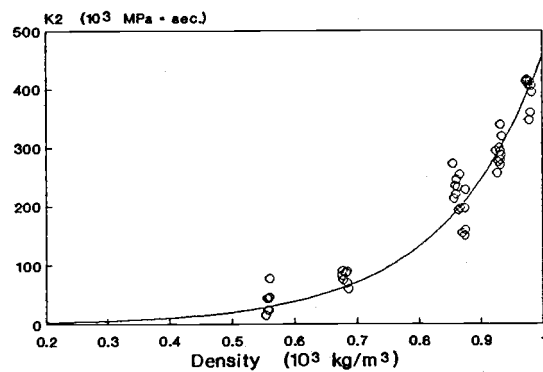
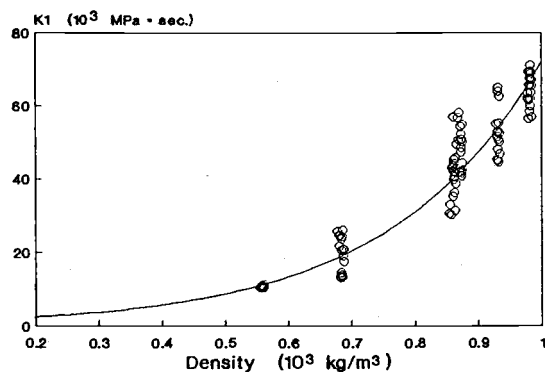
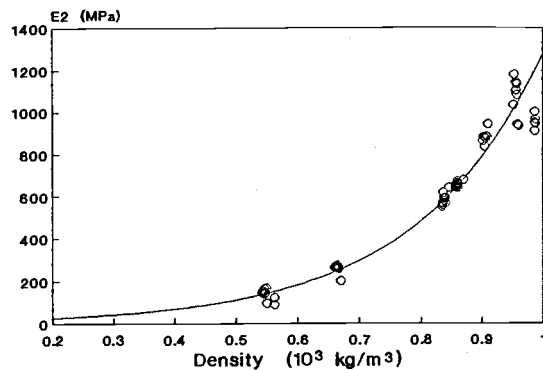
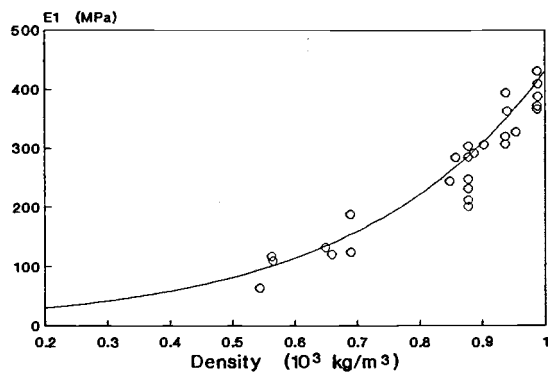
Element properties on $T = 25^\circ \text{C}$, $\text{MC} = 16\%$.



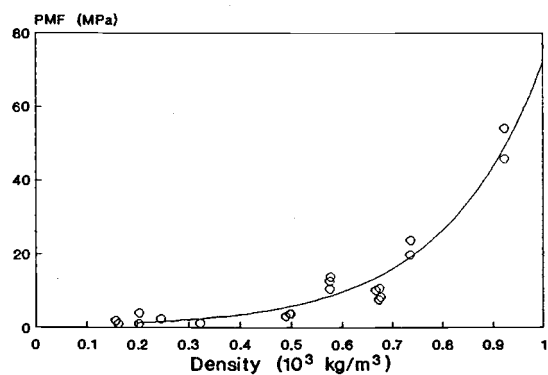
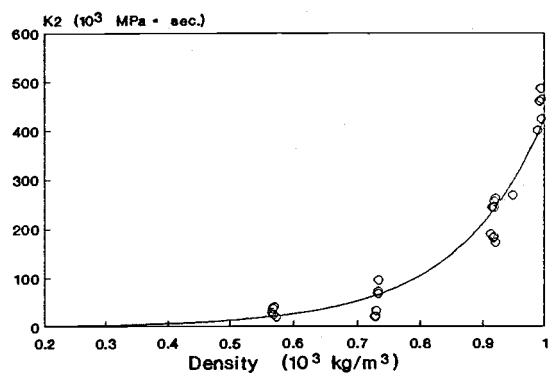
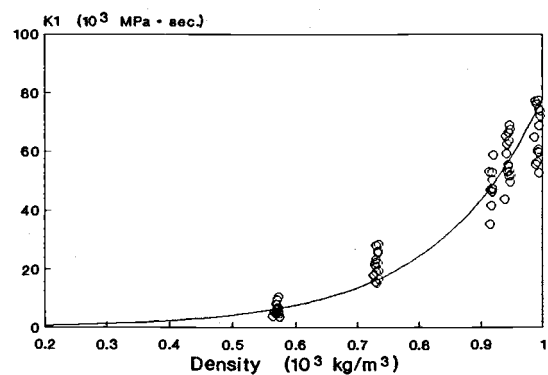
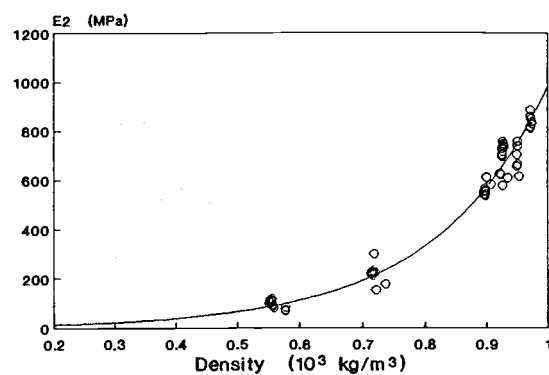
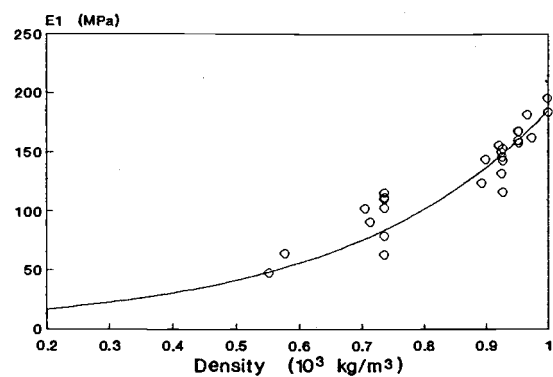
Element properties on $T = 100\text{ }^{\circ}\text{C}$, $MC = 0\%$.



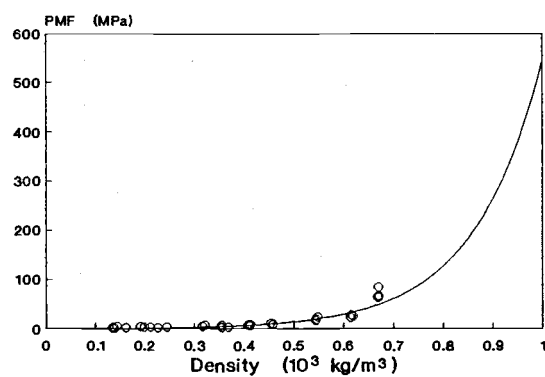
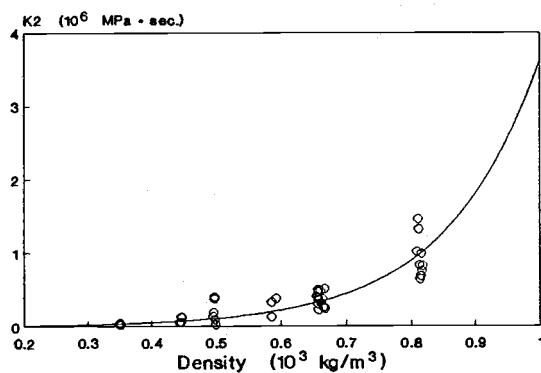
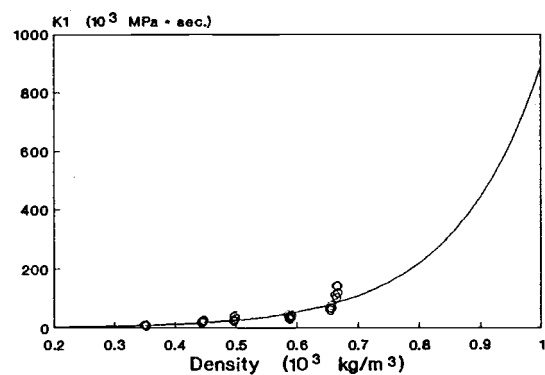
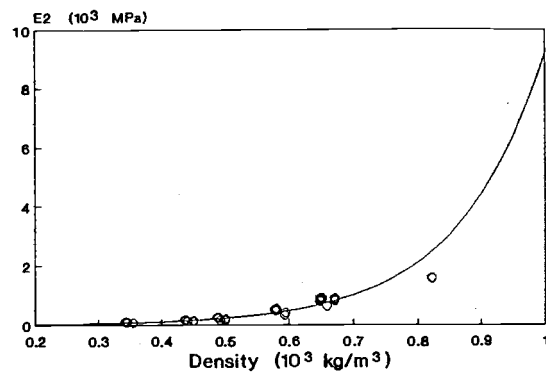
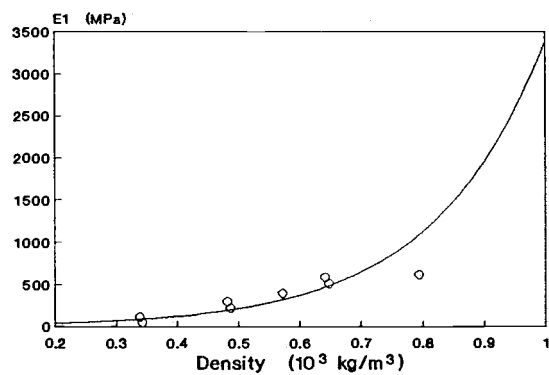
Element properties on $T = 100^\circ\text{C}$, $\text{MC} = 4\%$.



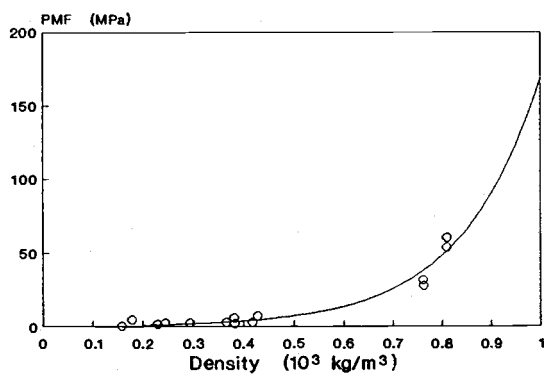
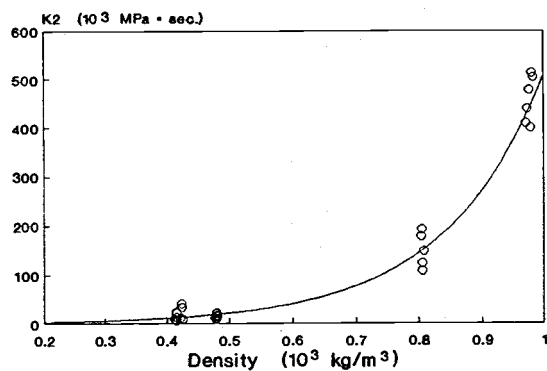
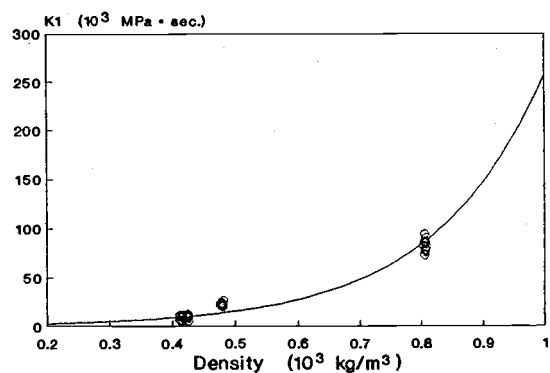
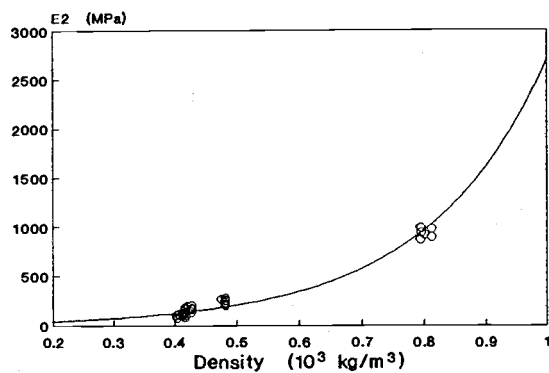
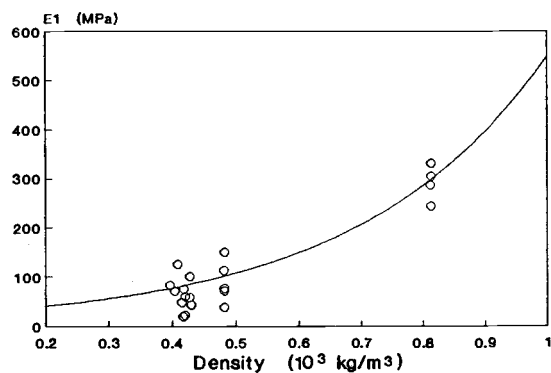
Element properties on $T = 100^\circ\text{C}$, $\text{MC} = 10\%$.



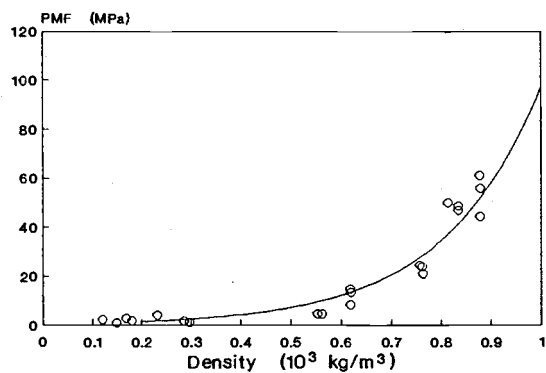
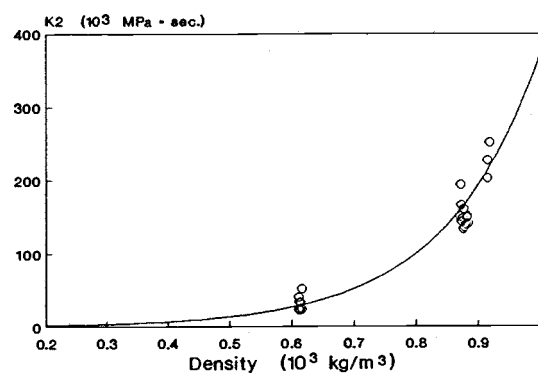
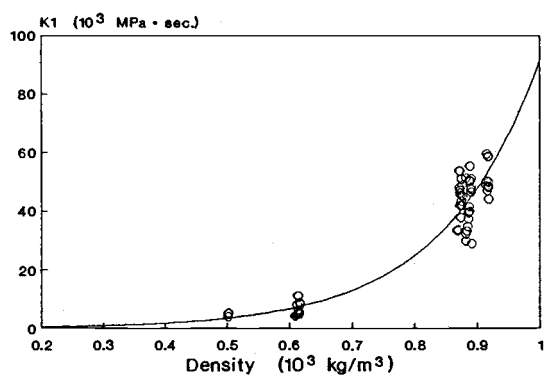
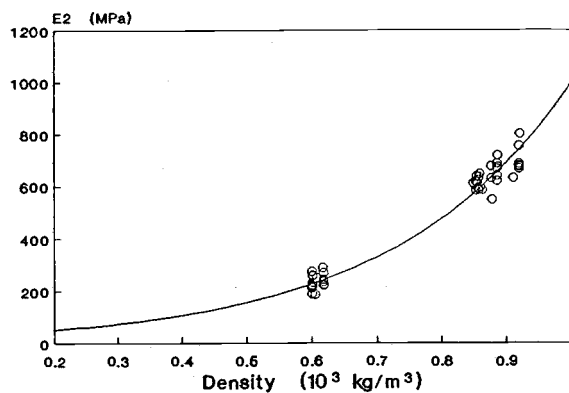
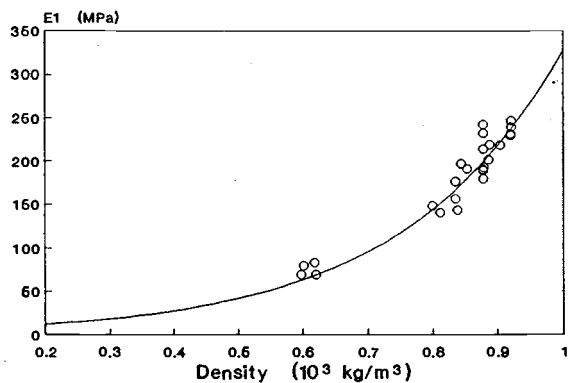
Element properties on $T = 100^\circ \text{C}$, $\text{MC} = 16\%$.



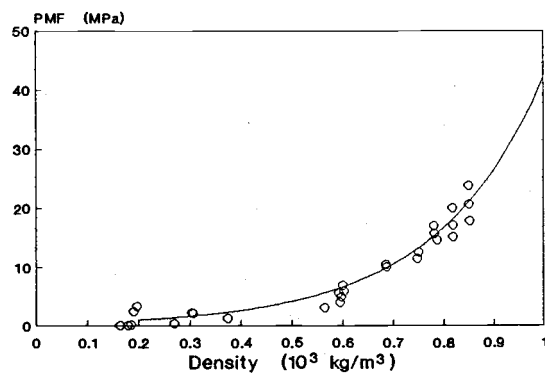
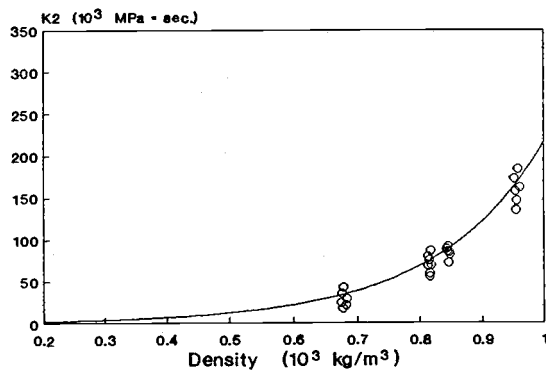
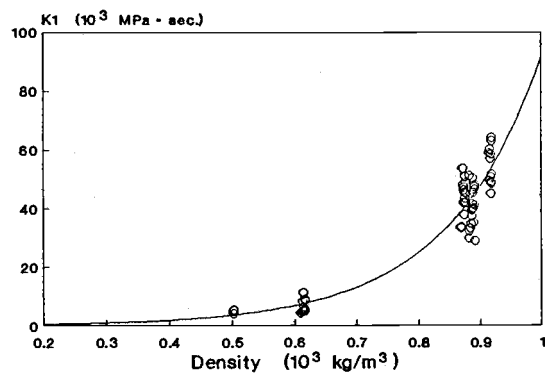
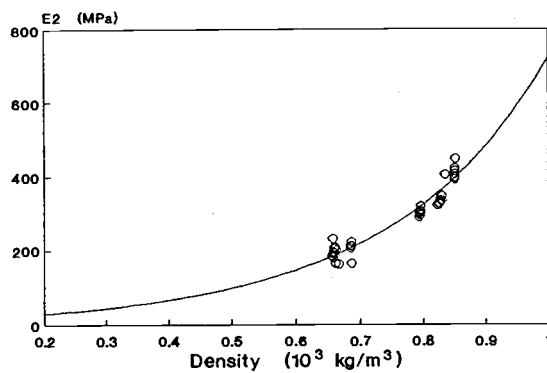
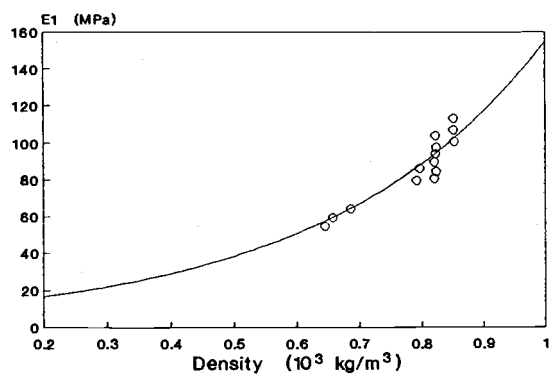
Element properties on $T = 120^\circ \text{C}$, $\text{MC} = 0\%$.



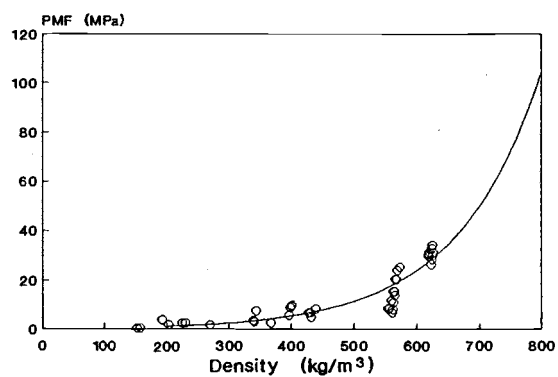
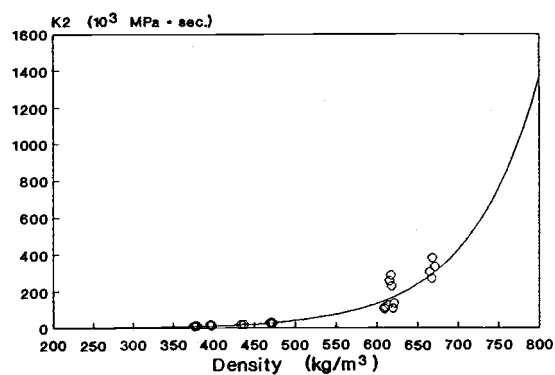
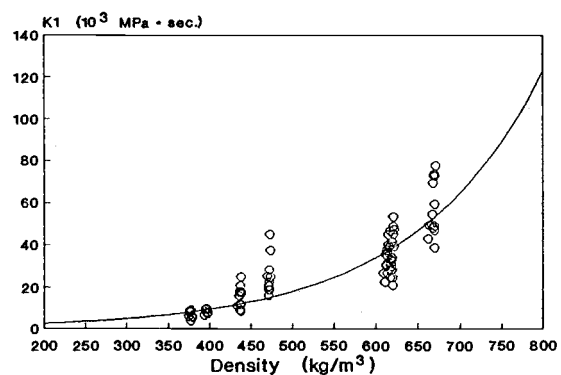
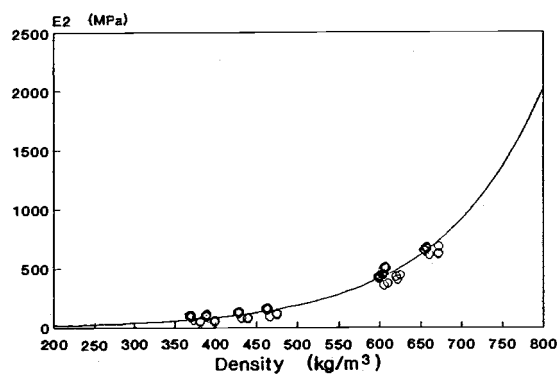
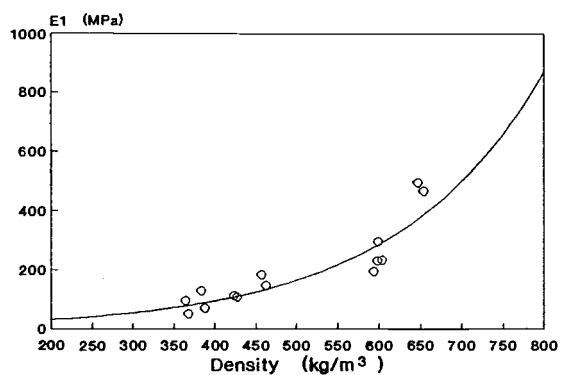
Element properties on $T = 120^\circ \text{C}$, $\text{MC} = 4\%$.



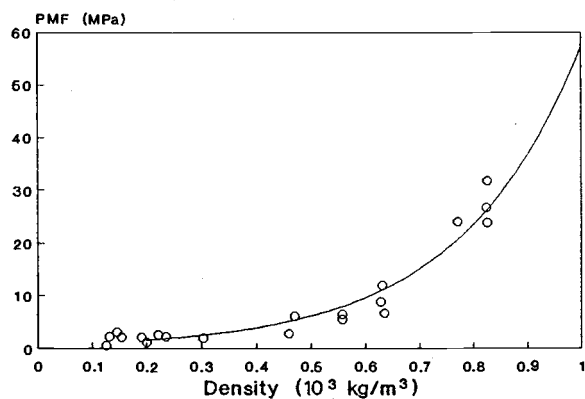
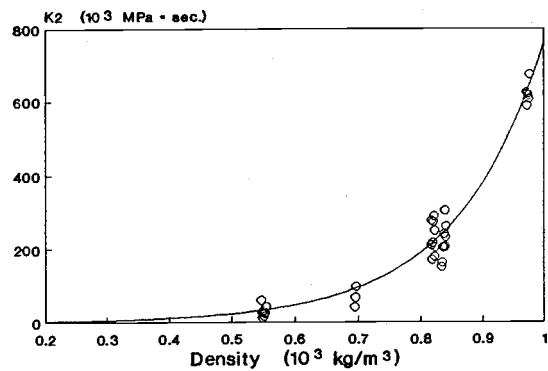
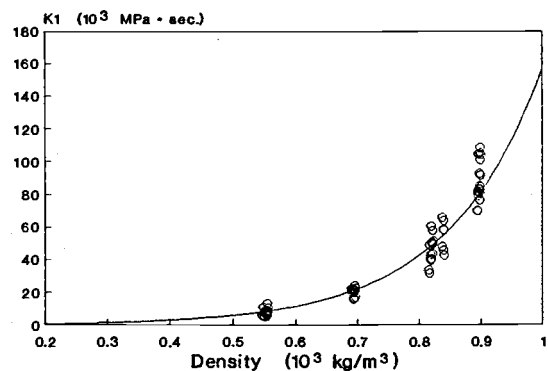
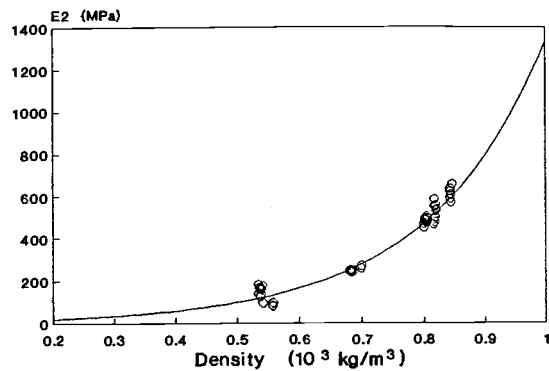
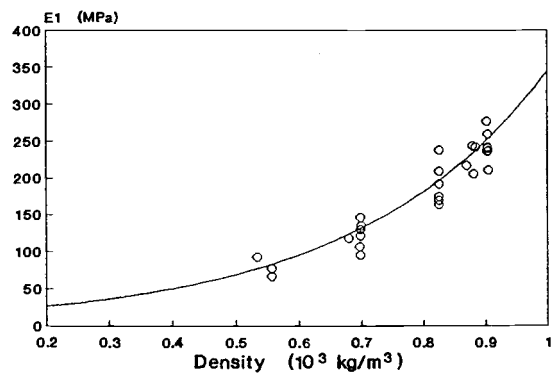
Element properties on $T = 120^\circ \text{C}$, $MC = 10\%$.



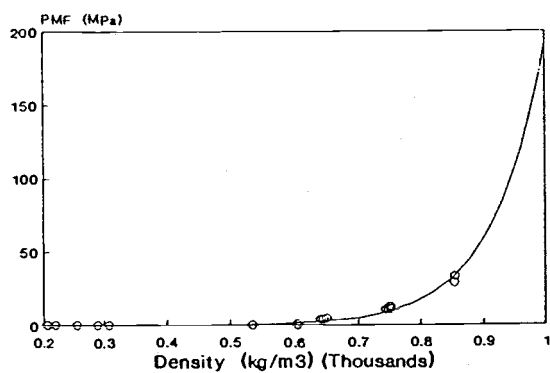
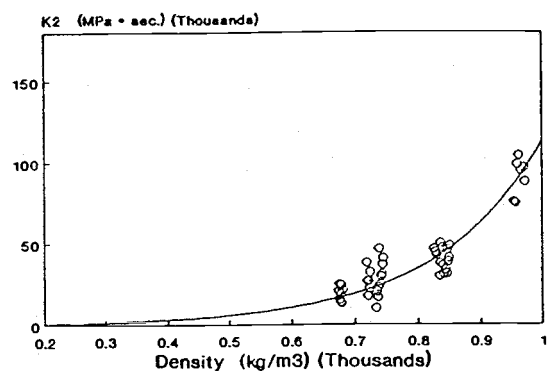
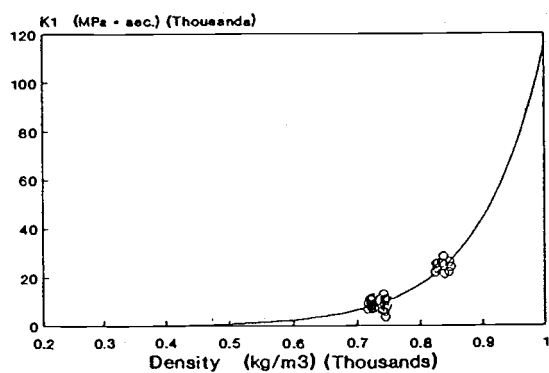
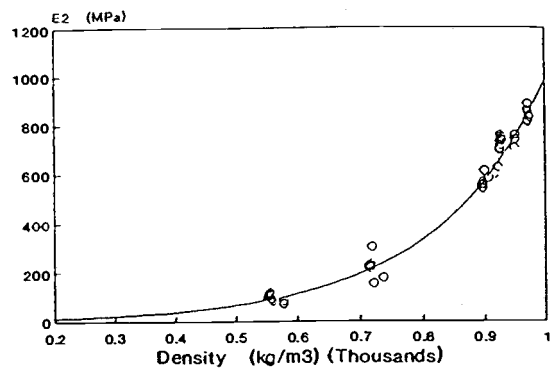
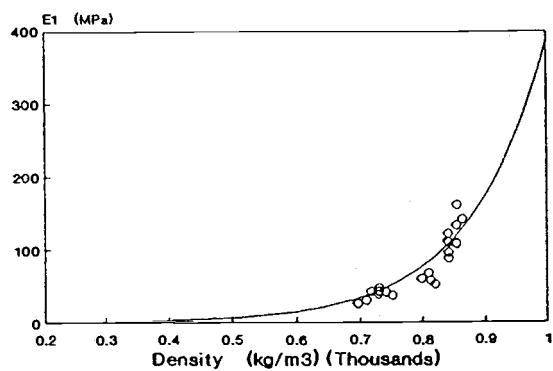
Element properties on $T = 120^\circ \text{C}$, $\text{MC} = 16\%$.



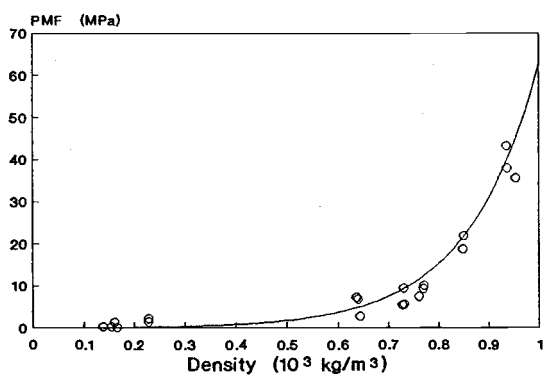
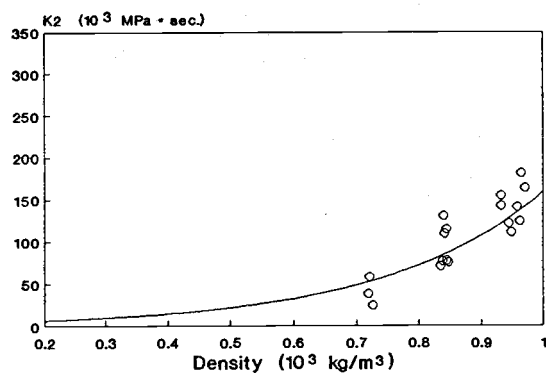
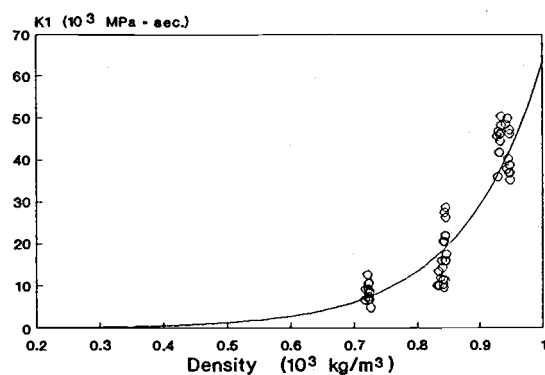
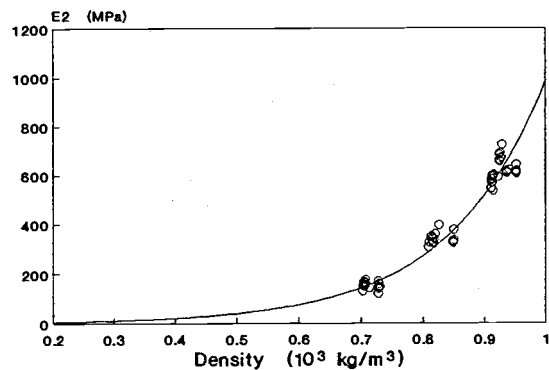
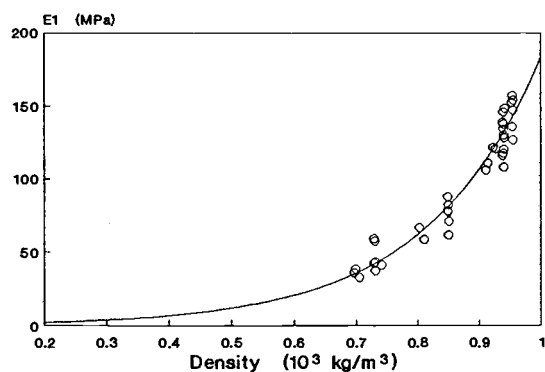
Element properties on $T = 150^\circ\text{C}$, $\text{MC} = 0\%$.



Element properties on $T = 150^\circ\text{C}$, $\text{MC} = 4\%$.



Element properties on $T = 150\text{ }^{\circ}\text{C}$, $MC = 10\%$.



Element properties on $T = 150^\circ \text{C}$, $\text{MC} = 16\%$.

APPENDIX III

Regression results

Regression Analysis - Exponential model: $Y = \exp(a+bX)$

Dependent variable: El250 Independent variable: del250

Parameter	Estimate	Standard Error	T Value	Prob. Level
Intercept	2.72063	0.277983	9.78704	.00000
Slope	6.36424E-3	5.86637E-4	10.8487	.00000

Analysis of Variance

Source	Sum of Squares	Df	Mean Square	F-Ratio	Prob. Level
Model	3.97536	1	3.97536	117.6939	.00000
Error	.3039937	9	.0337771		
Total (Corr.)	4.2793507	10			

Correlation Coefficient = 0.963827 R-squared = 92.90 percent
 Std. Error of Est. = 0.183785

Regression Analysis - Exponential model: $Y = \exp(a+bX)$

Dependent variable: El254 Independent variable: del254

Parameter	Estimate	Standard Error	T Value	Prob. Level
Intercept	1.88442	0.430679	4.37546	.00054
Slope	6.62003E-3	8.10843E-4	8.16437	.00000

Analysis of Variance

Source	Sum of Squares	Df	Mean Square	F-Ratio	Prob. Level
Model	7.043969	1	7.043969	66.65693	.00000
Error	1.585125	15	.105675		
Total (Corr.)	8.629094	16			

Correlation Coefficient = 0.903496 R-squared = 81.63 percent
 Std. Error of Est. = 0.325077

Regression Analysis - Exponential model: $Y = \exp(a+bX)$

Dependent variable: El2510 Independent variable: del2510

Parameter	Estimate	Standard Error	T Value	Prob. Level
Intercept	1.79215	0.394418	4.54378	.00067
Slope	6.47299E-3	7.29727E-4	8.87042	.00000

Analysis of Variance

Source	Sum of Squares	Df	Mean Square	F-Ratio	Prob. Level
Model	6.972136	1	6.972136	78.68437	.00000
Error	1.063307	12	.088609		
Total (Corr.)	8.035443	13			

Correlation Coefficient = 0.93149 R-squared = 86.77 percent
 Std. Error of Est. = 0.297672

Regression Analysis - Exponential model: $Y = \exp(a+bX)$

Dependent variable: El2516 Independent variable: del2516

Parameter	Estimate	Standard Error	T Value	Prob. Level
Intercept	2.47814	0.196622	12.6036	.00000
Slope	3.67729E-3	3.1394E-4	11.7134	.00000

Analysis of Variance

Source	Sum of Squares	Df	Mean Square	F-Ratio	Prob. Level
Model	7.29773	1	7.29773	137.2027	.00000
Error	.957410	18	.053189		
Total (Corr.)	8.255143	19			

Correlation Coefficient = 0.940225 R-squared = 88.40 percent
 Std. Error of Est. = 0.230628

Regression Analysis - Exponential model: $Y = \exp(a+bx)$

Dependent variable: P25 Independent variable: dnp25

Parameter	Estimate	Standard Error	T Value	Prob. Level
Intercept	-0.50492	0.322201	-1.5671	.13136
Slope	8.3318E-3	9.18032E-4	9.07572	.00000

Analysis of Variance

Source	Sum of Squares	Df	Mean Square	F-Ratio	Prob. Level
Model	24.062700	1	24.062700	82.36865	.00000
Error	6.426953	22	.292134		
Total (Corr.)	30.489653	23			

Correlation Coefficient = 0.888374 R-squared = 78.92 percent
 Stnd. Error of Est. = 0.540494

Regression Analysis - Exponential model: $Y = \exp(a+bx)$

Dependent variable: P254 Independent variable: dnp254

Parameter	Estimate	Standard Error	T Value	Prob. Level
Intercept	-1.37294	0.412225	-3.33055	.00372
Slope	9.03376E-3	1.10158E-3	8.20074	.00000

Analysis of Variance

Source	Sum of Squares	Df	Mean Square	F-Ratio	Prob. Level
Model	26.800684	1	26.800684	67.25211	.00000
Error	7.173192	18	.398511		
Total (Corr.)	33.973876	19			

Correlation Coefficient = 0.888179 R-squared = 78.89 percent
 Stnd. Error of Est. = 0.631277

Regression Analysis - Exponential model: $Y = \exp(a+bx)$

Dependent variable: P2510 Independent variable: dnp2510

Parameter	Estimate	Standard Error	T Value	Prob. Level
Intercept	-0.715827	0.304929	-2.34752	.02748
Slope	6.83013E-3	7.43402E-4	9.18767	.00000

Analysis of Variance

Source	Sum of Squares	Df	Mean Square	F-Ratio	Prob. Level
Model	29.748193	1	29.748193	84.41323	.00000
Error	8.457876	24	.352412		
Total (Corr.)	38.206070	25			

Correlation Coefficient = 0.882397 R-squared = 77.86 percent
 Stnd. Error of Est. = 0.593643

Regression Analysis - Exponential model: $Y = \exp(a+bx)$

Dependent variable: P2516 Independent variable: dnp2516

Parameter	Estimate	Standard Error	T Value	Prob. Level
Intercept	-0.20318	0.172393	-1.17858	.25175
Slope	4.80322E-3	2.95054E-4	16.2791	.00000

Analysis of Variance

Source	Sum of Squares	Df	Mean Square	F-Ratio	Prob. Level
Model	30.35691	1	30.35691	265.0097	.00000
Error	2.405554	21	.114550		
Total (Corr.)	32.762466	22			

Correlation Coefficient = 0.962588 R-squared = 92.66 percent
 Stnd. Error of Est. = 0.338453

Regression Analysis - Exponential model: $Y = \exp(a+bX)$

Dependent variable: K1250 Independent variable: dnk1250

Parameter	Estimate	Standard Error	T Value	Prob. Level
Intercept	7.03929	0.125363	56.1511	.00000
Slope	8.5716E-3	2.69966E-4	31.7506	.00000

Analysis of Variance

Source	Sum of Squares	Df	Mean Square	F-Ratio	Prob. Level
Model	38.2613	1	38.2613	1008.103	.00000
Error	1.897690	50	.037954		
Total (Corr.)	40.159037	51			

Correlation Coefficient = 0.976087
Std. Error of Est. = 0.194817

R-squared = 95.27 percent

Regression Analysis - Exponential model: $Y = \exp(a+bX)$

Dependent variable: K1254 Independent variable: dnk1254

Parameter	Estimate	Standard Error	T Value	Prob. Level
Intercept	7.2095	0.0800122	90.1051	.00000
Slope	6.74147E-3	1.58251E-4	42.5999	.00000

Analysis of Variance

Source	Sum of Squares	Df	Mean Square	F-Ratio	Prob. Level
Model	25.3121	1	25.3121	1814.750	.00000
Error	.739242	53	.013948		
Total (Corr.)	26.051322	54			

Correlation Coefficient = 0.98571
Std. Error of Est. = 0.118102

R-squared = 97.16 percent

Regression Analysis - Exponential model: $Y = \exp(a+bX)$

Dependent variable: K12510 Independent variable: dnk12510

Parameter	Estimate	Standard Error	T Value	Prob. Level
Intercept	6.99715	0.150285	46.5592	.00000
Slope	6.35302E-3	3.07489E-4	20.6609	.00000

Analysis of Variance

Source	Sum of Squares	Df	Mean Square	F-Ratio	Prob. Level
Model	15.28876	1	15.28876	426.8742	.00000
Error	1.396809	39	.035816		
Total (Corr.)	16.685569	40			

Correlation Coefficient = 0.957229
Std. Error of Est. = 0.18925

R-squared = 91.63 percent

Regression Analysis - Exponential model: $Y = \exp(a+bX)$

Dependent variable: K12516 Independent variable: dnk12516

Parameter	Estimate	Standard Error	T Value	Prob. Level
Intercept	7.3551	0.0859624	85.5618	.00000
Slope	4.35375E-3	1.37715E-4	31.6141	.00000

Analysis of Variance

Source	Sum of Squares	Df	Mean Square	F-Ratio	Prob. Level
Model	36.88287	1	36.88287	999.4514	.00000
Error	2.583218	70	.036903		
Total (Corr.)	39.466093	71			

Correlation Coefficient = 0.966719
Std. Error of Est. = 0.192102

R-squared = 93.45 percent

Regression Analysis - Exponential model: $Y = \exp(a+bX)$

Dependent variable: E2250 Independent variable: dne2250

Parameter	Estimate	Standard Error	T Value	Prob. Level
Intercept	2.09391	0.074518	28.0994	.00000
Slope	8.59909E-3	1.60754E-4	53.4921	.00000

Analysis of Variance

Source	Sum of Squares	Df	Mean Square	F-Ratio	Prob. Level
Model	51.0094	1	51.0094	2861.408	.00000
Error	1.194386	67	.017827		
Total (Corr.)	52.203750	68			

Correlation Coefficient = 0.988494
Std. Error of Est. = 0.133517

R-squared = 97.71 percent

Regression Analysis - Exponential model: $Y = \exp(a+bX)$

Dependent variable: E2254 Independent variable: dne2254

Parameter	Estimate	Standard Error	T Value	Prob. Level
Intercept	1.50248	0.130198	11.54	.00000
Slope	8.20522E-3	2.7849E-4	29.4633	.00000

Analysis of Variance

Source	Sum of Squares	Df	Mean Square	F-Ratio	Prob. Level
Model	35.69034	1	35.69034	868.0868	.00000
Error	2.343486	57	.041114		
Total (Corr.)	38.033822	58			

Correlation Coefficient = 0.968702
Std. Error of Est. = 0.202765

R-squared = 93.84 percent

Regression Analysis - Exponential model: $Y = \exp(a+bX)$

Dependent variable: E22510 Independent variable: dne22510

Parameter	Estimate	Standard Error	T Value	Prob. Level
Intercept	1.94875	0.100181	19.4523	.00000
Slope	7.29642E-3	2.12318E-4	34.3655	.00000

Analysis of Variance

Source	Sum of Squares	Df	Mean Square	F-Ratio	Prob. Level
Model	47.4078	1	47.4078	1180.989	.00000
Error	2.729689	68	.040142		
Total (Corr.)	50.137526	69			

Correlation Coefficient = 0.972397
Std. Error of Est. = 0.200356

R-squared = 94.56 percent

Regression Analysis - Exponential model: $Y = \exp(a+bX)$

Dependent variable: E22516 Independent variable: dne22516

Parameter	Estimate	Standard Error	T Value	Prob. Level
Intercept	2.56073	0.116276	22.0228	.00000
Slope	4.83953E-3	1.86035E-4	26.0141	.00000

Analysis of Variance

Source	Sum of Squares	Df	Mean Square	F-Ratio	Prob. Level
Model	50.21551	1	50.21551	676.7322	.00000
Error	5.194205	70	.074203		
Total (Corr.)	55.409719	71			

Correlation Coefficient = 0.951976
Std. Error of Est. = 0.272402

R-squared = 90.63 percent

Regression Analysis - Exponential model: $Y = \exp(a+bX)$

Dependent variable: K2250 Independent variable: dnk2250

Parameter	Estimate	Standard Error	T Value	Prob. Level
Intercept	7.71583	0.365215	21.1268	.00000
Slope	0.0104692	7.2948E-4	14.3516	.00000

Analysis of Variance

Source	Sum of Squares	Df	Mean Square	F-Ratio	Prob. Level
Model	29.07047	1	29.07047	205.9692	.00000
Error	3.810778	27	.141140		

Total (Corr.) 32.881250 28

Correlation Coefficient = 0.940268 R-squared = 88.41 percent
Std. Error of Est. = 0.375686Regression Analysis - Exponential model: $Y = \exp(a+bX)$

Dependent variable: K2254 Independent variable: dnk2254

Parameter	Estimate	Standard Error	T Value	Prob. Level
Intercept	6.67971	0.252709	26.4324	.00000
Slope	0.0107715	4.96976E-4	21.674	.00000

Analysis of Variance

Source	Sum of Squares	Df	Mean Square	F-Ratio	Prob. Level
Model	44.47599	1	44.47599	469.7622	.00000
Error	2.556297	27	.094678		

Total (Corr.) 47.032289 28

Correlation Coefficient = 0.972444 R-squared = 94.56 percent
Std. Error of Est. = 0.307697Regression Analysis - Exponential model: $Y = \exp(a+bX)$

Dependent variable: K22510 Independent variable: dnk2510

Parameter	Estimate	Standard Error	T Value	Prob. Level
Intercept	5.89205	0.289344	20.3635	.00000
Slope	0.0120526	6.23932E-4	19.3171	.00000

Analysis of Variance

Source	Sum of Squares	Df	Mean Square	F-Ratio	Prob. Level
Model	59.57899	1	59.57899	373.1506	.00000
Error	4.789942	30	.159665		

Total (Corr.) 64.368931 31

Correlation Coefficient = 0.962074 R-squared = 92.56 percent
Std. Error of Est. = 0.399581Regression Analysis - Exponential model: $Y = \exp(a+bX)$

Dependent variable: K22516 Independent variable: dnk22516

Parameter	Estimate	Standard Error	T Value	Prob. Level
Intercept	7.48219	0.236305	31.6633	.00000
Slope	6.74908E-3	3.65764E-4	18.452	.00000

Analysis of Variance

Source	Sum of Squares	Df	Mean Square	F-Ratio	Prob. Level
Model	40.91912	1	40.91912	340.4763	.00000
Error	3.244914	27	.120182		

Total (Corr.) 44.164031 28

Correlation Coefficient = 0.962562 R-squared = 92.65 percent
Std. Error of Est. = 0.346673

Regression Analysis - Exponential model: $Y = \exp(a+bx)$

Dependent variable: E11000 Independent variable: del1000

Parameter	Estimate	Standard Error	T Value	Prob. Level
Intercept	2.65174	0.277593	9.55262	.00000
Slope	5.479E-3	5.00077E-4	10.9563	.00000

Analysis of Variance

Source	Sum of Squares	Df	Mean Square	F-Ratio	Prob. Level
Model	6.08540	1	6.08540	120.0407	.00000
Error	.709723	14	.050695		
Total (Corr.)	6.795125	15			

Correlation Coefficient = 0.946337
Std. Error of Est. = 0.225154

R-squared = 89.56 percent

Regression Analysis - Exponential model: $Y = \exp(a+bx)$

Dependent variable: E11004 Independent variable: del1004

Parameter	Estimate	Standard Error	T Value	Prob. Level
Intercept	2.39771	0.243719	9.83799	.00000
Slope	4.41083E-3	3.41455E-4	12.9178	.00000

Analysis of Variance

Source	Sum of Squares	Df	Mean Square	F-Ratio	Prob. Level
Model	11.69207	1	11.69207	166.8687	.00000
Error	1.261215	18	.070067		
Total (Corr.)	12.953287	19			

Correlation Coefficient = 0.95007
Std. Error of Est. = 0.264703

R-squared = 90.26 percent

Regression Analysis - Exponential model: $Y = \exp(a+bx)$

Dependent variable: E110010 Independent variable: del10010

Parameter	Estimate	Standard Error	T Value	Prob. Level
Intercept	2.73551	0.461197	5.93133	.00001
Slope	3.33078E-3	5.57662E-4	5.97276	.00001

Analysis of Variance

Source	Sum of Squares	Df	Mean Square	F-Ratio	Prob. Level
Model	5.452407	1	5.452407	35.67392	.00001
Error	2.903963	19	.152840		
Total (Corr.)	8.356371	20			

Correlation Coefficient = 0.807766
Std. Error of Est. = 0.390948

R-squared = 65.25 percent

Regression Analysis - Exponential model: $Y = \exp(a+bx)$

Dependent variable: E110016 Independent variable: del10016

Parameter	Estimate	Standard Error	T Value	Prob. Level
Intercept	2.22265	0.263393	8.43853	.00000
Slope	2.99797E-3	3.11289E-4	9.63083	.00000

Analysis of Variance

Source	Sum of Squares	Df	Mean Square	F-Ratio	Prob. Level
Model	3.944767	1	3.944767	92.75284	.00000
Error	.723008	17	.042530		
Total (Corr.)	4.667775	18			

Correlation Coefficient = 0.919297
Std. Error of Est. = 0.206228

R-squared = 84.51 percent

Regression Analysis - Exponential model: $Y = \exp(a+bX)$

Dependent variable: P1000 Independent variable: dnp1000

Parameter	Estimate	Standard Error	T Value	Prob. Level
Intercept	-1.45454	0.389264	-3.73665	.00102
Slope	8.57181E-3	9.12743E-4	9.39126	.00000

Analysis of Variance

Source	Sum of Squares	Df	Mean Square	F-Ratio	Prob. Level
Model	38.746038	1	38.746038	88.19582	.00000
Error	10.543640	24	.439318		
Total (Corr.)	49.289678	25			

Correlation Coefficient = 0.886616
Std. Error of Est. = 0.662811

R-squared = 78.61 percent

Regression Analysis - Exponential model: $Y = \exp(a+bX)$

Dependent variable: P1004 Independent variable: dnp1004

Parameter	Estimate	Standard Error	T Value	Prob. Level
Intercept	-0.736199	0.280678	-2.62293	.01725
Slope	5.97381E-3	5.79341E-4	10.3114	.00000

Analysis of Variance

Source	Sum of Squares	Df	Mean Square	F-Ratio	Prob. Level
Model	33.22947	1	33.22947	106.3245	.00000
Error	5.625519	18	.312529		
Total (Corr.)	38.854985	19			

Correlation Coefficient = 0.92478
Std. Error of Est. = 0.559043

R-squared = 85.52 percent

Regression Analysis - Exponential model: $Y = \exp(a+bX)$

Dependent variable: P10010 Independent variable: dnp10010

Parameter	Estimate	Standard Error	T Value	Prob. Level
Intercept	-0.942334	0.303597	-3.10389	.00777
Slope	5.70627E-3	5.11295E-4	11.1604	.00000

Analysis of Variance

Source	Sum of Squares	Df	Mean Square	F-Ratio	Prob. Level
Model	32.51344	1	32.51344	124.5552	.00000
Error	3.654509	14	.261036		
Total (Corr.)	36.167945	15			

Correlation Coefficient = 0.948134
Std. Error of Est. = 0.510917

R-squared = 89.90 percent

Regression Analysis - Exponential model: $Y = \exp(a+bX)$

Dependent variable: P10016 Independent variable: dnp10016

Parameter	Estimate	Standard Error	T Value	Prob. Level
Intercept	-0.728678	0.276844	-2.63209	.01642
Slope	5.0081E-3	4.74661E-4	10.5509	.00000

Analysis of Variance

Source	Sum of Squares	Df	Mean Square	F-Ratio	Prob. Level
Model	28.44971	1	28.44971	111.3213	.00000
Error	4.855713	19	.255564		
Total (Corr.)	33.305421	20			

Correlation Coefficient = 0.924233
Std. Error of Est. = 0.505533

R-squared = 85.42 percent

Regression Analysis - Exponential model: $Y = \exp(a+bx)$

Dependent variable: K11000 Independent variable: dnk11000

Parameter	Estimate	Standard Error	T Value	Prob. Level
Intercept	7.05826	0.19028	37.0941	.00000
Slope	6.73133E-3	3.33237E-4	20.1998	.00000

Analysis of Variance

Source	Sum of Squares	Df	Mean Square	F-Ratio	Prob. Level
Model	46.64891	1	46.64891	408.0320	.00000
Error	8.688823	76	.114327		
Total (Corr.)	55.337736	77			

Correlation Coefficient = 0.918142
Std. Error of Est. = 0.338122

R-squared = 84.30 percent

Regression Analysis - Exponential model: $Y = \exp(a+bx)$

Dependent variable: K11004 Independent variable: dnk11004

Parameter	Estimate	Standard Error	T Value	Prob. Level
Intercept	7.69316	0.182474	42.1602	.00000
Slope	4.50446E-3	2.88447E-4	15.6162	.00000

Analysis of Variance

Source	Sum of Squares	Df	Mean Square	F-Ratio	Prob. Level
Model	30.80655	1	30.80655	243.8672	.00000
Error	5.810954	46	.126325		
Total (Corr.)	36.617499	47			

Correlation Coefficient = 0.917228
Std. Error of Est. = 0.355422

R-squared = 84.13 percent

Regression Analysis - Exponential model: $Y = \exp(a+bx)$

Dependent variable: K110010 Independent variable: dnk110010

Parameter	Estimate	Standard Error	T Value	Prob. Level
Intercept	6.97595	0.140979	49.4821	.00000
Slope	4.20846E-3	1.64857E-4	25.528	.00000

Analysis of Variance

Source	Sum of Squares	Df	Mean Square	F-Ratio	Prob. Level
Model	32.90959	1	32.90959	651.6771	.00000
Error	5.25198	104	.05050		
Total (Corr.)	38.16157	105			

Correlation Coefficient = 0.928642
Std. Error of Est. = 0.224722

R-squared = 86.24 percent

Regression Analysis - Exponential model: $Y = \exp(a+bx)$

Dependent variable: K110016 Independent variable: dnk110016

Parameter	Estimate	Standard Error	T Value	Prob. Level
Intercept	5.4637	0.128274	42.5941	.00000
Slope	5.80376E-3	1.57136E-4	36.9346	.00000

Analysis of Variance

Source	Sum of Squares	Df	Mean Square	F-Ratio	Prob. Level
Model	77.6756	1	77.6756	1364.164	.00000
Error	4.555206	80	.056940		
Total (Corr.)	82.230823	81			

Correlation Coefficient = 0.971908
Std. Error of Est. = 0.238621

R-squared = 94.46 percent

Regression Analysis - Exponential model: $Y = \exp(a+bx)$

Dependent variable: E21000 Independent variable: dne21000

Parameter	Estimate	Standard Error	T Value	Prob. Level
Intercept	2.0031	0.109849	18.235	.00000
Slope	7.89901E-3	2.06269E-4	38.2947	.00000

Analysis of Variance

Source	Sum of Squares	Df	Mean Square	F-Ratio	Prob. Level
Model	70.8169	1	70.8169	1466.486	.00000
Error	3.814928	79	.048290		
Total (Corr.)	74.631838	80			

Correlation Coefficient = 0.974106
Std. Error of Est. = 0.21975

R-squared = 94.89 percent

Regression Analysis - Exponential model: $Y = \exp(a+bx)$

Dependent variable: E21004 Independent variable: dne21004

Parameter	Estimate	Standard Error	T Value	Prob. Level
Intercept	2.10239	0.096715	21.738	.00000
Slope	5.65738E-3	1.54493E-4	36.6191	.00000

Analysis of Variance

Source	Sum of Squares	Df	Mean Square	F-Ratio	Prob. Level
Model	67.7831	1	67.7831	1340.959	.00000
Error	3.588925	71	.050548		
Total (Corr.)	71.372027	72			

Correlation Coefficient = 0.974533
Std. Error of Est. = 0.224829

R-squared = 94.97 percent

Regression Analysis - Exponential model: $Y = \exp(a+bx)$

Dependent variable: E210010 Independent variable: dne210010

Parameter	Estimate	Standard Error	T Value	Prob. Level
Intercept	2.27419	0.0816051	27.8682	.00000
Slope	4.87903E-3	1.01709E-4	47.9706	.00000

Analysis of Variance

Source	Sum of Squares	Df	Mean Square	F-Ratio	Prob. Level
Model	38.9100	1	38.9100	2301.183	.00000
Error	1.183609	70	.016909		
Total (Corr.)	40.093621	71			

Correlation Coefficient = 0.985129
Std. Error of Est. = 0.130033

R-squared = 97.05 percent

Regression Analysis - Exponential model: $Y = \exp(a+bx)$

Dependent variable: E210016 Independent variable: dne210016

Parameter	Estimate	Standard Error	T Value	Prob. Level
Intercept	1.47303	0.0908486	16.2141	.00000
Slope	5.41741E-3	1.10598E-4	48.9829	.00000

Analysis of Variance

Source	Sum of Squares	Df	Mean Square	F-Ratio	Prob. Level
Model	56.0551	1	56.0551	2399.320	.00000
Error	1.705493	73	.023363		
Total (Corr.)	57.760615	74			

Correlation Coefficient = 0.985126
Std. Error of Est. = 0.152849

R-squared = 97.05 percent

Regression Analysis - Exponential model: $Y = \exp(a+bX)$

Dependent variable: K21000 Independent variable: dnk21000

Parameter	Estimate	Standard Error	T Value	Prob. Level
Intercept	7.14709	0.294248	24.2893	.00000
Slope	9.68855E-3	5.01388E-4	19.3235	.00000

Analysis of Variance

Source	Sum of Squares	Df	Mean Square	F-Ratio	Prob. Level
Model	52.89470	1	52.89470	373.3968	.00000
Error	5.807985	41	.141658		
Total (Corr.)	58.702690	42			

Correlation Coefficient = 0.949242
Std. Error of Est. = 0.376375

R-squared = 90.11 percent

Regression Analysis - Exponential model: $Y = \exp(a+bX)$

Dependent variable: K221004 Independent variable: dnk21004

Parameter	Estimate	Standard Error	T Value	Prob. Level
Intercept	8.06327	0.242736	33.2182	.00000
Slope	5.701E-3	3.33853E-4	17.0764	.00000

Analysis of Variance

Source	Sum of Squares	Df	Mean Square	F-Ratio	Prob. Level
Model	47.76560	1	47.76560	291.6019	.00000
Error	5.077928	31	.163804		
Total (Corr.)	52.843525	32			

Correlation Coefficient = 0.95074
Std. Error of Est. = 0.404727

R-squared = 90.39 percent

Regression Analysis - Exponential model: $Y = \exp(a+bX)$

Dependent variable: K210010 Independent variable: dnk210010

Parameter	Estimate	Standard Error	T Value	Prob. Level
Intercept	6.81938	0.287715	23.7019	.00000
Slope	6.62128E-3	3.44714E-4	19.208	.00000

Analysis of Variance

Source	Sum of Squares	Df	Mean Square	F-Ratio	Prob. Level
Model	46.42884	1	46.42884	368.9492	.00000
Error	5.788674	46	.125841		
Total (Corr.)	52.217509	47			

Correlation Coefficient = 0.942944
Std. Error of Est. = 0.35474

R-squared = 88.91 percent

Regression Analysis - Exponential model: $Y = \exp(a+bX)$

Dependent variable: K210016 Independent variable: dnk210016

Parameter	Estimate	Standard Error	T Value	Prob. Level
Intercept	5.97159	0.564853	10.5719	.00000
Slope	6.98959E-3	6.77673E-4	10.3141	.00000

Analysis of Variance

Source	Sum of Squares	Df	Mean Square	F-Ratio	Prob. Level
Model	29.55107	1	29.55107	106.3806	.00000
Error	6.389084	23	.277786		
Total (Corr.)	35.940156	24			

Correlation Coefficient = 0.906769
Std. Error of Est. = 0.527054

R-squared = 82.22 percent

Regression Analysis - Exponential model: $Y = \exp(a+bX)$

Dependent variable: Ell200 Independent variable: dell200

Parameter	Estimate	Standard Error	T Value	Prob. Level
Intercept	2.59871	0.563975	4.60785	.00366
Slope	5.53004E-3	1.01399E-3	5.45377	.00158

Analysis of Variance

Source	Sum of Squares	Df	Mean Square	F-Ratio	Prob. Level
Model	5.164701	1	5.164701	29.74360	.00158
Error	1.0418448	6	.1736408		

Total (Corr.) 6.2065462 7

Correlation Coefficient = 0.912216
Std. Error of Est. = 0.416702

R-squared = 83.21 percent

Regression Analysis - Exponential model: $Y = \exp(a+bX)$

Dependent variable: Ell204 Independent variable: dell204

Parameter	Estimate	Standard Error	T Value	Prob. Level
Intercept	3.05273	0.311445	9.80185	.00000
Slope	3.25517E-3	5.47392E-4	5.94669	.00007

Analysis of Variance

Source	Sum of Squares	Df	Mean Square	F-Ratio	Prob. Level
Model	4.442044	1	4.442044	35.36307	.00007
Error	1.507350	12	.125613		

Total (Corr.) 5.949394 13

Correlation Coefficient = 0.864082
Std. Error of Est. = 0.354419

R-squared = 74.66 percent

Regression Analysis - Exponential model: $Y = \exp(a+bX)$

Dependent variable: Ell2010 Independent variable: dell2010

Parameter	Estimate	Standard Error	T Value	Prob. Level
Intercept	1.68379	0.650413	2.58881	.01853
Slope	4.10871E-3	7.70403E-4	5.33319	.00005

Analysis of Variance

Source	Sum of Squares	Df	Mean Square	F-Ratio	Prob. Level
Model	4.081843	1	4.081843	28.44292	.00005
Error	2.583179	18	.143510		

Total (Corr.) 6.665022 19

Correlation Coefficient = 0.782577
Std. Error of Est. = 0.378827

R-squared = 61.24 percent

Regression Analysis - Exponential model: $Y = \exp(a+bX)$

Dependent variable: Ell2016 Independent variable: dell2016

Parameter	Estimate	Standard Error	T Value	Prob. Level
Intercept	2.25415	0.537061	4.1972	.00105
Slope	2.78735E-3	6.74188E-4	4.13438	.00118

Analysis of Variance

Source	Sum of Squares	Df	Mean Square	F-Ratio	Prob. Level
Model	.546208	1	.546208	17.09308	.00118
Error	.415414	13	.031955		

Total (Corr.) .961623 14

Correlation Coefficient = 0.753662
Std. Error of Est. = 0.178759

R-squared = 56.80 percent

Regression Analysis - Exponential model: $Y = \exp(a+bX)$

Dependent variable: P1200 Independent variable: dnp1200

Parameter	Estimate	Standard Error	T Value	Prob. Level
Intercept	-0.992936	0.248188	-4.00073	.00035
Slope	7.29628E-3	5.75441E-4	12.6795	.00000

Analysis of Variance

Source	Sum of Squares	Df	Mean Square	F-Ratio	Prob. Level
Model	54.81822	1	54.81822	160.7685	.00000
Error	10.911236	32	.340976		
Total (Corr.)	65.729461	33			

Correlation Coefficient = 0.913235 R-squared = 83.40 percent
 Stnd. Error of Est. = 0.583932

Regression Analysis - Exponential model: $Y = \exp(a+bX)$

Dependent variable: P1204 Independent variable: dnp1204

Parameter	Estimate	Standard Error	T Value	Prob. Level
Intercept	-1.15077	0.420045	-2.73964	.01520
Slope	6.2807E-3	8.1507E-4	7.70571	.00000

Analysis of Variance

Source	Sum of Squares	Df	Mean Square	F-Ratio	Prob. Level
Model	34.587181	1	34.587181	59.37795	.00000
Error	8.737379	15	.582492		
Total (Corr.)	43.324560	16			

Correlation Coefficient = 0.893492 R-squared = 79.83 percent
 Stnd. Error of Est. = 0.763212

Regression Analysis - Exponential model: $Y = \exp(a+bX)$

Dependent variable: P12010 Independent variable: dnp12010

Parameter	Estimate	Standard Error	T Value	Prob. Level
Intercept	-0.601202	0.241469	-2.48977	.02170
Slope	5.18172E-3	3.94092E-4	13.1465	.00000

Analysis of Variance

Source	Sum of Squares	Df	Mean Square	F-Ratio	Prob. Level
Model	43.88805	1	43.88805	172.8827	.00000
Error	5.077206	20	.253860		
Total (Corr.)	48.965261	21			

Correlation Coefficient = 0.946737 R-squared = 89.63 percent
 Stnd. Error of Est. = 0.503846

Regression Analysis - Exponential model: $Y = \exp(a+bX)$

Dependent variable: P12016 Independent variable: dnp12016

Parameter	Estimate	Standard Error	T Value	Prob. Level
Intercept	-2.81699	0.600547	-4.69071	.00008
Slope	7.34071E-3	9.70587E-4	7.56317	.00000

Analysis of Variance

Source	Sum of Squares	Df	Mean Square	F-Ratio	Prob. Level
Model	89.922497	1	89.922497	57.20147	.00000
Error	40.872809	26	1.572031		
Total (Corr.)	130.79531	27			

Correlation Coefficient = 0.82916 R-squared = 68.75 percent
 Stnd. Error of Est. = 1.25381

Regression Analysis - Exponential model: $Y = \exp(a+bX)$

Dependent variable: K11200 Independent variable: dnk11200

Parameter	Estimate	Standard Error	T Value	Prob. Level
Intercept	6.72563	0.164998	40.7619	.00000
Slope	6.97454E-3	3.21185E-4	21.7151	.00000

Analysis of Variance

Source	Sum of Squares	Df	Mean Square	F-Ratio	Prob. Level
Model	35.76259	1	35.76259	471.5435	.00000
Error	4.929701	65	.075842		
Total (Corr.)	40.692293	66			

Correlation Coefficient = 0.937472 R-squared = 87.89 percent
 Stnd. Error of Est. = 0.275393

Regression Analysis - Exponential model: $Y = \exp(a+bX)$

Dependent variable: K11204 Independent variable: dnk11204

Parameter	Estimate	Standard Error	T Value	Prob. Level
Intercept	6.8686	0.163999	41.8819	.00000
Slope	5.59056E-3	2.91482E-4	19.1798	.00000

Analysis of Variance

Source	Sum of Squares	Df	Mean Square	F-Ratio	Prob. Level
Model	40.84505	1	40.84505	367.8647	.00000
Error	5.107508	46	.111033		
Total (Corr.)	45.952553	47			

Correlation Coefficient = 0.94279 R-squared = 88.89 percent
 Stnd. Error of Est. = 0.333216

Regression Analysis - Exponential model: $Y = \exp(a+bX)$

Dependent variable: K112010 Independent variable: dnk112010

Parameter	Estimate	Standard Error	T Value	Prob. Level
Intercept	4.95519	0.346262	14.3105	.00000
Slope	6.46935E-3	4.13009E-4	15.664	.00000

Analysis of Variance

Source	Sum of Squares	Df	Mean Square	F-Ratio	Prob. Level
Model	45.35210	1	45.35210	245.3596	.00000
Error	15.711341	85	.184839		
Total (Corr.)	61.063438	86			

Correlation Coefficient = 0.861803 R-squared = 74.27 percent
 Stnd. Error of Est. = 0.429929

Regression Analysis - Exponential model: $Y = \exp(a+bX)$

Dependent variable: P12016 Independent variable: dnp12016

Parameter	Estimate	Standard Error	T Value	Prob. Level
Intercept	-0.866036	0.37644	-2.30059	.03520
Slope	4.60574E-3	5.95737E-4	7.73117	.00000

Analysis of Variance

Source	Sum of Squares	Df	Mean Square	F-Ratio	Prob. Level
Model	23.080752	1	23.080752	59.77104	.00000
Error	6.178445	16	.386153		
Total (Corr.)	29.259197	17			

Correlation Coefficient = 0.888165 R-squared = 78.88 percent
 Stnd. Error of Est. = 0.621412

Regression Analysis - Exponential model: $Y = \exp(a+bX)$

Dependent variable: E21200 Independent variable: dne21200

Parameter	Estimate	Standard Error	T Value	Prob. Level
Intercept	1.76593	0.105175	16.7903	.00000
Slope	7.36038E-3	1.93852E-4	37.969	.00000

Analysis of Variance

Source	Sum of Squares	Df	Mean Square	F-Ratio	Prob. Level
Model	87.8200	1	87.8200	1441.646	.00000
Error	5.908894	97	.060916		
Total (Corr.)	93.728852	98			

Correlation Coefficient = 0.967966 R-squared = 93.70 percent
 Stnd. Error of Est. = 0.246813

Regression Analysis - Exponential model: $Y = \exp(a+bX)$

Dependent variable: E21204 Independent variable: dne21204

Parameter	Estimate	Standard Error	T Value	Prob. Level
Intercept	2.76024	0.134204	20.5675	.00000
Slope	5.13917E-3	2.56191E-4	20.0599	.00000

Analysis of Variance

Source	Sum of Squares	Df	Mean Square	F-Ratio	Prob. Level
Model	24.26484	1	24.26484	402.4009	.00000
Error	2.351706	39	.060300		
Total (Corr.)	26.616546	40			

Correlation Coefficient = 0.954801 R-squared = 91.16 percent
 Stnd. Error of Est. = 0.245561

Regression Analysis - Exponential model: $Y = \exp(a+bX)$

Dependent variable: E212010 Independent variable: dne212010

Parameter	Estimate	Standard Error	T Value	Prob. Level
Intercept	3.19372	0.073577	43.4066	.00000
Slope	3.71192E-3	9.44866E-5	39.2852	.00000

Analysis of Variance

Source	Sum of Squares	Df	Mean Square	F-Ratio	Prob. Level
Model	12.2490	1	12.2490	1543.325	.00000
Error	.365092	46	.007937		
Total (Corr.)	12.614125	47			

Correlation Coefficient = 0.985422 R-squared = 97.11 percent
 Stnd. Error of Est. = 0.0890886

Regression Analysis - Exponential model: $Y = \exp(a+bX)$

Dependent variable: E212016 Independent variable: dne212016

Parameter	Estimate	Standard Error	T Value	Prob. Level
Intercept	2.60589	0.161503	16.1352	.00000
Slope	3.97485E-3	2.10659E-4	18.8687	.00000

Analysis of Variance

Source	Sum of Squares	Df	Mean Square	F-Ratio	Prob. Level
Model	4.33491	1	4.33491	356.0270	.00000
Error	.560087	46	.012176		
Total (Corr.)	4.895000	47			

Correlation Coefficient = 0.941053 R-squared = 88.56 percent
 Stnd. Error of Est. = 0.110344

Regression Analysis - Exponential model: $Y = \exp(a+bX)$

Dependent variable: K21200 Independent variable: dnk21200

Parameter	Estimate	Standard Error	T Value	Prob. Level
Intercept	8.13388	0.298658	27.2348	.00000
Slope	6.96735E-3	4.81963E-4	14.4562	.00000

Analysis of Variance

Source	Sum of Squares	Df	Mean Square	F-Ratio	Prob. Level
Model	49.32130	1	49.32130	208.9811	.00000
Error	8.968319	38	.236008		

Total (Corr.) 58.289618 39

Correlation Coefficient = 0.91986 R-squared = 84.61 percent
Std. Error of Est. = 0.485807Regression Analysis - Exponential model: $Y = \exp(a+bX)$

Dependent variable: K21204 Independent variable: dnk21204

Parameter	Estimate	Standard Error	T Value	Prob. Level
Intercept	6.86583	0.290803	23.6099	.00000
Slope	6.27431E-3	4.39502E-4	14.276	.00000

Analysis of Variance

Source	Sum of Squares	Df	Mean Square	F-Ratio	Prob. Level
Model	93.92307	1	93.92307	203.8028	.00000
Error	15.208139	33	.460853		

Total (Corr.) 109.13121 34

Correlation Coefficient = 0.927709 R-squared = 86.06 percent
Std. Error of Est. = 0.678861Regression Analysis - Exponential model: $Y = \exp(a+bX)$

Dependent variable: K212010 Independent variable: dnk212010

Parameter	Estimate	Standard Error	T Value	Prob. Level
Intercept	6.26179	0.484432	12.926	.00000
Slope	6.56798E-3	6.00369E-4	10.9399	.00000

Analysis of Variance

Source	Sum of Squares	Df	Mean Square	F-Ratio	Prob. Level
Model	17.30103	1	17.30103	119.6816	.00000
Error	3.324852	23	.144559		

Total (Corr.) 20.625881 24

Correlation Coefficient = 0.915861 R-squared = 83.88 percent
Std. Error of Est. = 0.380209Regression Analysis - Exponential model: $Y = \exp(a+bX)$

Dependent variable: K212016 Independent variable: dnk212016

Parameter	Estimate	Standard Error	T Value	Prob. Level
Intercept	6.52881	0.524022	12.459	.00000
Slope	5.75833E-3	5.90513E-4	9.75139	.00000

Analysis of Variance

Source	Sum of Squares	Df	Mean Square	F-Ratio	Prob. Level
Model	24.394804	1	24.394804	95.08965	.00000
Error	5.900542	23	.256545		

Total (Corr.) 30.295347 24

Correlation Coefficient = 0.897348 R-squared = 80.52 percent
Std. Error of Est. = 0.506503

Regression Analysis - Exponential model: $Y = \exp(a+bX)$

Dependent variable: Ell500 Independent variable: del1500

Parameter	Estimate	Standard Error	T Value	Prob. Level
Intercept	2.33204	0.360524	6.46848	.00003
Slope	5.54424E-3	7.08821E-4	7.82177	.00000

Analysis of Variance

Source	Sum of Squares	Df	Mean Square	F-Ratio	Prob. Level
Model	4.939833	1	4.939833	61.18015	.00000
Error	.968909	12	.080742		
Total (Corr.)	5.908742	13			

Correlation Coefficient = 0.914342 R-squared = 83.60 percent
 Std. Error of Est. = 0.284152

Regression Analysis - Exponential model: $Y = \exp(a+bX)$

Dependent variable: Ell504 Independent variable: del1504

Parameter	Estimate	Standard Error	T Value	Prob. Level
Intercept	2.63164	0.375165	7.01463	.00000
Slope	3.21019E-3	4.63401E-4	6.92746	.00000

Analysis of Variance

Source	Sum of Squares	Df	Mean Square	F-Ratio	Prob. Level
Model	3.030541	1	3.030541	47.98965	.00000
Error	1.010398	16	.063150		
Total (Corr.)	4.040939	17			

Correlation Coefficient = 0.866002 R-squared = 75.00 percent
 Std. Error of Est. = 0.251296

Regression Analysis - Exponential model: $Y = \exp(a+bX)$

Dependent variable: ell15010 Independent variable: del15010

Parameter	Estimate	Standard Error	T Value	Prob. Level
Intercept	-2.0938	0.992395	-2.10984	.05000
Slope	8.05393E-3	1.25686E-3	6.40797	.00001

Analysis of Variance

Source	Sum of Squares	Df	Mean Square	F-Ratio	Prob. Level
Model	4.531550	1	4.531550	41.06204	.00001
Error	1.876096	17	.110359		
Total (Corr.)	6.407646	18			

Correlation Coefficient = 0.840958 R-squared = 70.72 percent
 Std. Error of Est. = 0.332203

Regression Analysis - Exponential model: $Y = \exp(a+bX)$

Dependent variable: Ell5016 Independent variable: del15016

Parameter	Estimate	Standard Error	T Value	Prob. Level
Intercept	-0.219869	0.295128	-0.744995	.46351
Slope	5.43054E-3	3.40137E-4	15.9657	.00000

Analysis of Variance

Source	Sum of Squares	Df	Mean Square	F-Ratio	Prob. Level
Model	6.07832	1	6.07832	254.9041	.00000
Error	.572292	24	.023846		
Total (Corr.)	6.650613	25			

Correlation Coefficient = 0.956007 R-squared = 91.39 percent
 Std. Error of Est. = 0.15442

Regression Analysis - Exponential model: $Y = \exp(a+bx)$

Dependent variable: P1500

Independent variable: dnp1500

Parameter	Estimate	Standard Error	T Value	Prob. Level
Intercept	-1.26273	0.270732	-4.66414	.00003
Slope	7.39144E-3	5.49877E-4	13.442	.00000

Analysis of Variance

Source	Sum of Squares	Df	Mean Square	F-Ratio	Prob. Level
Model	51.84782	1	51.84782	180.6870	.00000
Error	12.051825	42	.286948		
Total (Corr.)	63.899645	43			

Correlation Coefficient = 0.900774
Std. Error of Est. = 0.535675

R-squared = 81.14 percent

Regression Analysis - Exponential model: $Y = \exp(a+bx)$

Dependent variable: P1504

Independent variable: dnp1504

Parameter	Estimate	Standard Error	T Value	Prob. Level
Intercept	-0.391305	0.254276	-1.5389	.14122
Slope	4.43776E-3	4.97679E-4	8.91691	.00000

Analysis of Variance

Source	Sum of Squares	Df	Mean Square	F-Ratio	Prob. Level
Model	25.242518	1	25.242518	79.51131	.00000
Error	5.714474	18	.317471		
Total (Corr.)	30.956992	19			

Correlation Coefficient = 0.902998
Std. Error of Est. = 0.563445

R-squared = 81.54 percent

Regression Analysis - Exponential model: $Y = \exp(a+bx)$

Dependent variable: P15010

Independent variable: dnp15010

Parameter	Estimate	Standard Error	T Value	Prob. Level
Intercept	-6.58683	0.329051	-20.0177	.00000
Slope	0.0118416	5.39503E-4	21.9491	.00000

Analysis of Variance

Source	Sum of Squares	Df	Mean Square	F-Ratio	Prob. Level
Model	182.84000	1	182.84000	481.7651	.00000
Error	7.210901	19	.379521		
Total (Corr.)	190.05090	20			

Correlation Coefficient = 0.980846
Std. Error of Est. = 0.616053

R-squared = 96.21 percent

Regression Analysis - Exponential model: $Y = \exp(a+bx)$

Dependent variable: P15016

Independent variable: dnp15016

Parameter	Estimate	Standard Error	T Value	Prob. Level
Intercept	-2.94695	0.762001	-3.86738	.00096
Slope	7.08643E-3	1.13046E-3	6.2686	.00000

Analysis of Variance

Source	Sum of Squares	Df	Mean Square	F-Ratio	Prob. Level
Model	87.495885	1	87.495885	39.29531	.00000
Error	44.532479	20	2.226624		
Total (Corr.)	132.02836	21			

Correlation Coefficient = 0.814067
Std. Error of Est. = 1.49219

R-squared = 66.27 percent

Regression Analysis - Exponential model: $Y = \exp(a+bX)$

Dependent variable: K11500 Independent variable: dnk11500

Parameter	Estimate	Standard Error	T Value	Prob. Level
Intercept	6.58855	0.166467	39.5787	.00000
Slope	6.41284E-3	3.1339E-4	20.4628	.00000

Analysis of Variance

Source	Sum of Squares	Df	Mean Square	F-Ratio	Prob. Level
Model	48.72665	1	48.72665	418.7280	.00000
Error	11.520458	99	.116368		
Total (Corr.)	60.247110	100			

Correlation Coefficient = 0.899322
Std. Error of Est. = 0.341128

R-squared = 80.88 percent

Regression Analysis - Exponential model: $Y = \exp(a+bX)$

Dependent variable: K11504 Independent variable: dnk11504

Parameter	Estimate	Standard Error	T Value	Prob. Level
Intercept	5.44764	0.200747	27.1368	.00000
Slope	6.51524E-3	2.61459E-4	24.9188	.00000

Analysis of Variance

Source	Sum of Squares	Df	Mean Square	F-Ratio	Prob. Level
Model	59.22254	1	59.22254	620.9456	.00000
Error	7.153107	75	.095375		
Total (Corr.)	66.375649	76			

Correlation Coefficient = 0.944581
Std. Error of Est. = 0.308828

R-squared = 89.22 percent

Regression Analysis - Exponential model: $Y = \exp(a+bX)$

Dependent variable: K115010 Independent variable: dnk115010

Parameter	Estimate	Standard Error	T Value	Prob. Level
Intercept	2.09287	0.627903	3.3331	.00180
Slope	9.55994E-3	8.20806E-4	11.647	.00000

Analysis of Variance

Source	Sum of Squares	Df	Mean Square	F-Ratio	Prob. Level
Model	10.03067	1	10.03067	135.6530	.00000
Error	3.105631	42	.073944		
Total (Corr.)	13.136300	43			

Correlation Coefficient = 0.873833
Std. Error of Est. = 0.271926

R-squared = 76.36 percent

Regression Analysis - Exponential model: $Y = \exp(a+bX)$

Dependent variable: K115016 Independent variable: dnk115016

Parameter	Estimate	Standard Error	T Value	Prob. Level
Intercept	3.31537	0.383584	8.64312	.00000
Slope	7.73948E-3	4.49237E-4	17.2281	.00000

Analysis of Variance

Source	Sum of Squares	Df	Mean Square	F-Ratio	Prob. Level
Model	24.30991	1	24.30991	296.8069	.00000
Error	4.422859	54	.081905		
Total (Corr.)	28.732766	55			

Correlation Coefficient = 0.91982
Std. Error of Est. = 0.28619

R-squared = 84.61 percent

Regression Analysis - Exponential model: $Y = \exp(a+bX)$

Dependent variable: E21500 Independent variable: dne21500

Parameter	Estimate	Standard Error	T Value	Prob. Level
Intercept	1.29433	0.1097	11.7988	.00000
Slope	7.89805E-3	2.13653E-4	36.9668	.00000

Analysis of Variance

Source	Sum of Squares	Df	Mean Square	F-Ratio	Prob. Level
Model	87.5769	1	87.5769	1366.542	.00000
Error	7.88264	123	.06409		
Total (Corr.)	95.45952	124			

Correlation Coefficient = 0.957823 R-squared = 91.74 percent
Std. Error of Est. = 0.253153Regression Analysis - Exponential model: $Y = \exp(a+bX)$

Dependent variable: E21504 Independent variable: dne21504

Parameter	Estimate	Standard Error	T Value	Prob. Level
Intercept	1.96528	0.156253	12.5775	.00000
Slope	5.23009E-3	2.18193E-4	23.97	.00000

Analysis of Variance

Source	Sum of Squares	Df	Mean Square	F-Ratio	Prob. Level
Model	23.33567	1	23.33567	574.5608	.00000
Error	2.396272	59	.040615		
Total (Corr.)	25.731937	60			

Correlation Coefficient = 0.9523 R-squared = 90.69 percent
Std. Error of Est. = 0.201531Regression Analysis - Exponential model: $Y = \exp(a+bX)$

Dependent variable: E215010 Independent variable: dne15010

Parameter	Estimate	Standard Error	T Value	Prob. Level
Intercept	-0.889025	0.529778	-1.67811	.10042
Slope	0.0117268	6.83454E-4	17.1581	.00000

Analysis of Variance

Source	Sum of Squares	Df	Mean Square	F-Ratio	Prob. Level
Model	32.28466	1	32.28466	294.4010	.00000
Error	4.825137	44	.109662		
Total (Corr.)	37.109793	45			

Correlation Coefficient = 0.932725 R-squared = 87.00 percent
Std. Error of Est. = 0.331153Regression Analysis - Exponential model: $Y = \exp(a+bX)$

Dependent variable: E215016 Independent variable: dne215016

Parameter	Estimate	Standard Error	T Value	Prob. Level
Intercept	0.450063	0.135986	3.30962	.00157
Slope	6.44301E-3	1.61418E-4	39.9152	.00000

Analysis of Variance

Source	Sum of Squares	Df	Mean Square	F-Ratio	Prob. Level
Model	22.0397	1	22.0397	1593.221	.00000
Error	.843840	61	.013833		
Total (Corr.)	22.883557	62			

Correlation Coefficient = 0.981389 R-squared = 96.31 percent
Std. Error of Est. = 0.117616

Regression Analysis - Exponential model: $Y = \exp(a+bX)$

Dependent variable: K21500 Independent variable: dnk21500

Parameter	Estimate	Standard Error	T Value	Prob. Level
Intercept	4.82398	0.221183	21.8099	.00000
Slope	0.0116318	4.33441E-4	26.836	.00000

Analysis of Variance

Source	Sum of Squares	Df	Mean Square	F-Ratio	Prob. Level
Model	51.13161	1	51.13161	720.1691	.00000
Error	2.200983	31	.070999		
Total (Corr.)	53.332591	32			

Correlation Coefficient = 0.979148 R-squared = 95.87 percent
 Stnd. Error of Est. = 0.266457

Regression Analysis - Exponential model: $Y = \exp(a+bX)$

Dependent variable: K21504 Independent variable: dnk21504

Parameter	Estimate	Standard Error	T Value	Prob. Level
Intercept	6.61729	0.464207	14.255	.00000
Slope	6.92548E-3	5.75409E-4	12.0357	.00000

Analysis of Variance

Source	Sum of Squares	Df	Mean Square	F-Ratio	Prob. Level
Model	50.44192	1	50.44192	144.8592	.00000
Error	11.839255	34	.348213		
Total (Corr.)	62.281175	35			

Correlation Coefficient = 0.899948 R-squared = 80.99 percent
 Stnd. Error of Est. = 0.590096

Regression Analysis - Exponential model: $Y = \exp(a+bX)$

Dependent variable: K215010 Independent variable: dnk215010

Parameter	Estimate	Standard Error	T Value	Prob. Level
Intercept	5.7481	0.414446	13.8694	.00000
Slope	5.89133E-3	4.68958E-4	12.5626	.00000

Analysis of Variance

Source	Sum of Squares	Df	Mean Square	F-Ratio	Prob. Level
Model	91.46906	1	91.46906	157.8190	.00000
Error	27.819945	48	.579582		
Total (Corr.)	119.28900	49			

Correlation Coefficient = 0.875663 R-squared = 76.68 percent
 Stnd. Error of Est. = 0.761303

Regression Analysis - Exponential model: $Y = \exp(a+bX)$

Dependent variable: K215016 Independent variable: dnk215016

Parameter	Estimate	Standard Error	T Value	Prob. Level
Intercept	7.9956	0.563614	14.1863	.00000
Slope	3.9836E-3	5.72342E-4	6.96018	.00000

Analysis of Variance

Source	Sum of Squares	Df	Mean Square	F-Ratio	Prob. Level
Model	14.640082	1	14.640082	48.44406	.00000
Error	4.835295	16	.302206		
Total (Corr.)	19.475377	17			

Correlation Coefficient = 0.867019 R-squared = 75.17 percent
 Stnd. Error of Est. = 0.549733